Combinatorics of Cluster Algebras from Surfaces

A DISSERTATION
SUBMITTED TO THE FACULTY OF THE GRADUATE SCHOOL
OF THE UNIVERSITY OF MINNESOTA
BY

Emily Gunawan

IN PARTIAL FULFILLMENT OF THE REQUIREMENTS
FOR THE DEGREE OF
Doctor of Philosophy

Gregg Musiker, Advisor

August, 2016

Acknowledgements

First and foremost, I am very grateful for my advisor Gregg Musiker, without whom this thesis would not have been possible. He introduced me to cluster algebras and have given me interesting problems as well as tremendous support and encouragement through every stage of my graduate school experience. I would also like to thank the other members of my committee Christine Berkesch Zamaere, Ravi Janardan, and Vic Reiner, for showing an interest in my work. I also thank Karin Baur, Pasha Pylyavskyy, Vic Reiner, Ralf Schiffler, Hugh Thomas, Peter Webb for their helpful feedback on this thesis.

I am thankful for my collaborator Hannah Vogel for teaching me about frieze patterns and welcoming me to write Chapter 3 with her.

I want to thank the wonderful mathematics department at University of Minnesota, including Al, Alex, Becky, Eric, Elise, Heidi, Jed, Joel, Julie, Kevin, Max, Mike, Sebastian, Shannon, Theo, Thomas, Travis, and many others not named here, for all their support.

I am grateful for the Center for Women in Mathematics at Smith College, and all my former math professors, including Yuri Berest, Michael Bush, Chris Golé, Ruth Haas, Jim Henle, Dick McGehee, and Carol Shilepsky.

I thank Manuela Tschabold and Hannah Vogel for allowing me to use some of their tikz figures. Some of the images and Laurent polynomial computations were done with the help of SageMath [Dev16, SCc08] and code written by Ana García Elsener and Jorge Nicolás López of Universidad Nacional de Mar del Plata.

I am thankful for the travel support and research assistantships provided to me through the Combinatorics Groups' RTG Grant (NSF/DMS-1148634) and SageMath Grant (NSF/OCI-1147161).

Dedication

To my parents.

Abstract

We construct a periodic infinite frieze using a class of peripheral elements of a cluster algebra of type D or $\widetilde{A}$. We discover new symmetries and formulas relating the entries of this frieze and bracelet elements. We also present a correspondence between Broline, Crowe and Isaacs's classical matching tuples and various recent interpretations of elements of cluster algebras from surfaces.

We extend a T-path expansion formula for arcs on an unpunctured surface to the case of arcs on a once-punctured polygon and use this formula to give a combinatorial proof that cluster monomials form the atomic basis of a cluster algebra of type D.

We further generalize our work and present T-path formulas for tagged arcs with one or two notchings on a marked surface with punctures.

Contents

List of Figures

Chapter 1

Introduction

Cluster algebras, introduced by S. Fomin and A. Zelevinsky at the beginning of this century in the seminal paper [FZ02], are a class of algebraic objects with rich combinatorial structure. They appear in many areas of mathematics and theoretical physics including string theory, discrete dynamical systems, Lie theory, representation theory, and geometry.

A *surface with marked points* [FST08] gives rise to a cluster algebra. The *arcs* (that is, the internal edges) of all possible triangulations are in bijection with generators of the corresponding cluster algebra. Every two triangulations are connected by a sequence of *arc flips*

Example. *The following is a sequence of arc flips for a disk with* 6 *boundary points.*

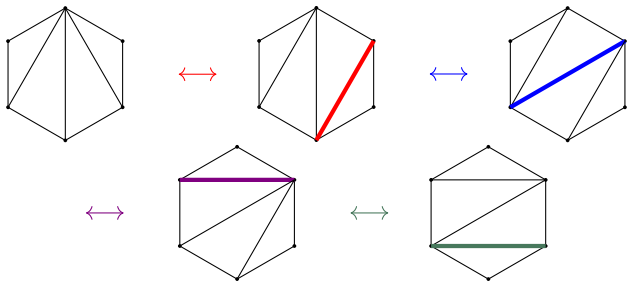

The class of cluster algebras from surfaces is an important subclass of a larger class

of cluster algebras that correspond to *quivers*[1] . A *cluster algebra* $\mathcal{A}(Q)$ corresponding to a quiver Q with n nodes (in the coefficient-free setting) is a $\mathbb{Z}$-subalgebra of the field of rational functions in n independent variables with coefficients in $\mathbb{Q}$. It is equipped with a distinguished set of generators, the *cluster variables*, which are grouped into overlapping sets of constant cardinality n, the *clusters*. These generators are not given from the outset but are produced by an iterative process.

Starting from an initial *seed* (*i.e.* a cluster $\{x_1, x_2, \ldots, x_n\}$ and a quiver Q with n nodes), the cluster variables are computed by an iteration of the form

$$\text{new variable at } k = \frac{\prod_{\text{arrows } j\to k} \text{variables at } j + \prod_{\text{arrows } k\to j} \text{variables at } j}{\text{old variable at position } k}$$

where the products are over all arrows $k \to j$ and $j \to k$ of Q. At each iteration (called a *mutation*), the new variable replaces the old variable, and the arrows of Q change following a simple rule[2] . Every seed can be mutated at every node k.

It is clear that all cluster variables are rational functions in the initial cluster variables $x_1, x_2, \ldots, x_n$. Surprisingly, every cluster variable u turns out to be a Laurent polynomial in $x_1, \ldots, x_n$ with positive coefficients [FZ02, LS15, GHKK14], that is, u can be written as a reduced fraction

$$u = \frac{f(x_1, x_2, \ldots, x_n)}{\prod_{i=1}^{n} x_i^{d_i}}, \tag{1.0.1}$$

where $f \in \mathbb{Z}_{\geq 0}[x_1, x_2, \ldots, x_n]$ and $d_i \geq 0$. The right hand side of equation (1.0.1) is called the *expansion of u in the cluster* $\{x_1, \ldots, x_n\}$.

This thesis is concerned with cluster algebras arising from surfaces. From a classification point of view, this class is significant because, for $n \geq 3$, all but 11 cluster algebras of *finite mutation type* belong to this class [FST12]. (A cluster algebra $\mathcal{A}$ is said to be of finite mutation type if there are finitely many quivers Q although $\mathcal{A}$ may

[1] A *quiver* is a directed graph with no loop $\circlearrowleft$ and no 2-cycles $i \leftrightarrows j$. Cycles longer than 2 are allowed, and multiple arrows between two nodes are allowed.

[2] *Mutating* Q at node k creates a new quiver $\mu_k(Q)$ constructed as follows: (1) For every $i \to k \to j$ in Q, add an arrow $i \to j$. (2) Reverse the direction of all arrows incident to k. (3) Remove any 2-cycles $i \leftrightarrows j$ created by steps (1) and (2). See Example 1.0.1.

have infinitely many cluster variables.) Each triangulation T with n internal edges corresponds to a quiver Q_T with n nodes. The mutation rules for changing arrows of Q_T correspond to *arc flips* of T. See Example 1.0.1.

Example 1.0.1. *The following is a sequence of arc flips connecting ideal triangulations of a once-punctured square, and the corresponding sequence of quiver mutations connecting quivers of type D_4.*

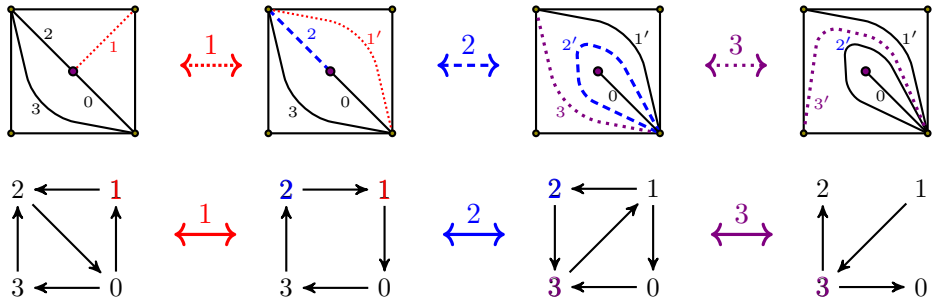

In Chapter 3, we study frieze patterns which are constructed from triangulations of surfaces. In Chapters 4 and 5, we discuss T-path formulas for computing cluster variables. In the second half Chapter 4, we use the T-paths to write a combinatorial proof involving a basis which consists of positive indecomposable elements (of a cluster algebra arising from a once-punctured polygon).

1.1 Results in Chapter 3

Chapter 3 is joint work with H. Vogel and G. Musiker. We use cluster algebraic techniques to study frieze patterns, classical objects which were first introduced by Conway and Coxeter in the 1970s.

- We construct of an infinite frieze where the entries of the frieze correspond to Laurent polynomials associated to generalized peripheral arcs (Theorem 3.3.1).
- We describe *progressions* and *growth coefficients* of entries in this frieze. We provide a geometric interpretation of these growth coefficients, and show that they correspond to so-called *bracelets* in the surface. Bracelets are associated to important cluster algebra elements which have been studied by many, including [SZ04, DT13, MW13, MSW13].

- We define *complementary arcs*, which are arcs between the same two vertices in a surface, but of alternate directions. Complementary arcs give rise to a special type of symmetry, which we call *complement symmetry*, in an infinite frieze. We state algebraic and combinatorial results involving the relationship between complementary arcs.

- We prove a bijection between T-paths (as studied by Schiffler and Thomas [Sch08a, ST09]) and the BCI matchings of vertices (as studied by Broline, Crowe, and Isaacs [BCI74]). This bijection preserves a natural distributive lattice structure which the T-paths are known to have.

1.2 Results in Chapter 4

When the surface has punctures, there are triangulations in which not all arcs may be flipped. This leads to *tagged arcs* (*i.e.* arcs where each endpoint is assigned a choice of two decorations, denoted by a notching $\bowtie$ or no notching) and *tagged arc flips* such as

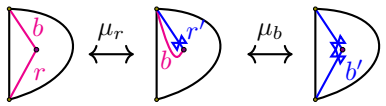

This causes technical difficulties which do not exist when working with unpunctured surfaces. Consequently, there are important results and constructions that were worked out for cluster algebras arising from unpunctured surfaces which were not yet extended to surfaces with punctures. Chapter 4 (which were jointly written with G. Musiker [GM15]) generalizes results that are known for unpunctured surfaces to surfaces with punctures.

- We generalize a cluster expansion formula (called T-path formula) for ordinary arcs for a cluster algebra of type D. Such a cluster algebra arises from a once-punctured polygon. The formula is given in terms of paths along a triangulation and generalizes work by Schiffer and Thomas [ST09, Sch10].

- An application of this T-path formula is a combinatorial proof that the families of non-crossing inner diagonals (which form a basis) form the set of all *positive indecomposable elements* for type D cluster algebras.

1.3 Results in Chapter 5

Chapter 5 generalizes the formula from the previous chapter.

- We work in the more general settings of cluster algebras arising from surfaces (with punctures) with so-called *principal coefficients*.
- We present a formula for ordinary arcs (as in the previous chapter).
- We present formulas for so-called *tagged arcs* with one or two notchings.

Chapter 2

Preliminaries

2.1 Cluster algebras with principal coefficients

This background section follows very closely the exposition written by Musiker, Schiffler, Williams in [MSW11, Sec. 2].

We recall an important type of cluster algebra $\mathcal{A}$, which is of *geometric type*, and a special type of so-called *coefficients* is called *principal coefficients*. These were introduced by Fomin and Zelevinsky in [FZ02, FZ07].

Let $\mathbb{P} = \mathrm{Trop}(u_1, \ldots, u_n)$ be an abelian group (written multiplicatively) freely generated by the u_j. We define $\oplus$ in $\mathrm{Trop}(u_1, \ldots, u_m)$ by

$$\prod_j u_j^{a_j} \oplus \prod_j u_j^{b_j} = \prod_j u_j^{\min(a_j, b_j)}, \tag{2.1.1}$$

and call $(\mathrm{Trop}(u_1, \ldots, u_m), \oplus, \cdot)$ a *tropical semifield*. Note that the group ring of $\mathrm{Trop}(u_1, \ldots, u_m)$ is the ring of Laurent polynomials in the variables u_j .

As an *ambient field* for $\mathcal{A}$, we take a field $\mathcal{F}$ isomorphic to the field of rational functions in n independent variables (here n is the *rank* of $\mathcal{A}$), with coefficients in $\mathbb{QP}$.

Definition 2.1.1 (labeled seeds)**.** *A* labeled seed *in $\mathcal{F}$ is a triple $(\mathbf{x}, \mathbf{y}, B)$, where*

- $\mathbf{x} = (x_1, \ldots, x_n)$ *is an n-tuple of elements of $\mathcal{F}$ forming a* free generating set *over $\mathbb{QP}$,*
- $\mathbf{y} = (y_1, \ldots, y_n)$ *is an n-tuple of elements of $\mathbb{P}$, and*

- $B = (b_{ij})$ *is an* $n \times n$ *integer matrix which is* skew-symmetrizable.

That is, $x_1, \ldots, x_n$ *are algebraically independent over* $\mathbb{QP}$*, and* $\mathcal{F} = \mathbb{QP}(x_1, \ldots, x_n)$*. We refer to* $\mathbf{x}$ *as the (labeled)* cluster *of a labeled seed* $(\mathbf{x}, \mathbf{y}, B)$*, to the tuple* $\mathbf{y}$ *as the* coefficient tuple*, and to the matrix* B *as the* exchange matrix*.*

We obtain (*unlabeled*) *seeds* from labeled seeds by identifying labeled seeds that differ from each other by simultaneous permutations of the components in $\mathbf{x}$ and $\mathbf{y}$, and of the rows and columns of B.

We use the notation $[x]_+ = \max(x, 0)$, $[1, n] = \{1, \ldots, n\}$, and

$$\operatorname{sgn}(x) = \begin{cases} -1 & \text{if } x < 0; \\ 0 & \text{if } x = 0; \\ 1 & \text{if } x > 0. \end{cases}$$

Definition 2.1.2 (seed mutations)**.** *Let* $(\mathbf{x}, \mathbf{y}, B)$ *be a labeled seed in* $\mathcal{F}$*, and let* $k \in [1, n]$*. The* seed mutation μ_k *in direction* k *transforms* $(\mathbf{x}, \mathbf{y}, B)$ *into the labeled seed* $\mu_k(\mathbf{x}, \mathbf{y}, B) = (\mathbf{x}', \mathbf{y}', B')$ *defined as follows:*

- *The entries of* $B' = (b'_{ij})$ *are given by*

$$b'_{ij} = \begin{cases} -b_{ij} & \text{if } i = k \text{ or } j = k; \\ b_{ij} + \operatorname{sgn}(b_{ik})\ [b_{ik} b_{kj}]_+ & \text{otherwise.} \end{cases} \tag{2.1.2}$$

- *The coefficient tuple* $\mathbf{y}' = (y'_1, \ldots, y'_n)$ *is given by*

$$y'_j = \begin{cases} y_k^{-1} & \text{if } j = k; \\ y_j y_k^{[b_{kj}]_+} (y_k \oplus 1)^{-b_{kj}} & \text{if } j \neq k. \end{cases} \tag{2.1.3}$$

- *The cluster* $\mathbf{x}' = (x'_1, \ldots, x'_n)$ *is given by* $x'_j = x_j$ *for* $j \neq k$*, whereas* $x'_k \in \mathcal{F}$ *is determined by the* exchange relation

$$x'_k = \frac{y_k \prod x_i^{[b_{ik}]_+} + \prod x_i^{[-b_{ik}]_+}}{(y_k \oplus 1) x_k}\,. \tag{2.1.4}$$

We say that two exchange matrices B and B' are *mutation-equivalent* if one can get from B to B' by a sequence of mutations.

Definition 2.1.3 (patterns)**.** *Consider the* n-regular tree $\mathbb{T}_n$ *whose edges are labeled by the numbers* $1, \ldots, n$*, so that the* n *edges emanating from each vertex receive different labels. A* cluster pattern *is an assignment of a labeled seed* $\Sigma_t = (\mathbf{x}_t, \mathbf{y}_t, B_t)$ *to every vertex* $t \in \mathbb{T}_n$*, such that the seeds assigned to the endpoints of any edge* $t \overset{k}{\text{——}} t'$ *are obtained from each other by the seed mutation in direction* k*. The components of* Σ_t *are written as:*

$$\mathbf{x}_t = (x_{1;t}\,, \ldots, x_{n;t})\,, \quad \mathbf{y}_t = (y_{1;t}\,, \ldots, y_{n;t})\,, \quad B_t = (b^t_{ij})\,. \tag{2.1.5}$$

A cluster pattern is uniquely determined by an arbitrary seed.

Definition 2.1.4 (Cluster algebra)**.** *Given a cluster pattern, we denote*

$$\mathcal{X} = \bigcup_{t \in \mathbb{T}_n} \mathbf{x}_t = \{x_{i,t} \,:\, t \in \mathbb{T}_n\,,\ 1 \le i \le n\}\ , \tag{2.1.6}$$

the union of clusters of all the seeds in the pattern. The elements $x_{i,t} \in \mathcal{X}$ *are called* cluster variables*. The* cluster algebra $\mathcal{A}$ *associated with a given pattern is the* $\mathbb{ZP}$*-subalgebra of the ambient field* $\mathcal{F}$ *generated by all cluster variables:* $\mathcal{A} = \mathbb{ZP}[\mathcal{X}]$*. We denote* $\mathcal{A} = \mathcal{A}(\mathbf{x}, \mathbf{y}, B)$*, where* $(\mathbf{x}, \mathbf{y}, B)$ *is any seed in the underlying cluster pattern.*

Cluster variables satisfy the following remarkable *Laurent phenomenon.*

Theorem 2.1.1. *[FZ02, Theorem 3.1] The cluster algebra* $\mathcal{A}$ *associated with a seed* $(\mathbf{x}, \mathbf{y}, B)$ *is contained in the Laurent polynomial ring* $\mathbb{ZP}[\mathbf{x}^{\pm 1}]$*, i.e. every element of* $\mathcal{A}$ *is a Laurent polynomial over* $\mathbb{ZP}$ *in the cluster variables from* $\mathbf{x} = (x_1, \ldots, x_n)$*.*

Furthermore, the long-standing conjecture that this Laurent polynomial has coefficients which are non-negative integer linear combinations of elements in $\mathbb{P}$ was recently proven in [GHKK14, LS15].

Given a seed Σ and a cluster variable a of $\mathcal{A}$, we refer to the expression of a as a Laurent polynomial in terms of the cluster variables from Σ as the *cluster expansion* of a in terms of Σ.

Remark 2.1.5. *In cluster algebras whose ground ring is* $\mathrm{Trop}(u_1, \ldots, u_m)$ *(the tropical semifield), it is convenient to replace the matrix* B *by an* $(n+m) \times n$ *matrix* $\tilde{B} = (b_{ij})$ *whose upper part is the* $n \times n$ *matrix* B *and whose lower part is an* $m \times n$ *matrix that encodes the coefficient tuple via*

$$y_k = \prod_{i=1}^{m} u_i^{b_{(n+i)k}}. \tag{2.1.7}$$

Then the mutation of the coefficient tuple in equation (2.1.3) is determined by the mutation of the matrix $\tilde{B}$ *in equation (2.1.2) and the formula (2.1.7); and the exchange relation (2.1.4) becomes*

$$x_k' = x_k^{-1} \left(\prod_{i=1}^{n} x_i^{[b_{ik}]_+} \prod_{i=1}^{m} u_i^{[b_{(n+i)k}]_+} + \prod_{i=1}^{n} x_i^{[-b_{ik}]_+} \prod_{i=1}^{m} u_i^{[-b_{(n+i)k}]_+} \right). \tag{2.1.8}$$

Fomin and Zelevinsky introduced in [FZ07] a special type of coefficients, called *principal coefficients*. A motivation for working with principal coefficients is that, knowing the cluster expansions for a cluster algebra with principal coefficients allows one to compute the cluster expansions for the "same" cluster algebra with an arbitrary coefficient system (see [FZ07, Theorem 3.7])

Definition 2.1.6 (principal coefficients)**.** *We say that a cluster pattern* $t \mapsto (\mathbf{x}_t, \mathbf{y}_t, B_t)$ *on* $\mathbb{T}_n$ *(or the corresponding cluster algebra* $\mathcal{A}$*) has* principal coefficients at a vertex t_0 *if* $\mathbb{P} = \mathrm{Trop}(y_1, \ldots, y_n)$ *and* $\mathbf{y}_{t_0} = (y_1, \ldots, y_n)$*. In this case, we denote* $\mathcal{A} = \mathcal{A}_\bullet(B_{t_0})$*.*

Remark 2.1.7. *Definition 2.1.6 can be rephrased as follows: a cluster algebra* $\mathcal{A}$ *has principal coefficients at a vertex* t_0 *if* $\mathcal{A}$ *is of geometric type, and is associated with the matrix* $\tilde{B}_{t_0}$ *of order* $2n \times n$ *whose upper part is* B_{t_0}*, and whose complementary (i.e., bottom) part is the* $n \times n$ *identity matrix ([FZ02, Corollary 5.9]).*

2.2 Cluster algebras from surfaces

We provide a brief background on cluster algebras arising from marked surfaces [FST08].

2.2.1 Triangulations of marked surfaces

Definition 2.2.1 (marked surface)**.** *Let S be a connected, oriented, Riemann surface with (possibly empty) boundary, and M a non-empty, finite set of marked points in the closure of S, such that there is at least one marked point on each boundary component of S. Then (S, M) is called a* marked surface*, and the interior points of S are called* punctures*.*

For technical reasons, assume that (S, M) is not the following: a sphere with fewer than four punctures; a monogon with zero or one puncture; or a bigon or triangle without punctures.

Definition 2.2.2 (ordinary arc)**.** *An* ordinary arc γ in (S, M) *is a curve in S, considered up to isotopy, such that: (1) the endpoints of γ are in M, (2) γ does not cross itself (except its endpoints may coincide), (3) the interior of γ is disjoint from M and from the boundary of S, and (4) γ does not cut out an unpunctured monogon or bigon. A* boundary edge *is a curve that connects two marked points and lies entirely on the boundary of S without passing through a third marked point.*

We say that two ordinary arcs α, β are *compatible* if there exist representatives α', β' in their respective isotopy classes such that α' and β' do not intersect in the interior of S.

Definition 2.2.3 (ideal triangulation)**.** *An* ideal triangulation *is a maximal (by inclusion) collection of distinct, pairwise compatible ordinary arcs. The ordinary arcs of an ideal triangulation cut the surface into* ideal triangles *(see Fig. 2.1).*

Remark 2.2.4 (possible types of ideal triangles)**.** *There are two types of ideal triangles in a triangulation: triangles that have three distinct sides (Figs. 2.1(a), 2.1(b), and 2.1(d)), and* self-folded triangles *(Fig. 2.1(c)). A self-folded triangle consists of an arc ℓ (which we will refer to as an ℓ-*loop*) whose endpoints coincide, along with an arc r (called a* radius*) that goes from the endpoint of ℓ to an enclosed puncture.*

Definition 2.2.5 (peripheral and radial arcs)**.** *Let γ be an ordinary arc of (S, M). We say that γ is a* peripheral arc *if: (1) both its endpoints are on a boundary component Bd of S, and (2) γ is isotopic to a concatenation of two or more boundary edges of a*

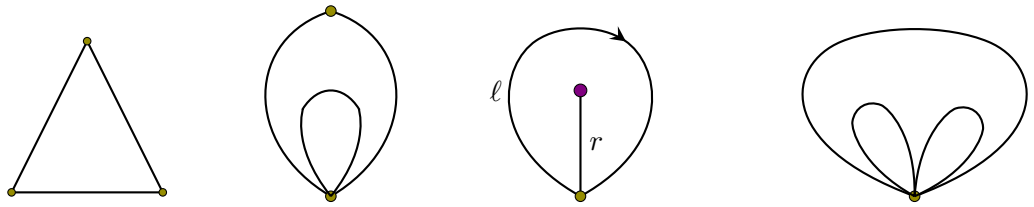

(a) Ordinary triangle. (b) Two vertices. (c) Self-folded triangle. (d) One vertex, 3 edges.

Figure 2.1: Possible types of ideal triangles.

boundary component Bd. Note that an ℓ-loop that is based at a boundary marked point is considered an ordinary peripheral arc. We call an arc connecting a marked point on a boundary component to a puncture (or a different boundary component) a radial arc*.*

Definition 2.2.6 (ordinary flip)**.** *A* (ordinary) flip *is a move that replaces an ordinary arc γ in an ideal triangulation T with a (unique) arc $\gamma' \neq \gamma$ such that $(T \setminus \gamma) \cup \gamma'$ forms a new ideal triangulation.*

Any two ideal triangulations of a surface are connected to each other by a sequence of flips (see Fig. 2.2 for an example).

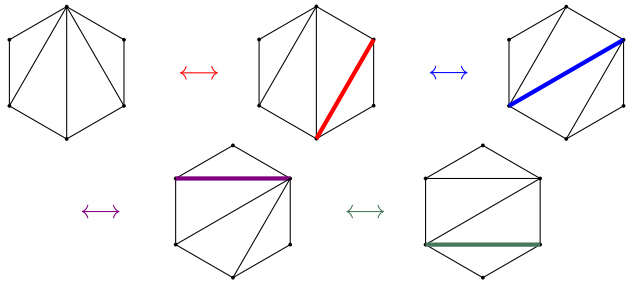

Figure 2.2: Sequence of flips.

When working with a cluster algebra associated to a surface with punctures, it is not sufficient to work with ordinary arcs and ideal triangulations. The authors of [FST08] introduced *tagged arcs* and *tagged triangulations*, and showed that they are in bijection with cluster variables and clusters.

Definition 2.2.7 (tagged arcs)**.** *A* tagged arc *is obtained by taking an ordinary arc (that is not an ℓ-loop) γ and marking ("tagging") each end γ with one of two options,* plain *or* notched*, such that:*

1) an endpoint lying on the boundary must be tagged plain, and

2) both ends of a loop must be tagged the same way.

A notched tagging is usually indicated by a bow tie, and a plain tagging is usually denoted by no marking. Note that a tagged arc never cuts out a once-punctured monogon, i.e., an ℓ-loop is not *a tagged arc. For a list of tagged arcs, see [FST08, Remark 7.3].*

Compatibility of two tagged arcs is defined in [FST08, Def. 7.4]. A maximal (by inclusion) collection of distinct, pairwise compatible tagged arcs is called a *tagged triangulation*. Fig. 2.3 (center) gives an example of a tagged triangulation. The *flip* of a tagged arc is defined in [FST08, Section 9.3].

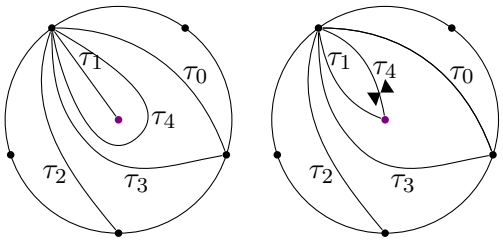

$$\begin{pmatrix} 0 & 1 & 0 & -1 & 1 \\ -1 & 0 & 0 & 1 & 0 \\ 0 & 0 & 0 & -1 & 0 \\ 1 & -1 & 1 & 0 & -1 \\ -1 & 0 & 0 & 1 & 0 \end{pmatrix}$$

Figure 2.3: An ideal triangulation, a corresponding tagged triangulation of the once-punctured 5-gon, and the corresponding signed adjacency matrix

Definition 2.2.8 (representing ordinary arcs as tagged arcs)**.** *Any ordinary arc γ can be represented by a tagged arc $\iota(\gamma)$ as follows. Suppose γ is an ℓ-loop (based at marked point v) which encloses a puncture p. Let r be the unique arc which is compatible with γ and which connects v and p. Then $\iota(\gamma)$ is obtained by tagging r plain at v and notched at p. Otherwise, $\iota(\gamma)$ is simply γ tagged plain at both endpoints. For example, see Fig. 2.3.*

2.2.2 From surfaces to cluster algebras

We can associate an exchange matrix [FST08, Def. 4.1 and 9.6], and hence a cluster algebra, to (S, M). Note that our convention agrees with, for example,[Sch10, MS10], but is opposite of the more recent papers [MSW11, MW13, MSW13].

Definition 2.2.9 (signed adjacency matrix of an ideal triangulation)**.** *Let T be an ideal triangulation, and $\tau_1, \tau_2, \ldots, \tau_n$ arcs of T. For any non-self folded triangle Δ in T, we define a matrix $B^\Delta = \left(b_{ij}^\Delta\right)_{1\le i\le n, 1\le j\le n}$ as follows:*

- *$b_{ij}^\Delta = 1$ and $b_{ji}^\Delta = -1$ in the following cases:*
  - *(a) τ_i and τ_j are sides of Δ with τ_j following τ_i in the counterclockwise order;*
  - *(b) τ_j is a radial arc in a self-folded triangle enclosed by an ℓ-loop τ_ℓ, and τ_i and τ_ℓ are sides of Δ with τ_ℓ following τ_i in the counterclockwiseorder;*
  - *(c) τ_i is a radial arc in a self-folded triangle enclosed by an ℓ-loop τ_ℓ, and τ_ℓ and τ_j are sides of Δ with τ_j following τ_ℓ in the counterclockwiseorder;*
- *$b_{ij}^\Delta = 0$ otherwise.*

Then define the signed adjacency matrix *$B_T = (b_{ij})_{1\le i\le n, 1\le j\le n}$ of T by $b_{ij} = \sum_\Delta b_{ij}^\Delta$, where the sum is taken over all triangles in T that are not self-folded.*

Definition 2.2.10 (signed adjacency matrix of a tagged triangulation)**.** *Let T be a tagged triangulation. We construct a tagged triangulation $\widehat{T}$ as follows: for each puncture such that all endpoints are notched, we change their tags to plain. Let T^o be the ideal triangulation which is represented by $\widehat{T}$. For each tagged arc in T, the corresponding ordinary arc in T^o retains the same label. The* signed adjacency matrix *B_T of T is defined to be the signed adjacency matrix B_{T^o} of T^o (as in Definition 2.2.9).*

See Fig. 2.3.

Theorem 2.2.11 ([FST08] Theorem 7.11, and [FT12] Theorem 6.1)**.** *Let (S, M) be a marked surface, and let $\mathcal{A}$ be the coefficient-free cluster algebra associated to the signed adjacency matrix of a tagged triangulation (as in Definition 2.2.10) Then the (unlabeled) seeds Σ_T of $\mathcal{A}$ are in bijection with tagged triangulations T of (S, M), and the cluster variables are in bijection with the tagged arcs of (S, M) (so we can denote each cluster variable by x_γ or $x(\gamma)$, where γ is a tagged arc). Moreover, each seed in $\mathcal{A}$ is uniquely determined by its cluster. Furthermore, if a tagged triangulation T' is obtained from another tagged triangulation T by flipping a tagged arc $\gamma \in T$ and obtaining γ', then $\Sigma_{T'}$ is obtained from Σ_T by the seed mutation replacing x_γ by $x_{\gamma'}$.*

If ℓ is an unnotched ℓ-loop with (based at marked point v) which encloses a radius r and a puncture P, then we set $x_\ell = x_r\, x_{r^{(P)}}$, where $r^{(P)}$ denote the arc obtained from r by changing its notching at P. If τ is a boundary edge, we set $x_\tau := 1$.

2.3 Cluster algebra elements associated to generalized arcs and closed loop

We now want to consider more complicated arcs, possibly with self-crossings, which correspond to Laurent polynomials in every cluster. In [MSW11], Musiker, Schiffler, and Williams gave a combinatorial formula for the Laurent expansion of any cluster variable in a cluster algebra associated to a marked surface. Their expansion formula, which is a weighted sum over perfect matchings of a *planar snake graph*, associates a cluster algebra element to an arc in the surface. In [MSW13, MW13], the same authors generalized this construction and associated cluster algebra elements to generalized arcs, as well as to closed loops (with or without self-crossings). Instead of perfect matchings of a planar graph, the Laurent polynomial associated to a closed curve is a weighted sum over good matchings in a *band graph* on a Mobius strip or annulus. In coefficient-free settings, these constructions for generalized arcs and loops work even in the existence of punctures.

2.3.1 Generalized arcs and closed loops

Definition 2.3.1 (generalized arcs)**.** *A* generalized (ordinary) arc *in* (S, M) *is a curve* γ *in* S*, considered up to isotopy, such that*

1. *the endpoints of* γ *are in* M*,*
2. *except for the endpoints,* γ *is disjoint from* M *and the boundary of* S*, and*
3. γ *does not cut out an unpunctured bigon or monogon. In other words,* γ *is not contractible to a point, and* γ *is not isotopic to a boundary edge.*

Generalized arcs are allowed to intersect themselves a finite number of times (possibly 0*). We consider these arcs up to isotopy of immersed arcs, that is, allowing Reidemeister moves of types II and III but not of type I. In particular, an isotopy cannot remove a*

contractible kink from a generalized arc. If an arc intersects itself, we say that the arc has a self-crossing*.*

Definition 2.3.2 (generalized peripheral arc)**.** *Suppose* (S, M) *contains a boundary component* Bd*. We say that a generalized (ordinary) arc* γ *is a* generalized peripheral arc on Bd *if* γ *starts at a marked point on* Bd*, wraps finitely many times (possibly 0)* Bd *and then ends at a marked point on* Bd *(possibly at the same starting point). Our convention is to choose the orientation of* γ *so that* Bd *is to the right of* γ *when looking from above.*

In the case of the punctured disk (respectively, annulus), a generalized peripheral arc γ wraps finitely many times around the puncture (respectively, the other boundary) such that the puncture (respectively, the other boundary) is always to the left of γ.

We can draw a generalized arc in the universal cover, for both the annulus and the punctured disk as in [BPT16].

Example 2.3.3. *In Fig. 2.4, we draw copies of the arc* $(2, 9)$ *along the lower (outer) boundary in the universal cover of the annulus* $C_{5,q}$*:*

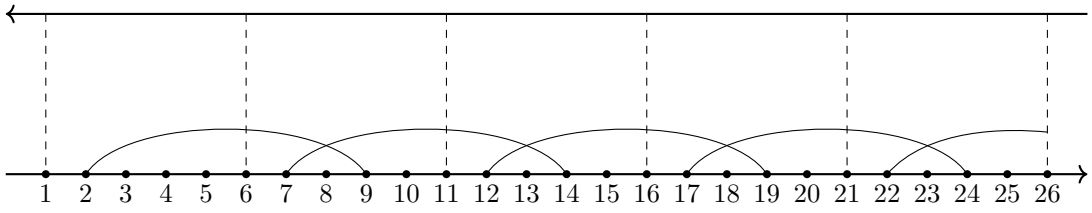

Figure 2.4: Universal cover of the annulus $C_{n,m}$, for $n = 5$.

Note that the arc $(2, 9)$ *has a self-crossing in the annulus.*

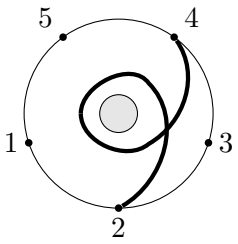

This can be see in the universal cover by the arc crossing into another frame *(denoted by the dashed lines).*

Definition 2.3.4 (closed loops)**.** *A* closed loop *in (S, M) is a closed curve γ in S which is disjoint from the boundary of S. Again, we allow closed loops to have a finite number of self-crossings, and we consider closed loops up to isotopy.*

Definition 2.3.5 (bracelets)**.** *A closed loop obtained by following a (non-contractible, non-self-crossing, kink-free) loop k times, and thus creating $k-1$ self-crossings, is called a* k-bracelet *and is denoted by $Brac_k$. See Fig. 2.5.*

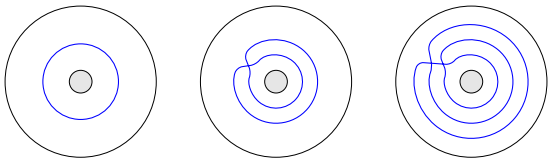

Figure 2.5: Bracelets $Brac_1$, $Brac_2$, and $Brac_3$.

2.3.2 Tiles G_j

Let γ be an ordinary arc in (S, M) which is not in T. Choose an orientation on γ, and let $s \in M$ be its starting point, and $t \in M$ its endpoint. We denote by $s = p_0, p_1, p_2, \ldots, p_{d+1} = t$ the points of intersection of γ and T in order. Let τ_{i_j} be the arc of T containing p_j, and let Δ_{j-1} and Δ_j be the two ideal triangles in T on either side of τ_{i_j}.

To each p_j we associate a *tile* G_j, that is, a triangulated quadrilateral (see Fig. 2.6) which is the union of two edge-labeled triangles Δ_1^j and Δ_2^j glued at an edge labeled τ_{i_j}. The triangles Δ_1^j and Δ_2^j are determined by the ideal Δ_{j-1} and Δ_j as follows.

If each of Δ_{j-1} and Δ_j has three distinct sides (*i.e.*, not self-folded), then Δ_1^j and Δ_2^j are triangles with edges labeled as in Δ_{j-1} and Δ_j. We glue Δ_1^j and Δ_2^j at the end labeled τ_{i_j} such that the orientations of Δ_1^j and Δ_2^j both either agree or disagree with those of Δ_{j-1} and Δ_j. This gives two possible planar embeddings of a graph G_j.

If one of Δ_{j-1} and Δ_j is self-folded, then T^o has a local configuration of an ideal bigon (with sides a and b, possibly loops). This bigon contains a radius r incident to a

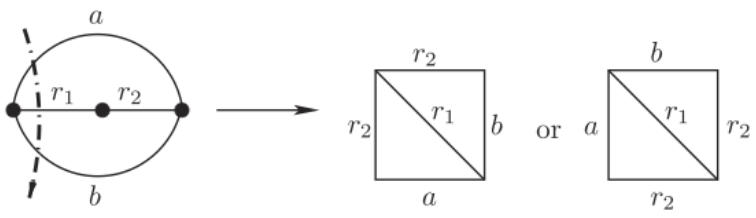

Figure 2.6: Possible tiles corresponding to a crossing radius of a bigon [MW13, Fig. 2].

puncture p inscribed inside an ℓ-loop ℓ, see [MW13, Fig. 3]. If γ has no self-crossing as it passes through the self- folded triangle, then γ must either

$$\text{intersect the } \ell\text{-loop } \ell \text{ and terminate at the puncture } p, \text{ or} \tag{2.3.1}$$

$$\text{intersect the } \ell\text{-loop } \ell, \text{ radius } r \text{ and then } \ell \text{ again.} \tag{2.3.2}$$

In case (2.3.1), we associate to p_j (the intersection point with ℓ) an ordinary tile G_j consisting of a triangle with sides $\{a, b, \ell\}$ which is glued along diagonal ℓ to a triangle with sides $\{\ell, r, r\}$. As before there are two possible planar embeddings of G_j.

In case (2.3.2), we associate to the triple of intersection points p_{j1}, p_j, and p_{j+1} a union of tiles $G_{j1} \cup G_j \cup G_{j+1}$, which we call a triple tile, based on whether γ enters and exits through different sides of the bigon or through the same side. These graphs are defined by the first three examples in 2.7.

Note that in each case there are two possible planar embeddings of the triple tile. We call the tiles G_{j1} and G_{j+1} within the triple tile ordinary tiles. On the other hand, if γ has a self-crossing inside the self-folded triangle, then the local configuration in the associated graph is as in the last two examples of Fig. 2.7.

Let G_j be the graph with 4 vertices and 5 edges, having the shape of a square with a diagonal, such that there is a bijection between the edges of G_j and the 5 arcs in the two triangles Δ_{j-1} and Δ_j, which preserves the signed adjacency of the arcs up to sign and such that the diagonal in G_j corresponds to the arc τ_{i_j} containing the crossing point p_j. We call the graph G_j a *tile*. Thus the tile G_j is given by the quadrilateral in the triangulation T whose diagonal is τ_{i_j}.

Definition 2.3.6. *Given a planar embedding $\tilde{G}_j$ of a tile G_j, we define the* relative

orientation $\mathrm{rel}(\tilde{G}_j, T)$ *of* $\tilde{G}_j$ *with respect to* T *to be* ± 1*, based on whether its triangles agree or disagree in orientation with those of* T*.*

Using the notation above, the arcs τ_{i_j} and $\tau_{i_{j+1}}$ form two edges of a triangle Δ_j in T. Define $\tau_{[\gamma_j]}$ to be the third arc in this triangle.

2.3.3 Snake graphs and band graphs

We now recursively glue together the tiles $G_1, \ldots, G_d$ in order from 1 to d, so that:

- Triple tiles must stay glued together as in Fig. 2.7.
- For two adjacent tiles, we glue G_{j+1} to $\tilde{G}_j$ along the edge labeled $\tau_{[\gamma_j]}$, choosing a planar embedding $\tilde{G}_{j+1}$ for G_{j+1} so that $\mathrm{rel}(\tilde{G}_{j+1}, T) \neq \mathrm{rel}(\tilde{G}_j, T)$.

After gluing together the d tiles, we obtain a graph (embedded in the plane), which we denote by $\overline{G}_\gamma$.

Definition 2.3.7. *The* snake graph G_γ *associated to* γ *is obtained from* $\overline{G}_\gamma$ *by removing the diagonal in each tile. Abusing notation, we will also use the word* tile *to refer to the graph obtained from a tile by deleting its diagonal.*

Now we associate a similar graph to closed loops. Let ζ be a closed loop in (S, M) (possibly with self-crossings) which is not contractible and has no contractible kinks. Choose an orientation for ζ, and a triangle Δ which is crossed by γ. Let p be a point in the interior of Δ which lies on γ, and let b and c be the two sides of the triangle crossed by γ immediately before and following its travel through point p. Let a be the third side of Δ. We let $\tilde{\gamma}$ denote the arc from p back to itself that exactly follows closed loop γ. Note that these definitions make sense even if Δ is self-folded. See Fig. 2.8.

We start by building the snake graph $G_{\tilde{\gamma}}$ as defined above. In the first tile of $G_{\tilde{\gamma}}$, let x denote the vertex at the corner of the edge labeled a and the edge labeled b, and let y denote the vertex at the other end of the edge labeled a. Similarly, in the last tile of $G_{\tilde{\gamma}}$, let x' denote the vertex at the corner of the edge labeled a and the edge labeled c, and let y' denote the vertex at the other end of the edge labeled a.

Definition 2.3.8. *The* band graph $\widetilde{G}_\zeta$ *associated to the loop* ζ *is the graph obtained from* $G_{\tilde{\zeta}}$ *by identifying the edges labeled* a *in the first and last tiles so that the vertices* x

and x' and the vertices y and y' are glued together. We refer to the two vertices obtained by identification as x and y, and to the edge obtained by identification as the cut edge. *The resulting graph lies on an annulus or a Möbius strip.*

2.3.4 Laurent polynomials associated to generalized arcs and closed loops

Recall from Theorem 2.2.11 that for unlabeled seeds Σ_T of a cluster algebra $\mathcal{A}$, the tagged arcs of (S, M) are in bijection with the cluster variables, and we denote these variables by x_τ for τ a tagged arc.

Definition 2.3.9. *If γ is a generalized arc of a closed loop, and $\tau_{i_1}, \tau_{i_2}, \ldots, \tau_{i_d}$ is the sequence of arcs in T which γ crosses, then the* crossing monomial *of γ with respect to T is defined to be*

$$cross(T, \gamma) = \prod_{j=1}^{d} x_{\tau_{i_j}}.$$

Recall that if τ is a boundary segment, then let $x_\tau := 1$.

Definition 2.3.10 ([MW13, Def. 3.7])**.** *A* perfect matching *of a graph G is a subset P of the edges of G such that each vertex of G is incident to exactly one edge of P. If G is a snake or band graph, and the edges of a perfect matching P of G are labeled $\tau_{j_1}, \ldots, \tau_{j_r}$, then we define the* weight *$x(P)$ of P to be $x_{\tau_{j_1}} \cdots x_{\tau_{i_r}}$.*

Definition 2.3.11 ([MW13, Def. 3.12])**.** *Let (S, M) be a surface, T an ideal triangulation, and $\mathcal{A} = \mathcal{A}(B_T)$ be the cluster algebra associated to B_T. Let γ be a generalized arc and let $G_{T,\gamma}$ denote its snake graph. We define a Laurent polynomial which lies in (the fraction field) of $\mathcal{A}$.*

1. *If γ cuts out a contractible monogon, then X_γ^T is equal to zero.*
2. *if γ has a contractible kink, let $\overline{\gamma}$ denote the corresponding tagged arc with this kink removed, and define $X_\gamma^T := (-1)X_{\overline{\gamma}}^T$.*
3. *Otherwise, define*

$$X_\gamma^T := \frac{1}{cross(T, \gamma)} \sum_P x(P),$$

where the sum is over all perfect matchings P of $G_{T,\gamma}$.

Theorem 2.3.12 ([MSW11, Thm 4.10]). *When γ is an arc (with no self-crossings), X_γ^T is equal to the Laurent expansion of the cluster variable $x_\gamma \in \mathcal{A}$ with respect to the seed Σ_T.*

Definition 2.3.13 ([MW13, Def. 3.18]). *Let ζ be a closed loop. A perfect matching P of the band graph $\tilde{G}_\zeta$ is called a* good matching *if either the vertices x and y are matched to each other (i.e. $P(x) = y$ and $P(y) = x$) or if both edges $(x, P(x))$ and $(y, P(y))$ lie on one side of the cut edge.*

We can now define a Laurent polynomial X_ζ for every closed loop ζ.

Definition 2.3.14 ([MW13, Def. 3.21]). *Let (S, M) be a surface, T an ideal triangulation, and $\mathcal{A}$ be the cluster algebra associated to B_T. Let ζ be a closed loop. We define a Laurent polynomial X_ζ^T which lies in (the fraction field) of $\mathcal{A}$.*

1. *If ζ is a contractible loop, then let $X_\zeta^T := -2$.*
2. *If ζ is a closed loop without self-crossings enclosing a single puncture p and T contains a self-folded triangle containing p, then let $X_\zeta^T := 2$.*
3. *If ζ has a contractible kink, let $\overline{\zeta}$ denote the corresponding closed loop with this kink removed, and define $X_\zeta^T := (-1)X_{\overline{\zeta}}$.*
4. *Otherwise, let*
$$X_\zeta^T = \frac{1}{cross(T, \gamma)} \sum_P x(P),$$
where the sum is over all good matchings P of the band graph $\tilde{G}_\zeta$.

Remark 2.3.15 ([MW13]). *If ζ is a loop contractible to a single puncture, then $X_\zeta^T = 2$.*

In our study of infinite friezes, we only consider marked surfaces (S, M) which has nonempty boundary. In this situation, the Laurent polynomials given in Definitions 2.3.11 and 2.3.14 in fact lie in $\mathcal{A}$, due to [Mul13, Theorem 4.1] and [CLS15, Theorem 5].

Example 2.3.16 (Example of a Laurent expansion corresponding to a generalized arc). *Consider the ideal triangulation T of a once-punctured disk and a generalized arc in Fig.*

2.9. We obtain the graph $\overline{G}_\gamma$ in Fig. 2.10. Following Definition 2.3.11, we compute

$$X_\gamma^T = \frac{x_0x_1x_4 + 2x_1x_3x_4 + 2x_0^2 + 4x_0x_3 + 2x_3^2}{x_0x_1x_4}$$

by specializing $x(\tau) = 1$ for each boundary edge τ. In particular, the snake graph G_γ has 11 perfect matchings (see Fig. 2.11).

Example 2.3.17 (Example of the Laurent polynomial corresponding to Brac_2 in an annulus)**.** *Consider the ideal triangulation T of an annulus and the $Brac_2$ in Fig. 2.12 (left). We obtain the graph $\widetilde{G}_{Brac_2}$ in Fig. 2.12 (right).*

Following Definition 2.3.14, we compute

$$X_{Brac_2}^T = \frac{x_1^4x_3^2 + x_2^4x_3^2 + 2x_0x_1^3x_3 + 2x_0x_1x_2^2x_3 + x_0^2x_1^2 + 2x_1^2x_2x_3 + 2x_2^3x_3 + 2x_0x_1x_2 + x_2^2}{x_1^2x_2^2x_3^2}$$

by specializing $x(\tau) = 1$ for each boundary edge τ. In particular, the band graph $\widetilde{G}_{Brac_2}$ has 14 good matchings.

For the rest of the paper, we will use the notation x_γ or $x(\gamma)$ to denote the cluster algebra element corresponding to γ, where γ is a generalized arc or loop.

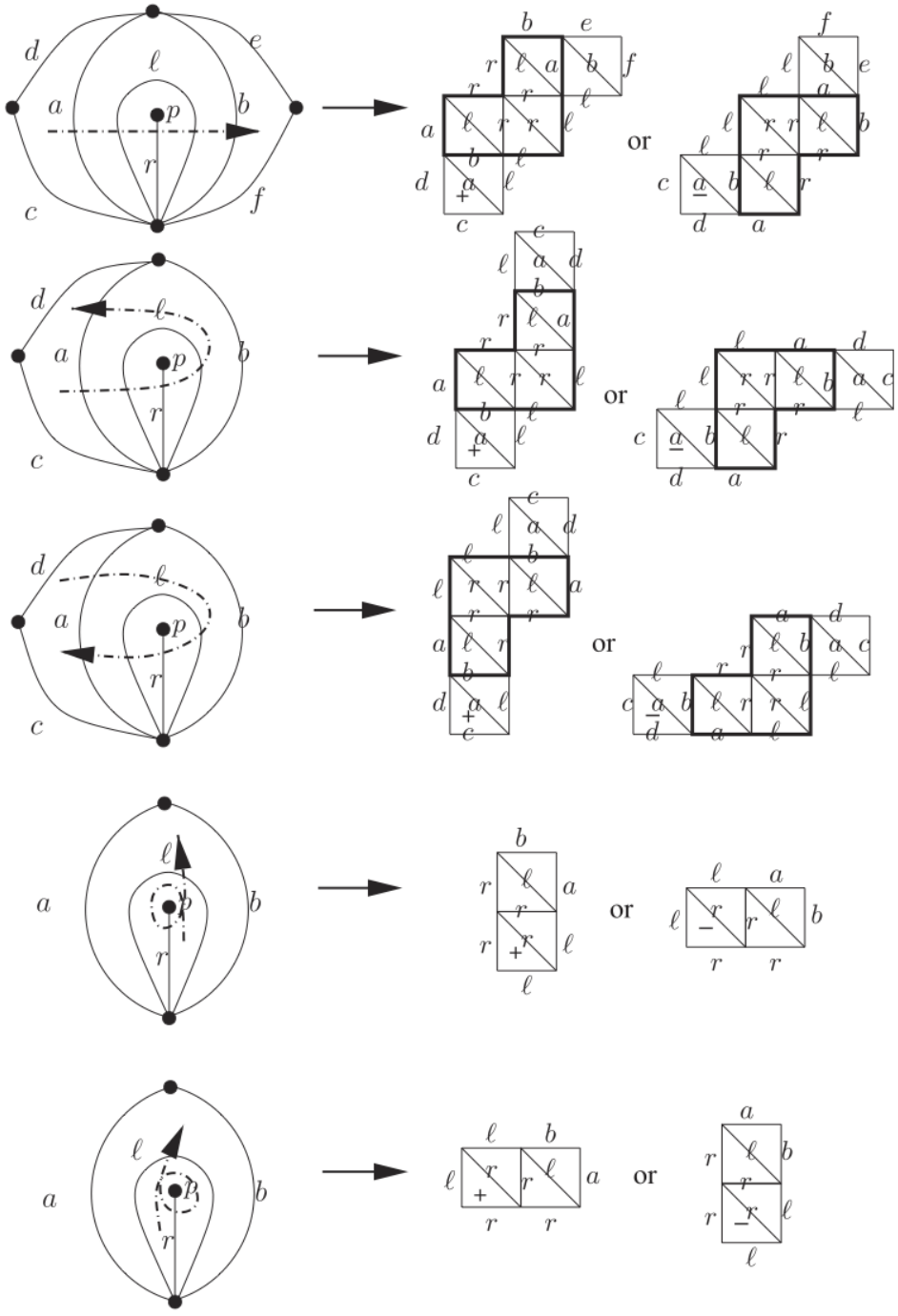

Figure 2.7: Possible triple tiles for crossing a self-folded triangulation [MW13, Fig. 3].

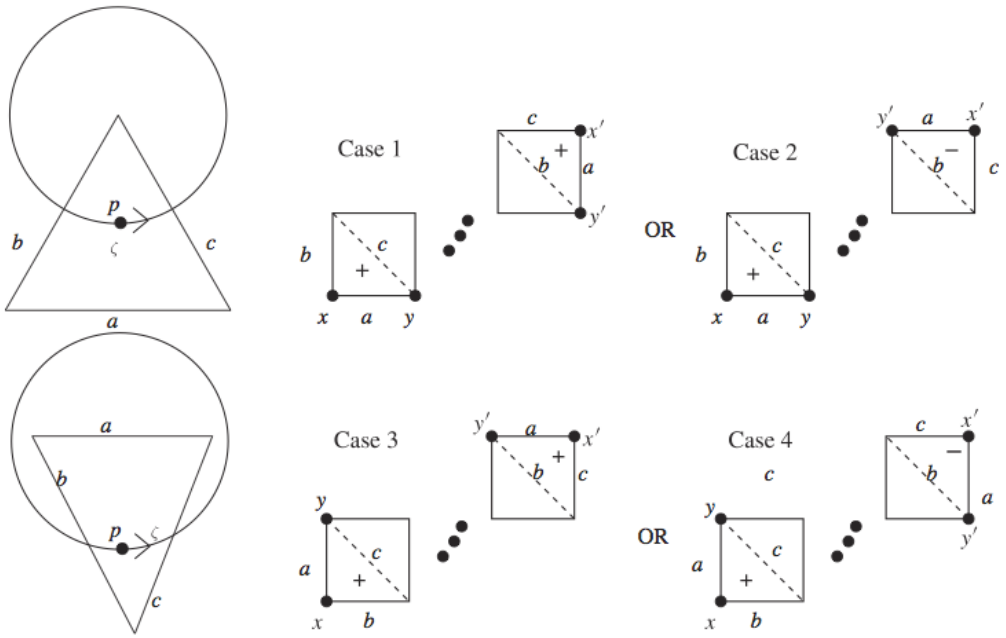

Figure 2.8: Left: triangle containing p along a closed loop ζ. Right: the corresponding band graph (with $x \sim x'$ and $y \sim y'$), depending on whether ζ crosses an odd or even number of arcs; the $+$ and $-$ symbols indicate the relative orientation of each tile [MSW13, Fig. 9].

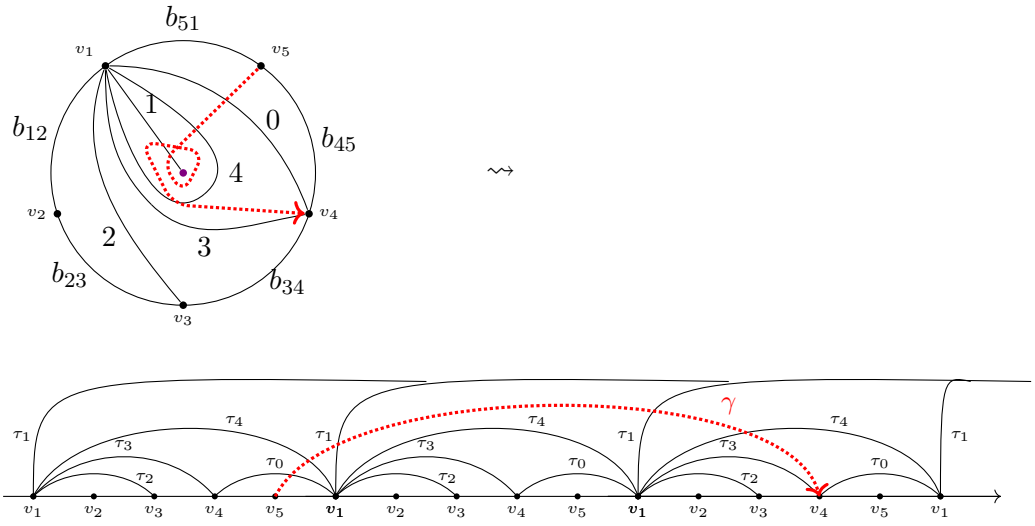

Figure 2.9: Top: An ideal triangulation T and a generalized arc γ of a once-punctured disk. Bottom: T drawn on a strip

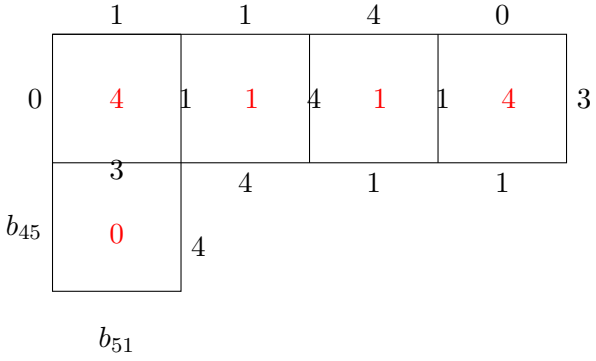

Figure 2.10: The snake graph corresponding to the generalized arc γ of Fig. 2.9.

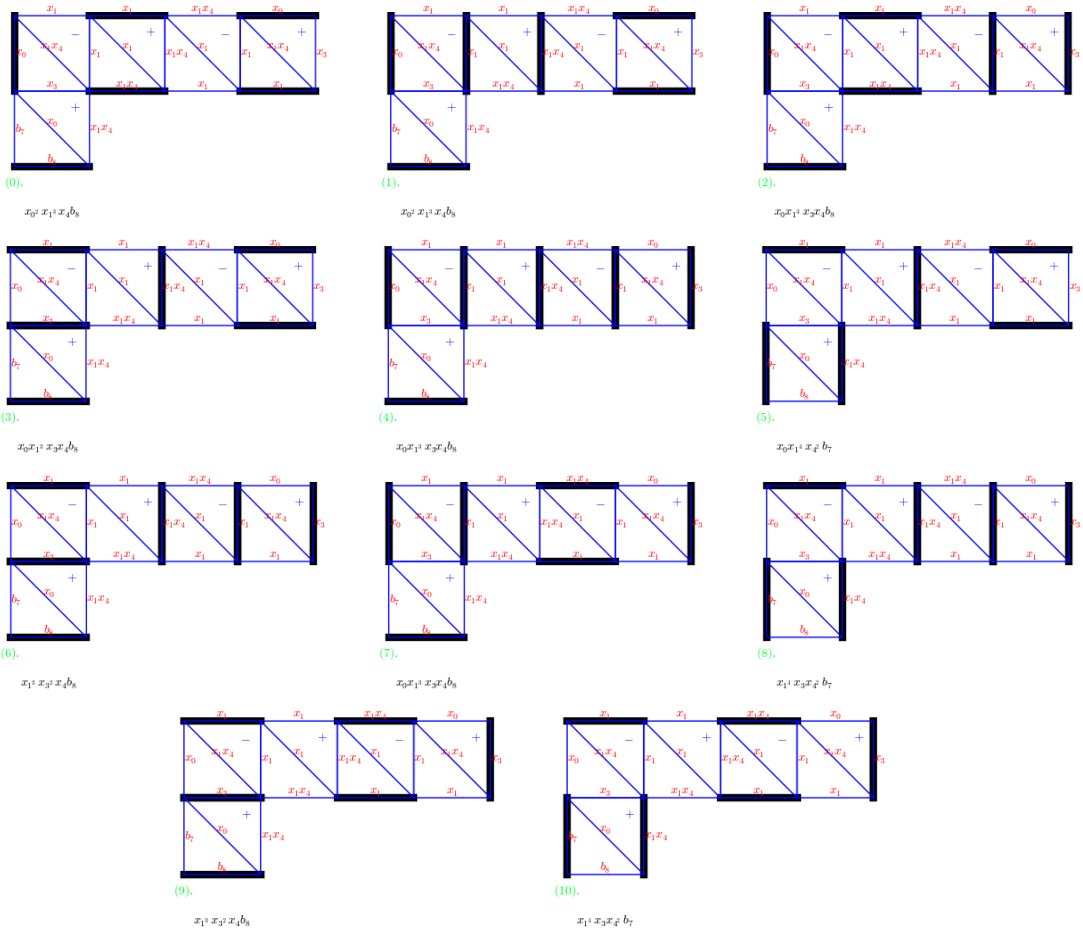

Figure 2.11: The 11 perfect matchings of the snake graph from Fig. 2.10, created using the help of SageMath [Dev16, SCc08]

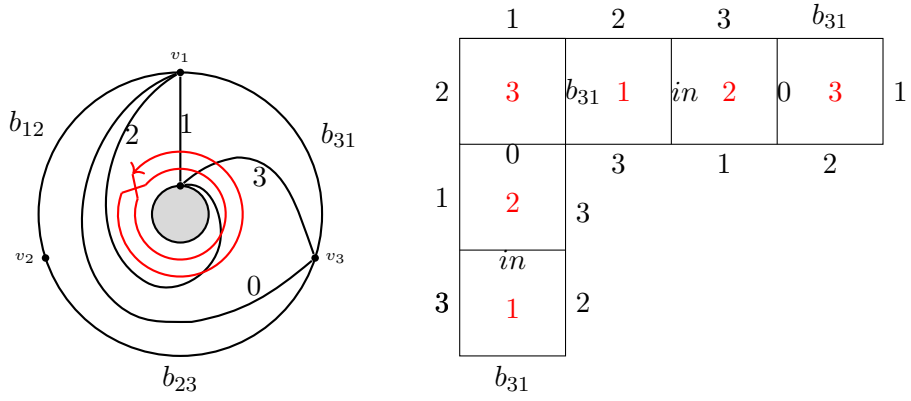

Figure 2.12: Left: An ideal triangulation T and the bracelet Brac_2. Right: Corresponding band graph $\widetilde{G}_\gamma$.

Chapter 3

Cluster algebraic interpretation of infinite friezes

3.1 Introduction

A *finite frieze* is an array of bi-infinite (infinite along the positive and negative x-axis) rows of positive integers, bounded above and below by a row of 1s, where the entries of the frieze satisfy a diamond relation. That is, for every diamond

$$\begin{array}{ccc} & c & \\ a & & b \\ & d & \end{array}$$

of entries in the frieze, the equation $ab - cd = 1$ is satisfied. We say that a frieze has period n if the rows repeat after n entries. Note that n may not be minimal.

If every entry in the frieze is a positive integer, then it is said to be a *frieze of positive integers*. Finite friezes of positive integers were first studied by Coxeter [Cox71], and then by Conway and Coxeter [CC73]. They showed that these patterns are invariant under a glide reflection, and give a bijection between finite friezes and triangulations of polygons.

The first non-trivial row (*i.e.*, the row following the row of 1s) of a frieze is called a *quiddity sequence*. The quiddity sequence defines a finite frieze, and the entries of

this row can be read off directly from a corresponding triangulation. The period n is the number of marked points on the boundary of the associated triangulated polygon. We label vertices $v_1, \ldots, v_n$ counter-clockwise around a triangulated polygon (we often write i for vertex v_i), and for each vertex v_i, the corresponding entry a_i in the quiddity sequence $(a_1, \ldots, a_n)$ is the number of triangles incident to i in T. See the following for an example.

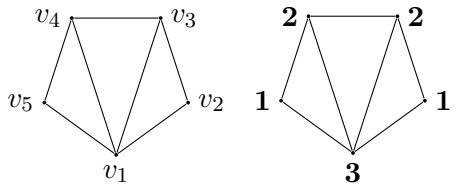

$$
\begin{array}{ccccccccccccccccc}
 & 1 & & 1 & & 1 & & 1 & & 1 & & 1 & & 1 & & \cdots \\
\cdots & & \mathbf{3} & & \mathbf{1} & & \mathbf{2} & & \mathbf{2} & & \mathbf{1} & & \mathbf{3} & & \mathbf{1} & \\
 & 2 & & 2 & & 1 & & 3 & & 1 & & 2 & & 2 & & \cdots \\
\cdots & & 1 & & 1 & & 1 & & 1 & & 1 & & 1 & & 1 &
\end{array}
$$

In [BCI74], Broline, Crowe, and Isaacs further studied the geometry of these finite frieze patterns associated to triangulated polygons. They found that every entry in such a frieze corresponds to a *matching number* associated to a diagonal in a triangulation T. A matching of vertices $v_{i_1}, \ldots, v_{i_r}$ "underneath" a diagonal is an r-tuple $(t_1, \ldots, t_r)$ of pairwise-distinct triangles in T, such that t_j is incident to vertex v_{i_j}. This motivated the work in Sections 3.7 and 3.8, where we present a bijection between these matchings (which we refer to as *BCI tuples*) and T-paths (as studied by [CP03, Sch08b, ST09]).

Caldero and Chapoton in [CC06] showed that finite frieze patterns appear in the context of cluster algebras of type A. Baur and Marsh in [BM09] used matching numbers to consider finite frieze patterns coming from triangulations of punctured disks, and thereby gave a definition of a finite frieze pattern corresponding to a cluster algebra of type D. See also [Sch08b] by Schiffler, for his study of the corresponding cluster category.

Infinite friezes (of positive integers) arising from triangulations of once-punctured disks were introduced and studied in [Tsc15] by Tschabold. A frieze is said to be *infinite* if it is not bounded below. Given an ideal triangulation T (in the sense of [FST08]) of a

once-punctured disk with n marked boundary points labeled $1, 2, \ldots, n$ counterclockwise around the boundary (note: this is the opposite to [Tsc15] convention), we can read off a quiddity sequence for the corresponding frieze pattern in a similar way, but now with some special rules on how to count self-folded triangles. See Fig. 3.1.

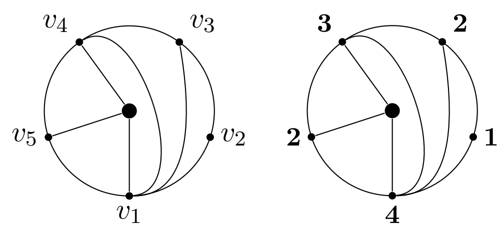

1 1 1 1 1 1 1 1 1 1

4 **1** **2** **3** **2** **4** **1** **2** **3** **2**

3 1 5 5 7 3 1 5 5 7 ···

··· 2 2 8 17 5 2 2 8 17 5

3 3 27 12 3 3 3 27 12 3

Figure 3.1: First level of an infinite frieze pattern corresponding to a punctured disk.

A finite frieze pattern that is associated to a triangulation of a polygon is said to be of type A, and an infinite frieze pattern is said to be of type D or type $\tilde{A}$, if is associated to a triangulation of a punctured disk or annulus, respectively. In [BPT16], Baur, Parsons, and Tschabold provide a complete classification of infinite frieze patterns. Other work on frieze patterns of type D and $\tilde{A}$ include [Smi15, BFPT16].

We study infinite friezes whose entries are Laurent polynomials (as opposed to positive integers). The first result (Theorem 3.3.1) of this chapter is a construction of an infinite frieze pattern where the entries of the frieze correspond to Laurent polynomials associated to generalized peripheral arcs. Once we have this frieze pattern of Laurent polynomials, we go on to describe nice symmetries and properties that this frieze pattern satisfies. We describe *progressions* of arcs in the frieze pattern, and *growth coefficients* of the frieze. These growth coefficients were first defined in [BFPT16], and are denoted by s_k, $k \in \mathbb{N}$. We provide a geometric interpretation of these growth coefficients, and show that they correspond to so-called *bracelets*, $Brac_k$, in the surface. Bracelets are

associated to important cluster algebra elements which have been studied by many, including [MW13, MSW13]. We then define *complementary arcs*, which are arcs between the same two vertices in a surface, but of alternate direction. Complementary arcs give rise to a special type of symmetry, which we call *complement symmetry*, in an infinite frieze. This complement symmetry reduces to glide-symmetry in a finite frieze pattern, because complementary arcs in an unpunctured surface give rise to the same entry (matching number/arc/Laurent polynomial) in a finite frieze. We state some algebraic and combinatorial results involving the relationship between complementary arcs. Our last result is a bijection between T-paths and the BCI matchings of vertices. This bijection preserves a natural distributive lattice structure which the T-paths are known to have.

The chapter is organized as follows: We first provide the background needed to present our results. In Sections 3.2.2 and 3.2.1, we recall some facts about infinite friezes, and explain how triangulations (of punctured disks and annuli) give rise to infinite friezes. Recall from Section 2.3 that we can define cluster algebra elements associated to generalized arcs and closed loops (with or without self-crossings) via snake graphs and band graphs, as per [MW13, MSW11, MSW13]. In Section 3.3, we state our first theorem, Theorem 3.3.1, and recall how to resolve crossings in multi-curves via skein relations (the cluster algebra element associated to a multi-curve obeys these skein relations [MW13]). We then use skein relations to prove our result. In Section 3.4, we state and prove our second result (Theorem 3.4.3); We present formulas which give relations between the entries in our (Laurent polynomial) friezes. We define a geometric interpretation of growth coefficients in Section 3.5. Section 3.6 then discusses geometrical relations, recursions, and symmetries among the entries in our friezes. Finally, in Section 3.7, we use T-paths to give a combinatorial formula for computing cluster algebra elements using BCI tuples. We discuss the lattice structure of the BCI tuples in Section 3.8.

3.2 Infinite frieze patterns

In this section, we review the definition of infinite frieze patterns.

3.2.1 Infinite friezes from once-punctured disks

Tschabold in [Tsc15] showed that triangulations of once-punctured disks give rise to periodic (positive integral) infinite friezes, and that infinite friezes arising in this way satisfy a certain arithmetic property. Baur, Parsons, and Tschabold showed in [BPT16] that all infinite friezes can be obtained via triangulations of surfaces, and non-periodic infinite friezes can be obtained via triangulations of an infinite strip in the plane. We will define and give examples of the arithmetic properties of infinite friezes arising from triangulations of punctured disks, and other properties of infinite friezes.

Definition 3.2.1. *An* infinite frieze $\mathcal{F}$ *of positive integers is an array* $(m_{ij})_{i,j\in\mathbb{Z},j\geq i}$ *of infinite rows with shifted entries, such that* $(i,i)=0$*, and* $(i,i+1)=1$*, and* $m_{ij}\in\mathbb{Z}_{>0}$ *for all* $i\leq j$*:*

$$\begin{array}{ccccccccccccc}
 & & 0 & & 0 & & 0 & & 0 & & 0 & & \\
\cdots & & 1 & & 1 & & 1 & & 1 & & 1 & \cdots & \\
 & & (-1,1) & & (0,2) & & (1,3) & & (2,4) & & (3,5) & & \\
 & \cdots & & (-1,2) & & (0,3) & & (1,4) & & (2,5) & & (3,6) & \cdots \\
 & & & & (-1,3) & & (0,4) & & (1,5) & & (2,6) & & (3,7) \\
 & & & & & & & \ddots & & & & \ddots &
\end{array}$$

satisfying the diamond rule, that is, for every diamond in $\mathcal{F}$ *of the form*

$$\begin{array}{ccc}
 & (i+1,j) & \\
(i,j) & & (i+1,j+1) \\
 & (i,j+1) &
\end{array}$$

the relation $(i,j)(i+1,j+1)-(i+1,j)(i,j+1)=1$ *is satisfied.*

We often omit the row of 0s when writing a frieze pattern, as they do not provide any additional information. The first non-trivial row of a frieze is called a *quiddity row.* If $\mathcal{F}$ is periodic with minimal period n, then we call the n-tuple $(a_1,\ldots,a_n)$ a *quiddity sequence.*

Just as finite friezes of type A_n correspond to triangulations of a polygon P_{n+3}, triangulations of the punctured disk D_n give rise to infinite friezes of positive integers

via matching numbers. Given a triangulation T of a punctured disk D_n, the quiddity sequence for the corresponding frieze pattern $\mathcal{F}_T$ is $(a_1, \ldots, a_n)$ where a_i is the number of ideal triangles incident to a vertex i, such that, if i is adjacent to a self-folded triangle, both the self-folded triangle and the triangle with an ℓ-loop as one of its three sides, are counted twice. See Fig. 3.2 for an example of counting adjacent triangles in both the self-folded and non-self folded cases.

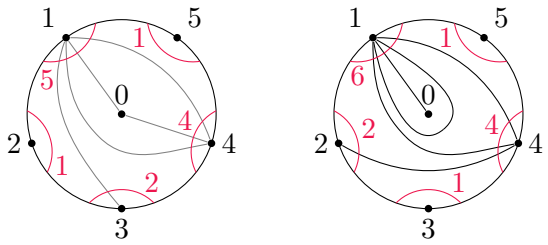

Figure 3.2: Counting triangles adjacent to marked boundary points in a triangulation (left), and in a triangulation with a self-folded triangle (right), of the punctured disk. Note that the self-folded triangle is counted twice for vertex 1 in the right-most figure.

Now that we have a way to read off the quiddity sequence from a triangulation, we can construct an infinite frieze pattern. The frieze pattern coming from the quiddity sequence of Fig. 3.2 (left) is given in Fig. 3.3. We write the $k\,n$-th, for $k \in \mathbb{N}$, rows of the frieze in bold.

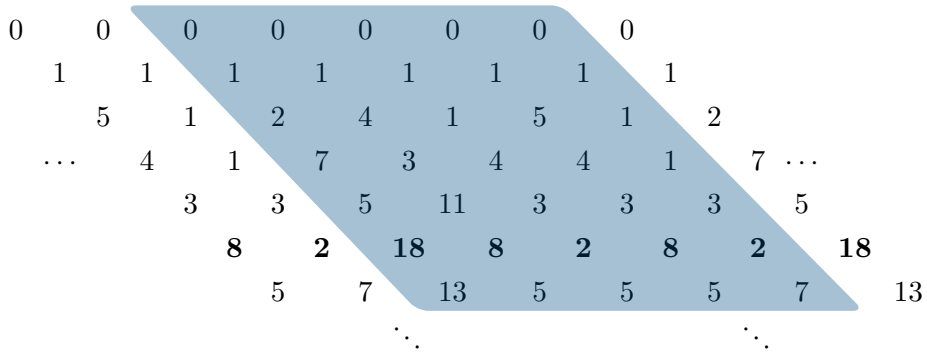

Figure 3.3: Infinite frieze with quiddity sequence $(2, 4, 1, 5, 1)$, with shaded fundamental region.

Theorem 3.2.2 (Thm. 3.6, 3.7, [Tsc15]). *Let T be a triangulation of a punctured disk D_n or an annulus $C_{n,m}$. Then the quiddity sequence $q_T = (a_1, \ldots, a_n)$ of T is a quiddity sequence of an infinite frieze $\mathcal{F}_T$ of period n.*

3.2.2 Infinite friezes from infinite strips

In [BPT16], the authors gave a complete characterization of infinite frieze patterns of positive integers via triangulations of an infinite strip in the plane. Periodic frieze patterns arise from triangulations of the annulus. We refer the reader to Lemma 3.6 of [BPT16] for a description on how to draw a triangulation of a punctured disk as an asymptotic triangulation in the annulus, but we provide an example in Fig. 3.4.

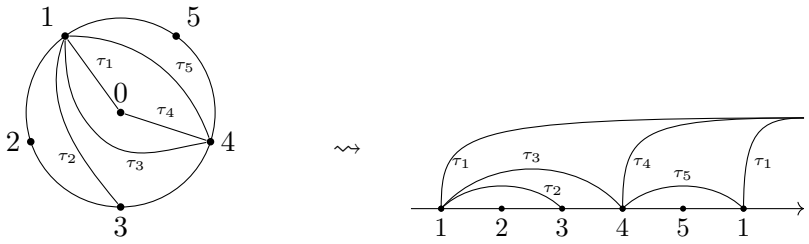

Figure 3.4: Triangulation of D_5 drawn as an asymptotic triangulation.

Consider a triangulation of the annulus $C_{n,m}$, where the outer boundary component has n marked points, and the inner boundary component has m marked points.

Both the outer boundary and inner boundary give a quiddity sequence, and thus an infinite frieze. Unless otherwise stated, we consider the quiddity sequence coming from the outer boundary of an annulus.

Definition 3.2.3 (Def. 3.8, [BPT16]). *Let $(a_1, \ldots, a_n)$ be the quiddity sequence of a periodic frieze. We say that $(a_1, \ldots, a_n)$ can be* realized (in an annulus) *if there is some $m \geq 0$ and a triangulation of $C_{n,m}$ such that $(a_1, \ldots, a_n)$ is the quiddity sequence of T.*

Let $\mathcal{U}$ be the universal cover as described in Section 3.3 of [BPT16]. Then every quiddity sequence can be realized in $\mathcal{U}$, and every triangulation of $\mathcal{U}$ gives rise to an infinite frieze (Theorem 5.2, [BPT16]). Every entry of these infinite friezes can still be described in terms of matching numbers.

Example 3.2.4. *Let T be the following triangulation of $\mathcal{U}$, and $\gamma(i,j)$ be the arc from i to j on the outer boundary ∂:*

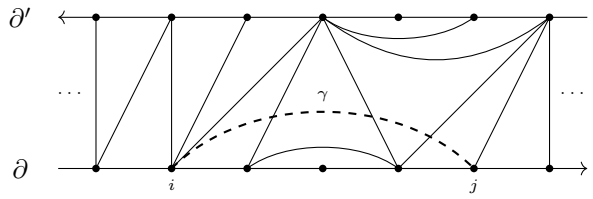

Then the arc $\gamma(i,j)$, corresponds to the (i,j)-th entry in the infinite frieze pattern arising from this triangulation.

We can even consider non-periodic triangulations of an infinite strip. Starting with such a triangulation, we can read of the matching numbers for each set of marked points (i,j) and we obtain a frieze pattern in this way.

3.3 Infinite friezes of cluster algebra elements

Our first result is the construction of infinite frieze patterns consisting of certain elements of a cluster algebra arising from (S,M) with boundary.

Theorem 3.3.1. *Let T be an ideal triangulation of a punctured disk or an annulus, and let $\mathcal{A} = \mathcal{A}(B_T)$ be the coefficient-free cluster algebra associated to B_T. Let Bd be a boundary component with n marked points, where $n \geq 2$. Then the Laurent polynomials corresponding to generalized peripheral arcs on Bd form an infinite frieze pattern.*

Before we prove the theorem, we recall *skein relations*, and the related terminology.

Definition 3.3.2. *A* multicurve *is a finite multiset of generalized arcs and closed loops such that there are only a finite number of pairwise crossings among the collection. A multicurve is said to be* simple *if there are no pairwise crossings among the collection, and no self-crossings.*

Now if a multicurve is not simple, then there are two ways to resolve a crossing so that we obtain a multicurve that no longer contains crossings. This process is known as *smoothing*:

Definition 3.3.3. *Let γ, γ_1, and γ_2 be generalized arcs or closed loops such that we have one of the following two cases:*

1. *γ_1 crosses γ_2 at a point c, or*

2. *γ has a self-crossing at a point c.*

Then we let C be the multicurve $\{\gamma_1, \gamma_2\}$ or $\{\gamma\}$ depending on which of the two cases we are in. We define the smoothing of C at the point x *to be the pair of configurations C_+ and C_-. The multicurve C_+ (respectively, C_-) is the same as C except for the local change that replaces the (self-)crossing $\times$ with the pair of segments $\cup\!\!\cap$ (resp., $\supset\!\subset$). See Fig. 3.5.*

Figure 3.5: Skein relation for ordinary arcs

Theorem 3.3.4 ([MW13, Props. 6.4,6.5,6.6 and Cor. 6.18])**.** *Let (S, M) be a marked surface, with or without punctures. Let C, C_+, C_- be as in Definition 3.3.3. Then we have the following identity in $\mathcal{A}_\cdot(B_T)$:*

$$x_C = x_{C_+} + x_{C_-},$$

We now look at an example of resolving a crossing using skein relations:

Example 3.3.5. *Consider the generalized arc $\gamma(2, 9)$ in the annulus. Using skein relations, we get that the Laurent polynomial $x(\gamma(2, 9))$ corresponding to $\gamma(2, 9)$ is the sum*

$$x(\gamma(4, 7)) \; + \; x(\gamma(2, 4))\, x(Brac_1).$$

See Fig. 3.6.

The proof that the generalized (ordinary) arcs form an infinite frieze pattern now follows easily from the skein relation.

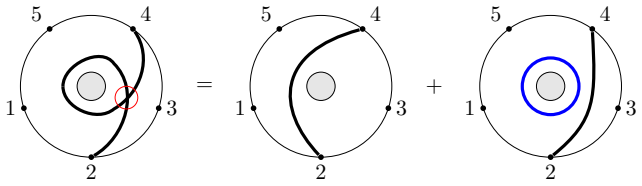

Figure 3.6: Resolving a self-crossing.

Proof of Theorem 3.3.1. Let Bd be a boundary component of a once-punctured disk or an annulus, drawn as a strip. We construct an array $\mathcal{F}$ corresponding to the set of all generalized arcs that are peripheral on Bd as follows: The entries of $\mathcal{F}$ are indexed by (i, j), $i \leq j \in \mathbb{Z}$ such that our labeling convention is the same as in Definition 3.2.1.

Set the entry at (i, i) to be 0. Now for every entry (i, j), $i < j$, we consider the (generalized) peripheral arc $\gamma(i, j)$ from a marked point i to another marked point j on Bd, following the orientation of the surface. We let the entry (i, j) of $\mathcal{F}$ be the Laurent polynomial $x(\gamma(i, j))$ corresponding to the generalized arc $\gamma(i, j)$ (see Definition 2.3.11). Note that $\gamma(i, i + 1)$ is a boundary edge, so $x(\gamma(i, i + 1)) = 1$ by definition.

To show that $\mathcal{F}$ is a frieze pattern, we need to check that for every diamond

$$\begin{array}{ccc} & b & \\ a & & d \\ & c & \end{array}$$

in $\mathcal{F}$, the equation $ad - bc = 1$ is satisfied.

From the labeling convention, every diamond in $\mathcal{F}$ has the form

$$\begin{array}{ccc} & (i+1, i+m) & \\ (i, i+m) & & (i+1, i+m+1) \\ & (i, i+m+1) & \end{array}$$

where $m \in \mathbb{N}$. We want to show that $(i, i+m)(i+1, i+m+1) = 1 + (i+1, i+m)(i, i+m+1)$.

Consider the arcs $\gamma(i, i+m), \gamma(i+1, i+m+1)$ drawn in the universal cover of our surface (Fig. 3.7, top). The arcs $\gamma(i, i+m), \gamma(i+1, i+m+1)$ have exactly one crossing

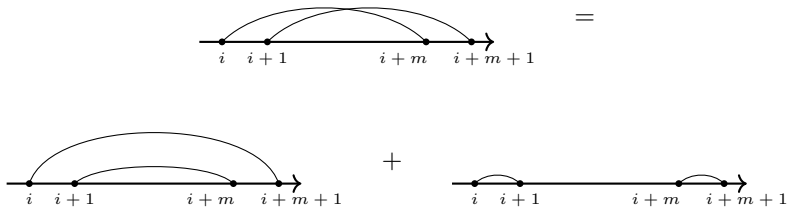

Figure 3.7: Applying skein relations to prove Theorem 3.3.1

point. Using the skein relations (Theorem 3.3.4), we have that

$$\begin{aligned} x(\gamma(i,i+m))\,x(\gamma(i+1,i+m+1)) =& x(\gamma(i,i+1))\,x(\gamma(i+m,i+m+1)) \\ &+ x(\gamma(i+1,i+m))\,x(\gamma(i,i+m+1)) \\ =& 1 + x(\gamma(i+1,i+m))\,x(\gamma(i,i+m+1)). \end{aligned}$$

This holds for every diamond in our pattern, and thus we have constructed a frieze pattern of Laurent polynomials corresponding to the set of all generalized peripheral arcs of Bd. □

3.4 Progression formulas

In Section 3.3, we constructed infinite frieze patterns of Laurent polynomial entries. In this section, we present formulas governing relations among these entries. These generalize the relations given in [BFPT16], in the sense that [BFPT16, Thm. 2.5] is a special case of the formulas.

3.4.1 Complementary arcs

Definition 3.4.1 (complementary arc)**.** *Let $\gamma_k(i,j)$ be the generalized peripheral arc in $C_{n,m}$ or D_n starting at marked point i and finishing at marked point j with $k-1$ self-crossings such that the boundary Bd is to the right of the curve as we trace it. We define the arc* complementary *to γ_k to be the generalized arc starting at marked point j and finishing at marked point i with $k-1$ self-crossings following the orientation of the surface. See Fig. 3.8. Let γ_k^C denote the arc complementary to γ_k.*

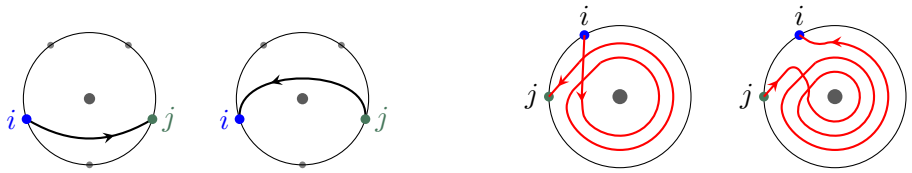

Figure 3.8: Examples of complementary arcs γ_1, γ_1^C and γ_3, γ_3^C.

Remark 3.4.2. *It is well-known that a finite frieze pattern has a so-called glide-symmetry. In an infinite frieze pattern $\mathcal{F}$, we don't have a glide-symmetry, but instead we have what we call a* complement-symmetry *along with the translation-symmetry. See Fig. 3.9 for an example. Note that each rn-th row ($r \in \mathbb{N}$) of $\mathcal{F}$ corresponds to self-complementary generalized arcs.*

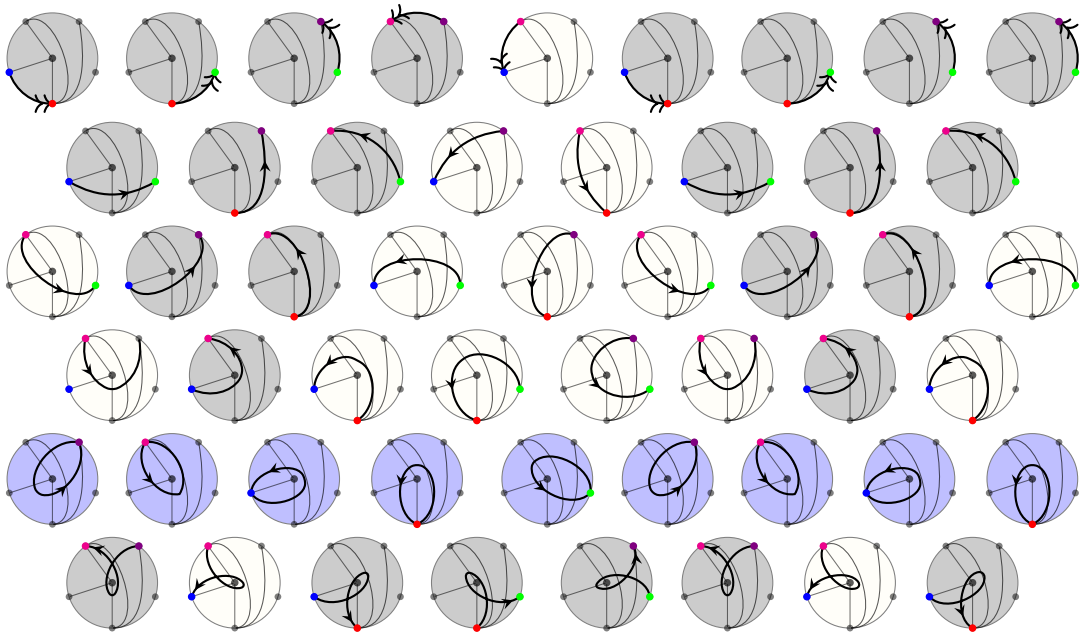

Figure 3.9: Symmetry of complementary arcs.

Theorem 3.4.3. *Let γ_1 be a peripheral arc or a boundary edge of (S, M) starting and finishing at points i and j. For $k = 1, 2, \ldots$ and $1 \leq m \leq k-1$, we have*

$$x(\gamma_k) = x(\gamma_m)x(Brac_{k-m}) + x(\gamma^C_{k-2m+1}).$$

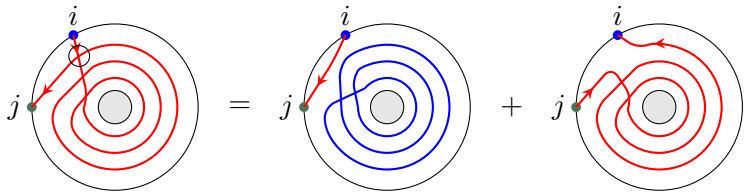

Figure 3.10: Case $m = 1$: By the progression formula (Theorem 3.4.3), we have $x(\gamma_4) = x(\gamma_1)x(Brac_3) + x(\gamma_3^C)$

For $r \geq 0$, γ_{-r}^C is defined to be the curve γ_{r+1} with a kink, so that $x(\gamma_{-r}^C) = -x(\gamma_{r+1})$. See Fig. 3.10.

Remark 3.4.4. *Special cases of above theorem are when $m = 1$ and $m = k - 1$. We have*

$$x(\gamma_k) = x(\gamma_1)x(Brac_{k-1}) + x(\gamma_{k-1}^C), \tag{3.4.1}$$

$$x(\gamma_k) = x(\gamma_{k-1})x(Brac_1) - x(\gamma_{k-2}) \tag{3.4.2}$$

Compare (3.4.2) with [BFPT16, Thm. 2.5].

If γ_1 is the boundary edge between i and $i + 1$, then $x(\gamma_1) = 1$, so

$$x(Brac_{k-1}) = x(\gamma_k) - x(\gamma_{k-1}^C). \tag{3.4.3}$$

3.4.2 Proof of Theorem 3.4.3

Let $\gamma_k := \gamma_k(i, j)$. We draw γ_k so that first it goes close to the other boundary (or the puncture) then spirals out.

In the strip covering, we draw the boundary Bd as the horizontal bottom line so that, in each frame, i is drawn to the left of j. We draw each representative of γ_k as follows. We start at a frame Reg_0. Starting from a vertex labeled i, our pencil goes north, passing all $k - 1$ crosses. When we get to the very north, we turn southeast, and finishes at a vertex labeled j, which is located in the frame $k - 1$ frames east of Reg_0. See Fig. 3.11.

Order the crossings of γ_k so that the first crossing is the one closest to Bd and the $(k-1)$-th crossing is the one furthest away from Bd. In each frame, consider the m-th crossing c of γ_k. Denote the segments meeting at c by $north_c$, $south_c$, $east_c$, and $west_c$, so that $north_c$ is the segment drawn north of c, $east_c$ is the segment drawn east of c, et cetera.

If we resolve all representatives of the m-th crossing c by glueing $north_c$ with $west_c$ as well as glueing $south_c$ with $east_c$, we get two curves, γ_m and $Brac_{k-m}$. This explains the first summand of Theorem 3.4.3. The following Lemma explains the second summand of Theorem 3.4.3.

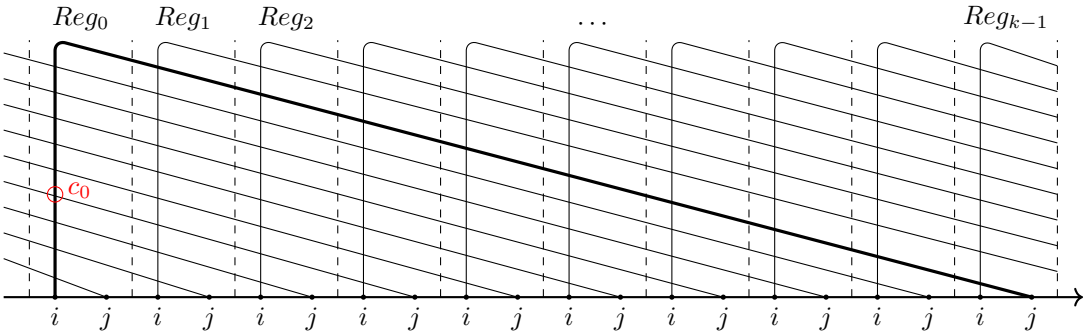

Figure 3.11: Lift of γ_k for $k = 10$, $m = 4$ drawn on the strip.

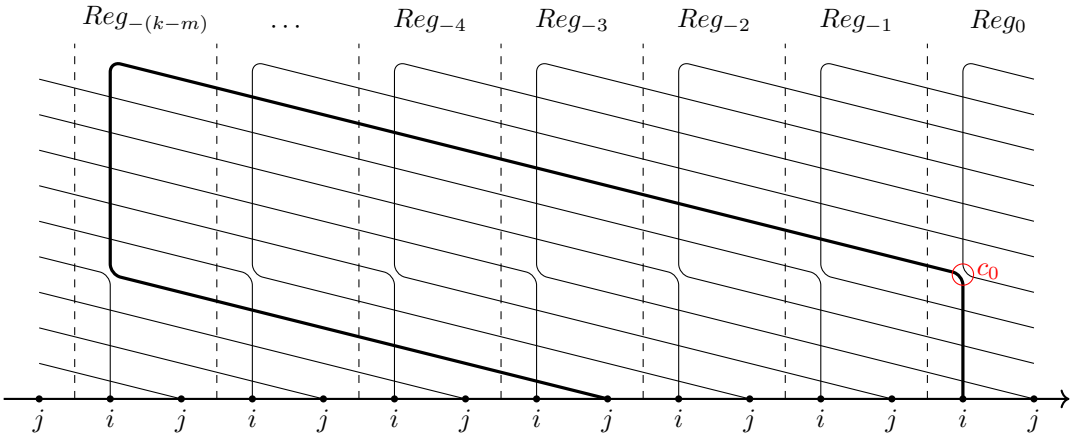

Figure 3.12: Lift of γ^C_{k-2m+1} for $k = 10$, $m = 4$ drawn on the strip.

Lemma 3.4.5. *Suppose we have the same setup as above for γ_k. Suppose we resolve all representatives of the m-th crossing c by glueing $north_c$ with $east_c$ as well as glueing*

$south_c$ with $west_c$. Then we get one curve, γ^C_{k-2m+1}. See Fig. 3.12.

Proof of Lemma 3.4.5. Our pencil starts at Reg_0 at the starting vertex i and heads north. Let c_0 denote the m-th crossing of γ_k at frame Reg_0. When we get to c_0, since the segment $south_{c_0}$ is glued to $west_{c_0}$, we pivot west of c_0. As we trace $west_{c_0}$ with our pencil, we pass through $k-m$ other frame west of Reg_0, denoted $Reg_{-1}, \ldots, Reg_{-(k-m)}$. When we get to $Reg_{-(k-m)}$, the curve bends south (because this is how we've chosen to draw γ_k). As our pencil traces south, we hit the m-th crossing c' in $Reg_{-(k-m)}$. Because we have glued $north_{c'}$ with $east_{c'}$, we bends east at c'.

Since this crossing is the m-th crossing closest to Bd, there are $m-1$ (possibly $m-1=0$) other crossings beneath it closer to Bd. Therefore, our pencil will end (at a representative of the vertex j) when we get to the frame that is $m-1$ frames away east of $Reg_{-(k-m)}$.

We consider the three possibilities: $k-m > m-1$ or $k-m = m-1$ or $k-m < m-1$. If $k-m > m-1$, we end at the frame $Reg_{-(k-m)+(m-1)} = Reg_{-(k-2m+1)}$, which we have passed earlier. Hence we have traced the curve γ^C_{k-2m+1}.

If $k-m = m-1$, we end at the original frame Reg_0, and we cross our pencil mark exactly once before ending at j. Hence we have traced the curve γ_1 with a kink. By definition, this curve is γ^C_0

If $k-m < m-1$, we pass Reg_0, crossing our pencil mark exactly once before continuing to another frame east of Reg_0. We end our drawing at a frame that is $m-1-(k-m) = -k+2m-1$ frames away east of Reg_0. Denote this frame $Reg_{(-k+2m-1)}$. Hence we have traced the curve $\gamma_{(-k+2m)}$ with a kink. By definition, this curve is γ^C_{k-2m+1}. □

3.5 Bracelets and Growth coefficients

The following tells us that the difference between the non-trivial entries directly above/below one another in the rows $n+1$ and $n-1$ in an n-periodic frieze is constant. (Note that the entries in row $n+1$ are the first row in the 2nd level and entries in row $n-1$ are the penultimate entries in the 1st level of the frieze.)

Proposition 3.5.1 (Analog of [BFPT16, Thm. 2.2])**.** *Let $\mathcal{F} = (i,j)_{i,j}$ be a periodic*

frieze pattern as described in Section 3.3. For all $i \in \mathbb{Z}$, we have

$$x(Brac_1) = x(\gamma(i, i+1+n)) - x(\gamma(i+1, i+n))$$

Proof. Let Bd be the boundary corresponding to $\mathcal{F}$, with n marked points. Let $i \in \mathbb{Z}$ and suppose γ_1 is the boundary edge from i to $i+1$ (taken modulo n). Then γ_2 corresponds to the entry $(i, i+1+n)$ and γ_1^C corresponds to the entry $(i+1, i+n)$. Due to (3.4.4), where $k = 2$, we have

$$x\left(Brac_1\right) = x\left(\gamma_2\right) - x\left(\gamma_1^C\right) = x\left(\gamma(i, i+1+n)\right) - x\left(\gamma(i+1, i+n)\right).$$

□

Remark 3.5.2. *In general, per (3.4.4), for $k \leq 1$ we have*

$$x(Brac_k) = x(\gamma_{k+1}) - x(\gamma_k^C) = x\left((i, i+1+kn)\right) - x\left((i+1, i+kn)\right) \tag{3.5.1}$$

for all $i \in \mathbb{Z}$. To see this, observe that, if γ_1 is the boundary edge from i to $i+1$ (taken modulo n), then γ_{k+1} corresponds to the entry at position $(i, i+1+kn)$ and γ_k^C corresponds to the entry at position $(i+1, i+kn)$.

3.5.1 Growth coefficients

Following [BFPT16, Def. 2.3], we now introduce the notion of *growth coefficients*.

Definition 3.5.3. *Let $\mathcal{F} = (m_{i,j})_{i,j}$ be a periodic frieze pattern as described in Section 3.3. Let n be the number of marked points on the outer boundary of the associated triangulated surface. For $k \geq 0$, the* kth growth coefficient *for $\mathcal{F}$ is given by $s_0 := 2$, and $s_k := m_{i,i+1+kn} - m_{i+1,i+kn}$, otherwise. In particular, we say that s_1 is the* principal growth coefficient *for $\mathcal{F}$.*

Remark 3.5.4. *Per Remark 3.5.2, $s_k = x(Brac_k)$ whenever $k \geq 1$, so we can use the two terms interchangeably.*

To see that $s_0 = 2$ makes sense in the frieze, see Fig. 3.13. We write in the row of 0s and then add a row of -1s above the row of 0s. Then $s_0 = 1 - (-1) = 2$.

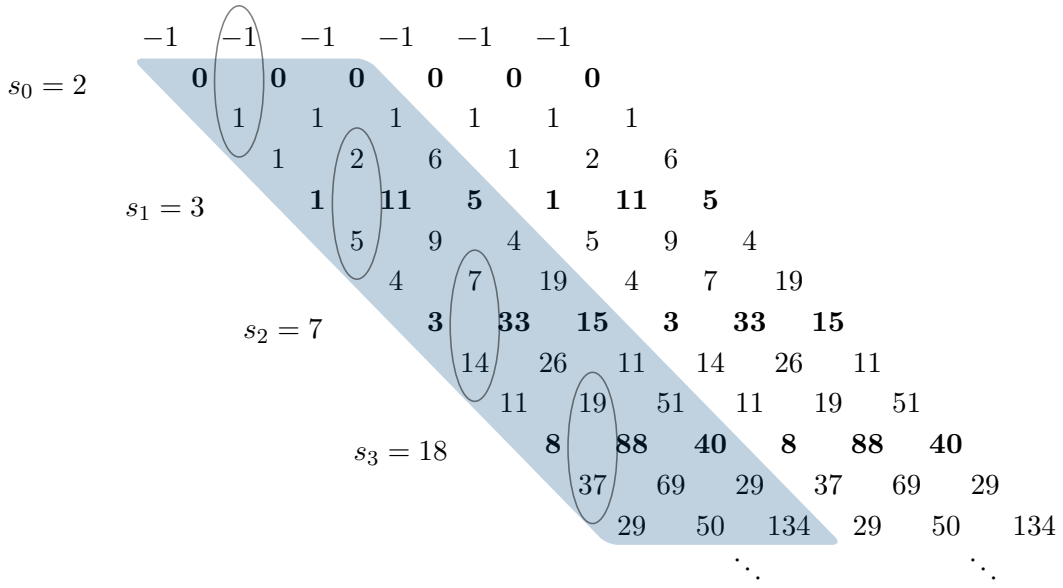

Figure 3.13: Growth coefficients in the frieze with quiddity sequence $(1, 2, 6)$.

In the case where $\mathcal{F}$ is an infinite frieze arising from a triangulation of a punctured disk, this common difference is equal to 2 for all k. This is *only* true for infinite friezes arising from triangulations of punctured disks.

Proposition 3.5.5 ([BFPT16, Cor. 3.8])**.** *Given a periodic infinite frieze that is realizable in the annulus but not in a punctured disk, we have $s_k > 2$ for all $k > 0$.*

Growth coefficients are also recursively related to each other, as seen in the following proposition.

Proposition 3.5.6 (Prop. 2.10, [BFPT16])**.** *Let $\mathcal{F} = \{(m_{i,j})\}_{i,j}$ be a periodic infinite frieze of positive integers. Then we have that $s_{k+2} = s_1 s_{k+1} - s_k$, for $k \geq 0$.*

As previously mentioned, given a triangulation of an annulus, we may get two different quiddity sequences q and $\overline{q}$ from the outer and inner boundaries, respectively. It turns out that $s_q = s_{\overline{q}}$ (Theorem 3.4, [BFPT16]).

Remark 3.5.7. *The progression formulas (Theorem 3.4.3) give us a way to compute entries on lower levels using the growth coefficients and entries on previous levels. Define*

$m(\gamma)$ to be the integer obtained from $x(\gamma)$ by specializing all the x_{τ_i} to 1. We demonstrate (3.4.1) on the frieze pattern in Fig. 3.14. Consider the underlined entry 5 (in the dotted

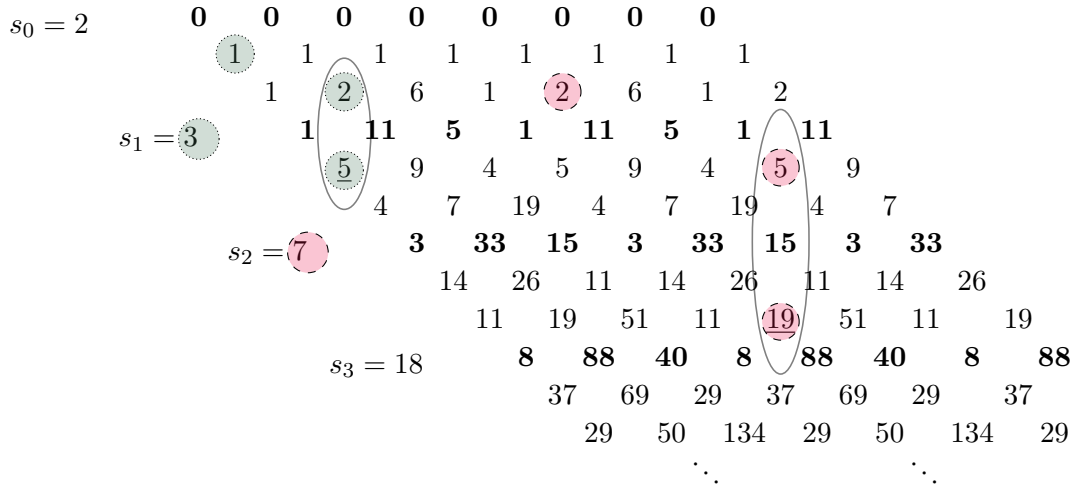

Figure 3.14: Computing entries in an infinite frieze pattern with quiddity sequence $(1, 2, 6)$

circle) on the fifth row and first column, which corresponds to the γ_2 for some boundary edge γ_1. This 5 is equal to $s_1\, m(\gamma_1) + m(\gamma_1^C) = 3(1) + 2$. Similarly, we compute the underlined entry $19 =: m(\gamma_3)$ which is equal to $s_2\, m(\gamma_1) + m(\gamma_2^C) = 7(2) + 5$. We can do this for every entry in a frieze pattern.

3.5.2 Chebyshev polynomials

We now recall some basic facts about Chebyshev polynomials (Section 2.5 of [MSW13]).

Definition 3.5.8 ([MSW13, Def. 2.33])**.** *Let T_k denote the k-th normalized Chebyshev polynomial defined by*

$$T_k\left(t + \frac{1}{t}\right) = t^k + \frac{1}{t^k}$$

Proposition 3.5.9 ([MSW13, Prop. 2.34])**.** *The normalized Chebyshev' polynomials $T_k(x)$ defined above can also be uniquely determined by the initial conditions $T_0(x) = 2$,*

$$\begin{aligned} T_0(x) &= 2 \\ T_1(x) &= x \\ T_2(x) &= x^2 - 2 \\ T_3(x) &= x^3 - 3x \\ T_4(x) &= x^4 - 4x^2 + 2 \\ T_5(x) &= x^5 - 5x^3 + 5x^2 \\ T_6(x) &= x^6 - 6x^4 + 9x^2 - 2 \end{aligned}$$

Table 3.1: The normalized Chebyshev polynomials $T_k(x)$ for small k.

$T_1(x) = x$, *and the recurrence*

$$T_k(x) = xT_{k-1}(x) - T_{k-2}(x).$$

Note that $T_k(x)$*'s can also be written as* $2Cheb_k(x/2)$*, where* $Cheb_k(x)$ *denotes the usual Chebyshev polynomial of the first kind, which satisfies* $Cheb_k(\cos x) = \cos(kx)$.

Table 3.1 shows the first few normalized Chebyshev polynomials.

The elements associated to the bracelets (Definition 2.3.14) satisfy the normalized Chebyshev polynomials.

Proposition 3.5.10 ([MSW13, Prop. 4.2])**.** *We have*

$$X_{Brac_k} = T_k(X_{Brac_1}),$$

where T_k *denotes the* k*th normalized Chebyshev polynomial.*

Remark 3.5.11. *Suppose* $Brac_1$ *is a closed loop without self-crossings enclosing a single puncture. Since* $X_{Brac_1} = 2$ *(per Remark 2.3.15),* $T_k(2) = 2$ *for all* $k \geq 0$ *(per Proposition 3.5.9), and* $X_{Brac_k} = T_k(X_{Brac_1})$ *(per Proposition 3.5.10), we have*

$$X_{Brac_k} = 2 \text{ for all } k \geq 0.$$

In particular, if (S, M) *is a once-punctured disk, all bracelets are associated* 2.

3.6 Recursive relationships

3.6.1 Difference between complementary arcs

We consider the difference between complementary arcs of two marked points. For punctured disk, this difference is constant across levels and is determined by the two marked points. For the annulus, this difference is determined by the level as well as the end points. Recall from Definition 3.5.3, that $s_k := m_{i,i+1+kn} - m_{i+1,i+kn}$ is the kth growth coefficient of a frieze $\mathcal{F}$.

Proposition 3.6.1. *Let $\mathcal{F}$ be a frieze pattern coming from a triangulation of a once-punctured disk or annulus. Let $\gamma_1 = \gamma$ be an ordinary arc from i to j or a boundary edge from i to $i+1$. Define $c_{k,\gamma} := x\left(\gamma_k^C\right) - x\left(\gamma_k\right)$ to be the difference between the complementary arcs γ_k^C and γ_k on level k of $\mathcal{F}$. (We write $c_k := c_{k,\gamma}$ since γ is understood.) Then we have the following relations for $k > 1$:*

(1) $c_k = (s_{k-1} - s_{k-2})c_1 + c_{k-2}$, *where we define $c_0 = c_1$;*

(2)

$$c_k = \begin{cases} c_1 \left(1 + \sum_{i=0}^{k-1} (-1)^{i+1} s_i\right) & \text{for } k \text{ even, and} \\ c_1 \left(1 + \sum_{i=1}^{k-1} (-1)^{i} s_i\right) & \text{for } k \text{ odd,} \end{cases}$$

where $c_1 = x(\gamma_1^C) - x(\gamma_1)$ is computed from the triangulation or the frieze.

Note that in the case of the punctured disk, since $s_i = 2$ for all i, the formula reduces to $c_k = c_1$ for all $k > 1$.

Proof. Per (3.4.1), we have $\gamma_k = s_{k-1}\, x(\gamma_1) + x(\gamma_{k-1}^C)$ and $x(\gamma_{k-1}^C) = s_{k-2}\, x(\gamma_1^C) + x(\gamma_{k-2})$. So $x(\gamma_k) = s_{k-1}\, x(\gamma_1) + s_{k-2}\, x(\gamma_1^C) + x(\gamma_{k-2})$. We get a similar equation $x(\gamma_k^C) = s_{k-1}\, x(\gamma_1^C) + s_{k-2}\, x(\gamma_1) + x(\gamma_{k-2}^C)$. Subtracting the two gives us (1).

Part (2) is proved by induction. For $k = 1$, we get that $c_1 = c_1$, and for $k = 2$, $c_2 = (s_1 - s_0)\, c_1 + c_0 = (s_1 - s_0)\, c_1 + c_1 = c_1 \left((-1)^2 s_1 + (-1)^1 s_0 + 1\right) = c_1 \left(\sum_{i=0}^{1} (-1)^{i+1} s_i + 1\right)$ by (1). Assume (2) holds for some n. If n is even, then $n+1$

is odd, and

$$\begin{aligned} c_{n+1} &= (s_n - s_{n-1})c_1 + c_{n-1} \\ &= c_1\left((-1)^n s_n + (-1)^{n-1}s_{n-1}\right) + c_1\left(\sum_{i=1}^{n-2}(-1)^i s_i + 1\right) \\ &= c_1\left(1 + \sum_{i=1}^{n}(-1)^i s_i\right). \end{aligned}$$

Similarly, if n is odd, then $n+1$ is even, and we have

$$\begin{aligned} c_{n+1} &= (s_n - s_{n-1})c_1 + c_{n-1} \\ &= c_1\left((-1)^{n+1} s_n + (-1)^n s_{n-1}\right) + c_1\left(\sum_{i=0}^{n-2}(-1)^{i+1} s_i + 1\right) \\ &= c_1\left(\sum_{i=0}^{n}(-1)^{i+1} s_i + 1\right). \end{aligned}$$

Thus the result holds true for all n. □

3.6.2 Arithmetic progressions

Friezes coming from triangulations of punctured disks satisfy a beautiful arithmetic property. Consider the frieze $\mathcal{F}_T$ in Fig. 3.15, where T is a triangulation of D_5; when jumping 5 steps along any diagonal in $\mathcal{F}_T$, we get a sequence of numbers that with a *common difference*. Thus these sequences of numbers form an increasing arithmetic progression (see Def. 3.10 of [Tsc15]). In Fig. 3.15, the dotted and dashed circles show examples of two 5-arithmetic progressions in the frieze.

Theorem 3.6.2 ([Tsc15, Thm. 3.11])**.** *Every n-periodic infinite frieze $\mathcal{F}_T$ associated to a triangulation T of D_n is n-arithmetic.*

The following is an analog of Theorem 3.6.2.

Proposition 3.6.3 (Corollary of Theorem 3.4.3)**.** *Suppose (S, M) is a once-punctured disk. Let γ_1 be an ordinary arc of (S, M) from i to j (possibly $j = i + 1$ or $j = i$, so*

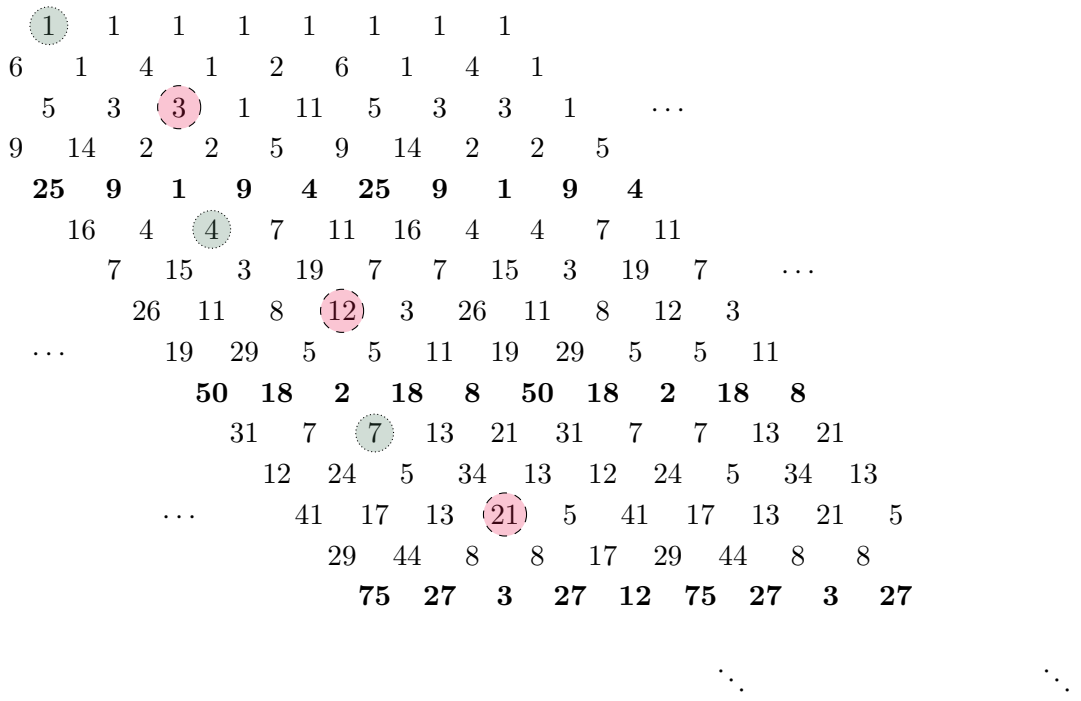

Figure 3.15: Arithmetic progression in a frieze. The dotted and dashed circles show two different arithmetic progressions. The dotted circles have a common difference of 3, the dashed circles of 9.

that γ_1 is a boundary edge, with $x(\gamma_1) = 1$). Then

$$x(\gamma_k) = x(\gamma_{k-1}) + \big(\ x(\gamma_1) + x(\gamma_1^C)\ \big)$$

Proof of proposition 3.6.3. We prove this by induction on k.

First, we have

$$\begin{aligned} x(\gamma_2) &= x(\mathrm{Brac}_1)\ x(\gamma_1) + x(\gamma_1^C) \text{ by Remark 3.4.4} \\ &= 2\ x(\gamma_1) + x(\gamma_1^C) \text{ by Remark 3.5.11} \\ &= x(\gamma_1) + \big(\ x(\gamma_1) + x(\gamma_1^C)\ \big) \text{ by, again, Remark 3.4.4.} \end{aligned}$$

Similarly, $x(\gamma_2^C) = x(\gamma_1^C) + \big(\ x(\gamma_1) + x(\gamma_1^C)\ \big)$.

Next, suppose we have $x(\gamma_k) = x(\gamma_{k-1}) + \big(\ x(\gamma_1) + x(\gamma_1^C)\ \big)$ and $x(\gamma_k^C) = x(\gamma_{k-1}^C) + \big(\ x(\gamma_1) + x(\gamma_1^C)\ \big)$. Then

$$\begin{aligned} x(\gamma_{k+1}) &= 2\ x(\gamma_k) + x(\gamma_k^C) \text{ by Remark 3.4.4 and Remark 3.5.11} \\ &= 2\ x(\gamma_1) + x(\gamma_{k-1}^C) + \big(\ x(\gamma_1) + x(\gamma_1^C)\ \big) \text{ by the inductive hypothesis} \\ &= x(\gamma_k) + \big(x(\gamma_1) + x(\gamma_1^C)\big) \text{ by Remark 3.4.4 and Remark 3.5.11.} \end{aligned}$$

□

3.7 A bijection between BCI tuples and T-paths

It is known that a combinatorial T-path formula can be used to compute the Laurent expansion of an arc in a polygon [Sch08a] (see also [ST09] and Chapters 4 and 5 for the case of a general surface). On the other hand, every entry in a finite (respectively, infinite) integral frieze counts the number of matchings between vertices of a polygon (respectively, punctured disk or annulus) and triangles of the associated triangulation [BCI74, Section 2] (respectively, [Tsc15, Section 4.5] and [BPT16, Section 5]) We give a bijection between these classical matching maps and the more recent T-paths. This bijection was also known to Carroll and Price [CP03, Pro05]. This allows us to present a combinatorial formula (Remark 3.7.8) for computing Laurent expansion formulas for cluster variables via these matching maps.

Throughout this section, let T be a triangulation of a general marked surface (S, M). Because matching maps have in the past been defined only for surfaces with with nonempty boundary, we assume that (S, M) has a boundary. Let γ be a generalized peripheral arc (allowing self-crossings) on a boundary component Bd of (S, M).

Choose the usual orientation so that Bd is to the right of γ. Per [MSW11, Theorem 10.1], for the purpose of computing the Laurent polynomial expansion of $x(\gamma)$, we can work with a finite polygon cover $\widetilde{S}_\gamma$ of T containing a lift of γ. By abuse of notation, we also denote the lift of γ in $\widetilde{S}_\gamma$ by γ. Let s and t be the starting and ending points of γ, respectively. Let $R_1, R_2, \ldots, R_r$ be the boundary vertices to the right of γ, not including s and t, and let $L_1, \ldots, L_l$ be the boundary vertices to the left of γ. These vertices are ordered so that $s, R_1, R_2, \ldots, R_r, t, L_l, \ldots, L_2, L_1$ go counterclockwise

around the polygon cover $\widetilde{S}_\gamma$. See Figures 3.16 and 3.17. We say that the R_i are the right vertices and the L_i are the left vertices.

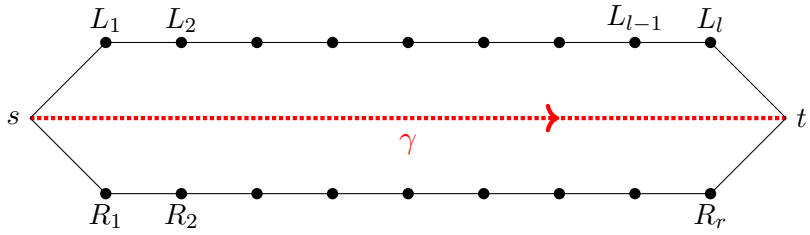

Figure 3.16: A generic polygon cover for a generalized arc γ.

3.7.1 BCI tuples and T-paths

Definition 3.7.1 ([BCI74, Section 2])**.** *A* BCI tuple for γ *is an* r*-tuple* $(t_1, \ldots, t_r)$ *such that:*

(B1) the i*-th entry* t_i *is a triangle of* $\widetilde{S_\gamma}$ *having* R_i *as a vertex. (We say that the vertex* R_i *is matched to the triangle in the* i*-th entry of the tuple, and write* $\triangle(R_i) := t_i$*).*

(B2) the entries are pairwise distinct.

Recall that $\Delta_0, \ldots, \Delta_d$ are the triangles of $\widetilde{S}_\gamma$ which are crossed by γ, in order.

Example 3.7.2. *The following are the BCI tuples for the generalized arc* γ *from Fig. 3.17. Note that* $A, B, C, D, E,$ *and* F *are the triangles which are* not *crossed by* γ *but which are adjacent to at least one of the vertices* $R_1, \ldots, R_8$ *(located to the right of* γ*).*

i. $(\Delta_3, A, B, C, D, \Delta_4, E, F)$

ii. $(\Delta_2, A, B, C, D, \Delta_5, E, F)$

iii. $(\Delta_2, A, B, C, D, \Delta_4, E, F)$

iv. $(\Delta_2, A, B, C, D, \Delta_3, E, F)$

v. $(\Delta_1, A, B, C, D, \Delta_5, E, F)$

vi. $(\Delta_1, A, B, C, D, \Delta_4, E, F)$

vii. $(\Delta_1, A, B, C, D, \Delta_3, E, F)$

viii. $(\Delta_0, A, B, C, D, \Delta_5, E, F)$

ix. $(\Delta_0, A, B, C, D, \Delta_4, E, F)$

x. $(\Delta_0, A, B, C, D, \Delta_3, E, F)$

xi. $(\Delta_3, A, B, C, D, \Delta_5, E, F)$

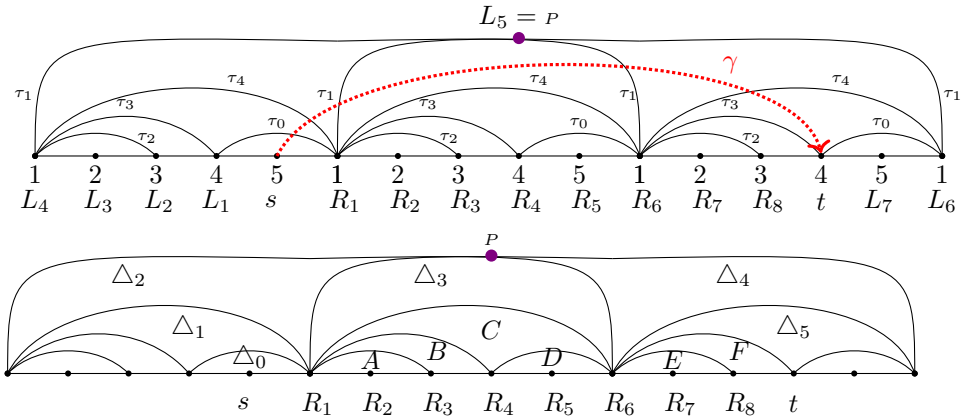

Figure 3.17: Finite polygon cover of T containing copies of triangles crossed by a lift of γ.

Definition 3.7.3 (BCI trail)**.** *Let b be a BCI tuple for γ. We define $trail(b) := \alpha = (\alpha_1, \ldots, \alpha_{length(\alpha)})$ to be a walk from the beginning to the ending point of γ along edges of the triangulation $\widetilde{S}_\gamma$ such that:*

(TR i) the triangles in b (called matched triangles*) are to the right of α, and*

(TR ii) the triangles not in b (called unmatched triangles*) are to the left of α.*

For example, Fig. 3.18 shows $trail(b) = (b_{40}, \tau_0, \tau_1, \tau_1, \tau_3)$ for a BCI tuple $b = (\Delta_0, A, B, C, D, \Delta_3, E, F)$ from Example 3.7.2.

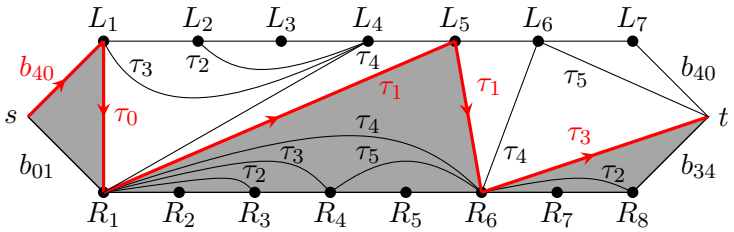

Figure 3.18: Trail $trail(b) = (b_{40}, \tau_5, \tau_1, \tau_1, \tau_3)$ in $\widetilde{S}_\gamma$ for a BCI tuple $b = (\Delta_0, A, B, C, D, \Delta_3, E, F)$ from Example 3.7.2.

We say that $trail(b)$ is the BCI trail *associated to b. By convention, if γ is an arc of T, the BCI tuple for γ is an empty tuple, and γ is the BCI trail of length 1 for itself.*

Remark 3.7.4. *To see that this is well-defined, we observe that, if $t_1 \neq \Delta_0$, the first step of α must go along the edge from s to R_1. Otherwise, the first step goes from s to L_1. Similarly, the last step of α goes from L_l to t if Δ_d is matched. If R_r is matched to a different triangle, then the last step of α goes from R_r to t. It is clear that no two distinct BCI tuples correspond to the same BCI trail.*

Since we are working on a polygonal cover, we only need to recall the definition of (*reduced*) T-paths of type A. However, T-paths can be defined directly on ideal triangulations of a general marked surface [ST09, Sch10] (possibly with punctures, see Chapters 4 and 5). We will introduce *complete* T-paths (a variant of the following definition) in Definition 3.8.7.

Definition 3.7.5 ([Sch08a, Definition 1], reduced T-paths)**.** *Let T denote the triangulation of $\widetilde{S}_\gamma$, where $\tau_1, \ldots, \tau_d$ are the inner diagonals, and $\tau_{d+1}, \ldots, \tau_{2d+3}$ are the boundary edges of the polygon cover $\widetilde{S}_\gamma$. A* reduced T-path *for $\gamma = (s, t)$ is a sequence*

$$\alpha = (a_0, a_1, \ldots, a_{length(\alpha)} | i_1, i_2, \ldots, i_{length(\alpha)})$$

such that

(T1) $s = a_0, a_1, \ldots, a_{length(\alpha)} = t$ are vertices of $\widetilde{S}_\gamma$.

(T2) Each τ_{i_k} connects the vertices $a_{i_{k-1}}$ and a_{i_k} for each $k = 1, 2, \ldots, length(\alpha)$.

(T3) No step goes along the same edge twice.

(T4) The length of a T-path is odd.

(T5) Every even step crosses γ.

(T6) If $j < k$ and both τ_{i_j} and τ_{i_k} cross γ, then the crossing point of τ_{i_j} and γ is closer to the vertex s than the crossing point of τ_{i_k} and γ.

We will prove the following in Sections 3.7.3 and 3.7.4.

Theorem 3.7.6. *Let γ be a generalized arc. The BCI trail map defined in Definition 3.7.3 gives a bijection between the set of BCI tuples for γ and the set of reduced T-paths for γ.*

3.7.2 Cluster expansion formula in terms of BCI tuples

We assign to a BCI tuple b the same weight as the reduced T-path corresponding to it. This choice of weight agrees with the weighting given by Caroll and Price [CP03] and Propp [Pro05, pages 10-11]. An equivalent weighting is used in a recent article [Yur16, Lemma 4.4].

Definition 3.7.7 (Laurent monomial)**.** *To any BCI tuple b, we associate an element $x(b)$ in the cluster algebra $\mathcal{A}(S, M)$ by first considering trail$(b) = \alpha = (\alpha_1, \ldots, \alpha_{length(\alpha)})$ and setting*

$$x(b) = x(\alpha) = \frac{\prod_{i \text{ odd}} x_{\alpha_i}}{\prod_{i \text{ even}} x_{\alpha_i}}.$$

Due to Theorem 3.7.6, we can rewrite the reduced T-path cluster expansion formula [Sch08a, Theorem 1.2] in terms of BCI tuples as follows.

Remark 3.7.8 (BCI tuple expansion formula)**.** *Let $\mathcal{A}(S, M)$ be a cluster algebra arising from (S, M), as per Theorem 2.2.11. Let γ be a peripheral generalized arc. The Laurent polynomial corresponding to γ with respect to the cluster x_T is*

$$x_\gamma = \sum_b x(b) \tag{3.7.1}$$

where the sum is over all BCI tuples b for γ. This formula does not depend on our choice of orientation on γ.

Example 3.7.9 (Example of a Laurent expansion corresponding to a generalized arc)**.** *Consider the ideal triangulation T of a once-punctured disk and a generalized arc in Fig. 3.17. We obtain the 11 BCI tuples for γ, listed in Example 3.7.2. Following (3.7.1), we compute*

$$X_\gamma^T = \frac{x_0x_1x_4 + 2x_1x_3x_4 + 2x_0^2 + 4x_0x_3 + 2x_3^2}{x_0x_1x_4}$$

by specializing $x(\tau) = 1$ for each boundary edge τ.

Note that (3.7.1) holds for any marked surface (S, M), possibly with no boundary, and for any generalized ordinary arc γ. This is due to [MSW11, Thm. 10.1].

3.7.3 Proof that the trail map is well-defined

In this section, we show that the map

$$\{\text{BCI tuples for } \gamma\} \to \{\text{reduced } T\text{-paths for } \gamma\}$$
$$b \mapsto trail(b),$$

where $trail(b)$ is the BCI trail corresponding to b defined in Definition 3.7.3, is well-defined.

Lemma 3.7.10. *Suppose that the i-th right vertex R_i is not adjacent to a triangle which crosses γ. Then R can only be matched to one triangle, and so the i-th entry in every BCI tuple for γ is fixed.*

Proof. Let b be a BCI tuple for γ. If such a vertex exists, there must be a vertex R_j which is adjacent to exactly one triangle $\triangle$. Then $t_j = \triangle$ by (BCI1). As in [BCI74, Section 2], we can remove $\triangle$ from $\widetilde{S}_\gamma$ and get a smaller triangulated polygon. By induction, we can remove all vertices not adjacent to a triangle crossed by γ this way. □

Remark 3.7.11. *Due to Lemma 3.7.10, we can assume without loss of generality that all vertices of $\widetilde{S}_\gamma$ are adjacent to triangles crossed by γ. Note that this gives us the same triangulated polygon cover defined in [MSW11, Section 7] (see also an exposition in Section4.3.1).*

Every right vertex R_i is adjacent to at least 2 triangles of $\widetilde{S}_\gamma$, with the exception of the starting vertex s and the finishing vertex t, which are adjacent to exactly one triangle Δ_0, Δ_d, respectively.

Fig. 3.17 illustrates Lemma 3.7.10. The triangles A, B, C, D, E, and F (which do not cross γ) appear in every BCI tuple. Instead of Fig. 3.17, we work with Fig. 3.19. When drawing this "smaller" polygon cover, we relabel the vertices of $\widetilde{S}_\gamma$, so that the indices of R and L are consecutively ordered. For example, vertex R_6 in Fig. 3.17 is now vertex R_2 in Fig. 3.19. Compare Fig. 3.18 with Fig. 3.20.

Lemma 3.7.12. *Let $b = (t_1, \ldots, t_r) = (\triangle(R_1), \ldots, \triangle(R_r))$ be a BCI tuple for γ and let $\alpha = (\alpha_1, \ldots, \alpha_{length(\alpha)})$ be its corresponding BCI trail.*

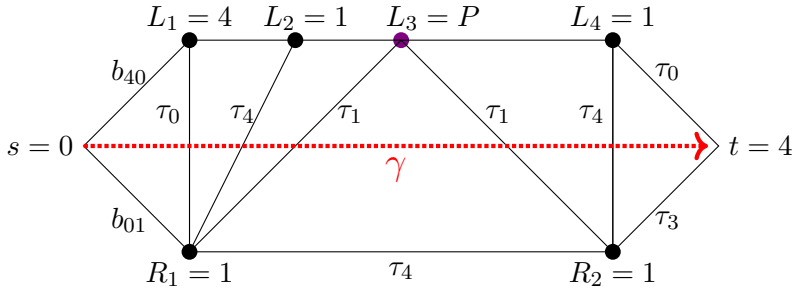

Figure 3.19: Finite $(5+3)$-gon cover $\widetilde{S}_\gamma$ from Figure 2.9.

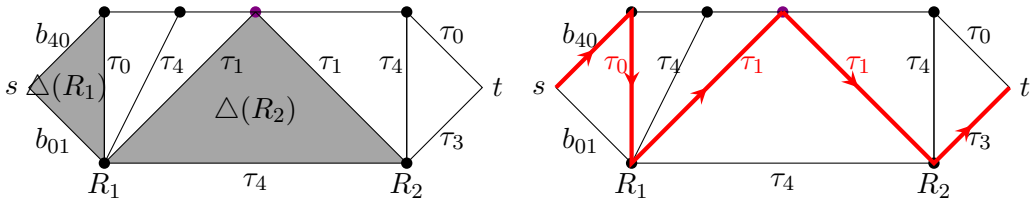

Figure 3.20: A BCI tuple $b = (\Delta_0, \Delta_3)$ for γ and corresponding BCI trail (b_{40}, τ_0, τ_1, τ_1, τ_3).

1. *If α_{2j} goes from a vertex R (to the right of γ) to a vertex L (to the left of γ), then, in the tuple b, R is matched to the triangle which is crossed by γ immediately after α_{2j}.*

2. *If α_{2j} goes from a vertex L (to the left of γ) to a vertex R (to the right of γ), then, in the tuple b, R is matched to the triangle which is crossed by γ immediately before α_{2j}.*

3. *Every even step α_{2j} crosses γ. So we have either situation (1) or (2).*

4. *Furthermore, the length of α is odd.*

Proof. We prove (1), (2), and (3) by induction on j. The first step must go from the starting point s of γ to either R_1 (the first vertex to the right of γ) or L_1 (the first vertex to the left of γ).

First, suppose R_1 is not matched to the first triangle Δ_0 crossed by γ. See Fig. 3.21. Since Δ_0 is not adjacent to other vertices to the right of γ, the BCI tuple b corresponding to α does not contain Δ_0. Then α_1 must go to R_1 because an unmatched

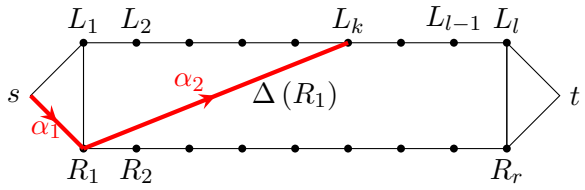

Figure 3.21: The first step α_1 ends at the right vertex R_1, and α_2 ends at a left vertex L_k for $k \geq 1$ (Lemma 3.7.12 Case 1).

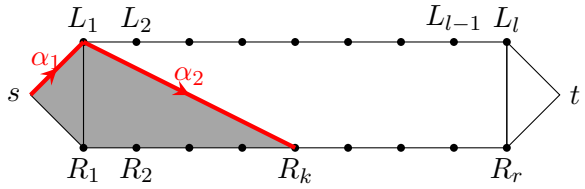

Figure 3.22: The first step α_1 ends at the left vertex L_1, and α_2 ends at a right vertex R_k for $k \geq 1$ (Lemma 3.7.12 Case 2). Shaded region represents triangles $\Delta_0, \ldots, \Delta_{k-1}$.

triangle of $\widetilde{S}_\gamma$ has to be to the left of α. Then R_1 is matched to a different triangle t_1 which γ crosses some time after Δ_0, and no other triangle (if any) between Δ_0 and t_1 is contained in b. Hence, by (TR i) and (TR ii), t_1 is immediately to the right of the next step α_2. Hence α crosses γ by going from R_1 to a left vertex. The converse follows from Definition 3.7.3. This is the base case for (1) and (3).

Second, suppose R_1 is matched to the first triangle Δ_0 crossed by γ. See Fig. 3.22. Then Δ_0 is the closest matched triangle to s. Then α_1 must go to L_1 because a matched triangle has to be to the right of γ. For some $k \geq 1$ (possibly $k = 1$), the triangles $t_1 = \Delta_0$, ..., $t_k = \Delta_{k-1}$ matched by R_1, R_2, ..., R_k form a maximal connected fan. Then α_2 crosses γ by going from L_1 to R_k. Furthermore, the triangle Δ_{k-1} matched to R_k appears immediately before α_2. This is the base case for (2) and (3).

Let j be given and assume α_{2j} crosses γ. First, assume (1): suppose α_{2j} starts from a right vertex R and ends at a vertex left L_k, and suppose that the triangle $\triangle(R)$ matched to R appears immediately after α_{2j}. See Figs. 3.23 and 3.24.

If $k = l$, then L_k is the last vertex to the left of γ before the ending point t of γ. Hence the triangles matched to vertices between R and R_r (inclusive) form a maximal

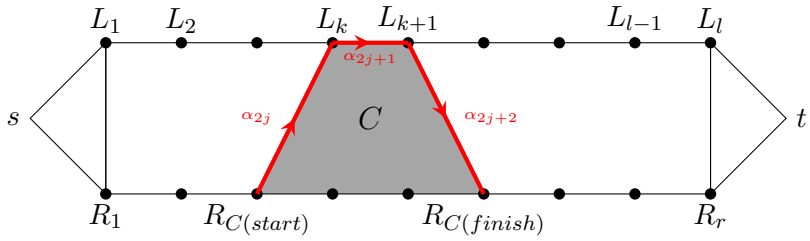

Figure 3.23: The subpath $\alpha_{2j}, \alpha_{2j+1}, \alpha_{2j+2}$ starts and finishes on the right of γ. Lemma 3.7.12 Case 1: When α_{2j} starts at a right vertex and α_{2j+2} ends at a right vertex

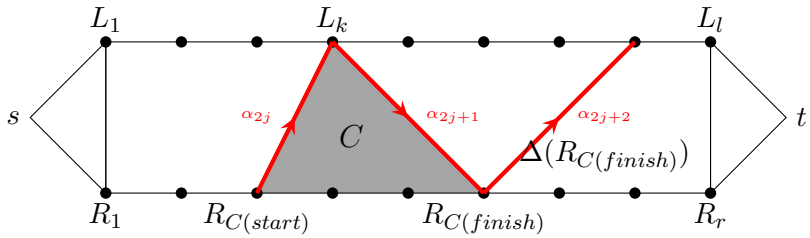

Figure 3.24: The subpath $\alpha_{2j}, \alpha_{2j+1}, \alpha_{2j+2}$ starts on the right and finishes on the left of γ. Lemma 3.7.12 Case 1: α_{2j} starts to the right of γ and α_{2j+2} ends to the left of γ.

connected fan which contains Δ_d. Therefore α_{2j+1} goes from L_l to t, proving (4). So suppose $k < l$.

Consider the maximal connected component C of matched triangles which $\triangle(R)$ is a part of. The edge between L_k and L_{k+1} is an edge of a triangle $\triangle[L_k, L_{k+1}]$. Consider these two possibilities: either $\triangle[L_k, L_{k+1}]$ is in C or it is not. Suppose it is. See Fig. 3.23. Then α_{2j+1} must go from L_k to L_{k+1} so that the matched triangles stay to the right of α. Furthermore, the right vertex $R_{C(finish)}$ that bounds C on the side that is closest to the end of γ must be matched to a triangle in C. (Note that vertex $R_{C(finish)}$ is equal to R if and only if C contains exactly one triangle, $\triangle(R)$). Also, C cannot include $\triangle[L_{k+1}, L_{k+2}]$. Then α_{2j+2} must go from L_{k+1} to $R_{C(finish)}$ in order to obey Definition 3.7.3. This satisfies (3) for $j+1$. Furthermore, the triangle which is matched to $R_{C(finish)}$ appears immediately before α_{2j+2}, satisfying (1) for $j+1$.

Consider the other possibility ($\triangle[L_k, L_{k+1}]$ not in C) as in Fig. 3.24. If the edge between L_k and L_{k+1} is not an edge of C, then α_{2j+1} must go to a right vertex $R_{C(finish)}$ in order to keep the unmatched triangles to the left of α. But in this situation $R_{C(finish)}$ is

not matched to a triangle in C, so $R_{C(finish)}$ must be matched to a triangle $\triangle(R_{C(finish)})$ outside of C. Since by assumption C is a maximal connected component of matched triangles, there must be at least one unmatched triangle immediately after C. Then α_{2j+2} needs to go to a left vertex in order to have the unmatched triangles stay to the left of α and the triangle $\triangle(R_{C(finish)})$ be to the right of α.

Second, assume (2): suppose α_{2j} ends at a vertex R_k (to the right of γ), and suppose that the triangle $\triangle(R_k)$ matched to R_k appears immediately before α_{2j}. See Figs. 3.25 and 3.26.

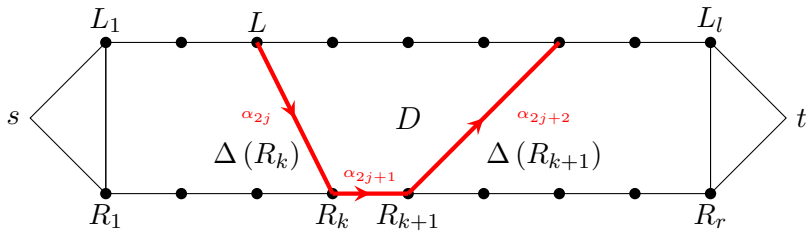

Figure 3.25: The subpath $\alpha_{2j}, \alpha_{2j+1}, \alpha_{2j+2}$ starts and finishes on the left of γ. Lemma 3.7.12 Case 2: α_{2j} starts to the left of γ and α_{2j+2} ends to the left of γ.

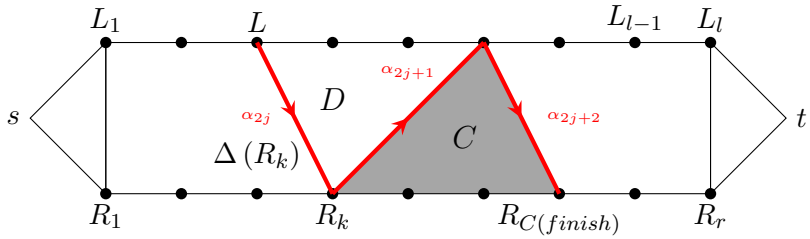

Figure 3.26: The subpath $\alpha_{2j}, \alpha_{2j+1}, \alpha_{2j+2}$ starts on the left and finishes on the right of γ. Lemma 3.7.12 Case 2: When α_{2j} starts to the left of γ and α_{2j+2} ends to the right of γ.

If $k = r$, then R_k is the last vertex before the ending point of γ. Then the rest of the triangles after $\triangle(R_r)$ (if any) are not matched, so they need to be to the left of α, and so α_{2j+1} goes from R_r to t. This proves (4). So suppose $k < r$.

Let D denote the maximal connected component of the unmatched triangles between $\triangle(R_k)$ and $\triangle(R_{(k+1)})$. Note that D needs to be to the left of α_{2j+1} by (TR ii). If the edge between R_k and R_{k+1} is an edge of D, then α_{2j+1} needs to go from R_k to R_{k+1}.

Then α_{2j+2} must go from R_{k+1} to a left (since R_{k+1} must be matched to the triangle adjacent to R_{k+1} which appears immediately after D). See Fig. 3.25.

If the edge between R_k and R_{k+1} is not an edge of D, then R_{k+1} must be matched to a triangle adjacent to R_k. So α_{2j+1} goes from R_k to a left vertex. See Fig. 3.26. Let C be the maximal connected fan of matched triangles which contain $\triangle(R_{(k+1)})$. Every right vertex in C must be matched to a triangle as close to the beginning of γ as possible. Hence this component forms a pyramid shape fan (with the base to the right of γ), and so α_{2j+2} goes from the left of γ to the right of γ. Furthermore, the endpoint of α_{2j+2} is matched to the triangle immediately before α_{2j+2}. This concludes our induction step for (2) and (3). □

Proposition 3.7.13. *A BCI trail for γ is a reduced T-path for γ.*

Proof. The definition of a BCI trail satisfies (T1), (T2), (T3), and (T6). Lemma 3.7.12 proves that a BCI trail satisfies (T4) and (T5). □

3.7.4 Triangles map

Conversely, given a reduced T-path α for γ, we show that the set of triangles to the right of γ forms a BCI tuple for γ. We define the map

$$\{\text{reduced } T\text{-paths for } \gamma\} \to \{\text{BCI tuples for } \gamma\}$$
$$\alpha \mapsto \mathit{triangles}(\alpha)$$

which associates to α a tuple $\mathit{triangles}(\alpha)$ of triangles of $\widetilde{S}_\gamma$ that are to the right of α. The following algorithm tells us the well-defined way to match the R_i's to triangles as we go along $\widetilde{S}_\gamma$ from R_1 to R_r.

If α_1 goes from s to the right vertex R_1, we assign $\triangle(R_1)$ to be the triangle immediately to the right of α_2. See Fig. 3.21.

If α_1 goes to the left vertex L_1, then α_2 goes from L_1 to some right vertex R_k. We match the first k vertices $R_1, \ldots, R_k$ to the triangles $\Delta_0, \ldots, \Delta_{k-1}$, in order. These triangles are represented by the shaded area in Fig. 3.22.

Since α_{2j} must cross γ, this step must go from the right to the left of γ (or vice versa). First, suppose α_{2j} goes from a right vertex $R_C(\mathit{start})$ to some left vertex L_k.

Then $R_C(start)$ has not been matched yet to any triangle which is crossed by γ prior to α_{2j}.

If α_{2j+1} goes from L_k to the next left vertex L_{k+1}, then α_{2j+2} goes from L_{k+1} to a right vertex $R_{C(finish)}$ where $C(start) \leq C(finish)$ (possibly $C(start) = C(finish)$). We we match the vertices $R_{C(start)}$, ..., $R_{C(finish)}$ to the triangles in the trapezoid bounded by the subpath α_{2j}, α_{2j+1}, α_{2j+2}. See Fig. 3.23.

If α_{2j+1} goes from L_k to a right vertex $R_{C(finish)}$ where $C(start) < C(finish)$, then we match the vertices $R_{C(start)}$, ..., $R_{C(finish)-1}$ to the triangles in the fan bounded by the subpath α_{2j}, α_{2j+1}, α_{2j+2}. See Fig. 3.24.

Second, suppose α_{2j} goes from a left vertex L to some right vertex R_k. Then R_k has been matched to the triangle (having α_{2j} as a side) which is crossed by γ prior to α_{2j}.

If α_{2j+1} goes from R_k to R_{k+1}, then α_{2j+2} goes from the right to the left of γ (see Fig. 3.25). This situation for α_{2j+2} has been discussed earlier.

If α_{2j+1} goes from R_k to a left vertex and α_{2j+2} goes to a right vertex $R_{C(finish)}$ (where $k < C(finish)$), then we match $R_{k+1}, \ldots, R_{C(finish)}$ to the triangles in the fan bounded by the subpath α_{2j+1}, α_{2j+2}. See Fig. 3.26.

Finally, the final (and hence odd) step of α either starts from L_l or from R_r. If it goes from L_l to t, then the previous even step finishes at a left vertex (Fig. 3.24 or 3.25). Hence R_r has not been matched to a triangle yet. We match R_r to the final triangle Δ_d. If it goes from R_r to t, then the previous even step finishes at a right vertex (Fig. 3.23 or 3.26). Hence R_r has been matched to the triangle having this even step as a side. By construction, the map *triangles* is well-defined.

Lemma 3.7.14. *The triangles map $\alpha \mapsto triangles(\alpha)$ is the inverse of the trail map $b \mapsto trail(b)$. In particular, both maps are bijections.*

Proof. Let $\alpha = (\alpha_1, \ldots, \alpha_{\text{length}(\alpha)})$ be a reduced T-path for γ. Then $triangles(\alpha)$ are the triangles to the right of α, which form a BCI tuple for γ. But $trail(triangles(\alpha))$ is the reduced T-path to the left of $triangles(\alpha)$, so $\alpha = trail(triangles(\alpha))$.

Conversely, let $b = (\triangle(R_1), \ldots, \triangle(R_r))$ be a BCI tuple for γ. Then $triangles(trail(b))$ is the tuple of all the triangles to the right of $trail(b)$. Since $trail(b)$ is the trail to the left of b, we have $b = triangles(trail(b))$ □

3.8 Natural lattice structure of the BCI tuples

It is known that the set of all snake graph perfect matchings has a natural distributive lattice structure [MSW13, Theorem 5.2] (as a consequence of [Pro02, Theorem 2]). Using a bijection of [MS10] between snake graph perfect matchings and complete T-paths (Definition 3.8.7), we will show that the BCI tuples have a natural lattice structure which is preserved by the bijection of Theorem 3.7.6. In the same spirit as [MS10, Sch10, MSW13], we define the *minimal* and *maximal* BCI tuples. We adopt the convention equivalent to the convention of [MS10, Sch10], which is opposite of the more recent papers [MSW11, MSW13].

3.8.1 Lattice structure

Let γ be the lift of a generalized peripheral arc of (S, M), as described in the previous section.

Definition 3.8.1 (Minimal and maximal BCI tuples)**.** *For a vertex R_i to the right of γ, denote by $FAN(R_i)$ the fan of all triangles adjacent to R_i which are crossed by γ. Per Remark 3.7.11, this fan contains at least two triangles. See Fig. 3.27. The orientation of γ determines an ordering of the triangles in this fan. Let $fan(R_i)_k$ be the k-th triangle in $FAN(R_i)$. Let $First(R_i) := fan(R_i)_1$ and $Last(R_i) := fan(R_i)_{|FAN(R_i)|}$ denote the first and last triangles in this fan. We say that a BCI tuple is the* minimal *BCI tuple if each vertex R_i is mapped to $First(R_i)$. Similarly, the* maximal *BCI tuple is defined to be $(Last(R_1), \ldots, Last(R_r))$. See Fig. 3.28.*

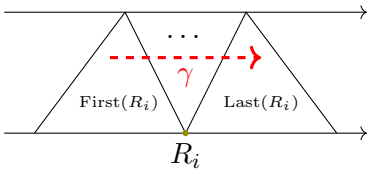

Figure 3.27: The collection $FAN(R_i)$ of triangles adjacent to R_i.

The lattice is graded by the sum of distances from the triangles $First(R_i)$ of the minimal BCI tuple.

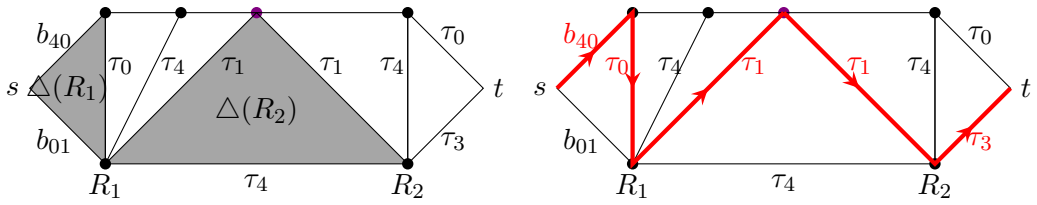

Figure 3.28: The (minimal) BCI tuple $(First(R_1), First(R_2))$ for γ from Figure 3.19 and its corresponding reduced T-path.

Definition 3.8.2 (twist)**.** *We define an* up twist *to be a local move that affects precisely one triangle $t_i = fan(R_i)_k$ of b, replacing $fan(R_i)_k$ with $fan(R_i)_{k+1}$. A* down twist *replaces $fan(R_i)_k$ with $fan(R_i)_{k-1}$.*

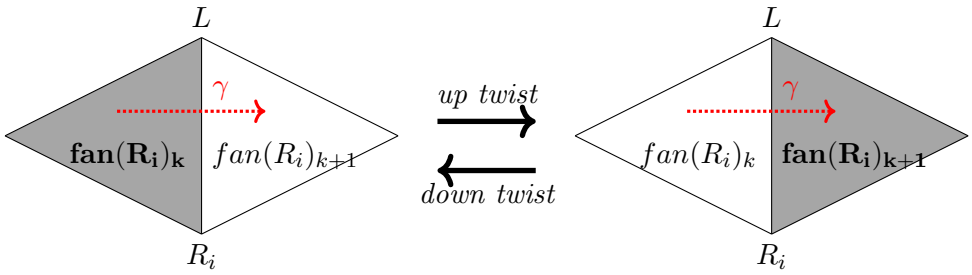

Unlike, for example, [Sch10, MW13], we do not work with principal coefficients. However, it still makes sense to define a *height function* for each BCI tuple.

Definition 3.8.3 (height function)**.** *Let*

$$\tau_{R_i,1}, \tau_{R_i,2}, \ldots, \tau_{R_i,f}$$

(where $f = |FAN(R_i)| - 1$) be the arcs crossed by γ and adjacent to R_i, ordered by the orientation of γ. Given an arbitrary BCI tuple $b = (t_1, \ldots, t_r) = (\triangle(R_1), \ldots, \triangle(R_r))$, we define its height function *$h(b)$ by the monomial*

$$\left(\prod_k w(\tau_{R_1,k})\right)\left(\prod_k w(\tau_{R_2,k})\right)\cdots\left(\prod_k w(\tau_{R_r,k})\right)$$

where each inner product is taken over every k such that $\tau_{R_i,k}$ is an edge between triangles $\triangle(R_i)$ and $First(R_i)$. By convention, if $\triangle(R_i) = First(R_i)$, there is no edge between

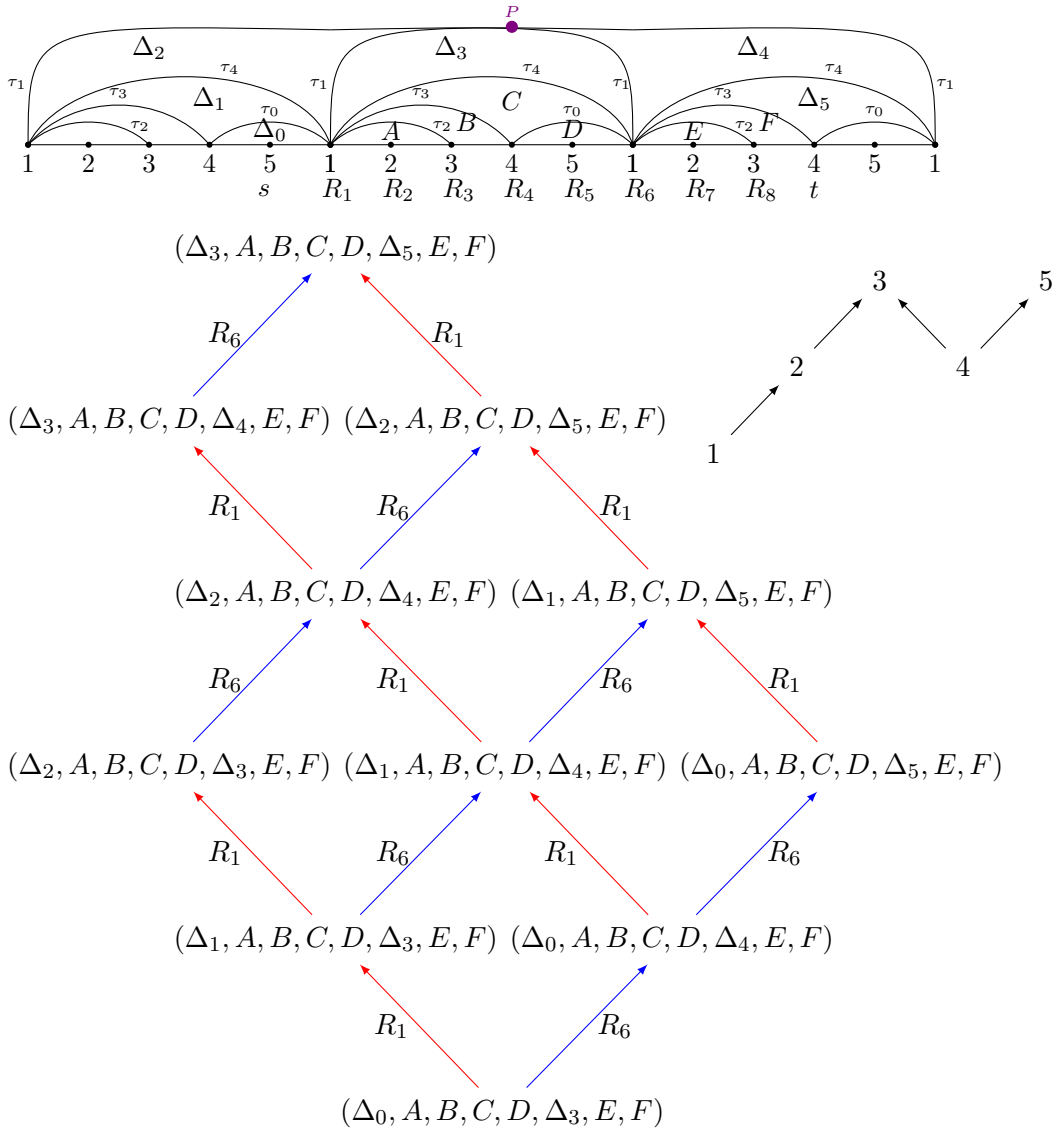

Figure 3.29: Based on the setup of Figure 3.17 (redrawn at the top). Left: the lattice $L_{BCI}(\gamma)$ of the BCI tuples for γ. Right: the poset Q_γ.

them, and the product equals 1.

Theorem 3.8.4 (Analog of [MSW13, Theorem 5.2])**.** *Construct a graph $L_{BCI}(\gamma)$ whose vertices are labeled by BCI tuples for γ, and whose edges connect two vertices if and only if the two tuples are related by an up or down twist. This graph is the Hasse diagram of*

a distributive lattice, whose minimal element is the minimal BCI tuple of γ. The lattice is graded by the degree of each height function.

We describe how to read off from T and γ a poset Q_γ whose lattice of order ideals $J(Q_\gamma)$ is equal to $L_{BCI}(\gamma)$. The following definition is equivalent to [MSW13, Def. 5.3].

Definition 3.8.5. *We associate to $\widetilde{S}_\gamma$ and γ a directed graph Q_γ whose vertices are labeled by $1, \ldots, d$, and whose directed edges are described as follows. Put an arrow from k to $k+1$ if and only if $\tau_{i_{k+1}}$ follows τ_{i_k} (considered as sides of Δ_k) in the counterclockwise order. (see Fig. 3.29). Because $\widetilde{S}_\gamma$ is a triangulated polygon, the underlying undirected graph of Q_γ is a Dynkin diagram of type A. By abuse of notation, let Q_γ denote the poset whose Hasse diagram is Q_γ*

For example, see Fig. 3.29 for $L_{BCI}(\gamma)$ and Q_γ, where γ is the generalized arc from our running example, Fig. 3.17.

Remark 3.8.6. *As a corollary of [MSW13, Theorem 5.4], we have the following facts. The lattice $L_{BCI}(\gamma)$ from Theorem 3.8.4 is the lattice of order ideals $J(Q_\gamma)$ of the poset Q_γ from Definition 3.8.5; the support of the height monomial of a BCI tuple b consists precisely of the elements in the corresponding order ideal. Moreover, an up twist of an entry of the tuple b corresponds to going up in the poset.*

3.8.2 Proof of Theorem 3.8.4

We now need to introduce *complete T-paths for γ*. Throughout this section, let τ_{i_k} be the k-th diagonal of $\widetilde{S}_\gamma$ that is crossed by γ. Furthermore, $p_0 = s, p_1, p_2, ..., p_{d+1} = t$ are the points of intersection of γ and $\widetilde{S}_\gamma$ in order, following the orientation on γ, and $i_1, i_2, ..., i_d$ are such that p_k lies on the arc $\tau_{i_k} \in \widetilde{S}_\gamma$. Let γ_k denote the segment of γ between the points p_k, p_{k+1}.

Definition 3.8.7 ([Sch10])**.** *A complete T-path for γ is a path $\overline{\alpha} = (\overline{\alpha}_1, \ldots, \overline{\alpha}_{2d+1})$ along edges of $\widetilde{S}_\gamma$ such that:*

(Com 1) The even arcs are precisely the arcs crossed by γ in order, that is, $\alpha_{2k} = \tau_{i_k}$.

(Com 2) For all $k = 0, 1, 2, \ldots, d$, the segment γ_k is homotopic to the segment of the path $\overline{\alpha}$ that starts at the point p_k, then goes along $\overline{\alpha}_{2k}$ to the starting point of

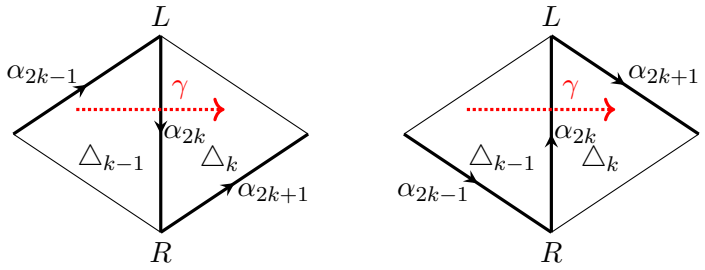

Figure 3.30: Two examples of a complete T-path subsequence $(\overline{\alpha}_{2k-1}, \overline{\alpha}_{2k}, \overline{\alpha}_{2k+1})$. On the left, $\overline{\alpha}_{2k}$ is *not* γ-oriented. On the right, $\overline{\alpha}_{2k}$ is γ-oriented.

$\overline{\alpha}_{2k+1}$, then along $\overline{\alpha}_{2k+1}$ to the starting point of $\overline{\alpha}_{2k+2}$, and then along $\overline{\alpha}_{2k+2}$ until the point p_{k+1}.

Remark 3.8.8. *Let $\overline{\alpha} = (\overline{\alpha}_1, \ldots, \overline{\alpha}_{2d+1})$ be a complete T-path for γ. We define a* backtrack *to be a pair of consecutive steps $(\overline{\alpha}_j, \overline{\alpha}_{j+1})$ along the same arc, forming a contractible loop. In contrast to the reduced T-paths (also known as BCI trails, per Theorem 3.7.6 above), complete T-paths allow backtracking. Although we are focusing on the case where $\widetilde{S}_\gamma$ is a polygon, Definition 3.8.7 works in the settings of general surfaces with no punctures (see Chapters 4 and 5 for the case with punctures).*

Remark 3.8.9. *The map $\{$complete T-paths for $\gamma\} \to \{$reduced T-paths for $\gamma\}$ which is given by removing all backtracks is a bijection.*

Although worded slightly differently, the following is equivalent to the definition given in [Sch10]. Recall that our convention matches [Sch10, MS10] but is the opposite of [MSW11, MSW13].

Definition 3.8.10 ([Sch10, Section 3.2])**.** *Let $\overline{\alpha} = (\overline{\alpha}_1, \ldots, \overline{\alpha}_{2d+1})$ be a complete T-path for γ. We say that $\overline{\alpha}_{2k}$ is γ-oriented if $\overline{\alpha}_{2k}$ goes from a right vertex R to a left vertex L. See Fig. 5.5.*

Definition 3.8.11 ([Sch10, Section 3.3])**.** *The height function for a complete T-path $\overline{\alpha} = (\overline{\alpha}_1, \ldots, \overline{\alpha}_{2d+1})$ for γ is given by*

$$h(\overline{\alpha}) = \prod_{k:\overline{\alpha}_{2k} \text{ is } \gamma\text{-oriented}} w_{i_k}.$$

Remark 3.8.12. *There is a unique complete T-path (denoted $\overline{\alpha}_-$) such that $h(\overline{\alpha}_-) = 1$. Every even step of $\overline{\alpha}$ goes from the left of γ to the right of γ. Every odd step (except for the first and last step) goes from a right vertex to a left vertex. We argue below in Proposition 3.8.13 that $\overline{\alpha}_-$ corresponds to the minimal BCI tuple $b_- = (First(R_1), \ldots, First(R_r))$.*

Similarly, there is a unique T-path $\overline{\alpha}_+$ with $h(\overline{\alpha}_+) = w_{i_1} \ldots w_{i_d}$ which corresponds to the maximal BCI tuple $b_+ = (Last(R_1), \ldots, Last(R_r))$. Every even step of $\overline{\alpha}_+$ goes from a left vertex to a right vertex. The odd steps (except for the first and last step) of $\overline{\alpha}_+$ go from the right vertices to the left vertices.

Proposition 3.8.13. *Let $\alpha_- = \left(\alpha_{-1}, \ldots, \alpha_{-length(\alpha_-)}\right)$ be the reduced T-path for γ which is associated to the minimal BCI tuple $b_- = (t_1, \ldots, t_r) = (First(R_1), \ldots, First(R_r))$ for γ by the trail map of Definition 3.7.3. Then α_- corresponds to the complete T-path $\overline{\alpha}$ for γ whose height function is 1.*

Proof. Since $First(R_1) = \Delta_0$, the first triangle crossed by γ, α_1 must go from s to L_1, the first left vertex.

For some r_1 (possibly $r_1 = 1$), the triangles $First(R_1)$, $\ldots$, $First(R_{r_1})$ form a maximal connected fan of triangles in b_-. Then α_2 goes from L_1 to R_{r_1}.

In fact, since $t_i = First(R_i)$ for all i, every maximal connected component of matched triangles is a fan sharing exactly one left vertex; every maximal connected component of unmatched triangles is a fan sharing exactly one right vertex. See Fig. 3.28. Hence, every odd step α_{2k+1} goes from R_{r_k} to some left vertex L_{r_k}. The last step α_{2d+1} goes from R_r to t. Every even step α_{2k} $(k > 1)$ goes from $L_{l_{k-1}}$ to R_{r_k}.

Next, consider the complete T-path $\overline{\alpha}$ corresponding to α_-. We claim that every even step $\overline{\alpha}$ goes from a left vertex to a right vertex, so that $h(\overline{\alpha}) = 1$.

If length$(\alpha) = 2d + 1$, then $\overline{\alpha} = \alpha$, and we are done. If length$(\alpha) < 2d + 1$, for every τ_{i_k} that is not an even step of α, we insert a backtrack (τ_{i_k}, τ_{i_k}) at the appropriate location. We either insert a backtrack at a left vertex or a right vertex. If we insert a backtrack at a left vertex L, since the only step of α_- which ends at a left vertex is an odd step α_{-2j+1}, the backtrack that we insert must start with an even step going from L to a right vertex. If we insert a backtrack at a right vertex R, since the only step of α_- which ends at a right vertex is an even step α_{-2j}, we insert an odd step going from R to the other end of τ_{i_k}, followed by an even step going back to R. □

Lemma 3.8.14 ([MSW13, Theorem 5.2])**.** *Consider the set of all perfect matchings of a snake graph G with tiles $G_1, \ldots, G_n$. Construct a graph $L_{MSW}(G)$ whose vertices are labeled by these matchings, and whose edges connect two vertices if and only if the two matchings are related by a twist. This graph is the Hasse diagram of a distributive lattice, whose minimal element is P_-. The lattice is graded by the degree of each height monomial.*

Lemma 3.8.15 ([MSW13, Theorem 5.4])**.** *Let G be a snake graph constructed from γ and $\widetilde{S}_\gamma$. An up twist of a tile G_k for a snake graph perfect matching P (going up in the lattice $L(G)$) is given as follows: If G_k has positive orientation, a vertical matching is replaced with a horizontal matching. If G_k has negative orientation, a horizontal matching is replaced with a vertical matching.*

The following follows from the construction of the snake graph and the bijection in [MS10].

Proposition 3.8.16. *A tile G_k can be twisted if and only if the corresponding steps $\overline{\alpha}_{2k-1}, \overline{\alpha}_{2k}, \overline{\alpha}_{2k+1}$ contain no backtracks.*

More precisely, an up twist of a complete T-path can be defined as follows.

Lemma 3.8.17. *Let $Quad_k$ be the quadrilateral consisting of exactly Δ_{k-1} and Δ_k. Let R and L denote the right and left endpoints of τ_{i_k}. An up twist of a tile G_k in the lattice $L_{MSW}(G)$ corresponds (via the bijection of [MS10]) to replacing consecutive steps $\overline{\alpha}_{2k-1}, \overline{\alpha}_{2k}(= \tau_{i_k}), \overline{\alpha}_{2k+1}$ such that:*

(i) $\overline{\alpha}_{2k}$ goes from L to R,

(ii) $\overline{\alpha}_{2k-1}$ traverses the edge of Δ_{k-1} which is counterclockwise to τ_{i_k},

(iii) and $\overline{\alpha}_{2k+1}$ traverses the edge of Δ_k which is counterclockwise to τ_{i_k},

with three steps $\overline{\alpha}_{2k-1}{}', \overline{\alpha}_{2k}{}'(= \tau_{i_k}), \overline{\alpha}_{2k+1}{}'$ such that:

(i) $\overline{\alpha}_{2k}{}'$ goes from R to L,

(ii) $\overline{\alpha}_{2k-1}{}'$ traverses the edge of Δ_{k-1} which is clockwise to τ_{i_k},

(iii) and $\overline{\alpha}_{2k+1}{}'$ traverses the edge of Δ_k which is clockwise to τ_{i_k}.

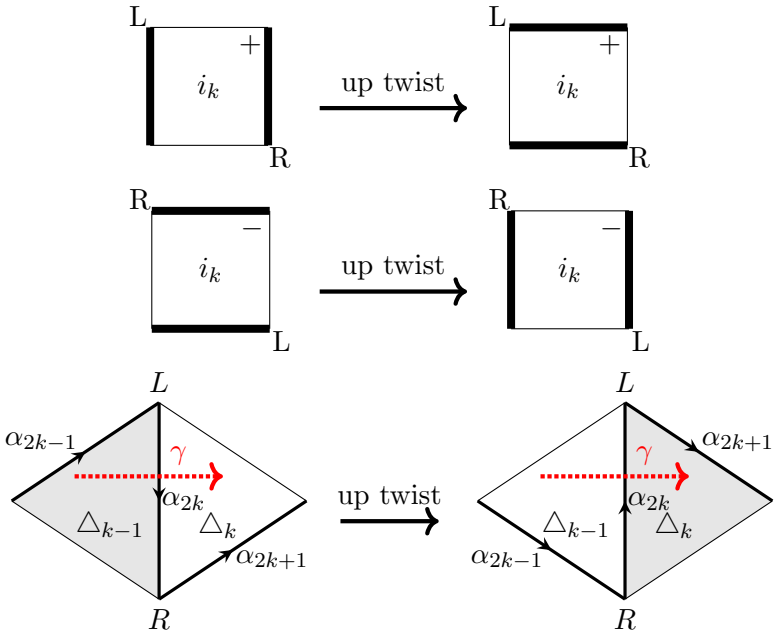

Figure 3.31: An up twist on a snake graph tile (the top two rows) and an up twist of a sequence of three steps $(\overline{\alpha}_{2k-1}, \overline{\alpha}_{2k}, \overline{\alpha}_{2k+1})$ of a complete T-path.

See Fig. 3.31.

Proof. This is a consequence of Lemma 3.8.15 and the bijection between snake graph matchings and complete T-paths [MS10]. □

To prove Theorem 3.8.4, it is sufficient to show that an up twist commutes with the bijection between the complete T-paths and the reduced T-paths. Let $\overline{\alpha}$ be a complete T-path for γ, and let $\mathrm{up}_k(\overline{\alpha})$ be the result of an up twist for $\overline{\alpha}$ which replaces $\overline{\alpha}_{2k-1}$, $\overline{\alpha}_{2k}$, and $\overline{\alpha}_{2k+1}$ with a sequence of three other steps along $Quad_k$, as described in Lemma 3.8.17. Let R and L denote the right and left endpoints of τ_{i_k}. Let α be the reduced T-path corresponding to $\overline{\alpha}$, and let b be the BCI tuple corresponding to α.

Since there is no backtrack (τ_{i_k}, τ_{i_k}) and since $\overline{\alpha}_{2k}$ goes L to R (by Lemma 3.8.17), we see that α contains an even step along τ_{i_k} from L to R. Immediately to the right (respectively, left) of this step is Δ_{k-1} (respectively, Δ_k). By Definition 3.7.3, every triangle to the right of α belongs to b and every triangle to the left of α does not belong

to b, so Δ_{k-1} belongs to b but Δ_k does not. Furthermore, by Lemma 3.7.12(2), the vertex R is matched to Δ_{k-1}.

Let α' be the reduced T-path and let b' be the BCI tuple corresponding to $\mathrm{up}_k(\overline{\alpha})$. By similar argument, we see that α' contains an even step along τ_{i_k} from R to L, and so Δ_{k-1} does not belong to b but Δ_k does. Furthermore, by Lemma 3.7.12(1), we see that R is matched to Δ_k in b'. All the other matched triangles in b' are the same as in b. Hence b' is the result of an up twist of b. This concludes the proof of Theorem 3.8.4.

Chapter 4

On type D cluster algebras: T-path formula and atomic bases

Cluster algebras, introduced by Fomin and Zelevinsky [FZ02] in 2000, are commutative algebras equipped with a distinguished set of generators, the *cluster variables*. The cluster variables are grouped into sets of constant cardinality n, the *clusters*, and the integer n is called the *rank* of the cluster algebra. Starting with an initial *seed* $(\mathbf{x}, B)$, that is, an initial cluster $\mathbf{x}$ together with a skew-symmetrizable integer $n \times n$ *exchange matrix* $B = (b_{ij})$, the set of cluster variables is obtained by repeated application of so called *mutations*. To be more precise, let $\{x_1, x_2, \ldots, x_n\}$ be indeterminates over $\mathbb{Z}$ and let $\mathcal{F} = \mathbb{Q}(x_1, x_2, \ldots, x_n)$. For every $k = 1, 2, \ldots, n$, the mutation $\mu_k(\mathbf{x})$ of the cluster $\mathbf{x} = \{x_1, x_2, \ldots, x_n\}$ is a new cluster $\mu(\mathbf{x}) = (\mathbf{x} \backslash \{x_k\}) \cup \{x_k'\}$ obtained from $\mathbf{x}$ by replacing the cluster variable x_k with the new cluster variable

$$x_k' = \frac{1}{x_k} \left(\prod_{b_{ik}>0} x_i^{b_{ik}} + \prod_{b_{ik}<0} x_i^{-b_{ik}} \right)$$

in $\mathcal{F}$. Mutations also change the attached matrix B, see [FZ02].

The set of all cluster variables is the union of all clusters obtained from an initial cluster $\mathbf{x}$ by repeated mutations. Note that this set may be infinite.

It is clear from the construction that every cluster variable is a rational function in the initial cluster variables $x_1, x_2, \ldots, x_n$. In [FZ02] it is shown that every cluster

variable u is actually a Laurent polynomial in the x_i, that is, u can be written as a reduced fraction

$$u = \frac{f(x_1, x_2, \ldots, x_n)}{\prod_{i=1}^{n} x_i^{d_i}}, \tag{4.0.1}$$

where $f \in \mathbb{Z}[x_1, x_2, \ldots, x_n]$ and $d_i \geq 0$. The right hand side of equation (4.0.1) is called the *cluster expansion of* u in $\mathbf{x}$.

The *coefficient-free cluster algebra* $\mathcal{A}(\mathbf{x}, B)$ is the subring of $\mathcal{F} = \mathbb{Q}(x_1, x_2, \ldots, x_n)$ generated by the cluster variables. When the set of cluster variables is finite, we say that $\mathcal{A}(\mathbf{x}, B)$ is of *finite type*.

We are interested in cluster algebras arising from *bordered surfaces with marked points* [FG06, FG09, FST08, GSV05]. In particular, we study cluster algebras of type D_n (type D for short), which are of finite type (as classified in [FZ03]) and correspond to once-punctured n-gons, as also described in detail in [Sch08b]. Other, related work on type D cluster algebra combinatorial models include [BM09, CP15, FZ03].

Our first result is a Laurent polynomial expansion formula for cluster variables arising from a once-punctured polygon in terms of certain paths (called T°-paths) on an ideal triangulation T° of the surface. This is an extension of the T-path formula (which we call the T°-path) given for any unpunctured surface by Schiffler and Thomas [Sch10, ST09]. Our proof takes advantage of two facts proven by the second author, Schiffler, and Williams: (1) a Laurent polynomial expansion formula for cluster variables arising from any surface in terms of perfect matchings of a *snake graph* [MSW11], and (2) a bijection between these perfect matchings and T°-paths arising from any unpunctured surface [MS10]. An application of the T°-path formula for type D is discussed in the next paragraph.

Our second result is a specific case of a result of [Cer11, CLF12], proven by representation theoretic methods, that the basis consisting of all *cluster monomials* is in fact the *atomic basis* for any skew-symmetric cluster algebra of finite type (see Section 4.4.1). We give a combinatorial proof of this fact for *coefficient-free* cluster algebras of type D. Our proof relies heavily on the T°-path formula for type D and is inspired by Dupont and Thomas' work in [DT13] on atomic bases for cluster algebras of type A and

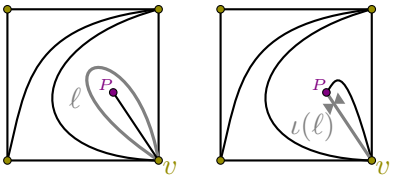

Figure 4.1: An ideal triangulation T^o and the corresponding tagged triangulation $T = \iota(T^o)$. The ℓ-loop ℓ and the corresponding tagged radius $\iota(\ell)$ (tagged notched at the puncture) are both in gray.

$\widetilde{A}$.

In Section 4.2, we present our first result (Theorem 4.2.1), an extension of the T°-path formula of [Sch10, ST09] to once-punctured polygons. We give the proof of this T°-path formula in Section 4.3. Finally, in Section 4.4, we give our second and main result (Theorem 4.4.2), which is a combinatorial proof, using the T°-path formula, that the cluster monomials form the atomic basis for a coefficient-free type D cluster algebra.

4.1 Once-punctured disks

See Chapter 2 for terminology arising in the theory of cluster algebras from general marked surfaces from [FST08, Sections 2 and 7]. In this chapter, we restrict our attention to the case of a once-punctured polygon, which often simplifies the notation. Let $\mathcal{C}_n$ denote a once-punctured n-gon, i.e., a disk with a marked point (called the puncture) in the interior and n marked points on the boundary.

Remark 4.1.1. *Three possible types of ideal triangles can appear in an ideal triangulation of $\mathcal{C}_n$: an ordinary triangle with 3 distinct vertices and 3 distinct sides (Fig. 2.1(a)), an ideal triangle with 2 distinct vertices and 3 distinct sides (Fig. 2.1(b)), and finally a self-folded triangle (Fig. 2.1(c)). The ideal triangulation of Fig. 4.1 (left) contains all 3 types of $\mathcal{C}_n$-ideal triangles. Note that the one-vertex ideal triangle (Fig. 2.1(d)) cannot appear.*

Remark 4.1.2. *Every tagged arc β of $\mathcal{C}_n$ belongs to one of the following three classes:*

- *β is a radius tagged plain at both endpoints (which we call a plain radius).*

- *β is a radius tagged notched at the puncture and plain at the boundary (which we call a notched radius).*
- *β is a peripheral arc connecting distinct endpoints tagged plain at both endpoints.*

Definition 4.1.3 (compatibility of tagged arcs, tagged triangulations, and multi-tagged triangulations of $\mathcal{C}_n$)**.** *The following is a complete list of possible compatible pairs $\{\alpha, \beta\}$ of tagged arcs of $\mathcal{C}_n$:*

- *α and β are two peripheral arcs (tagged plain at all endpoints) that do not intersect in the interior of $\mathcal{C}_n$.*
- *α and β are a peripheral arc and a radius (tagged plain at boundary endpoints) that do not intersect in the interior of $\mathcal{C}_n$.*
- *α and β are two radii both adjacent to the same boundary marked point (tagged plain) but α is tagged plain at the puncture and β is tagged notched at the puncture.*
- *α and β are two radii with distinct boundary endpoints (tagged plain at boundary endpoints) and tagged the same way at the puncture.*
- *α and β are equal.*

A maximal (by inclusion) collection of distinct, pairwise compatible tagged arcs is called a tagged triangulation*. A collection of pairwise compatible tagged arcs (considered with multiplicity) is called a* multi-tagged triangulation*. A multi-tagged triangulation Σ is* compatible *with T if $\sigma \in T$ for every tagged arc $\sigma \in \Sigma$.*

If r is a plain radius and ℓ is the ℓ-loop enclosing r, denote $x_\ell := x_r x_{r^{(p)}}$. If β is a boundary edge, set $x_\beta := 1$. When we say the *T-expansion* of a cluster variable $x(\gamma)$, we mean the cluster expansion of $x(\gamma)$ in the variables of the seed $\mathbf{x}_T$, i.e., a Laurent polynomial in the variables of $\mathbf{x}_T$, see equation (4.0.1).

Remark 4.1.4. *Due to the following proposition, it is enough to work with only two types of tagged triangulations T: one where T has all plain-tagged radii (so that T° has a local wheel-like triangulation as in Fig. 4.2(a)), and one where T has two parallel radii, one tagged plain and the other tagged notched at the puncture (so that T° has a self-folded triangle as in Fig. 4.2(b)).*

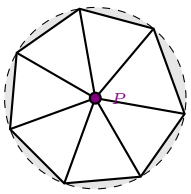

(a) Wheel-like triangulation around the puncture.

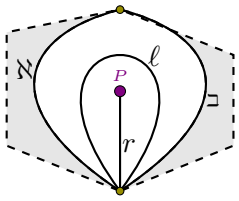

(b) A self-folded triangle around the puncture where ℵ, ב are peripheral arcs or boundary edges.

Figure 4.2: Local triangulations around the puncture. The shaded gray area consists only of peripheral arcs and boundary edges, each sector forming a polygon.

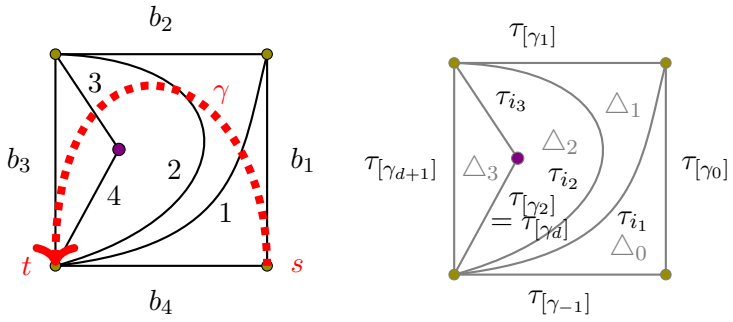

Figure 4.3: A triangulation T° and an arc γ of a once-punctured square. The first, second, third, and fourth ideal triangles crossed by γ are denoted by $\triangle_0$, $\triangle_1$, $\triangle_2$, and $\triangle_3$.

Proposition 4.1.5 ([MSW11, Proposition 3.15])**.** *Suppose $T = \{\tau_1, \ldots, \tau_n\}$ is a tagged triangulation of $\mathcal{C}_n$. Let $\gamma^{(p)}$ denote the arc obtained from γ by changing the notching at the puncture p. Let $T^{(p)}$ denote the tagged triangulation that is obtained from T by replacing each $\tau \in T$ by $\tau^{(p)}$. Let $x(\gamma)$ be the T-expansion of the cluster variable corresponding to γ. Then*

$$x\big(\gamma^{(p)}\big) = x(\gamma)\big|_{x(\tau_i)\leftarrow x(\tau_i{}^{(p)})}$$

is the $T^{(p)}$-expansion of the cluster variable corresponding to $\gamma^{(p)}$.

Recall that, if r is a plain radius and ℓ is the ℓ-loop enclosing r, denote $x_\ell := x_r x_{r^{(p)}}$. If β is a boundary edge, set $x_\beta := 1$. When we say the *T-expansion* of a cluster variable $x(\gamma)$, we mean the cluster expansion of $x(\gamma)$ in the variables of the seed $\mathbf{x}_T$,

i.e., a Laurent polynomial in the variables of $\mathbf{x}_T$, see equation (4.0.1).

4.2 (T°, γ)-path expansion formula

We extend Schiffler and Thomas' work [Sch10, ST09] to once-punctured disks $\mathcal{C}_n$. Following [Sch10, Section 3], we will use the following setup throughout the rest of the paper.

- Let S be an unpunctured surface or $S = \mathcal{C}_n$. Let T° be an ideal triangulation of S and let $\gamma \notin T^\circ$ be an ordinary arc of S. Recall that an ℓ-loop is considered an ordinary arc.
- Choose an orientation on γ, and let s^γ and t^γ be the starting point and the finishing point of γ. Denote by

  $$s^\gamma = p_0^\gamma, p_1^\gamma, p_2^\gamma, \ldots, p_{d+1}^\gamma = t^\gamma$$

  the points of intersection of γ and T° in order. Since γ is considered up to homotopy, we pick a representative so that d is minimal. Let $i_1, i_2, \ldots, i_d$ be such that $\tau_{i_k}^\gamma$ is the arc of T° containing p_k^γ. See Fig. 4.3, where $\tau_{i_1}^\gamma = 1$, $\tau_{i_2}^\gamma = 2$, and $\tau_{i_3}^\gamma = 3$, and see Fig. 4.8(a), where $\tau_{i_k}^\gamma$ $(k = 1, \ldots, 5)$ are labeled 1, 2, ℓ, r and ℓ.
- For $k = 0, 1, \ldots, d$, let γ_k denote the segment of γ from the point p_k to the point p_{k+1}, and let $\triangle_k^\gamma$ denote the (unique) ideal triangle of T° that γ_k crosses. When it is clear from the context which arc we mean, we simply write p_k^γ as p_k, $\tau_{i_k}^\gamma$ as τ_{i_k}, $\triangle_k^\gamma$ as $\triangle_k$.
- The side/s of $\triangle_k$ that is not labeled τ_{i_k} or $\tau_{i_{k+1}}$ is labeled as in Figs. 4.4 and 4.5. In particular, for $k = 1, \ldots, d-1$, define arc $\tau_{[\gamma_k]}$ to be

  $$\tau_{[\gamma_k]} = \begin{cases} \text{the 3rd arc in } \triangle_k & \text{if } \triangle_k \text{ is not self-folded,} \\ \text{the radius in } \triangle_k & \text{if } \triangle_k \text{ is self-folded.} \end{cases}$$

  Define $\tau_{[\gamma_0]}$, $\tau_{[\gamma_{-1}]}$, $\tau_{[\gamma_d]}$, and $\tau_{[\gamma_{d+1}]}$ as follows:

  – If the ideal triangle $\triangle_0$ has three distinct edges, then $\triangle_0$ is formed by arc

τ_{i_1} and two distinct arcs/boundary edges $\tau_{[\gamma_0]}$, $\tau_{[\gamma_{-1}]}$ (not equal to τ_{i_1}) such that $\tau_{[\gamma_0]}$, $\tau_{[\gamma_{-1}]}$, τ_{i_1} are arranged in clockwise order around $\triangle_0$. Similarly, if the ideal triangle $\triangle_d$ has three distinct edges, then it is formed by the arcs τ_{i_d} and two distinct arcs/boundary edges $\tau_{[\gamma_d]}$, $\tau_{[\gamma_{d+1}]}$ (not equal to τ_{i_d}) such that $\tau_{[\gamma_d]}$, $\tau_{[\gamma_{d+1}]}$, τ_{i_d} are arranged in clockwise order around $\triangle_d$.

– If $\triangle_0$ (respectively, $\triangle_d$) is self-folded, then $\tau_{[\gamma_0]} = \tau_{[\gamma_{-1}]}$ (respectively, $\tau_{[\gamma_d]} = \tau_{[\gamma_{d+1}]}$) is the radius.

In Fig. 4.8(a), $\tau_{[\gamma_0]} = b_1$, $\tau_{[\gamma_{-1}]} = b_4$, $\tau_{[\gamma_d]} = 2$, $\tau_{[\gamma_{d+1}]} = b_3$.

Definition 4.2.1 (Quasi-arc)**.** *If τ is an ordinary radius of $\mathcal{C}_n$ between a marked point v on the boundary and the puncture p, let an associated* quasi-arc *τ' be a curve (not passing through p) which satisfies the following:*

1. *τ' is between v and a (non-marked) point p' in the vicinity of p. (Note that another quasi-arc associated to τ may use a different point p''.)*
2. *τ' agrees with the arc τ outside of a radius-ϵ disk D_ϵ around p, where ϵ is chosen small enough so that the intersection of τ with any other arc is outside of D_ϵ.*

If τ is a peripheral arc, we let the associated quasi-arc be τ itself. We label a quasi-arc with the label of the arc that it is associated to.

By abuse of notation, whenever we say we are going along an arc or a side of an ideal triangle $\triangle_k$ (as part of a T°-path), we mean traversing an associated quasi-arc. Note that except for the case when τ is a radius, no abuse of notation is actually needed. The following is an extension of the complete (T°, γ)-path definition as stated in [Sch10, Definition 2], [MS10, Section 4.1].

Definition 4.2.2 (complete (T°, γ)-path)**.** *A* path $\omega = (\omega_1, \omega_2, \ldots, \omega_{length(\omega)})$ *on T° is a concatenation of* steps*, i.e., oriented quasi-arcs and boundary edges of the ideal triangulation T° of S, such that the starting point of a step ω_i is the finishing point of the previous step ω_{i-1}. We say that $\omega = (\omega_1, \ldots, \omega_{2d+1})$ is a* complete (T°, γ)-path *if the following axioms hold:*

(T1) Each even step ω_{2k} $(k = 1, \ldots, d)$ is a quasi-arc associated to arc τ_{i_k}. Recall that $\tau_{i_1}, \ldots, \tau_{i_d}$ is the sequence of arcs crossed by γ in order.

(T2) For $k = 0, \ldots, d$, each ω_{2k+1} traverses a side of the ideal triangle $\triangle_k$. In addition, ω_1 traverses the edge $\tau_{[\gamma_0]}$ or $\tau_{[\gamma_{-1}]}$ (which is adjacent to s) and ω_{2d+1} traverses the edge $\tau_{[\gamma_d]}$ or $\tau_{[\gamma_{d+1}]}$ (which is adjacent to t).

i) Moreover, for $k = 1, 2, \ldots, d-1$, let $[p_k, p_{k+1}]_\omega$ denote the segment of ω starting at the point p_k following ω_{2k}, continuing along ω_{2k+1} and $\omega_{2(k+1)}$ until the point p_{k+1}. Then the segment γ_k is homotopic to $[p_k, p_{k+1}]_\omega$. If $S = \mathcal{C}_n$, then we mean homotopy in the disk minus the puncture.

ii) The segment γ_0 is homotopic to the segment $[s, p_1]_\omega$ of the path starting at the point $s = p_0$ following ω_1 and ω_2 until the point p_1;

iii) The segment γ_d is homotopic to the segment $[p_d, t]_\omega$ of the path starting at the point p_d following ω_{2d} and ω_{2d+1} until the point $p_{d+1} = t$.

(T3) The step ω_{2k+1} starts and finishes in the interior of $\triangle_k$ or at a boundary marked point. This means that, if ω_{2k+1} goes along a quasi-arc τ' associated to a radius, τ' must be chosen so that its endpoint p' near the puncture is located in the interior of $\triangle_k$.

See Examples 4.2.8 and 4.2.9.

It is clear that this definition agrees with the complete T°-paths of [MS10, Sch10] for unpunctured surfaces. For short, we will refer to a complete (T°, γ)-path as simply a (T°, γ)-path (or a T°-path) for the rest of this paper.

Remark 4.2.3. *Per (T2), a (T°, γ)-path is homotopic to γ. It is possible to have $\omega_j = \omega_{j+1}$ and, if j is odd, to have $\omega_j = \omega_{j+1} = \omega_{j+2}$. However, since for each k we have $\omega_{2k} = \tau_{i_k}$ and $\omega_{2(k+1)} = \tau_{i_{k+1}}$ by (T1) but $\tau_{i_k} \neq \tau_{i_{k+1}}$, no more than three consecutive steps can coincide.*

Definition 4.2.4 (backtrack cycle, non-backtrack cycle, quasi-backtrack)**.** *Let $\gamma \notin T^\circ$ and let $\omega = (\omega_1, \ldots, \omega_{2d+1})$ be a (T°, γ)-path. Let τ be an arc of T°, and let (ω_j, ω_{j+1}) be a pair of consecutive quasi-arcs going along τ. We say that (ω_j, ω_{j+1}) is a* cycle *if the starting point of ω_j coincides with the ending point of ω_{j+1}.*

i) A cycle (ω_j, ω_{j+1}) is called a backtrack*, denoted by $(\underline{\tau, \tau})$, if it is contractible.*

ii) A cycle (ω_j, ω_{j+1}) is called a non-backtrack*, denoted by $(\boldsymbol{\tau, \tau})$, otherwise.*

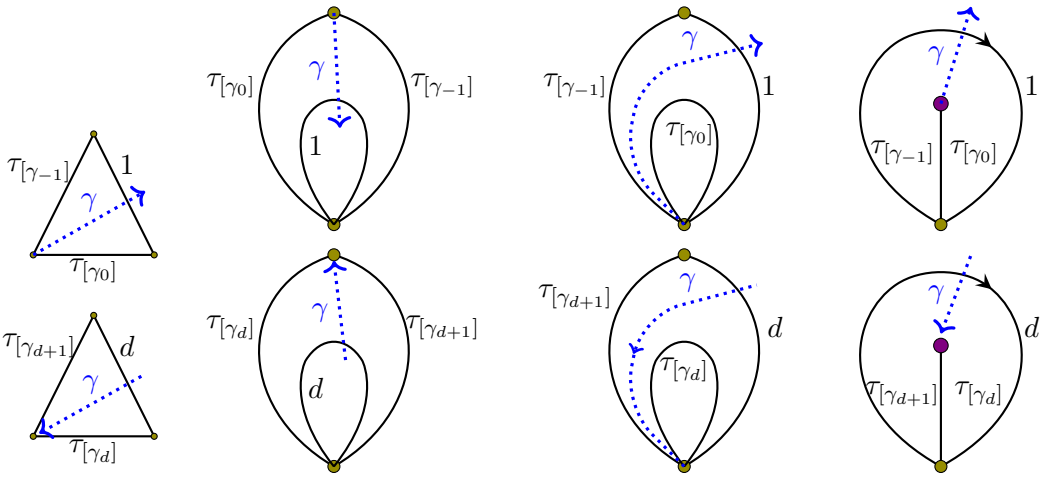

(a) Ordinary triangle.

(b) Two vertices where arc 1^γ or d^γ is a loop.

(c) Two vertices where arc 1^γ or d^γ is not a loop.

(d) Self-folded triangle.

Figure 4.4: Ways for γ to cross the ideal triangle $\triangle_0$ or $\triangle_d$.

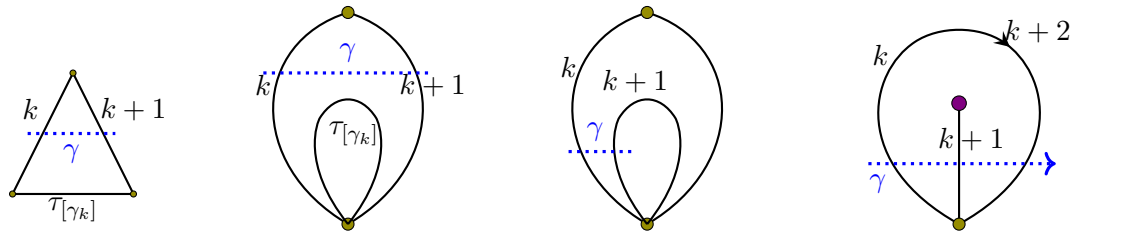

(a) Ordinary triangle.

(b) Two vertices where arc $\tau_{[\gamma_k]}$ is a loop.

(c) Two vertices where arc $k+1$ is a loop.

(d) γ crossing a self-folded triangle's radius in the counterclockwise direction.

Figure 4.5: Ways for γ to cross an ideal triangle $\triangle_k$ for $k = 1, \ldots, k-1$.

In the case that τ is a radius between the puncture p and a marked point v on the boundary, we say that (ω_j, ω_{j+1}), denoted by $(\overline{\tau, \tau})$, is a quasi-backtrack *if it is a concatenation of two quasi-arcs $p' \rightsquigarrow v \rightsquigarrow p''$ where p' and p'' are distinct points in the vicinity of p.*

Remark 4.2.5. *Assume (ω_j, ω_{j+1}) is a pair of steps going along τ, as in Definition 4.2.4.*

1) Suppose τ is peripheral.

i) Then (ω_j, ω_{j+1}) is a backtrack if and only if ω_j and ω_{j+1} are opposite orientations of τ. In particular, if τ has two distinct endpoints, (ω_j, ω_{j+1}) must be a backtrack cycle.

ii) If τ is an ℓ-loop, the concatenation of two steps going along the same orientation of τ would form a non-contractible cycle. However, we show in Proposition 4.2.13(1) that it is impossible for (ω_j, ω_{j+1}) to go along the same orientation of an ℓ-loop twice as part of a (T°, γ)-path.

2) Suppose τ is a radius between the puncture p and a marked point v on the boundary.

a) Suppose ω_j begins at v, so that (ω_j, ω_{j+1}) is a concatenation of two associated quasi-arcs $v \rightsquigarrow p' \rightsquigarrow v$.

i) Then (ω_j, ω_{j+1}) is a backtrack cycle if it is contractible to v. See Fig. 4.6(a) for the case where T° has a self-folded triangle and τ is its radius and Fig. 4.7(a) for the case where τ is not the only radius of T°.

ii) If (ω_j, ω_{j+1}) is not contractible, then due to (T2) it must be homotopic to a loop which goes around the puncture once. We say that (ω_j, ω_{j+1}) is a counterclockwise non-backtrack *if it goes counterclockwise (Fig. 4.6(b)), and a* clockwise non-backtrack *if it goes clockwise (Fig. 4.6(c)). We show in Proposition 4.2.13(2a) that in this case, τ must be the only radius of T°, i.e., T° contains a self-folded triangle.*

b) Suppose ω_j ends at v, so that (ω_j, ω_{j+1}) is a concatenation of two associated quasi-arcs $p' \rightsquigarrow v \rightsquigarrow p''$, where p' and p'' are in the vicinity of the puncture. We show in Proposition 4.2.13(2b) that p' and p'' must be distinct, so (ω_j, ω_{j+1}) is a quasi-backtrak. See Fig. 4.7(b).

Definition 4.2.6 (Laurent monomial from a T°-path)**.** *We identify each step with the label of the quasi-arc/boundary edge which it traverses and define the Laurent monomial $x(\omega)$ corresponding to a complete (T°, γ)-path ω by*

$$x(\omega) = \prod_{i \text{ odd}} x_{\omega_i} \prod_{i \text{ even}} x_{\omega_i}^{-1}.$$

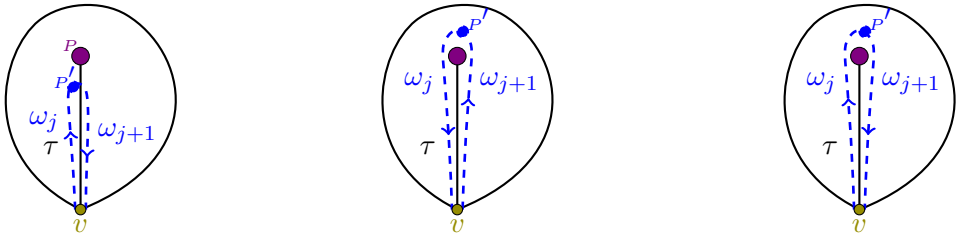

(a) Backtrack cycle. (b) Counterclockwise non-backtrack cycle. (c) Clockwise non-backtrack cycle.

Figure 4.6: The three possibilities of a pair (ω_j, ω_{j+1}) of consecutive steps along τ if T° has a self-folded triangle with τ as the radius.

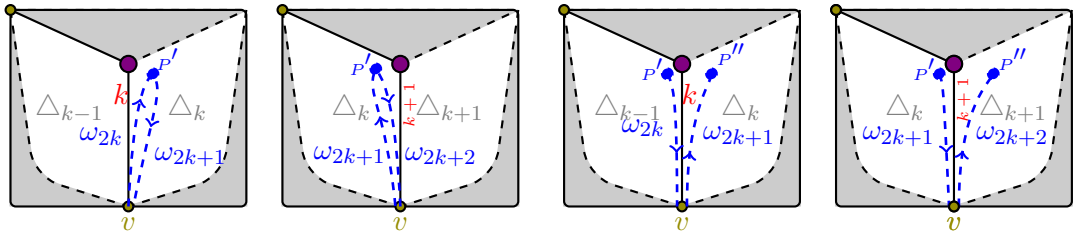

(a) Backtrack cycle $(\omega_{2k}, \omega_{2k+1})$ or $(\omega_{2k+1}, \omega_{2k})$. (b) Quasi-backtrack $(\omega_{2k}, \omega_{2k+1})$ or $(\omega_{2k+1}, \omega_{2k})$.

Figure 4.7: A pair (ω_j, ω_{j+1}) of consecutive steps along a radius τ is either a quasi-backtrack or a backtrack cycle if every ideal triangle of T° is an ordinary triangle.

Remark 4.2.7. *Two or more (T°, γ)-paths may correspond to the same Laurent monomial, e.g., see Example 4.2.9. For each (T°, γ)-path ω, the denominator of $x(\omega)$, before reducing, is equal to $x_{i_1}, x_{i_2}, \ldots, x_{i_d}$ which corresponds to the arcs $\tau_{i_1}, \ldots, \tau_{i_d}$ of T° which cross γ.*

Theorem 4.2.1 (T°-path formula for $\mathcal{C}_n$, an extension of [Sch10, Theorem 3.1], [ST09, Theorem 3.2])**.** *Let T° be an ideal triangulation of $\mathcal{C}_n$, let $\gamma \notin T^\circ$ be an ordinary arc of $\mathcal{C}_n$, and let x_γ denote the corresponding element in the cluster algebra which arises from $\mathcal{C}_n$ (see Theorem 2.2.11). Then*

$$x_\gamma = \sum_{\omega} x(\omega),$$

where the sum is taken over all (T°, γ)-paths. The formula does not depend on the

choice of orientation on γ.

The proof of Theorem 4.2.1 is given in Section 4.3.4. Note that, since $x_\ell := x_r x_{r^{(p)}}$, Theorem 4.2.1 also provides a formula for the cluster variable associated to every tagged arc of $\mathcal{C}_n$.

Example 4.2.8. *The following are the five (T°, γ)-paths for the situation of Fig. 4.3. Note that γ crosses 1, 2, 3 in order so $\tau_{i_1} = 1, \tau_{i_2} = 2$, and $\tau_{i_3} = 3$ in this example.*

1) $(b_1, 1, \underline{2, 2}, 4, 3, b_3)$,
2) $(b_1, 1, \underline{2, 2}, 2, 3, 4)$,
3) $(b_4, 1, b_2, \underline{2, 2}, 3, 4)$,
4) $(b_4, 1, b_2, 2, 4, 3, b_3)$,
5) $(b_4, \underline{1, 1}, 2, \underline{3, 3}, b_3)$.

Theorem 4.2.1 thus implies that

$$x_\gamma = \frac{x_{b_1}x_2x_4x_{b_3} + x_{b_1}x_2x_2x_4 + x_{b_4}x_{b_2}x_2x_4 + x_{b_4}x_{b_2}x_4x_{b_3} + x_{b_4}x_1x_3x_{b_3}}{x_1x_2x_3},$$

where $x_{b_j} = 1$ for each boundary edge b_j.

Example 4.2.9. *The nine (T°, γ)-paths from Fig. 4.8(a) are as follows (with the backtracks underlined):*

(1) $(b_4, 1, b_2, 2, b_3, \ell, \underline{r, r}, \underline{\ell, \ell}, b_3)$,
(2) $(b_4, \underline{1, 1}, 2, \underline{\ell, \ell}, \underline{r, r}, \underline{\ell, \ell}, b_3)$,
(3) $(b_1, 1, \underline{2, 2}, 2, \underline{\ell, \ell}, \underline{r, r}, \ell, 2)$,
(4) $(b_1, 1, \underline{2, 2}, b_3, \ell, \underline{r, r}, \underline{\ell, \ell}, b_3)$,
(5) $(b_4, 1, b_2, \underline{2, 2}, \underline{\ell, \ell}, \underline{r, r}, \ell, 2)$,
(6) $(b_4, 1, b_2, \underline{2, 2}, \underline{\ell, \ell}, \mathbf{r}, \mathbf{r}, \ell, b_3)$,
(7) $(b_4, 1, b_2, \underline{2, 2}, \ell, \mathbf{r}, \mathbf{r}, \underline{\ell, \ell}, b_3)$,
(8) $(b_1, 1, \underline{2, 2}, 2, \underline{\ell, \ell}, \mathbf{r}, \mathbf{r}, \ell, b_3)$,
(9) $(b_1, 1, \underline{2, 2}, 2, \ell, \mathbf{r}, \mathbf{r}, \underline{\ell, \ell}, b_3)$.

The last four of these (T°, γ)-paths contain a (counterclockwise) non-backtrack $(\mathbf{r}, \mathbf{r})$ and are illustrated in Fig. 4.8. They are drawn so that the backtrack cycles $(\underline{2, 2})$ and $(\underline{\ell, \ell})$ are ignored.

We apply Theorem 4.2.1 and replace each $(x_r x_\ell)/(x_\ell x_r x_\ell)$ *with* $1/x_\ell$ *and each* x_ℓ *with* $x_r x_{r^{(p)}}$ *to get*

$$x_\gamma = \big(x_{b_4}x_{b_2}x_{b_3}x_{b_3} + x_{b_4}x_1x_rx_{r^{(p)}}x_{b_3} + x_{b_1}x_2^3 + x_{b_1}x_{b_3}^2x_2 + x_{b_4}x_{b_2}x_2^2 + 2x_{b_4}x_{b_2}x_{b_3}x_2 + 2x_{b_1}x_{b_3}x_2^2\big)/(x_1x_2x_rx_{r^{(p)}}),$$

where $x_{b_j} = 1$ *for each boundary edge* b_j*.*

Example 4.2.10. *Consider the ideal triangulation* T *of a once-punctured disk and an arc* γ *in Fig. 4.10(a). Fig. 4.10 illustrates all five* (T°, γ)*-paths, which are listed as follows.*

1) $(b_1, 1, \overline{2, \underline{2}}, 2, 3, b_4)$ *3)* $(b_1, 1, \overline{2, 2}, 4, 3, b_3)$ *5)* $(4, \overline{1, \underline{1}}, 2, \underline{3, 3}, b_3)$

2) $(4, 1, b_2, \overline{2, \underline{2}}, 3, b_4)$ *4)* $(4, 1, b_2, 2, 4, 3, b_3)$

Note that the backtrack cycle $(\underline{3, 3})$ *in Fig. 4.10(f) is not drawn.*

Applying Theorem 4.2.1, we compute x_γ *to be*

$$x_\gamma = \frac{b_1\,x_2\,x_2\,b_4 + x_4\,b_2\,x_2\,b_4 + b_1\,x_2\,x_4\,b_3 + x_4\,b_2\,x_4\,b_3 + x_4\,x_1\,x_3\,b_3}{x_1\,x_2\,x_3}$$

where $x_{b_j} = 1$ *for each boundary edge* b_j*.*

Example 4.2.11. *Fig. 4.9 illustrates the four* (T°, γ)*-paths for the case where the ideal triangulation* T° *and the* ℓ*-loop* $\gamma \notin T^\circ$ *are illustrated in Fig. 4.9(a). In this example, no* (T°, γ)*-path contains any cycle* (ω_j, ω_{j+1})*.*

4.2.1 A non-backtrack cycle can only go along a self-folded triangle's radius

We prove the assertions from Remark 4.2.5.

Definition 4.2.12 (Crossing a self-folded triangle)**.** *Suppose that* T° *contains a self-folded triangle with radius* r*. We say that* γ *crosses* r *in the* counterclockwise direction *(respectively,* clockwise direction*) if it matches (respectively, if* γ *has the opposite orientation of) Fig. 4.5(d).*

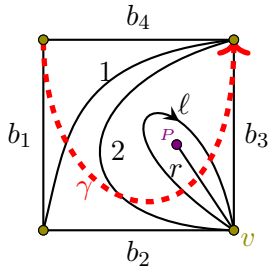

(a) An arc γ of $\mathcal{C}_4$ which crosses T° 5 times.

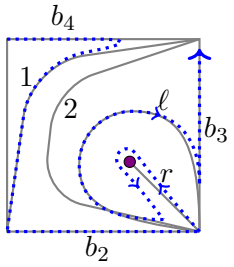

(b) $(b_4, 1, b_2, \underline{2, 2}, \underline{\ell, \ell}, \mathbf{r}, \mathbf{r}, \ell, b_3)$.

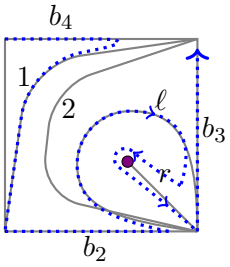

(c) $(b_4, 1, b_2, \underline{2, 2}, \ell, \mathbf{r}, \mathbf{r}, \underline{\ell, \ell}, b_3)$.

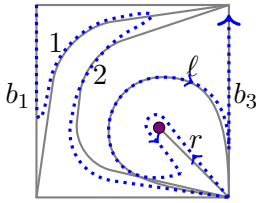

(d) $(b_1, 1, \underline{2, 2}, 2, \underline{\ell, \ell}, \mathbf{r}, \mathbf{r}, \ell, b_3)$.

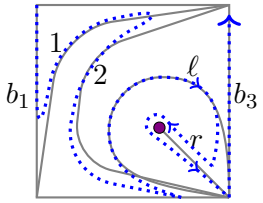

(e) $(b_1, 1, \underline{2, 2}, 2, \ell, \mathbf{r}, \mathbf{r}, \underline{\ell, \ell}, b_3)$.

Figure 4.8: The four (T°, γ)-paths (of T° and γ from Fig. 4.8(a)) which contain a (counterclockwise) non-backtrack cycle $(\mathbf{r}, \mathbf{r})$. All backtracks have been omitted, and steps are not drawn exactly along the arcs/boundary edges for illustration purposes

Proposition 4.2.13. *Let T° be an ideal triangulation of $\mathcal{C}_n$. Suppose γ is an ordinary arc which crosses $\tau \in T^\circ$, and let $\omega = (\omega_1, \ldots, \omega_{2d+1})$ be a (T°, γ)-path. Suppose (ω_j, ω_{j+1}) is a pair of steps both going along quasi-arcs associated to τ.*

1) *Suppose $\tau \in T^\circ$ is an ℓ-loop ℓ. Then (ω_j, ω_{j+1}) are two opposite orientations of ℓ, so that (ω_j, ω_{j+1}) is a backtrack cycle. See Remark* 4.2.5(1).

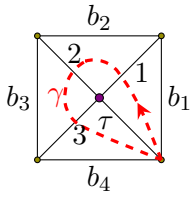

(a) An ℓ-loop γ of $\mathcal{C}_4$ which crosses T° 3 times.

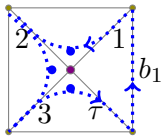

(b) $(b_1, 1, \overline{2,2}, \overline{3,3}, \tau)$.

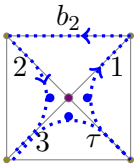

(c) $(\tau, 1, b_2, 2, \overline{3,3}, \tau)$.

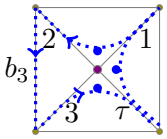

(d) $(\tau, \overline{1,1}, 2, b_3, 3, \tau)$.

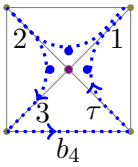

(e) $(\tau, \overline{1,1}, \overline{2,2}, 3, b_4)$.

Figure 4.9: The four (T°, γ)-paths of the ideal triangulation T° and the ℓ-loop γ of Fig. 4.9(a). Each path contains a quasi-backtrack $(\overline{1,1})$, $(\overline{2,2})$, or $(\overline{3,3})$.

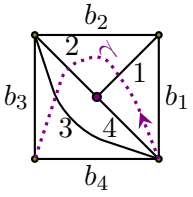

(a) An arc γ which crosses T° three times

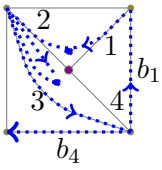

(b) $(b_1, 1, \overline{2,2}, 2, 3, b_4)$

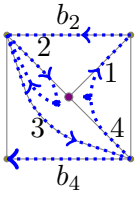

(c) $(4, 1, b_2, \overline{2,2}, 3, b_4)$

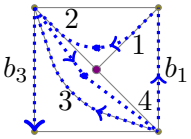

(d) $(b_1, 1, \overline{2,2}, 4, 3, b_3)$

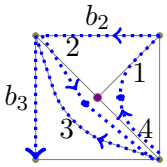

(e) $(4, 1, b_2, 2, 4, 3, b_3)$

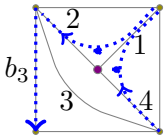

(f) $(4, \overline{1,1}, 2, \underline{3,3}, b_3)$

Figure 4.10: The five (T°, γ)-paths of the ideal triangulation T° and the arc γ of Fig. 4.10(a).

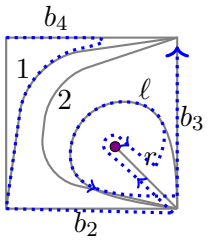

(a) A path with the same labels $(b_4, 1, b_2, \underline{2, 2}, \ell, \ell, \mathbf{r}, \mathbf{r}, \ell, b_3)$ as Fig. 4.8(b) but *fails* (T2) because $[p_4, p_5]_\omega$ is not homotopic to γ_4.

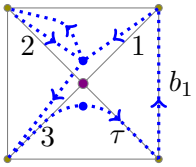

(b) A path with the same labels $(b_1, 1, \underline{2, 2}, \overline{3, 3}, \tau)$ as Fig. 4.9(b) but *fails* (T3) because $\omega_5 = 3$ starts outside $\triangle_2$.

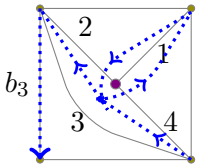

(c) A path with the same labels $(0, \overline{1, 1}, 2, \underline{3, 3}, b_3)$ as Fig. 4.10(f) but *fails* (T3) because $\omega_1 = 0$ starts outside $\triangle_0$ and $\omega_3 = 2$ finishes outside $\triangle_1$.

Figure 4.11: Examples of *non*-(T°, γ)-paths for the situations in Figs. 4.8(a), 4.9(a), and 4.10(a). Each path is homotopic to γ and satisfies (T1) but fails (T2) or (T3).

2) *Suppose T° does not contain any self-folded triangle, and let $\tau \in T^\circ$ be a radius between the puncture p and a marked point v on the boundary.*

   a) *Suppose that ω_j begins at v, so that (ω_j, ω_{j+1}) is a concatenation of two quasi-arcs $v \rightsquigarrow p' \rightsquigarrow v$ where p' is in the vicinity of the puncture. Then (ω_j, ω_{j+1}) is a backtrack cycle. See Remark* 4.2.5(2a).

   b) *Suppose that ω_j ends at v, so that (ω_j, ω_{j+1}) is a concatenation of two quasi-arcs $p' \rightsquigarrow v \rightsquigarrow p''$ where p' and p'' are in the vicinity of the puncture. Then $p' \neq p''$, and hence (ω_j, ω_{j+1}) is a quasi-backtrack. See Remark* 4.2.5(2b).

Remark 4.2.14. *In Examples 4.2.8 and 4.2.11, none of the (T°, γ)-paths include a non-backtrack cycle along a radius since T° contains no self-folded triangle (see Proposition 4.2.13(2a)). In contrast, four of the (T°, γ)-paths in Example 4.2.9 for (T°, γ)-paths*

contains a non-backtrack cycle. Furthermore, no cycle $p' \rightsquigarrow v \rightsquigarrow p'$ *can appear in general (see Proposition 4.2.13(2b)). See Fig. 4.11 and Example 4.2.17 for examples of non-*(T°, γ)*-paths.*

Proof of Proposition 4.2.13. First, we point out that the pair of steps (ω_j, ω_{j+1}) must be in the middle of the (T°, γ)-path, i.e.,

$$\text{the first step of } \omega \text{ cannot be } \omega_j \text{ and the last step of } \omega \text{ cannot be } \omega_{j+1}. \tag{4.2.1}$$

To see this, note that, by (T2), ω_1 goes along $\tau_{[\gamma_0]}$ or $\tau_{[\gamma_{-1}]}$, and ω_{2d+1} goes along $\tau_{[\gamma_d]}$ or $\tau_{[\gamma_{d+1}]}$. But, as illustrated in Fig. 4.4, $\tau_{[\gamma_j]} \neq \tau_{i_1}$ if $j \in \{0, -1\}$, and $\tau_{[\gamma_j]} \neq \tau_{i_d}$ if $j \in \{d, d+1\}$. Since, by (T1), ω_2 goes along τ_{i_1} and ω_{2d} goes along τ_{i_d}, we must have $1 < j$ and $j + 1 < d$.

We prove case (1): Suppose T° has a self-folded triangle with radius r and ℓ-loop ℓ, and $\tau = \ell$. For the sake of argument, suppose that ω_j and ω_{j+1} are the same orientation of ℓ. Note that every arc of T° other than ℓ has two distinct endpoints.

– First, suppose $j = 2k$ is even. Per (4.2.1), another even-indexed step $\omega_{2(k+1)}$ follows $(\omega_{2k}, \omega_{2k+1})$. Since ω_{2k+1} ends at v, the step ω_{2k+2} (crossing γ) must go from v along a different arc λ to a different marked point. Using the labels of Figs. 4.12(a), λ can be either r, א, or ב. We check all possible cases against (T1) and (T2) but only show one of the arguments here. Suppose $\lambda = r$ and γ is a peripheral arc crossing ℓ, r, and ℓ again in the counterclockwise direction as in Fig. 4.12(a) with $j = 2k$ and $j+1 = 2k+1$ so that $\omega_{2k} = \ell$ and $\omega_{2k+2} = r$. For contradiction, suppose $(\omega_{2k}, \omega_{2k+1})$ go along the clockwise orientation of ℓ twice. Recall that γ_k is the segment of γ from p_k (a point in the interior of ℓ) and p_{k+1} (a point in the interior of r) as in Fig. 4.12(b). By (T2), the segment γ_k must be homotopic to $[p_k, p_{k+1}]_\omega$ (see Definition 4.2.2 and Fig. 4.12(c)). However, as illustrated in Fig. 4.12(d), the concatenation of $[p_k, p_{k+1}]_\omega$ and the opposite orientation γ_k^- of γ_k is not contractible. Hence γ_k is not homotopic to $[p_k, p_{k+1}]_\omega$.

– Second, suppose $j = 2k + 1$ is odd. Again, per (4.2.1), there is another even-indexed step ω_{2k} (crossing γ, and going from a different marked point to v along a peripheral arc) which precedes $(\omega_{2k+1}, \omega_{2k+2})$. Using the same logic as in the previous paragraph, we show that $(\omega_{2k+1}, \omega_{2k+2})$ must go along two opposite orientations of ℓ in order for γ_k to be homotopic to $[p_k, p_{k+1}]_\omega$.

We prove case (2a): Suppose τ is a radius and a side of a regular triangle (hence T° has no self-folded triangle), and every arc of T° has two distinct endpoints.

– First, suppose $j = 2k$ is even. Per (4.2.1), another even-indexed step $\omega_{2(k+1)}$ follows $(\omega_{2k}, \omega_{2k+1})$. Since ω_{2k+1} ends at v, the step ω_{2k+2} (crossing γ) must be a peripheral step λ to a different point. But $(\omega_{2k}, \omega_{2k+1})$ would need to be contractible in order for γ_k to be homotopic to $[p_k, p_{k+1}]_\omega$.

– Second, suppose $j = 2k + 1$ is odd. Again, per (4.2.1), there is another even-indexed step ω_{2k} (crossing γ, and going from a different marked point to v along a peripheral arc λ) which precedes $(\omega_{2k+1}, \omega_{2k+2})$. But $(\omega_{2k+1}, \omega_{2k+2})$ would need to be contractible in order for γ_k to be homotopic to $[p_k, p_{k+1}]_\omega$.

We prove case (2b): First suppose $j = 2k+1$ is odd. Then ${}_P{}'$ is in the interior of $\triangle_k$ since ω_{2k+1} must start in the interior of $\triangle_k$ by (T3). The next step ω_{2k+2} then goes along τ from v to ${}_P{}''$. Since the last step of ω is an odd-indexed step, after ω_{2k+2} there must be another step ω_{2k+3} which starts at ${}_P{}''$. Again by (T3), ω_{2k+3} starts in the interior of $\triangle_{k+1}$. But $\triangle_k$ and $\triangle_{k+1}$ are distinct triangles since T° has no self-folded triangle. Hence ${}_P{}' \neq {}_P{}''$, and so $(\omega_{2k+1}, \omega_{2k+2})$ is a quasi-backtrack which starts in the interior of $\triangle_k$ and ends in the interior of $\triangle_{k+1}$.

If $j = 2k$ is even, then by a similar argument $(\omega_{2k}, \omega_{2k+1})$ is a quasi-backtrack which starts in the interior of $\triangle_{k-1}$ and ends in the interior of $\triangle_k$. See Fig. 4.7(b). □

4.2.2 A (T°, γ)-path ω on $\mathcal{C}_n$ is uniquely determined by its sequence of labels

Notation 4.2.15. *Let r and ℓ be the radius and ℓ-loop of a self-folded triangle, and let v be the boundary vertex on the boundary that is adjacent to ℓ. Let ℓ_+ (respectively, ℓ_-) denote the clockwise (respectively, counterclockwise) orientation along ℓ. (We mark each ℓ curve in our illustrations with an arrow pointing clockwise to remind the reader that ℓ_+ denotes the clockwise direction.)*

Consider the cycle (r, r)

$$v \rightsquigarrow {}_P{}' \rightsquigarrow v \text{ along } r$$

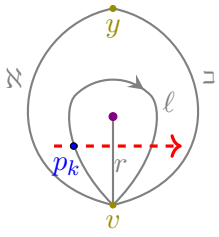

(a) γ crosses r in the counterclockwise direction

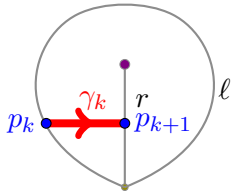

(b) γ_k is the segment of γ from p_k to p_{k+1}.

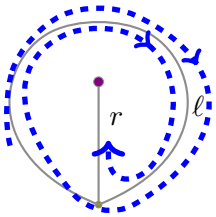

(c) $[p_k, p_{k+1}]_\omega$ goes along ℓ_+, ℓ_+, and r.

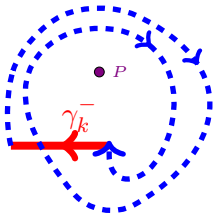

(d) Concatenation of $[p_k, p_{k+1}]_\omega$ and the opposite orientation of γ_k.

Figure 4.12: (ℓ_+, ℓ_+) is not a valid (T°, γ)-subpath.

from Remark 4.2.5(2a). Let $(\underline{r, r})$ denote the backtrack cycle and let $(\mathbf{r}, \mathbf{r})$ denote a (counterclockwise or clockwise) non-backtrack cycle.

The following proposition is an analogue of a remark from [Sch10, Section 3.1].

Proposition 4.2.16. *A (T°, γ)-path ω on $\mathcal{C}_n$ is uniquely determined by its sequence of labels $(\omega_1, \ldots, \omega_{2d+1})$, forgetting the orientations of the steps and whether a consecutive pair is a non-backtrack or a backtrack.*

Example 4.2.17. *To illustrate Proposition 4.2.16, consider the (T°, γ)-path of Fig. 4.8(b)*

$$\omega = (b_4, 1, b_2, 2, 2, \ell_+, \ell_-, \mathbf{r}, \mathbf{r}, \ell_+, b_3).$$

The pair $(\omega_8, \omega_9) = (\mathbf{r}, \mathbf{r})$ is a counterclockwise *non-backtrack along the radius r, and $\omega_{10} = \ell_+$ goes clockwise around ℓ. Consider a different path ω' (see Fig. 4.11(a)) which goes along the same sequence of arcs such that $(\omega'_8, \omega'_9) = (\mathbf{r}, \mathbf{r})$ is a* clockwise *non-backtrack along the radius, and $\omega'_{10} = \ell_-$ goes counterclockwise around ℓ. Even*

though ω' is homotopic to γ, the segment γ_4 is not homotopic to $[p_4, p_5]_\omega$, violating Definition 4.2.2(T2).

The paths illustrated in Figs. 4.11(b) and 4.11(c) go along associated quasi-arcs of the same arcs/edges as the (T°, γ)-paths of Figs. 4.9(b) and 4.10(f), but they fail axiom (T3), which requires each odd-indexed step ω_{2k+1} to start and finish in the interior of $\triangle_k$ or at a boundary marked point.

Proof of Proposition 4.2.16. For short, let the arcs $\tau_{i_1}, \ldots, \tau_{i_d}$ be denoted by arcs $1, \ldots, d$.

First, consider the subsequence $(\omega_1, \omega_2, \omega_3)$. There are four possibilities:

i) $\triangle_0$ is an ordinary triangle (Fig. 4.4(a)).

ii) $\triangle_0$ is an ideal triangle with two vertices where arc 1 is the loop (Fig. 4.4(b)).

iii) $\triangle_0$ is an ideal triangle with two vertices where arc 1 is not the loop (Fig. 4.4(c)).

iv) $\triangle_0$ is a self-folded triangle where arc 1 is the ℓ-loop (Fig. 4.4(d)).

For each of the first three cases, $\triangle_0$ has three distinct edges k, $\tau_{[\gamma_0]}$, and $\tau_{[\gamma_{-1}]}$. There are exactly two possible subpaths for (ω_1, ω_2), which are represented by two distinct sequences $(\tau_{[\gamma_0]}, 1)$ and $(\tau_{[\gamma_{-1}]}, 1)$.

In the fourth case, $\triangle_0$ is a self-folded triangle with radius r and ℓ-loop ℓ (see Fig. 4.4(d), top), so that $\tau_{[\gamma_0]} = \tau_{[\gamma_{-1}]} = r$. However, there are exactly two possible subpaths in this case as well.

Remark 4.2.18. *Suppose γ is a radius starting at the puncture, as in Fig. 4.4(d). Let v denote the vertex that ℓ is based at. Due to (T2), the first step ω_1 must go $_P{}' \rightsquigarrow v$ along $\tau_{[\gamma_0]} = \tau_{[\gamma_{-1}]} = r$, but there are two valid options for ω_2, to go counterclockwise or clockwise along ℓ, so that there are exactly two possibilities for (ω_1, ω_2):*

A1) (r, ℓ_-),

A2) (r, ℓ_+).

We continue with the proof of Proposition 4.2.16 in this fourth case. In particular, we show that (A1) and (A2) lead to distinct ways for the (T°, γ)-path to be finished. These two possible choices for (ω_1, ω_2) are represented by the same sequence $(\tau_{[\gamma_0]}, 1) = (\tau_{[\gamma_{-1}]}, 1)$, but we claim that the orientation of ω_2 determines the possible choices for

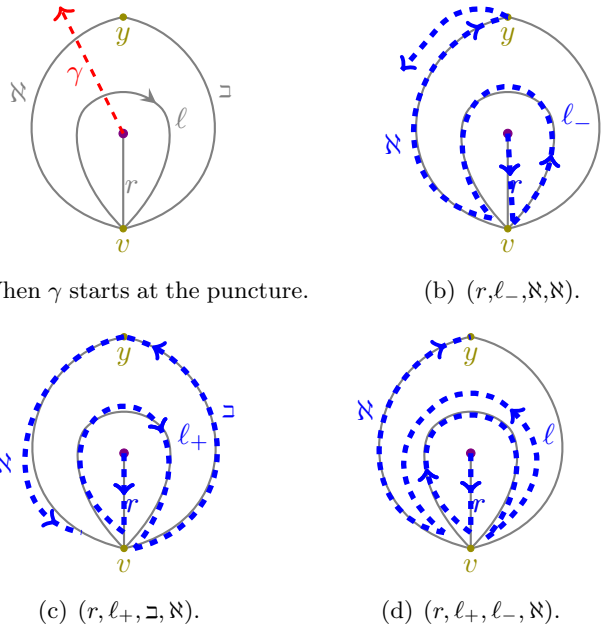

(a) When γ starts at the puncture.

(b) $(r,\ell_-,\aleph,\aleph)$.

(c) $(r,\ell_+,\beth,\aleph)$.

(d) $(r,\ell_+,\ell_-,\aleph)$.

Figure 4.13: The subpaths $(\omega_1,\ldots,\omega_4)$ of Remark 4.2.18(A1), (A2) when γ starts at p and crosses ℓ and $\aleph$. See Fig. 4.20.

the next term ω_3. Suppose that $\aleph$ (respectively, $\beth$) is the side of $\triangle_1$ which lies clockwise (respectively, counterclockwise) of ℓ, as illustrated in Fig. 4.13(a).

Suppose γ ends at the vertex y. If $\omega_2 = \ell_-$ is counterclockwise, then $\omega_3 = \aleph$ (Fig. 4.13(b)), otherwise $\omega_3 = \beth$ (Fig. 4.13(c)).

If γ does not end at y, then the second arc that γ crosses is either $\aleph$ or $\beth$ (say, $\aleph$). If $\omega_2 = \ell_-$ is counterclockwise, then $(\omega_3,\omega_4) = (\aleph,\aleph)$ (Fig. 4.13(b)). If $\omega_2 = \ell_+$ is clockwise, then $(\omega_3,\omega_4) = (\beth,\aleph)$ (Fig. 4.13(c)) or $(\ell_-,\aleph)$ (Fig. 4.13(d)). Hence, the subpath $(\omega_1,\omega_2,\omega_3)$ is either $(r,\ell_-,\aleph)$, (r,ℓ_+,b), or (r,ℓ_+,ℓ_-). As these are represented by three distinct subsequenes, each subsequence uniquely determines the first three steps of ω.

By the same logic, the subsequence $(\omega_{2d-1},\omega_{2d},\omega_{d+1})$ uniquely determines the last three steps of ω.

Next, consider any triple $(\omega_{2k},\omega_{2k+1},\omega_{2k+2})$. There are four possibilities:

i) $\triangle_k$ is an ordinary triangle (Fig. 4.5(a)).

ii) $\triangle_k$ is an ideal triangle with two vertices where neither arc k nor arc $k+1$ are loops (Fig. 4.5(b)).

iii) $\triangle_k$ is an ideal triangle with two vertices where one of arcs k and $k+1$ (say, $k+1$) is a loop (Fig. 4.5(c)).

iv) $\triangle_k$ is a self-folded triangle with radius r and ℓ-loop ℓ where one of arcs k and $k+1$ (say, $k+1$) is the radius r (Fig. 4.5(d)).

For each of the first three cases, $\triangle_k$ has three distinct edges k, $k+1$, and $\tau_{[\gamma_k]}$. There are exactly three legal subpaths for $(\omega_{2k}, \omega_{2k+1}, \omega_{2k+2})$, and they are represented by three distinct sequences $(k, k+1, k+1)$, $(k, k, k+1)$, and $(k, \tau_{[\gamma_k]}, k+1)$. In the case that one of these steps is an ℓ-loop, it is also clear that (T2) forces a specific orientation along ℓ as part of the (T°, γ)-path.

In the fourth case, γ crosses ℓ, r, then ℓ in either the counterclockwise or clockwise (say, the former) direction.

Lemma 4.2.19. *Suppose T° contains a self-folded triangle with radius r and ℓ-loop ℓ, and suppose that γ crosses r, say, in the counterclockwise direction. Let v be the boundary vertex on the boundary that is adjacent to ℓ. Suppose ℓ, r, ℓ are the k-th, $(k+1)$-th, and $(k+2)$-th arcs crossed by γ (see Fig. 4.5(d)). Then there are exactly three possible subpaths for $(\omega_{2k}, \omega_{2k+1}, \omega_{2(k+1)})$:*

*a*1) $(\ell_-, \underline{r, r})$*: follow ℓ_- then backtrack cycle $(\underline{r, r})$ (Fig. 4.14(1)),*

*a*2) (ℓ_+, ℓ_-, r)*: follow (ℓ_+, ℓ_-) then follow r from v to P' (a point in the vicinity of the puncture) (Fig. 4.14(2)),*

*a*3) $(\ell_+, \mathbf{r}, \mathbf{r})$*: follow ℓ_+ then counterclockwise non-backtrack cycle $(\mathbf{r}, \mathbf{r})$ (Fig. 4.14(3)).*

There are also exactly three possible subpaths for $(\omega_{2(k+1)}, \omega_{2k+3}, \omega_{2(k+2)})$:

*b*1) (r, ℓ_-, ℓ_+)*: follow r from P' (a point in the vicinity of the puncture) to v then (ℓ_-, ℓ_+) (see Fig. 4.15(1)),*

*b*2) $(\underline{r, r}, \ell_-)$*: backtrack cycle $(\underline{r, r})$ then ℓ_- (Fig. 4.15(2)),*

*b*3) $(\mathbf{r}, \mathbf{r}, \ell_+)$*: counterclockwise non-backtrack cycle $(\mathbf{r}, \mathbf{r})$ then ℓ_+ (Fig. 4.15(3)).*

The (ℓ, r, r, ℓ, ℓ)*-subsequence corresponds to exactly* 2 *valid subpaths for* $(\omega_{2k}, \ldots, \omega_{2k+2})$*, one where* $(\underline{r, r})$ *is a backtrack and the other where* $(\mathbf{r}, \mathbf{r})$ *is a non-backtrack. We get them by combining* $(a1)$ *with* $(b1)$ *and combining* $(a3)$ *with* $(b1)$*:*

I) $(\ell_-, \underline{r, r}, \ell_-, \ell_+)$*: follow* ℓ_- *then backtrack cycle* $(\underline{r, r})$ *then* (ℓ_-, ℓ_+)*.*

II) $(\ell_+, \mathbf{r}, \mathbf{r}, \ell_-, \ell_+)$*: follow* ℓ_+ *then counterclockwise non-backtrack cycle* $(\mathbf{r}, \mathbf{r})$ *then* (ℓ_-, ℓ_+)*.*

Similarly, the (ℓ, ℓ, r, r, ℓ)*-subsequence would correspond to exactly two valid subpaths, one where* $(\underline{r, r})$ *is a backtrack and the other where* $(\mathbf{r}, \mathbf{r})$ *is a non-backtrack. We get them by combining* $(a2)$ *with* $(b2)$*, and combining* $(a2)$ *with* $(b3)$*.*

III) $(\ell_+, \ell_-, \underline{r, r}, \ell_-)$*: follow* ℓ_+*, then* ℓ_- *then backtrack cycle* $(\underline{r, r})$ *then* ℓ_-*.*

IV) $(\ell_+, \ell_-, \mathbf{r}, \mathbf{r}, \ell_+)$*: follow* ℓ_+*, then* ℓ_- *then counterclockwise non-backtrack cycle* $(\mathbf{r}, \mathbf{r})$ *then* ℓ_+*.*

Remark 4.2.20. *In Lemma 4.2.19, note that the subpaths (I) and (III) are homotopic to a counterclockwise orientation of* ℓ*. The subpaths (II) and (IV) are contractible to* v*.*

Proof of Lemma 4.2.19. By (T1), since the k-th, $(k+1)$-th, $(k+2)$-th arcs crossed by γ are ℓ, r, and ℓ, the sequence

$$(\omega_{2k}, \omega_{2k+1}, \omega_{2(k+1)}, \omega_{2k+3}, \omega_{2(k+2)})$$

must be

$$(\ell, \quad , r, \quad , \ell).$$

For this to be a connected path, we must fill in the odd steps with ℓ then r (or r then ℓ) by (T2), so that the 5-term subsequence is either (ℓ, r, r, ℓ, ℓ) or (ℓ, ℓ, r, r, ℓ).

The two subpaths (a1) and (a3) (both represented by (ℓ, r, r)) satisfy (T2):

Case (a1) If $(\omega_{2k}, \omega_{2k+1}, \omega_{2(k+1)}) = (\ell_-, \underline{r, r})$ (where $(\underline{r, r})$ is a backtrack cycle), the concatenation of $[p_k, p_{k+1}]_\omega$ and the opposite orientation ${\gamma_k}^-$ of γ_k is contractible, so $[p_k, p_{k+1}]_\omega$ and γ_k are homotopic. See Fig. 4.16(a).

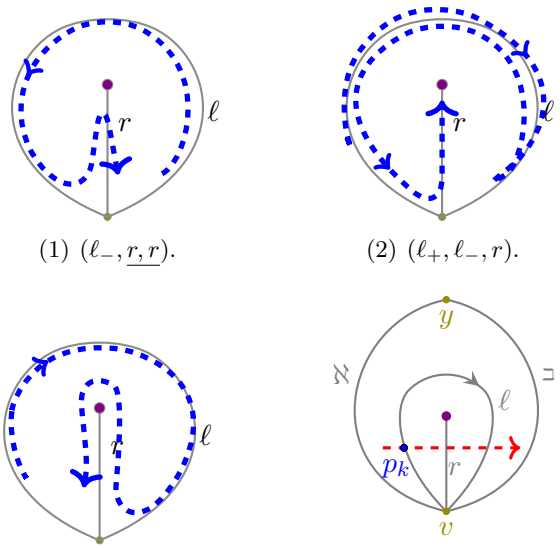

(1) $(\ell_-, \underline{r, r})$. (2) (ℓ_+, ℓ_-, r).

(3) $(\ell_+, \mathbf{r}, \mathbf{r})$. (4) γ crosses r in the counterclockwise direction.

Figure 4.14: The subpaths $(\omega_{2k}, \omega_{2k+1}, \omega_{2k+2})$ of Lemma 4.2.19(a1), (a2), (a3) if γ crosses arcs $\tau_{i_k} = \ell$, $\tau_{i_{k+1}} = r$, and $\tau_{i_{k+2}} = \ell$ in the counterclockwise order. See Fig. 4.21.

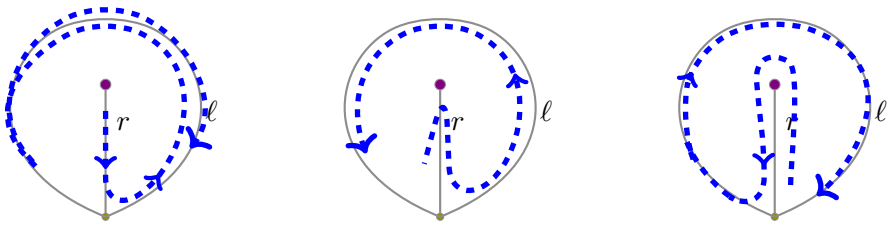

(1) (r, ℓ_-, ℓ_+). (2) $(\underline{r, r}, \ell_-)$. (3) $(\mathbf{r}, \mathbf{r}, \ell_+)$.

Figure 4.15: The subpaths $(\omega_{2k+2}, \omega_{2k+3}, \omega_{2k+4})$ of Lemma 4.2.19(b1), (b2), (b3) if γ crosses arcs $\tau_{i_k} = \ell$, $\tau_{i_{k+1}} = r$, and $\tau_{i_{k+2}} = \ell$ in the counterclockwise order. See Fig. 4.22.

Case (a3) If $(\omega_{2k}, \omega_{2k+1}, \omega_{2(k+1)}) = (\ell_+, \mathbf{r}, \mathbf{r})$ (where $(\mathbf{r}, \mathbf{r})$ is a counterclockwise non-backtrack cycle), the concatenation of $[p_k, p_{k+1}]_\omega$ and the opposite orientation $\gamma_k{}^-$ of γ_k is contractible, so $[p_k, p_{k+1}]_\omega$ and γ_k are homotopic. See Fig. 4.16(b).

The sequence (ℓ, r, r) may also represent a subpath $(\ell_+, \underline{r, r})$ where $(\underline{r, r})$ is a backtrack

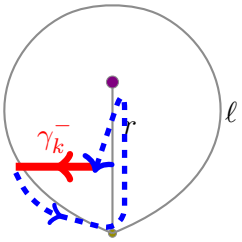

(a) Concatenation of $[p_k, p_{k+1}]_\omega$ (ℓ_-,$\underline{r, r}$(backtrack)) and γ_k^- *is* contractible, so $[p_k, p_{k+1}]_\omega$ is homotopic to γ_k.

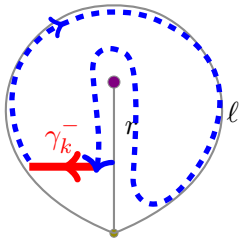

(b) Similarly, $[p_k, p_{k+1}]_\omega$ (ℓ_+,$\mathbf{r}, \mathbf{r}$ (counterclockwise non-backtrack)) is homotopic to γ_k.

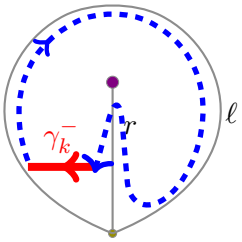

(c) $[p_k, p_{k+1}]_\omega$ (ℓ_+,$\underline{r, r}$(backtrack)) is *not* homotopic to γ_k.

Figure 4.16: Concatenation of $[p_k, p_{k+1}]_\omega$ (ℓ, r, r) and the opposite orientation of γ_k^- of γ_k.

or $(\ell_-, \mathbf{r}, \mathbf{r})$ where $(\mathbf{r}, \mathbf{r})$ is a non-backtrack cycle, but we claim that these are not valid T°-subpath: For contradiction, suppose $(\omega_{2k}, \omega_{2k+1}, \omega_{2k+2}) = (\ell_+, \underline{r, r})$ where $(\underline{r, r})$ is a backtrack. By (T2), the segment γ_k (Fig. 4.12(b)) must be homotopic to $[p_k, p_{k+1}]_\omega$. However, as illustrated in Fig. 4.16(c), the concatenation of $[p_k, p_{k+1}]_\omega$ and the opposite orientation ${\gamma_k}^-$ of γ_k is not contractible. Hence γ_k is not homotopic to $[p_k, p_{k+1}]_\omega$, and so this subpath does not appear. Similarly, no subpath $(\ell_-, \mathbf{r}, \mathbf{r})$ with a non-backtrack cycle $(\mathbf{r}, \mathbf{r})$ can appear.

By similar logic,

– (a2) is the only valid T°-subpath which can be represented by (ℓ, ℓ, r),

– (b1) is the only valid T°-subpath which can be represented by (r, ℓ, ℓ), and

– (b2) and (b3) are the only two valid T°-subpaths which can be represented by (r, r, ℓ).

This concludes our proof of Lemma 4.2.19. □

We continue with the proof of Proposition 4.2.16. Note that the subpaths (I) and (II) are represented by the same 5-term subsequence (ℓ, r, r, ℓ, ℓ). We claim that the steps ω_{2k-1} which precede (I) and (II) go along distinct arcs/edges. Note that the ideal triangle $\triangle_{k-1}$ is a two-vertex, three-edge triangle (Fig. 2.1(b)).

Case 1: Suppose $k = 1$, so that γ starts at the marked point y. Recall that the side of $\triangle_0$ that lies clockwise of ℓ is $\tau_{[\gamma_0]}$, and the side of $\triangle_0$ that lies counterclockwise of ℓ is $\tau_{[\gamma_{-1}]}$ (see Fig. 4.4(b)). In Fig. 4.14(4), $\tau_{[\gamma_0]} = \aleph$ and $\tau_{[\gamma_{-1}]} = \beth$.

- Since (I) starts with a counterclockwise ℓ_- step, the first step ω_1 must go along $\tau_{[\gamma_{-1}]}$. So the first six-term subsequence is $(\tau_{[\gamma_{-1}]}, \ell, r, r, \ell, \ell)$.
- Since (II) starts with a clockwise ℓ_+ step, the first step ω_1 must go along $\tau_{[\gamma_0]}$. So the first six-term subsequence is $(\tau_{[\gamma_0]}, \ell, r, r, \ell, \ell)$.

Case 2: Suppose $1 < k$, so that γ crosses arc $k-1$ (in Fig. 4.14(4), this arc is either $\aleph$ or $\beth$.) Suppose (without loss of generality) that arc $k-1$ lies clockwise of ℓ (i.e., arc $k-1$ is $\aleph$ in Fig. 4.14(4)). Then the third arc $\tau_{[\gamma_{k-1}]}$ of $\triangle_{k-1}$ lies counterclockwise of ℓ (i.e., side $\tau_{[\gamma_{k-1}]}$ is $\beth$ in Fig. 4.14(4)). Recall that ω_{2k-2} must traverse arc $k-1$ by (T1).

- Since (I) starts with a counterclockwise ℓ_- step, the previous step ω_{2k-1} must go along either ℓ or $\tau_{[\gamma_{k-1}]}$ (i.e., side $\beth$ in Fig. 4.14(4)), so that $(\omega_{2k-1}, \ldots, \omega_{2(k+2)})$ form a six-term subsequence $(\ell, \ell, r, r, \ell, \ell)$ or $(\tau_{[\gamma_{k-1}]}, \ell, r, r, \ell, \ell)$.
- Since (II) starts with a clockwise ℓ_+ step, the previous step ω_{2k-1} must go along arc $k-1$ (i.e., arc $\aleph$ in Fig. 4.14(4)), so that $(\omega_{2k-1}, \ldots, \omega_{2(k+2)}) = (k-1, \ell, r, r, \ell, \ell)$.

Similarly, the subpaths (III) and (IV) are represented by the same 5-term subsequence $(\ell, \ell, r,\ r, \ell)$. We claim that the steps $\omega_{2(k+2)+1}$ following (III) and (IV) go along distinct arc/edges. Note that the ideal triangle $\triangle_{k+2}$ is a two-vertex, three-edge triangle (Fig. 2.1(b)).

Case 1: Suppose $d = k+2$, so that γ ends at the marked point y. Recall that the side of $\triangle_d$ that lies clockwise of ℓ is $\tau_{[\gamma_d]}$, and the side of $\triangle_0$ that lies counterclockwise of ℓ is $\tau_{[\gamma_{d+1}]}$ (see Fig. 4.4(b)). In Fig. 4.14(4), $\tau_{[\gamma_d]} = \aleph$ and $\tau_{[\gamma_{d+1}]} = \beth$.

- Since (III) ends with a counterclockwise ℓ_-, the last step must go along $\tau_{[\gamma_d]}$, so that the last six-term subsequence is $(\ell, \ell, r, r, \ell, \tau_{[\gamma_d]})$
- Since (IV) ends with a clockwise ℓ_+, the last step must go along $\tau_{[\gamma_{d+1}]}$, so that the last six-term subsequence is $(\ell, \ell, r, r, \ell, \tau_{[\gamma_{d+1}]})$.

Case 2: Suppose $d > k+2$, so that γ crosses arc $k+3$ (in Fig. 4.14(4), this arc is either ℵ or ב.) Suppose (without loss of generality) that arc $k+3$ lies clockwise of ℓ (i.e., arc $k+3$ is ℵ in Fig. 4.14(4)). Then the third arc $\tau_{[\gamma_{k+2}]}$ of $\triangle_{k+2}$ lies counterclockwise of ℓ (i.e., side $\tau_{[\gamma_{k+2}]}$ is ב in Fig. 4.14(4)).

- Since (III) ends with a counterclockwise ℓ_-, the next step ω_{2k+5} must go along arc $k+3$ (i.e., arc ℵ in Fig. 4.14(4)), so that $(\omega_{2k}, \ldots, \omega_{2k+5}) = (\ell, \ell, r, r, \ell, k+3)$.
- Since (IV) ends with a clockwise ℓ_+, the next step ω_{2k+5} must go along either counterclockwise ℓ_- or $\tau_{[\gamma_{k+2}]}$ (i.e., arc/edge labeled ב in Fig. 4.14(4)), so that $(\omega_{2k}, \ldots, \omega_{2k+5})$ form a six-term subsequence $(\ell, \ell, r, r, \ell, \ell)$ or $(\ell, \ell, r, r, \ell, \tau_{[\gamma_{k+2}]})$. □

4.3 Proof of Theorem 4.2.1, the (T°, γ)-path expansion formula for a once-punctured disk

We begin with an outline of our proof. Let T° be an ideal triangulation of a once-punctured n-gon $\mathcal{C}_n$ and let $\gamma \notin T^\circ$ be an oriented ordinary arc (possibly an ℓ-loop).

Step 1: Following [MSW11, Section 7], we construct a triangulated $(d+3)$-gon $\widetilde{S_\gamma}$ (modeled after $\triangle_0, \ldots, \triangle_d$). See Section 4.3.1.

Step 2: In Section 4.3.2, we give a bijection $\overline{\pi}$: $\{(\widetilde{S_\gamma}, \widetilde{\gamma})\text{-paths}\} \to \{(T^\circ, \gamma)\text{-paths}\}$.

Step 3: Section 4.3.3 recaps [MSW11, Theorem 4.10], a T°-expansion of x_γ in terms of perfect matchings of a snake graph $G_{T^o,\gamma}$.

Step 4: [MS10, Lemma 4.5] gives a bijection F: {perfect matchings of $G_{T^o,\gamma}$} $\to$ $\{(\widetilde{S_\gamma}, \widetilde{\gamma})\text{-paths}\}$. See Section 4.3.4.

Step 5: The composition $\overline{\pi} \circ F$ gives a bijection between perfect matchings of $G_{T^o,\gamma}$ and (T°, γ)-paths. Applying $\overline{\pi} \circ F$ to [MSW11, Theorem 4.10] yields Theorem 4.2.1.

4.3.1 A triangulated polygon $\widetilde{S_\gamma}$ and a lifted arc $\widetilde{\gamma}$

Let T° be an ideal triangulation of a once-punctured n-gon $\mathcal{C}_n$ and let $\gamma \notin T^\circ$ be an oriented ordinary arc (possibly an ℓ-loop) from the point s to the point t. Let S_γ be the union of the ideal triangles $\triangle_k$ $(k = 0, \ldots, d)$ crossed by γ. First, for each $k = 0, \ldots, d$, we build a triangle $\widetilde{\triangle}_k$ with three distinct labels.

Definition 4.3.1 (triangles $\widetilde{\triangle}_k$)**.** *If $\triangle_k$ has three distinct sides, its lift $\widetilde{\triangle}_k$ is an ordinary triangle with the edge labels $\widetilde{\tau}_{i_k} = \tau_{i_k}$, $\widetilde{\tau}_{i_{k+1}} = \tau_{i_{k+1}}$, $\widetilde{\tau}_{[\gamma_k]} = \tau_{[\gamma_k]}$, and the same orientation as $\triangle_k$.*

When $\triangle_k$ is a self-folded triangle with radius r and ℓ-loop ℓ, its lift $\widetilde{\triangle}_k$ is formed by two lifts of r and a lift of ℓ, as follows:

Case $k = 1$ or d: If $k = 0$, then $\widetilde{\triangle}_0$ has edge labels $\widetilde{\tau}_{i_1} = \ell$, $\widetilde{\tau}_{[\gamma_0]} = r$, $\widetilde{\tau}_{[\gamma_{-1}]} = r^{cc}$ (arranged in clockwise order). Similarly, if $k = d$, then $\widetilde{\triangle}_d$ has edge labels $\widetilde{\tau}_{i_d} = \ell$, $\widetilde{\tau}_{[\gamma_d]} = r$, $\widetilde{\tau}_{[\gamma_{d+1}]} = r^{cc}$ (arranged in clockwise order). See Fig. 4.17(b).

Case $0 < k < d$: Suppose $k = \ell$, $k + 1 = r$, and $k + 2 = \ell$. Then $\widetilde{\triangle}_k$ has three distinct edge labels $\widetilde{\tau}_{i_k}$, $\widetilde{\tau}_{i_{k+1}}$, and $\widetilde{\tau}_{[\gamma_k]}$: If γ crosses r in counterclockwise (respectively, clockwise) direction, let $\widetilde{\tau}_{i_{k+1}} = r$ be the label of the edge of $\widetilde{\triangle}_k$ which lies counterclockwise (respectively, clockwise) of $\widetilde{\tau}_{i_k} = \ell$. Let $\widetilde{\tau}_{[\gamma_k]} = \dot{r}$ be the label of the third edge of $\widetilde{\triangle}_k$.

Similarly, $\widetilde{\triangle}_{k+1}$ has three distinct edge labels $\widetilde{\tau}_{i_{k+1}}$, $\widetilde{\tau}_{i_{k+2}}$, and $\widetilde{\tau}_{[\gamma_{k+1}]}$: If γ crosses r in counterclockwise (respectively, clockwise) direction, let $\widetilde{\tau}_{[\gamma_{k+1}]} = \ddot{r}$ be the label of the edge of $\widetilde{\triangle}_{k+1}$ which lies counterclockwise (respectively, clockwise) of $\widetilde{\tau}_{i_{k+2}} = \ell$. Let r be the label of the third edge of $\widetilde{\triangle}_{k+1}$. See Figs. 4.17(e) and 4.17(f).

Definition 4.3.2 (triangulated $(d+3)$-gon)**.** *Glue $\widetilde{\triangle}_1$ to $\widetilde{\triangle}_0$ along τ_{i_1}, glue $\widetilde{\triangle}_2$ to $\widetilde{\triangle}_1$ along τ_{i_2}, and so forth to form a triangulated $(d+3)$-gon $\widetilde{S_\gamma}$ with internal edges*

$$\widetilde{\tau}_{i_1}, \ldots, \widetilde{\tau}_{i_d}$$

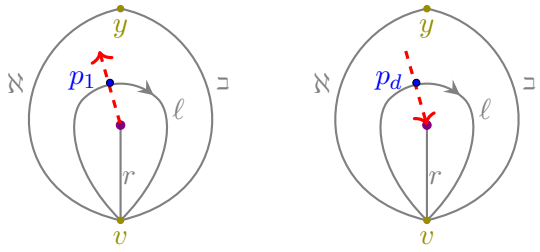

(a) γ is a radius starting or ending at the puncture.

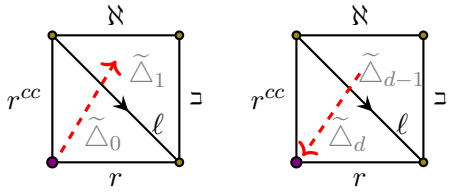

(b) The triangle $\widetilde{\triangle}_0$ or $\widetilde{\triangle}_d$ when γ is a radius starting or ending at the puncture.

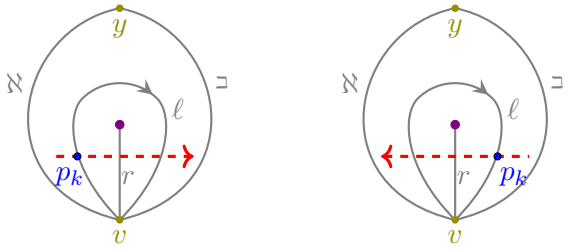

(c) γ crosses r in the counterclockwise direction.

(d) γ crosses r in the clockwise direction.

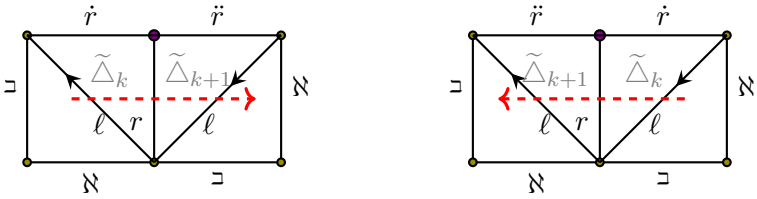

(e) The triangles $\widetilde{\triangle}_k$, $\widetilde{\triangle}_{k+1}$ when γ crosses a self-folded triangle's radius r in the counterclockwise direction.

(f) The triangles $\widetilde{\triangle}_k$, $\widetilde{\triangle}_{k+1}$ when γ crosses a self-folded triangle's radius r in the clockwise direction.

Figure 4.17: The triangles $\widetilde{\triangle}_k$ when γ crosses an ℓ-loop.

and boundary edges

$$\widetilde{\tau}_{[\gamma_{-1}]}, \widetilde{\tau}_{[\gamma_0]}, \ldots, \widetilde{\tau}_{[\gamma_{d+1}]}.$$

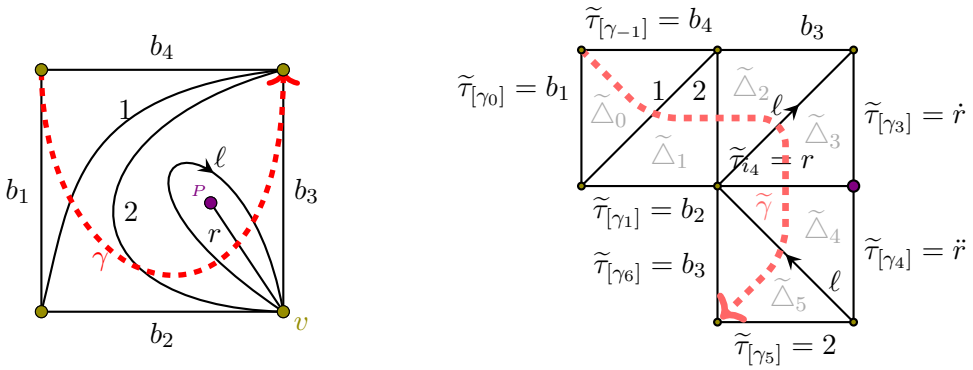

(a) Arc γ of $\mathcal{C}_4$ where $d = 5$. (b) Lifted arc $\widetilde{\gamma}$ on the constructed triangulated $(5+3)$-gon $\widetilde{S_\gamma}$.

Figure 4.18: The construction of the triangulated polygon $\widetilde{S_\gamma}$ and lifted arc $\widetilde{\gamma}$ for T° and γ from Fig. 4.18(a).

Let the lift $\widetilde{s} = \widetilde{p}_0$ of $s = p_0$ be the vertex of $\widetilde{\triangle}_0$ that is adjacent to the lifted edges $\widetilde{\tau}_{[\gamma_0]}$ and $\widetilde{\tau}_{[\gamma_{-1}]}$, and the lift $\widetilde{t} = \widetilde{p}_{d+1}$ of $t = p_{d+1}$ be the vertex of $\widetilde{\triangle}_d$ that is adjacent to the lifted edges $\widetilde{\tau}_{[\gamma_d]}$ and $\widetilde{\tau}_{[\gamma_{d+1}]}$. If $k = 1, \ldots, d-1$, let $\widetilde{p}_k$, $\widetilde{p}_{k+1}$ denote the lifts of p_k, p_{k+1} on $\widetilde{\triangle}_k$ which lies on the interior of $\widetilde{\tau}_{i_k}$, $\widetilde{\tau}_{i_{k+1}}$ (respectively).

Let $\widetilde{\gamma}$ be the arc in $\widetilde{S_\gamma}$ from $\tilde{s}$ to $\tilde{t}$. We call $\widetilde{\gamma}$ the lift *of γ. Let $\pi \colon \widetilde{S_\gamma} \to S_\gamma$ denote the covering map of $\widetilde{S_\gamma} \to S_\gamma$. See Fig. 4.18(b) for the lifts $\widetilde{\gamma}$ and $\widetilde{S_\gamma}$ of γ and S_γ of Fig. 4.18(a).*

Remark 4.3.3. *By construction, $\widetilde{\tau}_{i_k} = \tau_{i_k}$ for each k. Furthermore, $\widetilde{\tau}_{[\gamma_k]} = \tau_{[\gamma_k]}$ unless $\widetilde{\tau}_{[\gamma_k]}$ has label $\dot{r}$, $\ddot{r}$, or r^{cc}. In addition, $\widetilde{\tau}_{[\gamma_0]}, \widetilde{\tau}_{[\gamma_d]} \notin \{\dot{r}, \ddot{r}, r^{cc}\}$, so $\widetilde{\tau}_{[\gamma_0]} = \tau_{[\gamma_0]}$, $\widetilde{\tau}_{[\gamma_d]} = \tau_{[\gamma_d]}$.*

4.3.2 A bijection $\overline{\pi}$ between $(\widetilde{S_\gamma}, \widetilde{\gamma})$-paths and (T°, γ)-paths

Keep the same setup as in the previous section, where T° is an ideal triangulation of $\mathcal{C}_n$ and $\gamma \notin T^\circ$ is an ordinary arc of $\mathcal{C}_n$. As $\widetilde{S_\gamma}$ is a triangulation of a polygon, we can consider a $(\widetilde{S_\gamma}, \widetilde{\gamma})$-path $\widetilde{\omega} = (\widetilde{\omega}_1, \ldots, \widetilde{\omega}_{2d+1})$ as defined in Definition 4.2.2. For example, the $(\widetilde{S_\gamma}, \widetilde{\gamma})$-paths of Fig. 4.19 correspond to the four (T°, γ)-paths of Fig. 4.8.

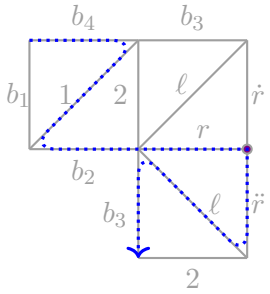

(a) $(b_4, 1, b_2, \underline{2, 2}, \underline{\ell, \ell}, \mathbf{r}, \ddot{\mathbf{r}}, \ell, b_3)$.

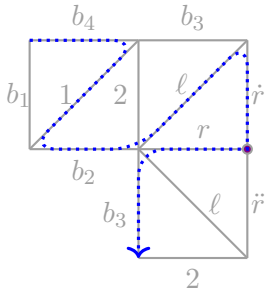

(b) $(b_4, 1, b_2, \underline{2, 2}, \ell, \dot{\mathbf{r}}, \mathbf{r}, \underline{\ell, \ell}, b_3)$.

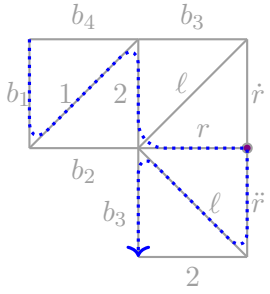

(c) $(b_1, 1, \underline{2, 2}, 2, \underline{\ell, \ell}, \mathbf{r}, \ddot{\mathbf{r}}, \ell, b_3)$.

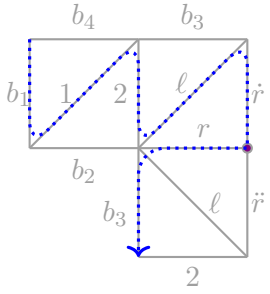

(d) $(b_1, 1, \underline{2, 2}, 2, \ell, \dot{\mathbf{r}}, \mathbf{r}, \underline{\ell, \ell}, b_3)$.

Figure 4.19: The $(\widetilde{T^o}, \widetilde{\gamma})$-paths corresponding to the four (T°, γ)-paths from Fig. 4.8. All backtracks have been omitted.

Lemma 4.3.4. *The covering map* $\pi\colon \widetilde{S_\gamma} \to S_\gamma$ *which gives*

$$\pi(\widetilde{\omega}_j) = \begin{cases} r & \text{if } \widetilde{\omega}_j \text{ has label } \dot{r},\ \ddot{r}, \text{ or } r^{cc}, \\ \text{the same label as } \widetilde{\omega}_j & \text{otherwise.} \end{cases}$$

induces a bijection

$$\overline{\pi}\colon\ \{(\widetilde{S_\gamma}, \widetilde{\gamma})\text{-paths in } \widetilde{S_\gamma}\} \to \{(T^\circ, \gamma)\text{-paths in } S_\gamma\},$$
$$\overline{\pi}(\widetilde{\omega}_1, \widetilde{\omega}_2, \ldots, \widetilde{\omega}_{2d+1}) = (\pi(\widetilde{\omega}_1), \pi(\widetilde{\omega}_2), \ldots, \pi(\widetilde{\omega}_{2d+1})).$$

Proof. Let $\widetilde{\omega}$ be a $(\widetilde{S_\gamma}, \widetilde{\gamma})$-path. Note that, since $\widetilde{S_\gamma}$ is a polygon, there is only one way to concatenate a pair $(\widetilde{\omega}_j, \widetilde{\omega}_{j+1})$ of steps. By (T1), every $\widetilde{\omega}_{2k}$ has label $\widetilde{\tau}_{i_k}$, and every ω_{2k} has label τ_{i_k}. Per Remark 4.3.3, $\widetilde{\tau}_{i_k}$ has the same label as τ_{i_k}, and $\widetilde{\tau}_{[\gamma_j]}$ has the same

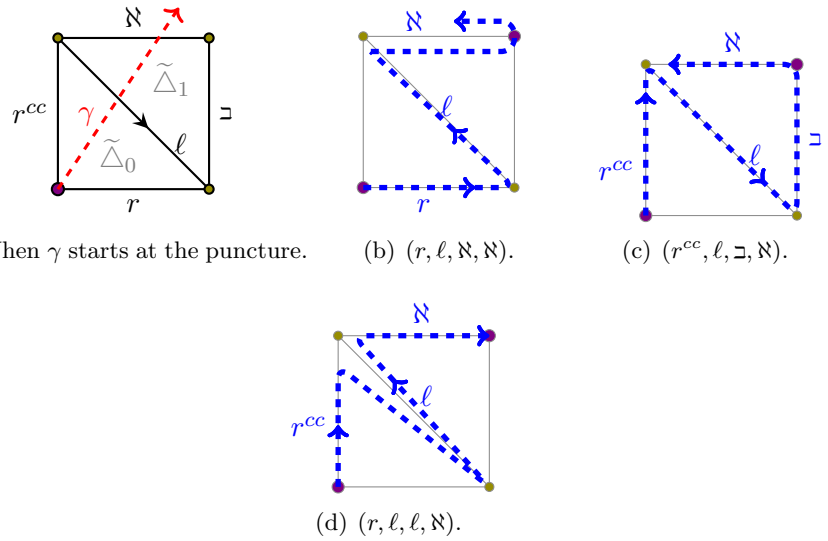

(a) When γ starts at the puncture. (b) $(r, \ell, \aleph, \aleph)$. (c) $(r^{cc}, \ell, \beth, \aleph)$.

(d) $(r, \ell, \ell, \aleph)$.

Figure 4.20: The lifts $(\widetilde{\omega}_1, \ldots, \widetilde{\omega}_4)$ of Remark 4.2.18(A1), (A2) when γ starts at the puncture, see Fig. 4.13.

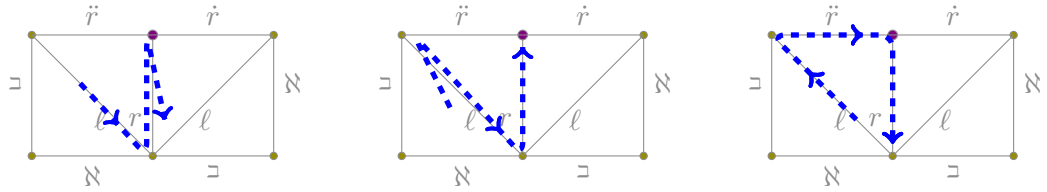

(1) $(\ell, \underline{r, r})$. (2) (ℓ, ℓ, r). (3) $(\ell, \dot{\mathbf{r}}, \mathbf{r})$.

Figure 4.21: The lifts $(\widetilde{\omega}_{2k}, \widetilde{\omega}_{2k+1}, \widetilde{\omega}_{2k+2})$ of the subpaths of Lemma 4.2.19(a1), (a2), (a3), see Fig. 4.14.

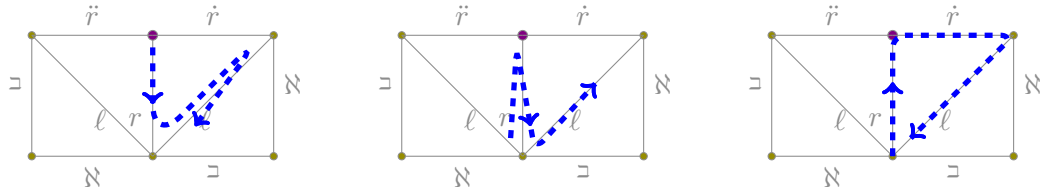

(1) (r, ℓ, ℓ). (2) $(\underline{r, r}, \ell)$. (3) $(r, \ddot{r}, \ell)$.

Figure 4.22: The lifts $(\widetilde{\omega}_{2k+2}, \widetilde{\omega}_{2k+3}, \widetilde{\omega}_{2k+4})$ of the subpaths of Lemma 4.2.19(b1), (b2), (b3), see Fig. 4.15.

label as $\tau_{[\gamma_j]}$ if $j \in \{0, d\}$.

By construction, $\widetilde{\triangle}_0$ has three distinct labels, τ_{i_1}, $\tau_{[\gamma_0]}$, and $\widetilde{\tau}_{[\gamma_{-1}]}$, and $\widetilde{\triangle}_d$ has three distinct labels, τ_{i_d}, $\tau_{[\gamma_d]}$, and $\widetilde{\tau}_{[\gamma_{d+1}]}$. Hence, as discussed in Section 4.2.2, the subpath $(\widetilde{\omega}_1, \widetilde{\omega}_2)$ is either $(\tau_{[\gamma_0]}, \tau_{i_1})$ or $(\widetilde{\tau}_{[\gamma_{-1}]}, \tau_{i_1})$, and the subpath $(\widetilde{\omega}_{2d}, \widetilde{\omega}_{2d+1})$ is either $(\tau_{i_d}, \tau_{[\gamma_d]})$ or $(\tau_{i_d}, \widetilde{\tau}_{i_{d+1}})$.

- If $\triangle_0$ has three distinct sides, τ_{i_1}, $\tau_{[\gamma_0]}$, and $\tau_{[\gamma_{-1}]}$, then $\widetilde{\tau}_{[\gamma_{-1}]} = \tau_{[\gamma_{-1}]}$, and $\overline{\pi}$ maps $(\widetilde{\omega}_1, \widetilde{\omega}_2)$ to the (T°, γ)-subpath (ω_1, ω_2) with the same labels.

  If $\triangle_0$ is a self-folded triangle with radius r and ℓ-loop ℓ, then recall that $\widetilde{\triangle}_0$ is an ordinary triangle with edge labels ℓ, r^{cc}, r (in counterclockwise order) as in Fig. 4.20(a). By (T1) and (T2), $\widetilde{\omega}_1$ goes along $\widetilde{\tau}_{[\gamma_0]}$ or $\widetilde{\tau}_{[\gamma_{-1}]}$ and $\widetilde{\omega}_2$ goes along ℓ. Hence, either $(\widetilde{\omega}_1, \widetilde{\omega}_2) = (r^{cc}, \ell)$ or $(\widetilde{\omega}_1, \widetilde{\omega}_2) = (r, \ell)$ (see Fig. 4.20). By Remark 4.2.18, there are two possible (T°, γ)-subpaths (ω_1, ω_2), either (r, ℓ_-) or (r, ℓ_+). We see that $\overline{\pi}$ maps

  $$(r, \ell) \longleftrightarrow \text{Remark 4.2.18(A1): } (r, \ell_-),$$
  $$(r^{cc}, \ell) \longleftrightarrow \text{Remark 4.2.18(A2): } (r, \ell_+).$$

- Similarly, if $\triangle_d$ has three distinct sides, then $(\widetilde{\omega}_{2d}, \widetilde{\omega}_{2d+1})$ is mapped to the subpath with the same labels. Otherwise, if $\triangle_d$ is a self-folded triangle with radius r and ℓ-loop ℓ, then recall that $\widetilde{\triangle}_d$ is an ordinary triangle with edges ℓ, r^{cc}, r (in counterclockwise order), see Fig. 4.17(b). Then either $(\widetilde{\omega}_{2d}, \widetilde{\omega}_{2d+1}) = (\ell, r^{cc})$ or $(\widetilde{\omega}_{2d}, \widetilde{\omega}_{2d+1}) = (\ell, r)$, and $\overline{\pi}$ maps

  $$(\ell, r^{cc}) \longleftrightarrow (\ell_-, r),$$
  $$(\ell, r) \longleftrightarrow (\ell_+, r).$$

Similarly, each $\widetilde{\triangle}_k$ has three distinct labels τ_{i_k}, $\tau_{i_{k+1}}$, and $\widetilde{\tau}_{[\gamma_k]}$. As discussed in Section 4.2.2, the subpath $(\widetilde{\omega}_{2k}, \widetilde{\omega}_{2k+1}, \widetilde{\omega}_{2k+2})$ is one of $(\tau_{i_k}, \tau_{i_{k+1}}, \tau_{i_{k+1}})$, $(\tau_{i_k}, \tau_{i_k}, \tau_{i_{k+1}})$, or $(\tau_{i_k}, \widetilde{\tau}_{[\gamma_k]}, \tau_{i_{k+1}})$.

- If $\triangle_k$ $(k = 1, \ldots, d)$ has three distinct sides, τ_{i_k}, $\tau_{i_{k+1}}$, and $\tau_{[\gamma_k]}$, then $\widetilde{\tau}_{[\gamma_k]} = \tau_{[\gamma_k]}$. Hence $(\widetilde{\omega}_{2k}, \widetilde{\omega}_{2k+1}, \widetilde{\omega}_{2k+2})$ is mapped to the (T°, γ)-subpath $(\omega_{2k}, \omega_{2k+1}, \omega_{2k+2})$ with the same labels.

Otherwise, suppose $\triangle_k$ is a self-folded triangle with radius r and ℓ-loop ℓ. Assume that ℓ, r, ℓ are the k-th, $(k+1)$-th, and $(k+2)$-th arcs crossed by γ and that γ crosses them in the counterclockwise direction (see Fig. 4.17(c)). By construction (see Definition 4.3.1 and Fig. 4.17(e)), $\widetilde{\triangle}_k$ has sides labeled $\widetilde{\tau}_{i_k} = \ell$, $\widetilde{\tau}_{i_{k+1}} = r$, and $\widetilde{\tau}_{[\gamma_k]} = \dot{r}$ (in counterclockwise order). The subpath $(\widetilde{\omega}_{2k}, \widetilde{\omega}_{2k+1}, \widetilde{\omega}_{2k+2})$ is one of $(\widetilde{\tau}_{i_k}, \widetilde{\tau}_{i_{k+1}}, \widetilde{\tau}_{i_{k+1}}) = (\ell, r, r)$, $(\widetilde{\tau}_{i_k}, \widetilde{\tau}_{i_k}, \widetilde{\tau}_{i_{k+1}}) = (\ell, \ell, r)$, or $(\widetilde{\tau}_{i_k}, \tau_{[\gamma_k]}, \widetilde{\tau}_{i_{k+1}}) = (\ell, \dot{r}, r)$. See Fig. 4.21. Per Lemma 4.2.19, there are three possible (T°, γ)-subpaths for $(\omega_{2k}, \omega_{2k+1}, \omega_{2k+2})$. We see that $\overline{\pi}$ maps

$(\ell, r, r) \longleftrightarrow$ Lemma 4.2.19(a1): $(\ell_-, \underline{r, r})$,
$(\ell, \ell, r) \longleftrightarrow$ Lemma 4.2.19(a2): (ℓ_+, ℓ_-, r),
$(\ell, \dot{r}, r) \longleftrightarrow$ Lemma 4.2.19(a3): $(\ell_+, \mathbf{r}, \mathbf{r}$ (counterclockwise non-backtrack)).

By construction (see Definition 4.3.1 and Fig. 4.17(e)), $\widetilde{\triangle}_{k+1}$ has sides labeled $\widetilde{\tau}_{i_{k+1}} = r$, $\widetilde{\tau}_{i_{k+2}} = \ell$, and $\widetilde{\tau}_{[\gamma_{k+1}]} = \ddot{r}$ (in counterclockwise order). The subpath $(\widetilde{\omega}_{2k+2}, \widetilde{\omega}_{2k+3}, \widetilde{\omega}_{2k+4})$ is one of $(\widetilde{\tau}_{i_{k+1}}, \widetilde{\tau}_{i_{k+2}}, \widetilde{\tau}_{i_{k+2}}) = (r, \ell, \ell)$, $(\widetilde{\tau}_{i_{k+1}}, \widetilde{\tau}_{i_{k+1}}, \widetilde{\tau}_{i_{k+2}}) = (r, r, \ell)$, or $(\widetilde{\tau}_{i_{k+1}}, \widetilde{\tau}_{[\gamma_{k+1}]}, \widetilde{\tau}_{i_{k+2}}) = (r, \ddot{r}, \ell)$. See Fig. 4.22. Per Lemma 4.2.19, there are three possible (T°, γ)-subpaths for $(\omega_{2k+2}, \omega_{2k+3}, \omega_{2k+4})$. We see that $\overline{\pi}$ maps

$(r, \ell, \ell) \longleftrightarrow$ Lemma 4.2.19(b1): (r, ℓ_-, ℓ_+),
$(r, r, \ell) \longleftrightarrow$ Lemma 4.2.19(b2): $(\underline{r, r}, \ell_-)$ then ℓ_-,
$(r, \ddot{r}, \ell) \longleftrightarrow$ Lemma 4.2.19(b3): $(\mathbf{r}, \mathbf{r}$ (counterclockwise non-backtrack) $, \ell_+)$.

□

We expect that Lemma 4.3.4 can be generalized to other punctured surfaces. However, other punctured surfaces can have more complication ideal triangulations (like those containing an ideal triangle of Fig. 2.1(d)) that have not been considered in our argument.

4.3.3 Perfect matching expansion formula

We recap the snake graph expansion formula of [MSW11, Theorem 4.10] for ordinary arcs of any bordered surface (including once-punctured polygons). We continue to restrict our attention to the case of the once-punctured n-gon $\mathcal{C}_n$.

Definition 4.3.5 (snake graph $G_{T^o,\gamma}$)**.** *We* unfold $\widetilde{S_\gamma}$ *into a graph* $\overline{G}_{T^o,\gamma}$*, called a* snake graph*, by inserting negative-oriented copies* $\widetilde{\triangle}_k^{(-)}$ *of* $\widetilde{\triangle}_k$ *(for* $k = 1, \ldots, d-1$*) into* $\widetilde{S_\gamma}$*. Fig. 4.23(a) is the graph* $\overline{G}_{T^o,\gamma}$ *that is built from* $\widetilde{S_\gamma}$ *of Fig. 4.18(b). See [MSW11, Section 4] for details. A* tile *consists of* $\widetilde{\triangle}_k$ *and* $\widetilde{\triangle}_{k+1}$ *(or* $\widetilde{\triangle}_k^{(-)}$ *and* $\widetilde{\triangle}_{k+1}^{(-)}$*) glued together along a* diagonal *labeled* $\widetilde{\tau}_{i_k}$*. Let* $G_{T^o,\gamma}$ *denote the graph obtained from* $\overline{G}_{T^o,\gamma}$ *by removing the diagonal from each tile.*

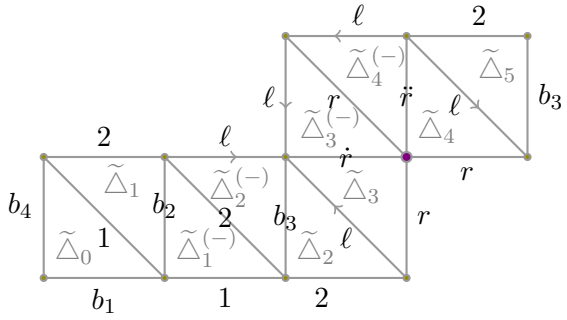

(a) The snake graph $\overline{G}_{T^o,\gamma}$ constructed from $\widetilde{S_\gamma}$ in Fig. 4.18(b).

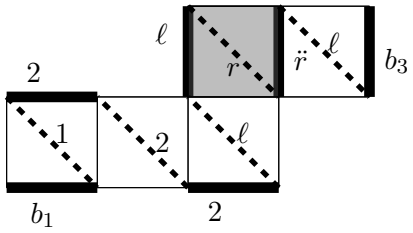

(b) A path corresponding to the $(\widetilde{S_\gamma}, \widetilde{\gamma})$-path of Fig. 4.19(c), with odd steps $(b_1, 2, 2, \ell, \ddot{r}, b_3)$, see Fig. 4.24(8), and even steps the diagonals 1, 2, ℓ, r, and ℓ.

Figure 4.23: The snake graph $\overline{G}_{T^o,\gamma}$ of Definition 4.3.5 and an example of a path on $\overline{G}_{T^o,\gamma}$, see Remark 4.3.8.

Definition 4.3.6 (crossing monomial)**.** *Define the* crossing monomial *of* γ *with respect to* T° *to be*

$$cross(T^\circ, \gamma) = \prod_{k=1}^{d} x(\tau_{i_k}).$$

Definition 4.3.7 (perfect matchings and weights)**.** *A* perfect matching *of a graph G is a subset E of the edges of G such that each vertex of G is incident to exactly one edge of E. See Fig. 4.24. If the edges of a perfect matching E are labeled $\beta_{j_1}, \ldots, \beta_{j_r}$, then the* weight $x(E)$ *of E is the product $x_{\beta_{j_1}} \cdots x_{\beta_{j_r}}$.*

Theorem 4.3.1 ([MSW11, Theorem 4.10], perfect matching expansion formula)**.** *Let T° be an ideal triangulation of any surface S and let $\gamma \notin T^\circ$ be an ordinary arc (note: γ may be an ℓ-loop). Let x_γ denote the element corresponding to γ in the cluster algebra which arises from S (see Theorem* 2.2.11*). Then*

$$x_\gamma = \sum_E \frac{x(E)}{\operatorname{cross}(T^\circ, \gamma)},$$

where the sum is over all perfect matchings E of $G_{T^o,\gamma}$.

4.3.4 Proof of the T°-path formula for $\mathcal{C}_n$ (Theorem 4.2.1)

Remark 4.3.8 ([MS10, Lemma 4.5])**.** *There is a bijection*

$$F\colon \{\text{perfect matchings of the graph } G_{T^o,\gamma}\} \to \{(\widetilde{S_\gamma}, \widetilde{\gamma})\text{-paths on } \widetilde{S_\gamma}\},$$
$$F\colon E \mapsto \widetilde{\omega}_E,$$

where the diagonals of $\overline{G}_{T^o,\gamma}$ correspond to the even-indexed steps of each $(\widetilde{S_\gamma}, \widetilde{\gamma})$-path (see Fig. 4.23(b)) and each matching E correspond to the odd-indexed steps of $\widetilde{\omega}_E$. See Figs. 4.25 and 4.26.

The bijections $\overline{\pi}$ (of Lemma 4.3.4) and F compose to form a bijection between the perfect matchings of the snake graph $G_{T^o,\gamma}$ and the (T°, γ)-paths on $\mathcal{C}_n$.

Theorem 4.3.2 (snake graph matchings to (T°, γ)-paths)**.** *Consider an arc γ of $\mathcal{C}_n$ and the (T°, γ)-paths and snake graph $G_{T^o,\gamma}$ corresponding to γ. The map*

$$\overline{\pi} \circ F\colon \{\text{perfect matchings in } G_{T^o,\gamma}\} \to \{(T^\circ, \gamma)\text{-paths on } \mathcal{C}_n\},$$
$$E \mapsto \omega_E := \overline{\pi}(\widetilde{\omega}_E)$$

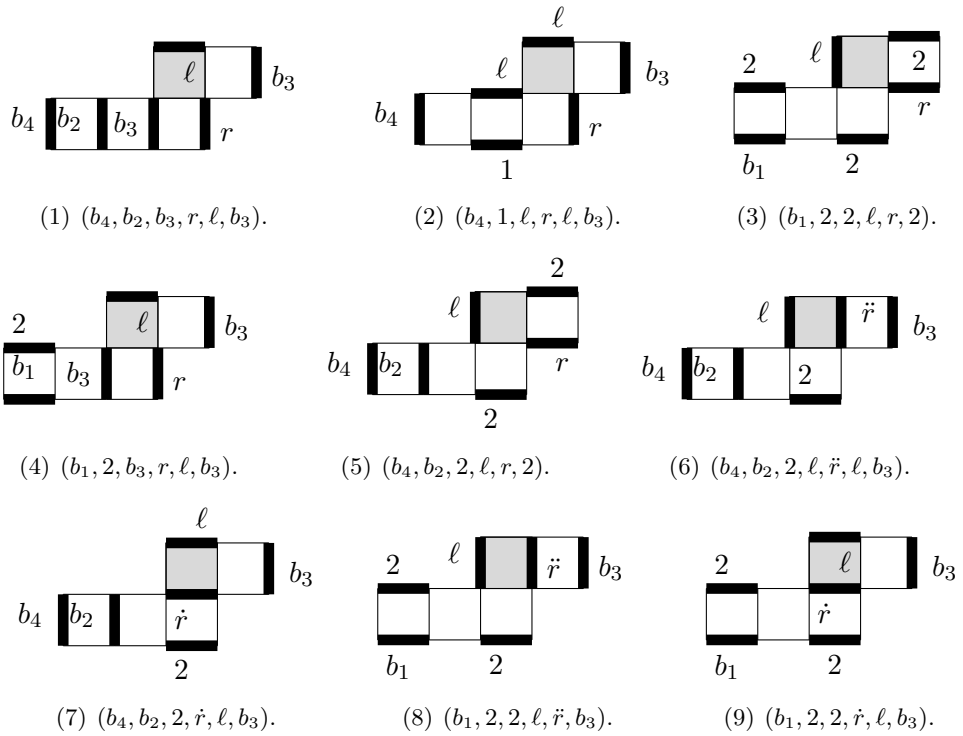

Figure 4.24: The nine perfect matchings of the snake graph $G_{T^\circ,\gamma}$ of Fig. 4.23(a). Matchings (6)–(9) correspond to the (T°, γ)-paths of Fig. 4.8. Note that these four are the only matchings where their restrictions to the gray-shaded tile are perfect matchings.

is a bijection where the edges of each matching E correspond to the odd-indexed steps of the (T°, γ)-path ω_E, see Fig. 4.23(b). *In particular, the weight $x(E)$ of the perfect matching E is equal to the numerator of the Laurent monomial $x(\omega_E)$ (see Definitions* 4.2.6 *and* 4.3.7).

Remark 4.3.9 (matching restrictions and (T°, γ)-subpaths)**.** *The four (T°, γ)-subpaths of Lemma 4.2.19(I)–(IV) correspond to the four possible matchings of the triple-tiles of $G_{T^\circ,\gamma}$. Compare Figs. 4.14–4.15, Figs. 4.21–4.22, and Figs. 4.25–4.26.*

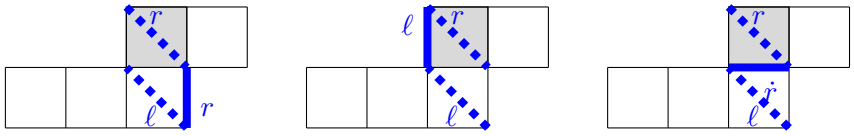

(1) edge $r \longleftrightarrow \widetilde{\omega}_{2k+1}$. (2) edge $\ell \longleftrightarrow \widetilde{\omega}_{2k+1}$. (3) edge $\ddot{r} \longleftrightarrow \widetilde{\omega}_{2k+1}$.

Figure 4.25: The subpaths on $\overline{G}_{T^o,\gamma}$ corresponding to the subpaths $(\widetilde{\omega}_{2k}, \widetilde{\omega}_{2k+1}, \widetilde{\omega}_{2k+2}) = (\ell, \quad, r)$ from Fig. 4.21.

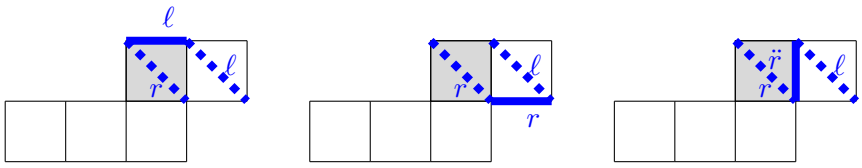

(1) edge $r \longleftrightarrow \widetilde{\omega}_{2k+3}$. (2) edge $\ell \longleftrightarrow \widetilde{\omega}_{2k+3}$. (3) edge $\ddot{r} \longleftrightarrow \widetilde{\omega}_{2k+3}$.

Figure 4.26: The subpaths on $\overline{G}_{T^o,\gamma}$ corresponding to the subpaths $(\widetilde{\omega}_{2k+2}, \widetilde{\omega}_{2k+3}, \widetilde{\omega}_{2k+4}) = (r, \quad, \ell)$ from Fig. 4.22.

Proof of Theorem 4.2.1. Applying the bijection $\overline{\pi} \circ F$ to the formula of [MSW11, Theorem 4.10] yields

$$x_\gamma = \frac{1}{\operatorname{cross}(T^\circ, \gamma)} \sum_{\substack{E \text{ perfect matchings} \\ \text{of } G_{T^o,\gamma}}} x(E) = \frac{1}{\operatorname{cross}(T^\circ, \gamma)} \sum_{(T^\circ,\gamma)\text{-paths } \omega} \left(\prod_{k=0}^{d} x(\omega_{2k+1}) \right).$$

Since $\prod_{k=1}^{d} x(\omega_{2k}) = \operatorname{cross}(T^\circ, \gamma)$, this concludes the proof. □

Example 4.3.10. *The nine perfect matchings of the graph $G_{T^o,\gamma}$ (from Fig. 4.23(a)) are listed in Fig. 4.24. Per Theorem 4.3.2, they correspond to the nine (T°, γ)-paths of Example 4.2.9.*

4.4 Combinatorial proof of atomic bases for type D

4.4.1 Atomic bases for the once-punctured n-gons (type D_n)

Definition 4.4.1 (cluster monomials)**.** *Let $\mathcal{A}$ be a coefficient-free cluster algebra. A* cluster monomial *is a monomial in cluster variables all belonging to a single cluster.*

Recall that, in the case that $\mathcal{A}$ arises from a surface, a cluster corresponds to a tagged triangulation and a cluster monomial corresponds to a multi-tagged triangulation (see Theorem 2.2.11). See Definition 4.1.3 for a list of compatible pairs of tagged arcs of $\mathcal{C}_n$.

The concepts of positive elements and atomic bases were first introduced in [SZ04] for the case of an annulus with one marked point on each boundary.

Definition 4.4.2 (positive elements and atomic bases)**.** *An element $y \in \mathcal{A}$ is called* positive *if the Laurent expansion of y in the variables of every cluster of $\mathcal{A}$ has non-negative coefficients.*

A $\mathbb{Z}$-linear basis $\mathcal{B}$ of $\mathcal{A}$ is called an atomic basis *of $\mathcal{A}$ if any positive element of $\mathcal{A}$ is a non-negative $\mathbb{Z}$-linear combination of $\mathcal{B}$. Note that, if such a $\mathcal{B}$ exists, $\mathcal{B}$ is the collection of all indecomposable positive elements (i.e., elements which cannot be written as a sum of positive elements) of $\mathcal{A}$, hence it is unique.*

Remark 4.4.3. *To prove that a collection $\mathcal{B} \subset \mathcal{A}$ is an atomic basis of $\mathcal{A}$, it suffices to verify the following:*

$$\text{every element of } \mathcal{B} \text{ is a positive element of } \mathcal{A}, \tag{4.4.1}$$

$$\mathcal{B} \text{ is a } \mathbb{Z}\text{-linear basis of } \mathcal{A}, \tag{4.4.2}$$

$$\text{every positive element } y \in \mathcal{A} \text{ can be written as a } \mathbb{Z}_{\geq 0}\text{-linear combination of } \mathcal{B}. \tag{4.4.3}$$

Theorem 4.4.1 ([Cer11])**.** *If $\mathcal{A}$ is a cluster algebra of type A, D, or E, the cluster monomials of $\mathcal{A}$ form the atomic basis of $\mathcal{A}$.*

Proof. [HL10, Nak11], [CK08], and [Cer11, CLF12] give representation theoretic proofs for (4.4.1), (4.4.2), and (4.4.3), respectively. [MSW11] and [MSW13] provide combinatorial arguments for (4.4.1) and (4.4.2), respectively, and [DT13] gives a combinatorial proof for type A for (4.4.3). We present in the remainder of this paper a combinatorial

proof for type D for (4.4.3) which relies on the T°-path formula (Theorem 4.2.1) and is inspired by [DT13]. □

Recall that a multi-tagged triangulation Σ is not compatible with a tagged triangulation T if Σ contains an arc σ which is not in T. Recall also that a *proper Laurent monomial in variables* u_i is a product of the form $u_1^{c_1} \cdots u_r^{c_r}$ where at least one of the c_i is negative.

Lemma 4.4.4. *Consider a once-punctured polygon $\mathcal{C}_n$. For every tagged triangulation T and every multi-tagged triangulation Σ which is not compatible with T, the T-expansion of x_Σ is a sum of proper Laurent monomials.*

Remark 4.4.5. *A general version of Lemma 4.4.4 is known as the* proper Laurent monomial property *(following [CLF12]) which was proven for cluster algebras from surfaces and any choice of coefficients in [CLF12] and then for any skew-symmetric cluster algebras in [CKLFP13], using representation theoretic arguments in both cases.*

Definition 4.4.6. *Let N be a subset of a tagged triangulation T. We write the* degree with respect to N *to mean the degree with respect to the cluster variables corresponding to N.*

Outline of proof of Lemma 4.4.4. Suppose x_Σ is a cluster monomial not compatible with a tagged triangulation T, i.e., Σ contains an arc σ which is not in T. For brevity, suppose that all tagged arcs of $\Sigma \backslash T$ are peripheral and the corresponding ideal triangulation T° has no self-folded triangle. For full details and the rest of the cases, see the remainder of this paper.

Step 1: Choose a tagged arc $\sigma \in \Sigma \backslash T$ such that σ is as close as possible to the puncture and, if possible, σ only crosses every arc of T at most once. Let (T, σ)-*cross* (respectively, (T, σ)-*doublecross*) be the set of arcs of T which σ crosses (respectively, the set of arcs of T which σ crosses twice).

Step 2: For each (T, σ)-path ω, we compare the number of odd-indexed steps (contributing to the numerator of $x(\omega)$) and the number of even-indexed steps (contributing to the denominator of $x(\omega)$) that belong to (T, σ)-*cross* and (T, σ)-*doublecross*. See Definition 4.2.6. This allows us to show that each term in

the T-expansion of x_σ is of *negative* degree either with respect to the cluster variables corresponding to (T, σ)-*cross* or with respect to the cluster variables corresponding to (T, σ)-*doublecross*.

Step 3: Similarly, for each factor x_β in the product of x_Σ, we consider a (T, β)-path and compare the number of odd steps versus the number of even steps to show that every term in the T-expansion of x_β has *non-positive* degree with respect to both the cluster variables corresponding to (T, σ)-*cross* and the cluster variables corresponding to (T, σ)-*doublecross*.

Step 4: It follows, since $\sigma \in \Sigma$ and every term in the T-expansion of x_Σ has non-positive degree with respect to both (T, σ)-*cross* and (T, σ)-*doublecross* that every term in the T-expansion of x_Σ has *negative* degree with respect to either (T, σ)-*cross* or (T, σ)-*doublecross*.

Since (T, γ)-*cross* and (T, γ)-*doublecross* are subsets of T, the T-expansion of x_Σ is a sum of proper Laurent monomials. □

Theorem 4.4.2. *If $\mathcal{A}$ is a coefficient-free cluster algebra of type D, every positive element $y \in \mathcal{A}$ is equal to a linear combination $y = \sum_\Gamma m_\Gamma x_\Gamma$ of cluster monomials where each m_Γ is non-negative.*

Proof of Theorem 4.4.2. We assume (4.4.1) and (4.4.2) for $\mathcal{B} = \{\text{cluster monomials}\}$. The following argument appears in [CLF12, DT13, SZ04], and we include it here for completeness. Let y be a positive element of a cluster algebra of type D. Write $y = \sum_\Gamma m_\Gamma x_\Gamma$ as a linear combination of cluster monomials. Then we prove that every m_Γ is non-negative as follows.

Let x_Γ be a cluster monomial from the sum, and let Γ denote the multi-tagged triangulation corresponding to it. Choose a tagged triangulation $T := T_\Gamma$ that is compatible with the multi-tagged triangulation Γ, i.e., so that $\gamma \in T$ for every arc $\gamma \in \Gamma$. Consider a different cluster monomial x_Σ from the sum. We argue that

$$x_\Gamma \text{ does not appear in the } T\text{-expansion of } x_\Sigma. \tag{4.4.4}$$

If all the arcs of Σ were in T, then x_Σ is its own T-expansion, and we are done. Suppose that Σ has an arc that is not in T. By Lemma 4.4.4, every term in the T-expansion

of x_Σ is a proper Laurent monomial in the cluster corresponding to T. Since x_Γ is a monomial (i.e., not a proper Laurent monomial) in this cluster, we have proven (4.4.4).

Hence, m_Γ is equal to the coefficient of x_Γ in the T-expansion of y. Since y is a positive element, the coefficient of x_Γ in the T-expansion of y is non-negative, as required. □

In Section 4.4.2, we provide notations and lemmas which are helpful toward proving the lemmas in Sections 4.4.3 and 4.4.4. Section 4.4.3 (respectively, Section 4.4.4) discusses lemmas which are needed to prove Lemma 4.4.4 for the case where all arcs of $\Sigma\backslash T$ are peripheral (respectively, for the case where $\Sigma\backslash T$ contains a radius). Even though a few of the lemmas can also be proven using the existing snake graph formula [MSW11, Theorem 4.3] (recapped in Section 4.3.3), many arguments (such as the proofs of Lemmas 4.4.21, 4.4.22, and 4.4.24) can be done more easily using the T°-path formula. Finally, we prove Lemma 4.4.4 in Section 4.4.5: if Σ is not compatible with the tagged triangulation T, we can choose a tagged arc $\sigma \in \Sigma\backslash T$ such that every term in the T-expansion of x_Σ has negative degree with respect to some subset N_σ^T of $T\backslash\Sigma$ by Lemmas 4.4.21, 4.4.22, 4.4.23, 4.4.26, 4.4.24, and 4.4.27.

4.4.2 Notations and technical lemmas to prove Lemma 4.4.4

Recall from Remark 4.1.2 that every tagged arc of $\mathcal{C}_n$ belongs to one of three classes: plain radius, notched radius, or peripheral.

Remark 4.4.7. *Per Remark 4.1.4, we only need to prove Lemma 4.4.4 and the related statements for two cases: one where T has all plain radii and one where T has 2 parallel radii r, $r^{(p)}$.*

Definition 4.4.8. *Let T be a tagged triangulation, T° the corresponding ideal triangulation, and λ a tagged arc. Let (T°, λ)-cross denote the arcs of T° that cross λ, and let (T°, λ)-doublecross denote be the arcs of T° that cross λ twice. (Note that, If T contains two parallel radii r, $r^{(p)}$, then (T°, λ)-cross and (T°, λ)-doublecross may contain the associated ℓ-loop.)*

If T contains two parallel radii r, $r^{(p)}$ (so that T° contains a self-folded triangle with

radius r and ℓ-loop ℓ), and if λ crosses the ℓ-loop ℓ, let

$$(T,\lambda)\text{-}cross := \{r^{(p)} \text{ and the peripheral arcs of } T \text{ that cross } \lambda\}, \text{ and}$$
$$(T,\lambda)\text{-}doublecross := \{r^{(p)} \text{ and the (peripheral) arcs of } T \text{ that cross } \lambda \text{ twice}\}.$$

Otherwise, if λ does not cross an ℓ-loop that belongs to T°, let

$$(T,\lambda)\text{-}cross := (T^\circ,\lambda)\text{-}cross \quad \text{and} \quad (T,\lambda)\text{-}doublecross := (T^\circ,\lambda)\text{-}doublecross.$$

Lemma 4.4.9. *Let T be a tagged triangulation with two parallel radii $r, r^{(p)}$ (so that T° has a self-folded triangle with radius r and ℓ-loop ℓ). Suppose β and σ (possibly $\beta = \sigma$) are compatible tagged arcs not in T, and either σ is a plain radius or β is peripheral. Let $w = (\omega_1, \ldots, \omega_{2d+1})$ be a (T°,β)-path. Recall that $x_\ell := x_r\, x_{r^{(p)}}$.*

Then $x(\omega)$ having negative (respectively, non-positive) degree with respect to (T°,σ)-cross implies that $x(\omega)$ has negative (respectively, non-positive) degree with respect to (T,σ)-cross.

Similarly, if (T°,σ)-doublecross is nonempty and if $x(\omega)$ has negative (respectively, non-positive) degree with respect to (T°,σ)-doublecross, then $x(\omega)$ has negative (respectively, non-positive) degree with respect to (T,σ)-doublecross.

Note that this statement is not necessarily true if σ is peripheral and β is a radius.

Proof. If σ is a radius (Fig. 4.17(a)), then it cannot cross r, so $r \notin (T^\circ,\sigma)$-*cross*. Since $r \notin (T,\sigma)$-*cross*, replacing the two gradings (T°,σ)-*cross* and (T,σ)-*cross* is equivalent to simply replacing ℓ in (T°,σ)-*cross* with $r^{(p)}$ in (T,σ)-*cross*, and the degree would stay the same.

If β is a peripheral arc crossing r (Figs. 4.17(d), 4.17(c)), then (T°,σ)-*cross* contains r, but ω goes along r exactly twice in a row, per Lemma 4.2.19(I)–(IV). So $x(\omega)$ (as a T°-monomial) has zero degree with respect to r, and we can again replace ℓ in (T°,σ)-*cross* with $r^{(p)}$ in (T,σ)-*cross* to arrive at the same conclusion.

Since r is a radius, σ can cross it at most once, so $r \notin (T^\circ,\sigma)$-*doublecross*. Since $r \notin (T,\sigma)$-*doublecross*, replacing the two gradings (T°,σ)-*doublecross* and (T,σ)-*doublecross* is equivalent to simply replacing ℓ in (T°,σ)-*doublecross* with $r^{(p)}$ in (T,σ)-*doublecross*, and the degree would stay the same. □

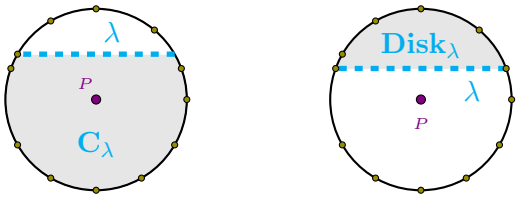

(a) Once-punctured disk $\mathbf{C}_\lambda$. (b) Disk $\mathbf{Disk}_\lambda$.

Figure 4.27: λ cuts out a smaller once-punctured disk $\mathbf{C}_\lambda$ and a disk $\mathbf{Disk}_\lambda$, shaded in gray.

Notation 4.4.10. *Every ordinary peripheral arc λ snips the surface into a smaller once-punctured disk (denoted $\boldsymbol{C}_\lambda$) and a region not containing the puncture (denoted $\boldsymbol{Disk}_\lambda$). See Fig. 4.27.*

Let σ be a peripheral arc with endpoints s and t (possibly $s = t$), and let β be another ordinary arc. We say that β lies in *$\boldsymbol{Disk}_\sigma$ (respectively, $\boldsymbol{C}_\sigma$) if the interior of β lies entirely in the interior of $\boldsymbol{Disk}_\sigma$ (respectively, $\boldsymbol{C}_\sigma$).*

Let v be an endpoint of β. We say that v lies in *$\boldsymbol{Disk}_\sigma$ if v is a marked point on the boundary of $\boldsymbol{Disk}_\sigma$, possibly $v = s$ or t. We say that v* lies in *$\boldsymbol{C}_\sigma$ if v is a marked point in the interior or on the boundary of $\boldsymbol{C}_\sigma$, possibly $v = s$ or t. We say that v* lies strictly in *$\boldsymbol{Disk}_\sigma$ (respectively, $\boldsymbol{C}_\sigma$) if v lies in $\boldsymbol{Disk}_\sigma$ (respectively, $\boldsymbol{C}_\sigma$) and v* is not equal to *s* nor *t. We say v* lies outside of *$\boldsymbol{Disk}_\sigma$ if v is not a marked point of $\boldsymbol{Disk}_\sigma$ (hence v is not equal to s nor t). We use the same language when the region is a disk cut out by two radii.*

We use Lemmas 4.4.11 and 4.4.12 to prove Lemma 4.4.13(iii), (iv).

Lemma 4.4.11. *Suppose γ and σ are distinct compatible ordinary arcs not in T°. If σ crosses $\tau_{[\gamma_k]}$, then σ crosses arc k^γ or $k+1^\gamma$, the k-th and $(k+1)$-th arcs crossed by γ.*

Proof. To simplify the proof, assume that $0 < k < d$. There are four possibilities for ways of γ to cross the ideal triangle $\triangle_k^\gamma$, see Fig. 4.5. If $\triangle_k^\gamma$ is self-folded, then $\tau_{[\gamma_k]}$ is equal to either arc k^γ or $k+1^\gamma$, and we are done. If arc k^γ, arc $k+1^\gamma$, and $\tau_{[\gamma_k]}$ are all distinct, then γ_k (the segment between p_k^γ and p_{k+1}^γ contained in $\triangle_k$) cuts $\triangle_k^\gamma$ into two regions, and one of the regions is an ideal quadrilateral $Q = \mathrm{Quad}(\triangle_k^\gamma)$ with sides $\tau_{[\gamma_k]}$, γ_k, part of arc k^γ, and part of arc $k+1^\gamma$ (see Figs. 4.5(a), 4.5(b), and 4.5(c)). By

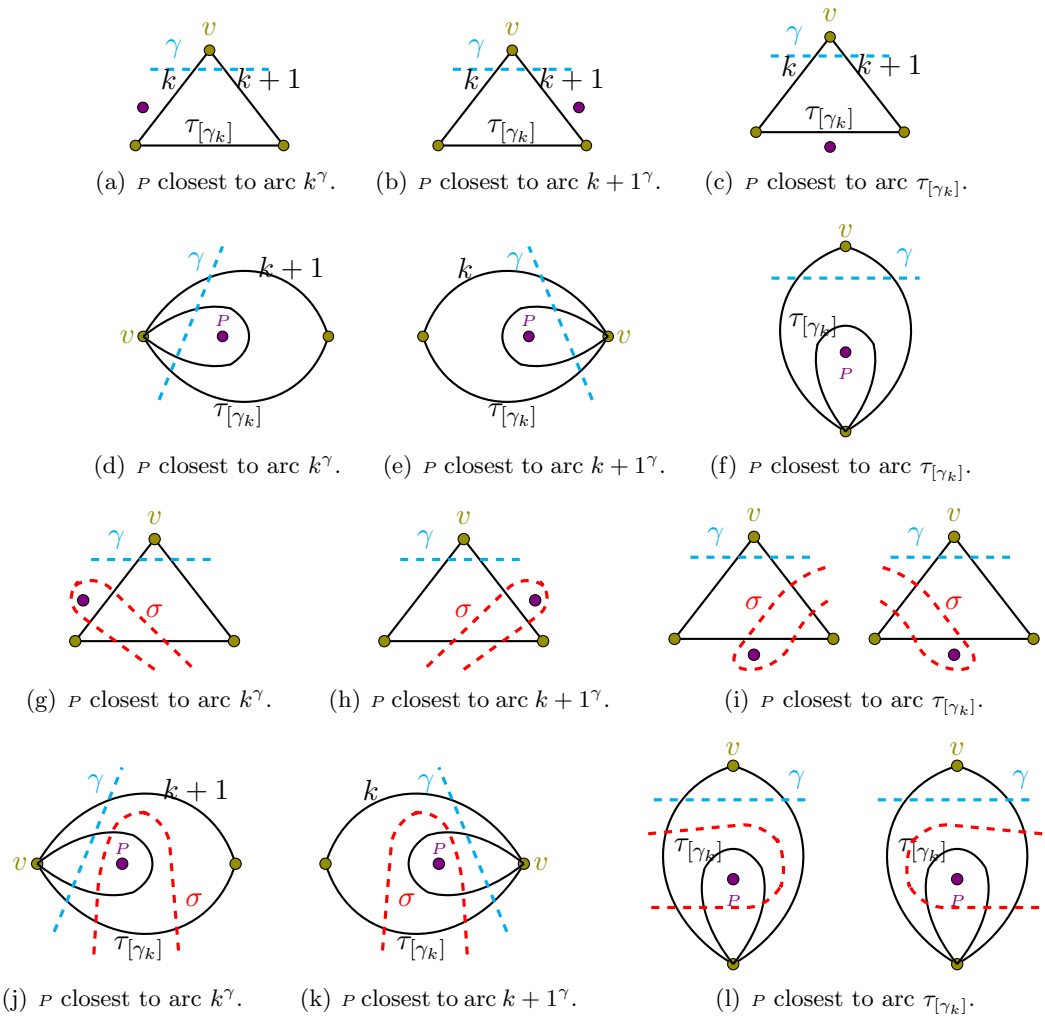

(a) P closest to arc k^γ. (b) P closest to arc $k+1^\gamma$. (c) P closest to arc $\tau_{[\gamma_k]}$.

(d) P closest to arc k^γ. (e) P closest to arc $k+1^\gamma$. (f) P closest to arc $\tau_{[\gamma_k]}$.

(g) P closest to arc k^γ. (h) P closest to arc $k+1^\gamma$. (i) P closest to arc $\tau_{[\gamma_k]}$.

(j) P closest to arc k^γ. (k) P closest to arc $k+1^\gamma$. (l) P closest to arc $\tau_{[\gamma_k]}$.

Figure 4.28: Lemma 4.4.12, when σ crosses $\tau_{[\gamma_k]}$ twice.

assumption, σ crosses $\tau_{[\gamma_k]}$, so σ cuts through Q. Since σ does not cross γ_k (because σ and γ are compatible by assumption), σ has to cross either arc k^γ or $k+1^\gamma$. □

Lemma 4.4.12. *Suppose γ and σ are (distinct, compatible) peripheral arcs such that γ that is contained in the interior of* $\mathbf{Disk}_\sigma$ *(i.e., σ is closer than γ to the puncture, see Fig.* 4.28*). If σ crosses $\tau_{[\gamma_k]}$ twice, then σ crosses arc k^γ twice or σ crosses $k+1^\gamma$ twice.*

Proof. To simplify the proof, assume $0 < k < d$. Let v be the marked point adjacent to both arcs k^γ and $k+1^\gamma$. Suppose σ crosses $\tau_{[\gamma_k]}$ twice. There are four possibilities for

ways of γ to cross the ideal triangle $\triangle_k$, see Fig. 4.5. If $\triangle_k^\gamma$ is self-folded, then $\tau_{[\gamma_k]}$ is equal to either arc k^γ or $k+1^\gamma$, and we are done.

Suppose arc k^γ, arc $k+1^\gamma$, and $\tau_{[\gamma_k]}$ are all distinct. Since γ is peripheral, γ cuts the surface $\mathcal{C}_n$ into two regions, the smaller once-punctured disk $\mathbf{C}_\gamma$ containing σ, and the disk $\mathbf{Disk}_\gamma$ containing v.

We claim that $\tau_{[\gamma_k]}$, arc k^γ, and arc $k+1^\gamma$ are all peripheral (one of them possibly an ℓ-loop). First, $\tau_{[\gamma_k]}$ must be peripheral because a radius can be crossed at most once. Because v is in the disk $\mathbf{Disk}_\gamma$, v is not the puncture, and so the arcs k and $k+1$ are also peripheral.

The puncture is either closest to arc k^γ, arc $k+1^\gamma$, or $\tau_{[\gamma_k]}$ (see Fig. 4.28). Since σ cuts out a disk containing γ, if the puncture is closest to arc k^γ (respectively, to arc $k+1^\gamma$), then σ has to cross arc k^γ (respectively, arc $k+1^\gamma$) twice. See Figs. 4.28(g) and 4.28(j) (respectively, Figs. 4.28(h) and 4.28(k)). If the puncture is closest to $\tau_{[\gamma_k]}$, then σ has to cross either arc k^γ or arc $k+1^\gamma$ twice (Figs. 4.28(i) and 4.28(l)). □

Lemma 4.4.13. *Let T° be an ideal triangulation. Suppose β and σ are compatible ordinary arcs, with $\beta \notin T^\circ$, and possibly $\beta = \sigma$. Let $\omega = (\omega_1, \ldots, \omega_{2d+1})$ be a (T°, β)-path. Suppose we have one of these four scenarios:*

i) Let $N_\sigma^{T^\circ} := \{$all radii of $T^\circ\}$ and suppose β is peripheral. (Note that $N_\sigma^{T^\circ}$ does not depend on σ here.)

ii) Let σ be a radius of T°, and let $N_\sigma^{T^\circ} := \{$all radii of $T^\circ\}\backslash\{\sigma\}$, and suppose β is peripheral.

iii) Let $N_\sigma^{T^\circ}$ denote (T°, σ)-cross, if $\sigma \notin T$.

iv) Let $N_\sigma^{T^\circ}$ denote (T°, σ)-doublecross if (T°, σ)-doublecross is non-empty, and suppose that β is a peripheral arc such that either $\beta = \sigma$ or β is contained in the interior of $\mathbf{Disk}_\sigma$.

In all four of these scenarios, if $\omega_{2k+1} \in N_\sigma^{T^\circ}$, then there is a step ω_{2k} or ω_{2k+2} which goes along an arc of $N_\sigma^{T^\circ}$.

Proof of Lemma 4.4.13. Suppose ω_{2k+1} belongs to $N_\sigma^{T^\circ}$. To simplify the proof, we only discuss cases where $k \neq 0, d$. Recall that (T1) requires β to cross each even step ω_{2i} of ω.

First, we prove the assertion in scenarios (i) and (ii). If ω_{2k+1} goes along a radius from the boundary to the puncture, we see that ω_{2k+2} must be a radius, as needed for scenario (i). Furthermore, since β crosses ω_{2k+2} but not σ, we see that ω_{2k+2} is a radius that is not equal to σ, proving scenario (ii). If ω_{2k+1} goes from the puncture to the boundary, we can repeat a similar argument to show that $\omega_{2k} \in N_\sigma^{T^\circ}$.

In scenarios (iii) and (iv), recall that the steps ω_{2k}, ω_{2k+1}, and ω_{2k+2} must go along edges in the $(k+1)$-th ideal triangle $\triangle_k^\beta$ crossed by β, and β crosses ω_{2k} and ω_{2k+2}. If ω_{2k+1} goes along the same arc as ω_{2k} or ω_{2k+2}, then we are done. Hence assume that the ideal triangle $\triangle_k^\beta$ has three distinct edges $\omega_{2k} = \tau_{i_k}^\beta$, $\omega_{2k+1} = \tau_{[\beta_k]}$, $\omega_{2k+2} = \tau_{i_{k+1}}^\beta$.

We consider scenario (iii): If $\beta = \sigma$, then ω_{2k} and ω_{2k+2} cross $\beta = \sigma$, and we are done. Assume that $\beta \neq \sigma$. By Lemma 4.4.11, since σ crosses $\tau_{[\beta_k]}$, then σ crosses $\tau_{i_k}^\beta$ or $\tau_{i_{k+1}}^\beta$.

Finally, we consider scenario (iv): By assumption, $\beta = \sigma$ or β is peripheral arc contained in the interior of $\mathbf{Disk}_\sigma$.

First, suppose $\beta = \sigma$. Having distinct ω_{2k}, ω_{2k+1}, and ω_{2k+2} means that the segment σ_k cuts $\triangle_k$ into two regions, and one of the regions contains ω_{2k+1}. Since σ cuts ω_{2k+1} twice, σ cuts $\triangle_k^\sigma$ three times. Since the surface $\mathcal{C}_n$ only contains one puncture, this is impossible, hence either $\omega_{2k} = \omega_{2k+1}$ or $\omega_{2k+2} = \omega_{2k+1}$.

Next, suppose β is a peripheral arc ($\beta \neq \sigma$) contained in the interior of $\mathbf{Disk}_\sigma$. By Lemma 4.4.12 (see Fig. 4.28), since σ crosses $\omega_{2k+1} = \tau_{[\beta_k]}$ twice, σ crosses $\tau_{i_k}^\beta$ or $\tau_{i_{k+1}}^\beta$ twice. Hence σ crosses ω_{2k} or $\omega_{2(k+1)}$, as needed. □

In particular, Lemma 4.4.13 implies Corollary 4.4.15.

Definition 4.4.14. *Let ω be a T°-path. Let N be a subset of T°. A consecutive subpath $\omega' = (\omega_a, \ldots, \omega_b)$ of ω is called an* N-subpath *if each step ω_j of ω' comes from N. We say that ω' is a* longest N-subpath *of ω if the step ω_{a-1} (if any) and the step ω_{b+1} (if any) do not come from N.*

Corollary 4.4.15. *Suppose we have the same setup as Lemma* 4.4.13.

a) If β does not cross any arc of $N_\sigma^{T^\circ}$, then ω does not contain any arc of $N_\sigma^{T^\circ}$, and the degree of $x(\omega)$ with respect to $N_\sigma^{T^\circ}$ is zero.

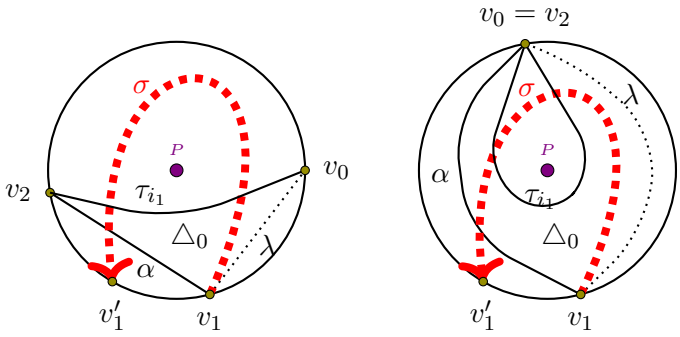

Figure 4.29: Lemma 4.4.16, when σ crosses two peripheral arcs α, τ_{i_1} of $\triangle_0$.

b) If the corresponding term $x(\omega)$ has positive degree with respect to $N_\sigma^{T^\circ}$, there must be an odd-length (of length three or greater) longest $N_\sigma^{T^\circ}$-subpath $\bar{\omega} = \omega_{2i-1}, \ldots, \omega_{2j+1}$ of ω.

Proof. a) If β does not cross any arc of $N_\sigma^{T^\circ}$, then by (T1) there is no even-indexed step ω_{2k} from $N_\sigma^{T^\circ}$. By Lemma 4.4.13, there is no odd-indexed step from $N_\sigma^{T^\circ}$.

b) Suppose $x(\omega)$ has a positive degree with respect to $N_\sigma^{T^\circ}$. Then $\left|\text{odd-indexed steps from } N_\sigma^{T^\circ}\right| > \left|\text{even-indexed steps from } N_\sigma^{T^\circ}\right|$ by the T°-path formula, and so there is at least one odd-indexed step from $N_\sigma^{T^\circ}$. By Lemma 4.4.13, each odd-indexed step $\omega_{2k+1} \in N_\sigma^{T^\circ}$ must either follow $\omega_{2k} \in N_\sigma^{T^\circ}$ or precede $\omega_{2k+2} \in N_\sigma^{T^\circ}$, and so the assertion follows. □

Lemma 4.4.16. *Suppose T° is an ideal triangulation and $\sigma \notin T^\circ$ is a peripheral arc from v_1 to v_1' (with $v_1 \neq v_1'$). Let $\tau := \tau_{i_1}$, the edge opposite v_1 in the first ideal triangle $\triangle_0$ through which σ passes. Let α and λ denote the two sides (the arcs $\tau_{[\sigma_0]}$, $\tau_{[\sigma_{-1}]}$, not necessarily in this order) of $\triangle_0$ adjacent to σ at v_1. Suppose σ crosses α (see Fig. 4.29). Then:*

a) α is a peripheral arc with distinct endpoints.

b) λ is a peripheral arc (or boundary edge) with distinct endpoints.

c) τ_{i_1} is peripheral (possibly an ℓ-loop) and $\tau_{i_1} \in (T^\circ, \sigma)$-doublecross.

d) There is no arc from (T°, σ)-cross that is adjacent to σ at v_1', and α is the only arc of (T°, σ)-cross that is adjacent to σ. Consequently, if $w = (\omega_1, \ldots, \omega_{2d+1})$ is a

(T°, σ)-*path, then either* $\omega_1 \notin (T^\circ, \sigma)$-*cross or* $\omega_{2d+1} \notin (T^\circ, \sigma)$-*cross.*

e) σ *crosses all radii of* T°*.*

Proof. Observe that, since v_1 lies on the boundary, the first ideal triangle σ crosses, $\triangle_0$, is not self-folded, and so all its edges τ_{i_1}, λ, α are pairwise distinct.

a) First, we prove part (a): We know that α cannot be a radius, because a radius from v_1 cannot cut an arc adjacent to v_1. Furthermore, since an ℓ-loop based at v_1 would have to lie entirely in $\mathbf{C}_\sigma$, no ℓ-loop based on v_1 can cross σ, hence α is a non-ℓ-loop peripheral arc.

b) Second, we prove part (b) of this lemma.

- Suppose for contradiction that λ is an ℓ-loop. Again, since no ℓ-loop based on v_1 can cross σ, we see that λ and σ do not cross. Hence λ would cut out a region $\mathbf{Disk}_\lambda$ not containing the puncture but containing σ as well as α. It is impossible for α and σ to both cross and be adjacent in this region, hence λ is not an ℓ-loop.
- Suppose for contradiction that λ is a radius. Then $\triangle_0$ is an ordinary triangle with the puncture as one of the vertices. Hence the region outside of $\triangle_0$ contains no puncture, so it is impossible for σ to cross $\triangle_0$ a second time. Therefore σ cannot cross α, contradicting our assumption.

Hence λ is a peripheral arc with distinct endpoints or a boundary edge.

c) We now prove part (c) of this lemma. By (a) and (b), $\tau = \tau_{i_1}$ is also a peripheral arc (possibly an ℓ-loop). Note that the puncture must be closer to τ_{i_1} than to α. Hence, the second arc crossed by σ is contained outside of $\mathbf{Disk}_\tau$, while α lies in $\mathbf{Disk}_\tau$. Since σ crosses α, σ must cross τ the second time, as needed for part (c).

d) Next, we prove part (d) of this lemma. Suppose that $\alpha' \in T^\circ$ is adjacent to the other endpoint v_1' of σ. Note that α cuts out a disk $\mathbf{Disk}_\alpha$ containing v_1', and no arc of T° in the interior of $\mathbf{Disk}_\alpha$ can both be adjacent to σ and belong to (T°, σ)-*cross*. But both α and α' belong to T° so they do not cross, hence α' is contained in $\mathbf{Disk}_\alpha$, and so α' cannot both be adjacent to σ and belong to (T°, σ)-*cross*.

Furthermore, by definition the only arcs that are adjacent to σ at v_1 are $\tau_{[\sigma_0]}$ and $\tau_{[\sigma_{-1}]}$ (i.e., α and λ). But λ is contained in $\mathbf{Disk}_\sigma$, so λ cannot cross σ.

e) Finally, we prove part (e) of this lemma. If τ_{i_1} is an ℓ-loop, then σ must cross the radius (which is the only radius of T°) containing it. Otherwise, since $\tau_{i_1} \in T^\circ$ is peripheral, all radii of T° are contained in $\mathbf{C}_\tau$. Since the segment of σ that is contained in $\mathbf{C}_\tau$ is homotopic to the segment of the original surface's boundary along $\mathbf{C}_\tau$ and since the two endpoints of σ lie *strictly* in $\mathbf{Disk}_\tau$, it follows that σ must cross all the radii. □

The following lemma is also used many times throughout the rest of this paper.

Lemma 4.4.17. *Suppose T° is an ideal triangulation, $\beta \notin T^\circ$ is an ordinary arc, and $\omega = (\omega_1, \ldots, \omega_{2d+1})$ is a (T°, β)-path. Let N be a subset of T°.*

a) If $|$even steps from $N| \geq |$odd steps from $N|$, then $x(\omega)$ has non-positive degree with respect to N. Furthermore, inequality implies negative degree.

b) $x(\omega)$ has non-positive degree with respect to (T°, β)-cross.

c) If $\omega_1, \omega_{2d+1} \notin (T^\circ, \beta)$-cross, then $x(\omega)$ has negative degree with respect to (T°, β)-cross. Hence, if β is not adjacent to any arc that crosses it, $x(\omega)$ has negative degree with respect to (T°, β)-cross.

Proof. Consider a (T°, β)-path $\omega = (\omega_1, \ldots, \omega_{2d+1})$. Part (a) follows from the T°-path formula.

The corresponding term $x(\omega)$ in the T°-expansion of x_β has $d+1$ factors in the numerator and d factors in the denominator. All the factors in the denominator correspond to the arcs of T° that cross β. By Lemma 4.4.16(d), at least one of the endpoints of β is not adjacent to any arc from (T°, β)-*cross*, so either the first step ω_1 or the last step ω_{2d+1} of ω does not come from (T°, β)-*cross* by (T2). Hence, there are at most d odd steps contributing to the degree. Since there are exactly d even steps from (T°, β)-*cross*, $x(\omega)$ has non-positive degree with respect to the arcs of T° which cross σ, satisfying part (b).

If the first and last steps ω_1, ω_{2d+1} of ω do not come from (T°, σ)-*cross*, there are at most $d-1$ odd steps which contribute to the degree, and (c) follows. Furthermore, if β is not adjacent to any arc from (T°, σ)-*cross*, then $\omega_1, \omega_{2d+1} \notin (T^\circ, \sigma)$-*cross* by (T2). □

4.4.3 Technical lemmas to prove Lemma 4.4.4 for cases where all arcs of $\Sigma\backslash T$ are peripheral

Proving that x_Σ has non-positive degree with respect to (T,σ)-*cross*

Lemma 4.4.18. *Let T be a tagged triangulation and suppose σ is a tagged peripheral arc not in T.*

a) Then each term in the T-expansion of x_σ has non-positive degree with respect to (T,σ)-cross.

b) If (T°,σ)-doublecross is empty, then each term in the T-expansion of x_σ has negative degree with respect to (T,σ)-cross.

Proof. By Lemma 4.4.17(b), each term in the T°-expansion of x_σ has non-positive degree with respect to (T°,σ)-*cross*.

By Lemma 4.4.16(c), if (T°,σ)-*doublecross* is empty, then σ is not adjacent to any arc from (T°,σ)-*cross*. Therefore, by Lemma 4.4.17(c), $x(\omega)$ has negative degree with respect to (T°,σ)-*cross*.

By Lemma 4.4.9, both assertions follow. □

Definition 4.4.19. *Let Λ be a multi-tagged triangulation containing only peripheral arcs. We say that $\lambda\in\Lambda$ is* central in Λ *if λ is as close as possibly to the puncture, i.e.,*

$$\text{if } \beta\in\Lambda\backslash\{\lambda\}, \text{ then the disk } \boldsymbol{Disk}_\beta \text{ does not contain } \lambda.$$

Remark 4.4.20. *Let $\{\lambda_1,\dots,\lambda_r\}$ be the set of central arcs of Λ. Then, by definition, every $\beta\in\Lambda$ is contained in $\boldsymbol{Disk}_{\lambda_j}$ for some j. See Fig. 4.30(a).*

Lemma 4.4.21. *Suppose Σ is a multi-tagged triangulation and T is a tagged triangulation. Suppose $\sigma\in\Sigma\backslash T$ is a tagged peripheral arc that is central in $\Sigma\backslash T$, i.e.,*

$$\text{if } \beta\in\Sigma\backslash T \text{ is not } \sigma, \text{ then the disk } \mathbf{Disk}_\beta \text{ does not contain } \sigma \text{ (see Fig. 4.31).} \quad (4.4.5)$$

Let β be any tagged arc in Σ such that, if $\beta\in\Sigma\backslash T$, then β is peripheral. See Figs. 4.31(a) *and* 4.31(b)*. Then each term in the T-expansion of x_β has non-positive degree with respect to (T,σ)-cross.*

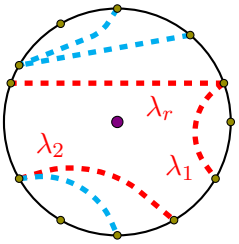

(a) The peripheral arcs $\lambda_1, \ldots, \lambda_r$ as close as possible to the puncture.

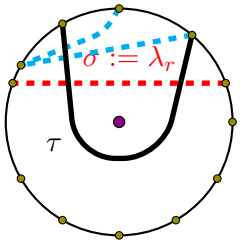

(b) If (T°, σ)-*doublecross* is non-empty, then $r = 1$.

Figure 4.30: Proof of Lemma 4.4.4: the case where $\Sigma \backslash T$ are all peripheral.

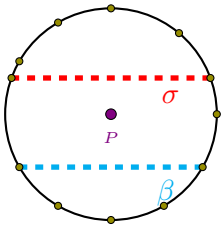

(a) Correct setup for Lemma 4.4.21 but wrong setup for Lemma 4.4.22: σ is not the only central arc.

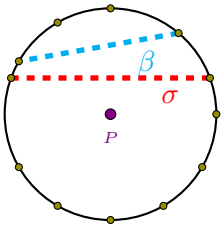

(b) Correct setup for both Lemmas 4.4.21 and 4.4.22: σ is the only central arc.

Figure 4.31: Setups for Lemmas 4.4.21 and 4.4.22.

Proof. Let s^σ be the starting point and let t^σ be the finishing point of σ. Since σ is not an ℓ-loop by assumption, $s^\sigma \neq t^\sigma$.

If $\beta \in T$, then its degree with respect to any of the above gradings is zero since it cannot cross σ. If $\beta = \sigma$, we are done by Lemma 4.4.18.

Otherwise, suppose $\beta \in \Sigma \backslash T$ and $\beta \neq \sigma$, and so β is peripheral by assumption. Let $\omega = (\omega_1, \ldots, \omega_{2d+1})$ be a (T°, β)-path. First, we prove that

the T°-expansion of $x(\omega)$ has non-positive degree with respect to (T°, σ)-*cross*. (4.4.6)

For contradiction, suppose otherwise. By Corollary 4.4.15(b), there must be a longest (T°, σ)-*cross*-subsequence $\bar{\omega} = (\omega_{2i-1}, \ldots, \omega_{2j+1})$ of ω (of length three or greater). Since σ and β are compatible, there are two possibilities for β: either β lies in the once-punctured disk $\mathbf{C}_\sigma$ or β lies in the disk $\mathbf{Disk}_\sigma$.

Case 1: *First, suppose β lies in $\boldsymbol{C}_\sigma$.* See Fig. 4.31(a). Per (4.4.5), β has the property that it cuts out the disk $\mathbf{Disk}_\beta$ not containing σ, so no radius can cross both β and σ. Hence each of the even-indexed arcs $\omega_{2i}, \ldots, \omega_{2j}$ is a peripheral arc because each of them crosses both β and σ. It then follows that each odd-indexed arc $\omega_{2i+1}, \ldots, \omega_{2j-1}$ is also a peripheral arc.

We claim that $\bar{\omega}$ begins and finishes in $\mathbf{C}_\sigma$ (recall that this means possibly at s^σ or t^σ):

- If $i = 1$, then ω_1 starts in $\mathbf{C}_\sigma$ since β lies in $\mathbf{C}_\sigma$. Otherwise, there is a previous step ω_{2i-2} which crosses β. Since ω_{2i-2} does not belong to (T°, σ)-*cross* by assumption, ω_{2i-2} ends in $\mathbf{C}_\sigma$.
- If $j = d$, then ω_{2d+1} finishes in $\mathbf{C}_\sigma$ since β lies in $\mathbf{C}_\sigma$. Otherwise, there is a next step ω_{2j+2} which crosses β. Since ω_{2j+2} does not belong to (T°, σ)-*cross* by assumption, ω_{2j+2} ends in $\mathbf{C}_\sigma$.

In fact, by induction starting from ω_{2i-1}, every odd-indexed arc of $\bar{\omega}$ must start from $\mathbf{C}_\sigma$. But this means that ω_{2j+1} is a peripheral arc which begins and ends in $\mathbf{C}_\sigma$ but also crosses σ, which is impossible.

Case 2: *Next, suppose that β lies in $\mathbf{Disk}_\sigma$.* See Figs. 4.31(b) and 4.32. To simplify our argument, consider

a 2-fold cover $\widetilde{T^o}$ of T°, a triangulated once-punctured disk containing two lifts of every arc $\tau \in T^\circ$ and of every boundary marked point of $\mathcal{C}_n$ (see Fig. 4.33),

every ideal triangle in $\widetilde{T^o}$ is an ordinary triangle, (4.4.7)

a lift of γ is a radius if and only if γ is a radius of $\mathcal{C}_n$.

Since every pair of arcs of $\mathcal{C}_n$ cross each other at most twice,

every pair of lifted arcs cross each other at most once on the two-fold cover. (4.4.8)

Hence, by Lemma 4.4.16(c),

a pair of adjacent lifted arcs do not cross on the two-fold cover. (4.4.9)

Choose a lift $\widetilde{\sigma}$ of σ going from $\tilde{s}^\sigma$ to $\tilde{t}^\sigma$. Here $\widetilde{\sigma}$ cuts out a disk $\mathbf{Disk}_{\widetilde{\sigma}}$ from $\widetilde{T^o}$. Let $\widetilde{\beta}$ denote the lift of β which lies in $\mathbf{Disk}_{\widetilde{\sigma}}$, and let $\widetilde{\omega}$ be the lift of ω which is a $(\widetilde{T^o}, \widetilde{\beta})$-path. We abuse notation by writing $\bar{\omega}$ to denote the subpath of $\widetilde{\omega}$ corresponding to $\bar{\omega}$.

i) First, assume that $\bar{\omega}$ has an earlier step ω_{2i-2} and a later step ω_{2j+2}. We see that $\bar{\omega}$ starts from inside $\mathbf{Disk}_{\widetilde{\sigma}}$ (otherwise, $\widetilde{\omega}_{2i-2}$ would have to cross $\widetilde{\sigma}$) and $\bar{\omega}$ ends inside $\mathbf{Disk}_{\widetilde{\sigma}}$ (otherwise, $\widetilde{\omega}_{2j+2}$ would have to cross $\widetilde{\sigma}$). Recall that by inside $\mathbf{Disk}_{\widetilde{\sigma}}$ we mean possibly at $\tilde{s}^\sigma$ or $\tilde{t}^\sigma$. In fact, by induction starting from ω_{2i-1}, every odd-indexed arc of $\bar{\omega}$ must start from inside $\mathbf{Disk}_{\widetilde{\sigma}}$. But this means that $\widetilde{\omega}_{2j+1}$ begins and ends inside $\mathbf{Disk}_{\widetilde{\sigma}}$ and also crosses $\widetilde{\sigma}$. This requires $\widetilde{\sigma}$ and $\widetilde{\omega}_{2j+1}$ to cross twice, contradicting (4.4.8).

ii) Second, assume that $i = 1$ or $j = d$. Without loss of generality, assume $i = 1$. There are two cases: either β and σ are adjacent at σ or not.

- If β and σ are adjacent at s, then $\widetilde{\omega}_1$ and $\widetilde{\sigma}$ are adjacent and so $\widetilde{\omega}_1$ cannot cross $\widetilde{\sigma}$ by (4.4.9). But ω_1 crosses σ by assumption, and so $\widetilde{\omega}_1$ must cross the other lift $\widetilde{\sigma}^2$ of σ which is outside of $\mathbf{Disk}_{\widetilde{\sigma}}$. Therefore $\widetilde{\omega}_1$ ends outside of $\mathbf{Disk}_{\widetilde{\sigma}}$.
- If β and σ are not adjacent at σ, then ω_1 starts inside of $\mathbf{Disk}_{\widetilde{\sigma}}$ because $\widetilde{\beta}$ lies in $\mathbf{Disk}_{\widetilde{\sigma}}$. Since ω_1 crosses σ by assumption, $\widetilde{\omega}_1$ has to cross $\widetilde{\sigma}$ and end outside of $\mathbf{Disk}_{\widetilde{\sigma}}$.

So, either way, $\widetilde{\omega}_1$ ends outside of $\mathbf{Disk}_{\widetilde{\sigma}}$. Hence $\widetilde{\omega}_2, \ldots, \widetilde{\omega}_{2j+1}$ forms a zig-zag pattern crossing $\widetilde{\sigma}$ an even number $(2j)$ of times, ending outside of $\mathbf{Disk}_{\widetilde{\sigma}}$. Since $\widetilde{\beta}$ lies in $\mathbf{Disk}_{\widetilde{\sigma}}$, there must be a step $\widetilde{\omega}_{2j+2}$ right after $\bar{\omega}$ which crosses $\widetilde{\omega}$, contradicting the assumption that $\bar{\omega}$ is a longest $(\widetilde{T^o}, \widetilde{\sigma})$-*cross*-subpath.

This ends the proof for (4.4.6). The conclusion follows from Lemma 4.4.9. □

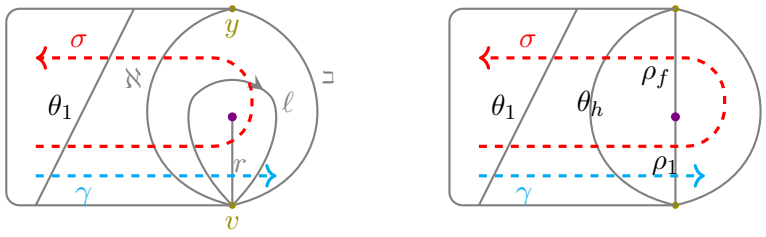

(a) T° contains a self-folded triangle with radius r and ℓ-loop ℓ.

(b) T° has radii $\rho_1, \ldots, \rho_f$ $(f \geq 2)$.

Figure 4.32: T° when (T°, σ)-*doublecross* $= \{\theta_1, \ldots, \theta_h\}$ is nonempty.

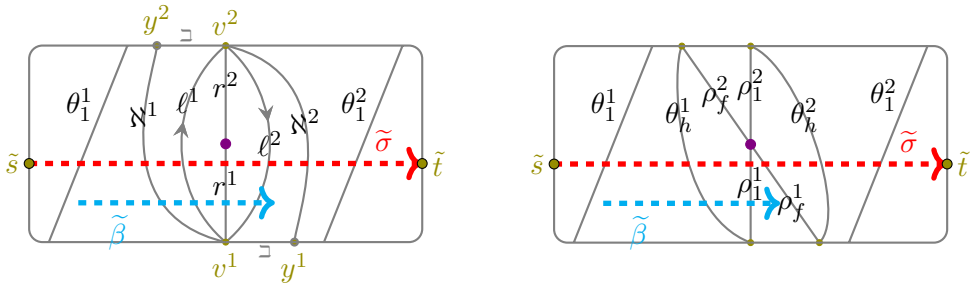

(a) T° contains a self-folded triangle with radius r and ℓ-loop ℓ.

(b) T° has radii $\rho_1, \ldots, \rho_f$ $(f \geq 2)$.

Figure 4.33: Two-fold cover $\mathbf{Disk}_{\widetilde{\sigma}}$ of T° when (T°, σ)-*doublecross* $= \{\theta_1, \ldots, \theta_h\}$ is nonempty.

Proving that x_Σ has non-positive degree with respect to (T, σ)-*doublecross*, and x_σ has negative degree with respect to (T, σ)-*cross* and (T, σ)-*doublecross*

Lemma 4.4.22. *Suppose Σ is a multi-tagged triangulation and T is a tagged triangulation. Let $\sigma \in \Sigma \backslash T$ be a tagged peripheral arc.*

1) *Assume (T, σ)-doublecross is non-empty, and σ is central in $\Sigma \backslash T$ and no other arc is central in $\Sigma \backslash T$. Let $\beta \in \Sigma$ (possibly $\beta = \sigma$). Then each term in the T-expansion of x_β has non-positive degree with respect to (T, σ)-doublecross.*

2) *Each term in the T-expansion of x_σ has negative degree with respect to (T, σ)-cross or (T, σ)-doublecross.*

Proof. If $\beta \in T$, then its degree with respect to (T°, σ)-*doublecross* is zero since it

cannot cross σ. Suppose $\beta \in \Sigma \backslash T$. By Remark 4.4.20, $\beta = \sigma$ or β lies in $\mathbf{Disk}_\sigma$, i.e., if $\beta \neq \sigma$, then σ is closer than β to the puncture. See Notation 4.4.10.

Let $\omega^\beta = (\omega_1, \ldots, \omega_{2e+1})$ be a (T°, β)-path. If β does not cross any arc from (T°, σ)-doublecross, then by Corollary 4.4.15(a) the degree of ω with respect to (T°, σ)-doublecross is zero. Suppose β crosses at least an arc from (T°, σ)-doublecross. See Figs. 4.32.

Suppose $x(\omega^\beta)$ has positive degree with respect to the θ_k's. Then by Corollary 4.4.15(b) there is a longest $\{\theta_k$'s$\}$-subpath $\bar{\omega}^\beta = (\omega_{2i-1}, \ldots, \omega_{2j+1})$ of ω.

Let arc $\tau_{i_1}, \ldots, \tau_{i_d}$ be the arcs crossed by σ, in order.

Let $\theta_1, \ldots, \theta_h$ $(h \geq 1)$ denote the arcs in that are crossed by σ twice (ordered so that θ_1 is the first and last arc from (T°, σ)-*doublecross* crossed by σ). Note that $\theta_1, \ldots, \theta_{h-1}$ are contained in the disk $\mathbf{Disk}_{\theta_h}$ cut by θ_h, see Fig. 4.32. Let $\rho_1, \ldots, \rho_f$ $(f \geq 1)$ be the radii of T°, in order of their intersections with σ. Recall that, by Lemma 4.4.16(e), σ crosses all radii of T°. Let $\tau_{i_1}, \ldots, \tau_{i_m}$ (if any) be the peripheral arcs which σ exactly once, right before σ crosses θ_1 for the first time. Let $\tau_{i_{m+h+f+h+1}}, \ldots, \tau_{i_d}$ (if any) be the peripheral arcs which σ exactly once, right after σ crosses θ_1 for the second time.

Consider a 2-fold cover $\widetilde{T^o}$ of T°, a triangulated once-punctured disk containing two lifts of every arc $\tau \in T^\circ$ and of every boundary marked point of $\mathcal{C}_n$, see (4.4.7) and Fig. 4.33.

Recall that (4.4.9) gives that

$$\text{a pair of adjacent lifted arcs on } \widetilde{T^o} \text{ do not cross.}$$

Let s^σ be the starting point of σ and let t^σ be the finishing point of σ. By assumption, σ is not an ℓ-loop, so $s \neq t$. Choose a lift $\widetilde{\sigma}$ of σ, running from a lift $\tilde{s}$ of s to a lift $\tilde{t}$ of t. Let $\mathbf{Disk}_{\widetilde{\sigma}}$ denote the disk that is cut out by $\widetilde{\sigma}$. Let $\widetilde{\sigma}^2$ be the other lift of σ, running from $\tilde{s}^2$ to $\tilde{t}^2$. Note that $\widetilde{\sigma}$ and $\widetilde{\sigma}^2$ never coincide, and, in particular,

$$\widetilde{\sigma} \text{ and } \widetilde{\sigma}^2 \text{ share no common endpoint.} \tag{4.4.10}$$

Let $\mathbf{Disk}^2_{\widetilde{\sigma}}$ be the disk that is cut out by $\widetilde{\sigma}$.

Let $\rho^1_1, \ldots, \rho^1_f$ denote the lifts of $\rho_1, \ldots, \rho_f$ which are crossed by $\widetilde{\sigma}$. Let $\rho^2_1, \ldots, \rho^2_f$

denote the other lifts of $\rho_1, \ldots, \rho_f$, lying entirely outside of $\mathbf{Disk}_{\widetilde{\sigma}}$. Let $\theta_1^1, \ldots, \theta_h^1$ (respectively, $\theta_1^2, \ldots, \theta_h^2$) denote the lifts of $\theta_1, \ldots, \theta_h$ which $\widetilde{\sigma}$ crosses first (respectively, second). In general, let τ^1 denote the lift of $\tau \in T^\circ$ in the region cut out by ρ_f^1 and ρ_f^2 which contains $\tilde{s}$, and let τ^2 denote the lift of $\tau \in T^\circ$ in the other region.

Since σ cuts $\tau_{i_1}, \ldots, \tau_{i_m}, \theta_1, \ldots, \theta_h, \rho_1, \ldots, \rho_f, \theta_h, \ldots, \theta_1, \tau_{i_{m+h+f+h+1}}, \ldots, \tau_{i_d}$, in this order, we see that $\widetilde{\sigma}$ cuts

$$\tau_{i_1}^1, \ldots, \tau_{i_m}^1, \theta_1^1, \ldots, \theta_h^1, \rho_1^1, \ldots, \rho_f^1, \theta_1^2, \ldots, \theta_h^2, \tau_{i_{m+h+f+h+1}}^2, \ldots, \tau_{i_d}^2,$$

in this order.

If $\tau \neq \theta_k$, then by assumption $\tau \in T^\circ$ cuts σ at most once, so

$$\begin{gathered}\text{if } \tau \neq \theta_k, \text{ then } \widetilde{\sigma} \text{ cuts at most one of the two lifts } \tau^1, \tau^2 \text{ of } \tau, \\ \text{and a lift of } \tau \text{ cuts at most one of the two lifts } \widetilde{\sigma}, \widetilde{\sigma}^2 \text{ of } \sigma. \end{gathered} \tag{4.4.11}$$

Since σ cuts each arc θ_k twice, $\widetilde{\sigma}$ cuts both lifts θ_k^1 and θ_k^2 of θ_k. Due to (4.4.9),

$$\widetilde{\sigma} \text{ cannot be adjacent to } \theta_k^1 \text{ or } \theta_k^2. \tag{4.4.12}$$

Let $\widetilde{\beta}$ be the lift of β that is contained in $\mathbf{Disk}_{\widetilde{\sigma}}$. Let $\widetilde{\omega}^\beta$ denote the $(\widetilde{T^o}, \widetilde{\beta})$-path corresponding to ω^β, and we abuse notation by writing $\bar{\omega}^\beta$ to refer to the subpath of $\widetilde{\omega}^\beta$ corresponding to $\bar{\omega}^\beta$.

If $\bar{\omega}^\beta$ contains both θ_a^1 and θ_b^2 for some $1 \leq a, b \leq h$, then $\bar{\omega}^\beta$ must contain the radius/radii $\rho_1^1, \ldots, \rho_f^1$, contradicting that the fact that $\bar{\omega}^\beta$ is a $\{\theta_k\text{'s}\}$-subpath. Without loss of generality, assume each step of $\bar{\omega}^\beta$ goes along θ_k^1 for some k.

Note that, because θ_k crosses σ twice,

$$\text{every } \theta_k^1 \text{ crosses both } \widetilde{\sigma} \text{ and } \widetilde{\sigma}^2.$$

Hence, since every step of $\bar{\omega}^\beta$ is θ_k^1 for some k,

$$\text{every step of } \bar{\omega}^\beta \text{ begins } \textit{strictly} \text{ inside } \mathbf{Disk}_{\widetilde{\sigma}} \text{ or } \mathbf{Disk}_{\widetilde{\sigma}}^2. \tag{4.4.13}$$

Recall that starting *strictly* inside $\mathbf{Disk}_{\widetilde{\sigma}}$ (respectively, $\mathbf{Disk}_{\widetilde{\sigma}}^2$) means at a marked point

of $\mathbf{Disk}_{\widetilde{\sigma}}$ (respectively, $\mathbf{Disk}^2_{\widetilde{\sigma}}$) that is not $\tilde{s}$ or $\tilde{t}$ (respectively, $\tilde{s}^2$ or $\tilde{t}^2$).

If $\beta = \sigma$, then $\bar{\omega}_1$ starts at $\tilde{s}$ and $\bar{\omega}_{2d+1}$ finishes at $\tilde{t}$, so by (4.4.13) there must be an earlier step $\widetilde{\omega}_{2i-2}$ and a later step ω_{2j+2} of $\widetilde{\omega}$. If $\beta \neq \sigma$, then it is possible to have $i = 1$ (if β is not adjacent to σ at its starting point) or $j = e$ (if β is not adjacent to σ at its finishing point).

We claim that $\bar{\omega}^\beta$ starts strictly inside $\mathbf{Disk}_{\widetilde{\sigma}}$. For the sake of argument, suppose that $\bar{\omega}^\beta = (\widetilde{\omega}_{2i-1}, \ldots, \widetilde{\omega}_{2j+1})$ starts strictly inside of $\mathbf{Disk}^2_{\widetilde{\sigma}}$.

Case 1: First, suppose that $\widetilde{\omega}^\beta$ has an earlier step $\widetilde{\omega}_{2i-2}$. Since $\widetilde{\omega}_{2i-2}$ must cross $\widetilde{\beta}$, which lies in $\mathbf{Disk}_{\widetilde{\sigma}}$, we see that $\widetilde{\omega}_{2i-2}$ must cross both $\widetilde{\sigma}$ and $\widetilde{\sigma}^2$ to get from strictly inside $\mathbf{Disk}_{\widetilde{\sigma}}$ to strictly inside $\mathbf{Disk}^2_{\widetilde{\sigma}}$. Since $\widetilde{\omega}_{2i-2}$ is not a lift of one of the θ_k's, this contradicts (4.4.11).

Case 2: Second, assume that $\beta \neq \sigma$, and we have $i = 1$. Since $\widetilde{\beta}$ lies in $\mathbf{Disk}_{\widetilde{\sigma}}$ by assumption, either $\widetilde{\omega}_1$ starts at $\tilde{s}^\sigma$ or $\tilde{t}^\sigma$, or $\widetilde{\omega}_1$ starts *strictly* inside of $\mathbf{Disk}_{\widetilde{\sigma}}$ (see Notation 4.4.10). By (4.4.13), $\widetilde{\omega}_1$ starts strictly in $\mathbf{Disk}_{\widetilde{\sigma}}$.

Either way, $\bar{\omega}^\beta$ starts strictly in $\mathbf{Disk}_{\widetilde{\sigma}}$. Per (4.4.13), we see that $(\widetilde{\omega}_{2i-1}, \ldots, \widetilde{\omega}_{2j+1})$ forms a zip-zag pattern bouncing back and forth between (strictly) $\mathbf{Disk}_{\widetilde{\sigma}}$ and (strictly) $\mathbf{Disk}^2_{\widetilde{\sigma}}$. So, by induction starting from $\widetilde{\omega}_{2i-1}$, every odd-indexed arc of $\bar{\omega}$ must start strictly in $\mathbf{Disk}_{\widetilde{\sigma}}$ and ends strictly in $\mathbf{Disk}^2_{\widetilde{\sigma}}$. Hence the last step $\widetilde{\omega}_{2j+1}$ ends strictly in $\mathbf{Disk}^2_{\widetilde{\sigma}}$.

The step $\widetilde{\omega}_{2j+1}$ cannot be the last step of $\widetilde{\omega}^\beta$ because the finishing point of $\widetilde{\beta}$ lies (strictly) outside of $\mathbf{Disk}^2_{\widetilde{\sigma}}$ per (4.4.10). Hence $\widetilde{\omega}^\beta$ has a next step $\widetilde{\omega}_{2j+2}$. Since $\widetilde{\omega}_{2j+2}$ must cross $\widetilde{\beta}$, which lies in $\mathbf{Disk}_{\widetilde{\sigma}}$, we see that $\widetilde{\omega}_{2j+2}$ must cross both $\widetilde{\sigma}$ and $\widetilde{\sigma}^2$ to go strictly from $\mathbf{Disk}^2_{\widetilde{\sigma}}$ to strictly in $\mathbf{Disk}_{\widetilde{\sigma}}$. Since $\widetilde{\omega}_{2j+2}$ is not a lift of one of the θ_k's, this contradicts (4.4.11).

We prove part (2):

Suppose $\omega = (\omega_1, \ldots, \omega_{2d+1})$ is a (T°, σ)-path. First, we claim that the T°-expansion of $x(\omega)$ has negative degree with respect to either (T°, σ)-*cross* or (T°, σ)-*doublecross*: By Lemma 4.4.16(d), either $\omega_1 \notin (T^\circ, \sigma)$-*cross* or $\omega_{2d+1} \notin (T^\circ, \sigma)$-*cross*. If necessary, reverse the orientation of ω so that $\omega_{2d+1} \notin (T^\circ, \sigma)$-*cross*. If not all the odd steps $\omega_1, \omega_3, \ldots, \omega_{2d-1}$ cross σ, then $x(\omega)$ has negative degree with respect to (T°, σ)-*cross*

by Lemma 4.4.17(c). Hence suppose that all steps of ω except ω_{2d+1} come from (T°, σ)-*cross*.

We claim that $\omega_{2h+1} \notin (T^\circ, \sigma)$-*doublecross*:

Since $\omega_1 \in (T^\circ, \sigma)$-*cross*, Lemma 4.4.16(c) gives us $\omega_2 = \theta_1$. Since ω_1 crosses σ, its lift $\widetilde{\omega}_1$ (which lies in $\mathbf{Disk}^1_{\widetilde{\theta}_1}$) must cross a lift of σ. Because $\widetilde{\omega}_1$ is adjacent to $\widetilde{\sigma}$, they cannot cross by (4.4.9), so $\widetilde{\omega}_1$ must cross the other lift $\widetilde{\sigma}^2$ of σ which is located (strictly) outside of $\mathbf{Disk}_{\widetilde{\sigma}}$. Hence $\widetilde{\omega}_1$ goes from $\tilde{s}$ to outside of $\mathbf{Disk}_{\widetilde{\sigma}}$, and $\widetilde{\omega}_2$ goes along θ^1_1 from outside to strictly inside of $\mathbf{Disk}_{\widetilde{\sigma}}$. By (T1) and (T2), the steps $\widetilde{\omega}_2, \widetilde{\omega}_3, \ldots, \widetilde{\omega}_{2h-1}, \widetilde{\omega}_{2h}$ make a zig-zag pattern along the arcs $\theta^1_1, \ldots, \theta^1_h$, so that $\widetilde{\omega}_{2h}$ goes along θ^1_h and ends strictly in $\mathbf{Disk}_{\widetilde{\sigma}}$. Hence, by (T2), $\widetilde{\omega}_{2h+1}$ either goes along θ^1_h or ρ^1_1. If $\widetilde{\omega}_{2h+1}$ goes along θ^1_h, it goes from strictly inside to outside of $\mathbf{Disk}_{\widetilde{\sigma}}$. Since the point of ρ^1_1 that is adjacent to θ^1_1 is strictly in $\mathbf{Disk}_{\widetilde{\sigma}}$, it is impossible for $\widetilde{\omega}_{2(h+1)}$ to go along ρ^1_1. This contradicts the fact that $\widetilde{\omega}_{2(h+1)}$ must go along ρ^1_1. Hence $\widetilde{\omega}_{2h+1}$ goes along ρ^1_1, as needed to show that $w_{2h+1} \notin (T^\circ, \sigma)$-*doublecross*.

By part (1), the odd-indexed steps $\omega_{2(h+f+1)-1}, \ldots, \omega_{2(h+f+h)+1}$ cannot all belong to (T°, σ)-*doublecross*, so there are at most h odd-indexed steps coming from $\omega_{2(h+f+1)-1}, \ldots, \omega_{2(h+f+h)+1}$. As there are at most $(h-1)+h$ odd-indexed steps from $\omega_3, \omega_5, \ldots, \omega_{2h-1}$, there are at most $(h-1)+h$ odd-indexed steps of ω coming from (T°, σ)-*doublecross* total. There are exactly $2h$ even steps of ω from (T°, σ)-*doublecross* by (T1). Hence, by Lemma 4.4.17(a), the term $x(\omega)$ has negative degree with respect to (T°, σ)-*doublecross*, as required.

Per Lemma 4.4.9, the conclusion follows. □

4.4.4 Technical lemmas to prove Lemma 4.4.4 for cases where Σ has a radius not in T

$\Sigma \backslash T$ contains a plain radius σ

Lemma 4.4.23 (Corollary of Lemma 4.4.17(c))**.** *Let T be a tagged triangulation and let $\sigma \notin T$ be a plain radius, see Figs.* 4.35(a) *and* 4.35(b)*. Then every term in the T-expansion of x_σ has negative degree with respect to*

$$N^T_\sigma := (T, \sigma)\text{-}cross.$$

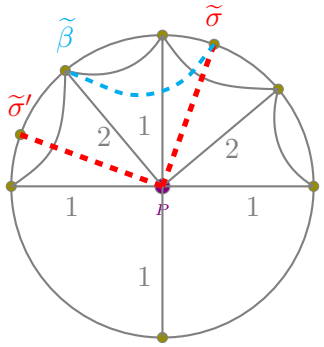

(a) 4-fold cover of T, which has at least two radii 1, 2, from Fig. 4.2(a), and σ is a radius.

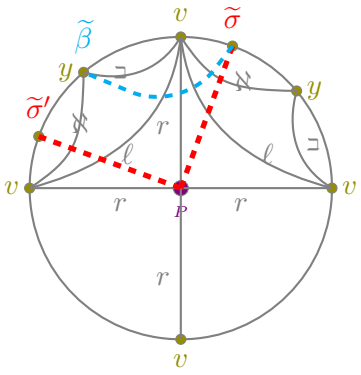

(b) 4-fold cover of T° from Fig. 4.2(b), where T° has a self-folded triangle r, ℓ. Here σ is a radius.

Figure 4.34: 4-fold cover $\widetilde{T^o}$ of T° where β is a peripheral arc, and σ is a peripheral arc (respectively, a radius), and $\mathbf{Disk}_{\widetilde{\sigma}}$ is a disk cut out by the peripheral $\widetilde{\sigma}$ (respectively, the fundamental domain area bounded by the two lifts $\widetilde{\sigma}$ and $\widetilde{\sigma}'$ of σ.)

As defined in Definition 4.4.8,

$$(T,\sigma)\text{-}cross = \begin{cases} (T^\circ,\sigma)\text{-}cross & \text{if } T \text{ has no parallel radii} \\ \{r^{(p)}, \text{ and the (peripheral) arcs of } T \text{ that cross } \sigma\} & \text{if } T \text{ has parallel radii } r,\ r^{(p)}. \end{cases}$$

Proof. Since σ is a radius, it is not adjacent to any arc from (T°,σ)-*cross*. Hence, by Lemma 4.4.17(c),

$$\text{each term in the } T^\circ\text{-expansion of } x_\sigma \text{ has negative degree with respect to } (T^\circ,\sigma)\text{-}cross, \tag{4.4.14}$$

and therefore, by Lemma 4.4.9, with respect to $N_\sigma^T := (T,\sigma)$-*cross*. □

Lemma 4.4.24. *Assume the same setup of T, σ, and N_σ^T as in Lemma* 4.4.23 *above, and let β be a tagged arc that is compatible with σ. Then each term in the T-expansion of x_β has non-positive degree with respect to $N_\sigma^T = (T,\sigma)$-cross.*

Proof of Lemma 4.4.24. Let $\rho_1,\dots,\rho_f$ denote the radii of T° and let σ run from the

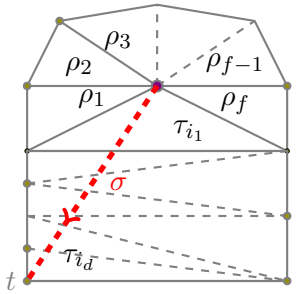

(a) T has no parallel radii.

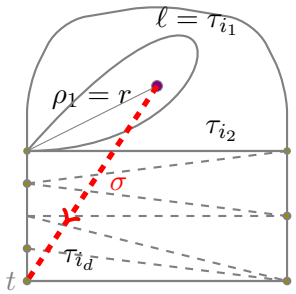

(b) T° has a self-folded triangle r, ℓ.

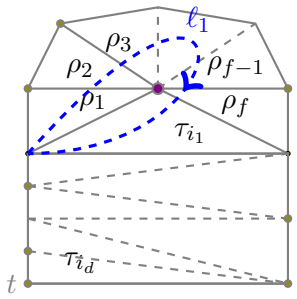

(c) ℓ_1 in dotted line is the loop surrounding the radius ρ_1.

Figure 4.35: Lemmas 4.4.23 and 4.4.24 assume that $\Sigma \backslash T$ contains a plain radius σ.

puncture to the boundary such that the radii ρ_1, ρ_f and peripheral arc τ_{i_1} (the first arc crossed by σ) form the first triangle that σ crosses. If T° has a self-folded triangle r, ℓ, then $f = 1$ and $\rho_1 = r = \rho_f$ and $\tau_{i_1} = \ell$. See Figs. 4.35(a) and 4.35(b).

If $\beta = \sigma$, we are done by the previous Lemma 4.4.23. Otherwise, since β must be compatible with σ, there are only four possibilities: β is an arc of T, another plain radius, the notched radius $\sigma^{(p)}$, or a peripheral arc.

Case 1: *First, suppose $\beta \in T$ is compatible with σ.* Then β cannot cross σ and β cannot be a notched radius, so $\beta \notin (T, \sigma)$-*cross*.

Case 2: *Second, suppose β is another plain radius (not in T°).* Let $\omega = (\omega_1, \ldots, \omega_{2d+1})$ be a (T°, β)-path which runs from the puncture to the boundary. Then ω_1 is a

radius, and hence ω_1 does not cross σ. Note that ρ_1 and ρ_f (possibly $\rho_1 = \rho_f$) bound a region (say, R) containing σ and all the (peripheral) arcs in (T°, σ)-*cross*. If β is outside of R, then ω does not contain any arc of (T°, σ)-*cross*. If β is contained in R, then the even-indexed arcs of ω that are crossed by σ form a consecutive string

$$\omega_2 = \tau_{i_1}, \ldots, \omega_{2j} = \tau_{i_j}.$$

By Lemma 4.4.13(iii), the only odd-indexed step/s that may belong to (T°, σ)-*cross* are $\omega_3, \ldots, \omega_{2j+1}$ since ω_1 is a radius (and hence does not cross σ). Hence ω has at j even-indexed steps and at most j odd-indexed steps from (T°, σ)-*cross*, so, by Lemma 4.4.17(a), $x(\omega)$ has non-positive degree with respect to (T°, σ)-*cross*, and hence, by Lemma 4.4.9, with respect to (T, σ)-*cross*.

Case 3: *Third, suppose* $\beta = \sigma^{(p)}$. First, suppose T has parallel radii r, $r^{(p)}$. By (4.4.14), each term of the T°-expansion of x_σ has negative degree with respect to (T°, σ)-*cross* $= \{\ell$, (peripheral) arcs of T which cross $\sigma\}$. Each term $x(\omega)$ (as a T°-monomial) corresponding to a (T°, σ)-path ω has degree $+1$ with respect to r, so $x(\omega)|_{r \leftrightarrow r^{(p)}}$ (as a ${T^{(p)}}^\circ$-monomial) has degree $+1$ with respect to $r^{(p)}$ and negative degree with respect to (T°, σ)-*cross* $= \{\ell$, (peripheral) arcs of T which cross $\sigma\}$, and, therefore, non-positive degree (as a T-monomial) with respect to (T, σ)-*cross*. Since $x_{\sigma^{(p)}} = x_\sigma|_{r \leftrightarrow r^{(p)}}$ by [MSW11, Proposition 3.15], every term in the T-expansion of $x_{\sigma^{(p)}}$ has non-positive degree with respect to (T, σ)-*cross*, as needed.

Next, suppose $f \geq 2$, and we have, by [MSW11, Proposition 3.15],

$$x_{\sigma^{(p)}} = x_\sigma|_{\rho_i \leftrightarrow \rho_i{}^{(p)}} = x_\sigma|_{\rho_1 \leftrightarrow \rho_1{}^{(p)}, \rho_f \leftrightarrow \rho_f{}^{(p)}}. \tag{4.4.15}$$

The second equality is due to the fact that no (T, σ)-path would contain the radii $\rho_2, \ldots, \rho_{f-1}$, as these radii are not adjacent to σ. Let ℓ_1 (respectively, ℓ_f) be the loop surrounding the radius ρ_1 (respectively, ρ_f), see Fig. 4.35(c).

Since only the starting endpoint (and not the finish endpoint) of σ is adjacent to ρ_1 and ρ_f, we see that every term in the T-expansion of x_σ has degree $+1$

with respect to $\{\rho_1, \rho_f\}$, so

$$\begin{gathered}\text{each term in the } T\text{-expansion of } \sigma^{(p)} \text{ has degree } +1 \\ \text{with respect to } \{x_{\rho_1^{(p)}} = x_{\ell_1}/x_{\rho_1},\, x_{\rho_f^{(p)}} = x_{\ell_f}/x_{\rho_f}\}. \end{gathered} \tag{4.4.16}$$

Furthermore, we observe that each term in the T-expansions of x_{ℓ_1} and x_{ℓ_f} has at most degree $+1$ with respect to (T, σ)-*cross*. Since $x_{\rho_i^{(p)}} = x_{\ell_i}/x_{\rho_i}$ for $i = 1, f$,

$$\begin{gathered}\text{each term in the } T\text{-expansions of } x_{\rho_1^{(p)}} \text{ and } x_{\rho_f^{(p)}} \text{ has at most degree } +1 \\ \text{with respect to } (T, \sigma)\text{-}cross. \end{gathered} \tag{4.4.17}$$

By Lemma 4.4.23, every term in the T-expansion of x_σ has negative degree with respect to (T, σ)-*cross*. Combining this fact with (4.4.15), (4.4.16), and (4.4.17), we see that each term in the T-expansion of $x_{\sigma^{(p)}}$ has non-positive degree with respect to (T, σ)-*cross*.

Case 4: *Fourth, suppose β is a peripheral arc (not in T) that does not cross σ.* Consider a 4-fold cover $\widetilde{T^o}$ of T°, a disk with one puncture ($\widetilde{P}$) and 4 lifts for every arc and marked point of T°. Let $\widetilde{\beta}$ be a lift of β. Since β and σ do not cross, there are two lifts of σ, say, $\widetilde{\sigma}$, $\widetilde{\sigma}'$, which bound exactly one fundamental domain containing $\widetilde{\beta}$. We denote this fundamental domain by $\mathbf{Disk}_{\widetilde{\sigma}}$. Let $\tilde{t}$ and $\tilde{t}'$ be the boundary endpoints of $\widetilde{\sigma}$ and $\widetilde{\sigma}'$, and let $\widetilde{P}$ be the puncture. See Fig. 4.34(a) (if T has no parallel radii) or 4.34(b) (if T° contains a self-folded triangle r, ℓ).

Let $\omega = (\omega_1, \ldots, \omega_{2d+1})$ denote a (T°, β)-path and also (by abuse of notation) its corresponding lifted $(\widetilde{T^o}, \widetilde{\beta})$-path. Per Corollary 4.4.15(b), in order for $x(\omega)$ to have a positive degree with respect (T°, σ)-*cross*, there must be a subsequence $\bar{\omega}$ of consecutive edges that cross σ, say, $\bar{\omega} = \omega_{2i-1}, \ldots, \omega_{2j+1}$, where the edges directly prior to $\bar{\omega}$ and directly after $\bar{\omega}$ do not cross σ. Since no radius of T° can cross σ, all edges in $\bar{\omega}$ are peripheral arcs.

We claim $\bar{\omega}$ starts and finishes strictly inside $\mathbf{Disk}_{\widetilde{\sigma}}$, i.e., at a marked point of $\mathbf{Disk}_\sigma$ that is none of $\widetilde{P}$, $\tilde{t}$, and $\tilde{t}'$.

If $i = 1$, then ω_1 starts strictly in $\mathbf{Disk}_\sigma$ because ω_1 is not adjacent to $\widetilde{\sigma}$ nor $\widetilde{\sigma}'$. Similarly, if $j = d$, then ω_{2d+1} ends strictly $\mathbf{Disk}_\sigma$ because ω_{2d+1} is not adjacent to $\widetilde{\sigma}$ nor $\widetilde{\sigma}'$.

Otherwise, $\bar{\omega}$ must start strictly in $\mathbf{Disk}_{\widetilde{\sigma}}$ because ω_{2i-2} must cross $\widetilde{\beta}$ but not $\widetilde{\sigma}$ nor $\widetilde{\sigma}'$, and $\bar{\omega}$ must end strictly in $\mathbf{Disk}_{\widetilde{\sigma}}$ because ω_{2j+2} must cross $\widetilde{\beta}$ but not $\widetilde{\sigma}$ nor $\widetilde{\sigma}'$.

By induction, every odd edge of $\bar{\omega}$ starts strictly in $\mathbf{Disk}_{\widetilde{\sigma}}$. But this means that ω_{2j+1} starts and ends strictly $\mathbf{Disk}_{\widetilde{\sigma}}$ even though ω_{2j+1} cuts one of $\widetilde{\sigma}$ and $\widetilde{\sigma}'$, which is impossible.

Hence, $x(\omega)$ has non-positive degree with respect to (T°, σ)-*cross*, and, by Lemma 4.4.9, also with respect to (T, σ)-*cross*, as needed. □

$\boldsymbol{\Sigma \backslash T}$ contains no plain radius but there is a notched radius $\boldsymbol{\sigma^{(p)} \in \Sigma \backslash T}$

The following lemma is helpful toward proving Lemmas 4.4.26 and 4.4.27.

Lemma 4.4.25. *Suppose T is a tagged triangulation with no parallel radii, so that $T = T^\circ$, and ρ is a radius of T. Then every term in the T-expansion of $x_{\rho^{(p)}}$ has negative degree with respect to $\{$all the radii of $T\}$.*

Proof of Lemma 4.4.25. Let $\rho_1, \ldots, \rho_f$ (with $f \geq 2$) denote all the (plain) radii (in consecutive order) of T such that $\rho = \rho_1$. Consider the loop ℓ_1 surrounding the radius ρ_1 which crosses ρ_2 first and crosses ρ_f last (see Fig. 4.35(c)). Consider a (T, ℓ_1)-path $\omega = (\omega_1, \ldots, \omega_{2d+1})$. Here $d = f - 1$.

We first show that $x(\omega)$ has non-negative degree with respect to $\{\rho_1, \ldots, \rho_f\}$. Since the arcs that are crossed by ℓ_1 are precisely $\rho_2, \ldots, \rho_f$, the even steps of ω are $\rho_2, \rho_3, \ldots, \rho_f$ by (T1). By Lemma 4.4.17(a), The only way for $x(\omega)$ to have positive degree with respect to $\{\rho_1, \ldots, \rho_f\}$ is if all the odd steps of ω come from $\{\rho_1, \ldots, \rho_f\}$. By induction, $\omega_1 = \rho_1, \omega_3 = \rho_2, \ldots, \omega_{2d-1} = \rho_f$ such that each one goes from the boundary to the puncture. But this requires $\omega_{2d} = \rho_f$ to go from the puncture to the boundary. Hence ω_{2d+1} goes from boundary to boundary, so $\omega_{2d+1} \notin \{\rho_1, \ldots, \rho_f\}$. Hence each term in the T-expansion of x_{ℓ_1} has non-negative degree with respect to $\{\rho_1, \ldots, \rho_f\}$.

Since $x_{\rho_1}^{(p)} = x_{\ell_1}/x_{\rho_1}$, every term in the T-expansion of $x_{\rho_1}^{(p)}$ has negative degree with respect to $\{\rho_1, \ldots, \rho_f\}$. □

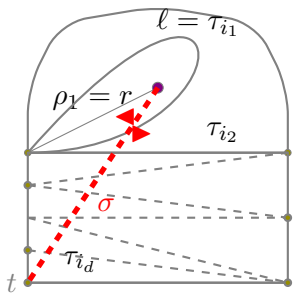

(a) T° has a self-folded triangle r, ℓ and $\Sigma\backslash T$ contains a notched radius $\sigma^{(p)}$.

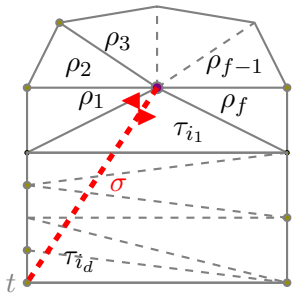

(b) T has no parallel radii and $\Sigma\backslash T$ contains no plain radius but it has a notched radius $\sigma^{(p)}$.

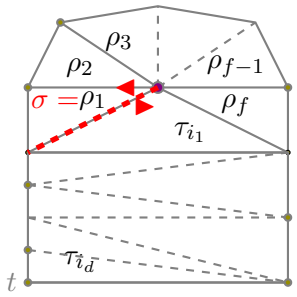

(c) T has no parallel radii and $\Sigma\backslash T$ contains no radius that crosses T, but $\Sigma\backslash T$ contains a notched radius parallel to ρ_1.

Figure 4.36: Three setups for Lemmas 4.4.26 and 4.4.27.

Lemma 4.4.26. *Suppose Σ is a multi-tagged triangulation and T is a tagged triangulation such that $\Sigma\backslash T$ does not contain any plain radius but it contains a notched radius $\sigma^{(p)}$. There are three cases to consider, Figs.* 4.36(a), 4.36(b), *and* 4.36(c).

If T has parallel radii r, $r^{(p)}$, we denote

$$N_\sigma^T := \{r, \text{ and the (peripheral) arcs of } T \text{ that cross } \sigma\},$$

where $\sigma^{(p)} \in \Sigma\backslash T$ is a notched radius such that $\sigma \notin T$ (see Fig. 4.36(a)).

If T has no parallel radii, we denote

$$N_\sigma^T := \begin{cases} \{\textit{all radii of } T\} & \textit{if } \sigma^{(p)} \in \Sigma\backslash T \textit{ is a notched radius such that } \sigma \notin T \\ & (\textit{see Fig. } 4.36(\text{b})), \\ \{\textit{all radii of } T\}\backslash\{\sigma\} & \textit{if } \Sigma\backslash T \textit{ contains no notched radius that crosses } T, \textit{ but} \\ & \sigma^{(p)} \in \Sigma\backslash T \textit{ is a notched radius where } \sigma \in T \,(\textit{see Fig. } 4.36(\text{c})). \end{cases}$$

Then each term in the T-expansion of $x_{\sigma^{(p)}}$ has negative degree with respect to N_σ^T.

Proof of Lemma 4.4.26. There are three cases to prove, Figs. 4.36(a), 4.36(b), and 4.36(c).

Fig. 4.36(a): In this case T has parallel radii r, $r^{(p)}$. The result follows from the proof of Lemma 4.4.23 by switching the roles of r, σ with $r^{(p)}$, $\sigma^{(p)}$.

For the remainder of this proof, assume T has no parallel radii. Let $\rho_1, \ldots, \rho_f$ denote the radii of T with $f \geq 2$.

Fig. 4.36(b): $\Sigma\backslash T$ contains a notched radius $\sigma^{(p)}$ such that $\sigma \notin T$. Let $N_\sigma^T := \{$all radii of $T\}$, per above assumption. Assume σ is adjacent to ρ_1 and ρ_f. First, recall that (4.4.15) gives us

$$x_{\sigma^{(p)}} = x_\sigma|_{\rho_i \leftrightarrow \rho_i{}^{(p)}} = x_\sigma|_{\rho_1 \leftrightarrow \rho_1{}^{(p)}, \rho_f \leftrightarrow \rho_f{}^{(p)}}.$$

Second, observe that every term in the T-expansion of x_σ has degree $+1$ with respect to $\{\rho_1, \rho_f\}$ and does not include any step from $\{\rho_2, \ldots, \rho_{f-1}\}$. Third, by Lemma 4.4.25, every term in the T-expansions of $x_{\rho_1}^{(p)}$ and $x_{\rho_f}^{(p)}$ has negative degree with respect to $\{\rho_1, \ldots, \rho_f\}$. Combing these three facts, every term in the T-expansion of $x_{\sigma^{(p)}} = x_\sigma|_{\rho_1 \leftrightarrow \rho_1{}^{(p)}, \rho_f \leftrightarrow \rho_f{}^{(p)}}$ has negative degree with respect to $\{\rho_1, \ldots, \rho_f\}$.

Fig. 4.36(c): $\Sigma\backslash T$ contains no radius that crosses T, but $\sigma^{(p)} \in \Sigma\backslash T$ is a notched radius where $\sigma \in T$. Let ρ_1 denote the radius σ of T. Let $N_\sigma^T := \{\rho_2, \ldots, \rho_f\}$, per above assumption. Consider the loop ℓ_1 around ρ_1 (see Fig. 4.35(c)) and a (T, ℓ_1)-path ω. Observe that ω has even steps $\rho_2, \rho_3, \ldots, \rho_f$, and

the first and last steps of ω are not in $\{\rho_2, \ldots, \rho_f\}$, so $x(\omega)$ has negative degree with respect to $\{\rho_2, \ldots, \rho_f\}$ by Lemma 4.4.17(a). Since

$$x_{\rho_1{}^{(p)}} = \frac{x_{\ell_1}}{x_{\rho_1}},$$

each term in the T-expansion of $x_{\rho_1^{(p)}}$ also has negative degree with respect to $\{\rho_2, \ldots, \rho_f\}$. □

Lemma 4.4.27. *Assume the same setup and three different cases as Lemma* 4.4.26 *above. If $\beta \in \Sigma$, then each term in the T-expansion of x_β is of non-positive degree with respect to N_σ^T.*

Proof. As in the proof of Lemma 4.4.26, there are three cases to prove, Figs. 4.36(a), 4.36(b), and 4.36(c).

We prove the case of Fig. 4.36(a) where T has parallel radii r, $r^{(p)}$ and $N_\sigma^T = \{r$, and the arcs of T that cross $\sigma\}$ by switching the roles of r, σ with $r^{(p)}$, $\sigma^{(p)}$ in the proof of Lemma 4.4.24.

For the remainder of this proof, we prove the two setups of Figs. 4.36(b) and 4.36(c) for when T has no parallel radii. Let $\rho_1, \ldots, \rho_f$ denote the radii of T with $f \geq 2$.

If $\beta = \sigma^{(p)}$, we are done by the previous Lemma 4.4.26. Otherwise, since β is compatible with $\sigma^{(p)}$, there are four possibilities: β is an arc of T, a notched radius that crosses T, a notched radius $\rho_k^{(p)}$ parallel to a radius of T, or a peripheral arc.

Case 1: *First, suppose $\beta \in T$.* Since β is compatible with the notched radius $\sigma^{(p)}$, we see that $\beta \notin N_\sigma^T$ since either $N_\sigma^T = \{$all radii of $T\}$ (if $\sigma \notin T$) or $N_\sigma^T = \{$all radii of $T\}\backslash\{\sigma\}$ (if σ is a radius of T).

Case 2: *Second, suppose β is a notched radius that crosses T.* The case of Fig. 4.36(b) where $N_\sigma^T = \{$all radii of $T\}$ is done by Lemma 4.4.26 (for the same case). We do not need to consider the case of Fig. 4.36(c) because it is assumed that $\Sigma\backslash T$ does not contain any notched radius that crosses T.

Case 3: *Third, suppose that β is a notched radius $\rho_k^{(p)}$ not equal to $\sigma^{(p)}$.* The case of Fig. 4.36(b) where $N_\sigma^T = \{$all radii of $T\}$ is done by Lemma 4.4.25.

To prove the case of Fig. 4.36(c), let ρ_1 denote σ. Suppose β is a notched arc $\rho_k^{(p)}$ with $k \neq 1$, and consider the loop ℓ_k around ρ_k and a (T, ℓ_k)-path ω. We claim that $x(\omega)$ has at most degree $+1$ with respect to $\{\rho_2, \ldots, \rho_f\}$. To prove this, note that the $f-1$ even arcs of ω are $\rho_{k+1}, \ldots, \rho_f, \rho_1, \ldots, \rho_{k-1}$, i.e., all the radii of T except for ρ_k. For $x(\omega)$ to have degree $+2$ or more with respect to $\{\rho_2, \ldots, \rho_f\}$, we need all f odd arcs of ω to be in $\{\rho_2, \ldots, \rho_f\}$. But either the step right before or right after the even-step along ρ_1 of ω needs to be either ρ_1 or another (peripheral) arc. Hence $x(\omega)$ has at most degree $+1$ with respect to $\{\rho_2, \ldots, \rho_f\}$. Since

$$x_{\rho_k{}^{(p)}} = \frac{x_{\ell_k}}{x_{\rho_k}},$$

each term of x_{ρ_k} has at most degree 0 with respect to $\{\rho_2, \ldots, \rho_f\}$, as needed.

Case 4: *Fourth, suppose β is a peripheral arc not crossing σ.* Let $\omega = (\omega_1, \ldots, \omega_{2d+1})$ be a (T, β)-path. Suppose for contradiction that $x(\omega)$ is of positive degree with respect to N_σ^T. By Corollary 4.4.15(b),

$$\begin{gathered}\text{we must have a subsequence } \bar{\omega} = \omega_{2i-1}, \ldots, \omega_{2j+1} \text{ of } \omega \\ \text{(of length three or greater) where all the steps of } \bar{\omega} \text{ belong to } N_\sigma^T \\ \text{while the step before and the one after do not belong to } N_\sigma^T. \qquad (4.4.18)\end{gathered}$$

We claim that $\bar{\omega}$ must starts at the boundary (as opposed to the puncture). Otherwise, ω would contain an earlier step ω_{2i-2} which must be a radius of T going from the boundary to the puncture. For the case where σ is not a radius of T and $N_\sigma^T = \{\text{all radii of } T\}$ (Fig. 4.36(b)), this shows that $\omega_{2i-2} \in N_\sigma^T$. For the case where $\sigma = \rho_1$ and $N_\sigma^T = \{\rho_2, \ldots, \rho_f\}$ (Fig. 4.36(c)), since β cannot cross ρ_1, we see that ω_{2i-2} has to come from $\{\rho_2, \ldots, \rho_f\} = N_\sigma^T$. For both cases, this contradicts the assumption (4.4.18) that no step before $\bar{\omega}$ comes from N_σ^T, hence $\bar{\omega}$ must starts at the boundary. Similarly, $\bar{\omega}$ must end at the boundary (as opposed to the puncture).

Since every step of $\bar{\omega}$ is a radius, it follows by induction that every odd step of $\bar{\omega}$ starts at the boundary. But this means that ω_{2j+1} is a radius that begins

and ends at the boundary, which is impossible. Hence $x(\omega)$ has non-positive degree with respect to N_σ^T. □

4.4.5 Proof of Lemma 4.4.4

Proof of Lemma 4.4.4. Suppose x_Σ is a cluster monomial not compatible with a tagged triangulation T.

Suppose that all tagged arcs of $\Sigma\backslash T$ are peripheral. We shall choose a tagged arc $\sigma \in \Sigma\backslash T$ that is central and, if possible, crosses every arc of T at most once, as follows. Let $\{\lambda_1, \ldots, \lambda_r\}$ be the set of central arcs in $\Sigma\backslash T$ (see Fig. 4.30(a)). If $r = 1$, then choose $\sigma := \lambda_r$.

If $r > 1$, we choose $\sigma \in \{\lambda_k\text{'s}\}$ such that (T°, σ)-*doublecross* $= \varnothing$. To see that we can do this, suppose that one of these λ_k (say, λ_r) cuts an arc $\tau \in T^\circ$ twice, see Fig. 4.30(b). Since τ must cut out a simply-connected region containing all of $\lambda_1, \ldots, \lambda_{r-1}$, each of $\lambda_1, \ldots, \lambda_{r-1}$ crosses every arc of T° at most once.

Hence, we satisfy the setup for

Lemma 4.4.21:σ is central in $\Sigma\backslash T$,

and for

Lemma 4.4.22:If (T°, σ)-*doublecross* is nonempty,

then σ is the only central arc in $\Sigma\backslash T$.

Lemma 4.4.22(2) tells us that each term in the T-expansion of x_σ is of negative degree with respect to either (T, σ)-*cross* or (T, σ)-*doublecross*. At the same time, Lemmas 4.4.21 and 4.4.22(1) tell us that every term in the T-expansion of x_Σ has non-positive degree with respect to both (T, σ)-*cross* and (T, σ)-*doublecross*. It follows, since $\sigma \in \Sigma$, that every term in the T-expansion of x_Σ has negative degree with respect to either (T, σ)-*cross* or (T, σ)-*doublecross*. Since (T, σ)-*cross* and (T, σ)-*doublecross* are subsets of T, the T-expansion of x_Σ is a sum of proper Laurent monomials.

Suppose now that $\Sigma\backslash T$ contains a radius σ. A very similar argument appears in the proof of [DT13, Proposition 2.3] but we repeat it here for completeness. Lemma 4.4.23 (if σ is a plain radius) or Lemma 4.4.26 (if all radii of $\Sigma\backslash T$ are notched) tells us that each term in the T-expansion of x_σ is of negative degree with respect to a subset N_σ^T. At the

same time, Lemma 4.4.24 (if σ is a plain radius) or Lemma 4.4.27 (if all radii of $\Sigma \backslash T$ are notched) tells us that each term in the T-expansion of the other factors of x_Σ are of non-positive degree with respect to the same grading N_σ^T. It follows that each term in the T-expansion of x_Σ has negative degree with respect to this grading. Since N_σ^T is a subset of T, the T-expansion of x_Σ is a sum of proper Laurent monomials. □

Remark 4.4.28. *Not every cluster algebra has an atomic basis. Examples of cluster algebras with no atomic bases are those of rank* 2 *where the exchange matrices looks like* $\begin{pmatrix} 0 & b \\ -c & 0 \end{pmatrix}$ *with* $bc \geq 5$ *[LLZ14]. See [MSW13, Conjecture 1.5] for a conjecture on the existence of atomic bases for cluster algebras from surfaces.*

Chapter 5

T-path formulas with principal coefficients and for notched arcs

In this chapter, we generalize our work in Chapter 4 and present several formulas for computing all cluster variables of a cluster algebra arising from a marked surface (possibly with punctures). Additionally, we work in the generality of principal coefficients.

The formula for ordinary arcs, given in Section 5.1, generalizes the work of Schiffler and Thomas [ST09, Sch10]. The proof is similar to the one we gave in Chapter 4.

For surfaces with punctures, we consider cluster variables which correspond to tagged arcs with one or two notchings. In Section 5.2, we introduce *equivalent classes of paths* and use them to present formulas for tagged arcs with one or two notchings. For the first formula, our proof was inspired by [MSW11]. For the second formula, our proof is a weight-preserving and height-preserving bijection between our equivalent classes of paths and certain perfect matchings of snake graphs defined in [MSW11].

5.1 A formula for ordinary arcs

Let (S, M) be a marked surface as defined in Section 2.2.

5.1.1 Paths for ordinary arcs

We extend Definition 4.2.2 for general marked surfaces.

Definition 5.1.1 (Quasi-arc)**.** *If τ is an arc whose endpoints are on the boundary, we let the* associated quasi-arc *of τ be τ itself. Otherwise, we define an associated quasi-arc as follows.*

- *Let τ be an ordinary arc between a boundary marked point and a puncture p. Then a* quasi-arc *τ' associated to τ is a curve (not passing through any puncture) which ends at a (non-marked) point p' in the vicinity of p. It agrees with τ outside of a radius-ϵ disk D_ϵ around p, where ϵ is chosen small enough so that the intersection of τ with any other arc is outside of D_ϵ. Note that another quasi-arc associated to τ may use a different point p''.*

- *Let τ be an ordinary arc whose two endpoints are distinct punctures p and q. Then an associated quasi-arc τ' of τ is a curve (not passing through any puncture) between two (non-marked) points p' and q' in the vicinities of p and q, respectively. The curve τ' agrees with τ outside of radius-ϵ disks D_P, D_Q centered around p, q (respectively), where ϵ is chosen small enough so that the intersection of τ with any other arc is outside of D_P and D_Q.*

- *Let τ be an ordinary arc which is a loop based at a puncture p. Then an associated quasi-arc τ' of τ is a curve (not passing through any puncture) between two (non-marked) points p' and p'' in the vicinity of p. The curve τ' agrees with τ outside of radius-ϵ disk D_ϵ centered around p, where ϵ is chosen small enough so that the intersection of τ with any other arc is outside of D_ϵ.*

As in Chapter 4, we label a quasi-arc with the label of the arc that it is associated to. By abuse of notation, whenever we say we are going along an arc or a side of an ideal triangle $\triangle_k$ (as part of a T^o-path), we mean traversing an associated quasi-arc. Note that, if τ has no puncture endpoints, no abuse of notation is actually needed. Let a *T^o-step* be an orientation of a quasi-arc or boundary edge of T°.

Definition 4.2.2 from Chapter 4 also makes sense when (S, M) is a more general marked surface (possibly with punctures). We repeat the definition here for the reader's convenience.

Definition 5.1.2 (complete (T^o, γ)-path)**.** *Let γ be an ordinary arc from the marked point s to the marked point t. Choose an orientation for γ. Denote by $s = p_0$, p_1, p_2,*

..., p_d, $t = p_{d+1}$ the points of intersection of γ and T^o, in order. Let τ_{i_k} be the arc containing p_k.

Let γ_0 denote the segment of γ between the points s and p_1. Let γ_d denote the segment of γ between the points p_d and t.

If $\triangle_0$ (respectively, $\triangle_d$) is self-folded, let $\tau_{[\gamma_0]} = \tau_{[\gamma_{-1}]}$ (respectively, $\tau_{[\gamma_d]} = \tau_{[\gamma_{d+1}]}$) denote the radius. Otherwise, let $\tau_{[\gamma_0]}$ and $\tau_{[\gamma_{-1}]}$ be the other two sides of $\triangle_0$ such that $\tau_{[\gamma_0]}$,$\tau_{[\gamma_{-1}]}$,τ_{i_1} are arranged in clockwise order around $\triangle_0$, and let $\tau_{[\gamma_d]}$ and $\tau_{[\gamma_{d+1}]}$ be the other two sides of $\triangle_d$ such that $\tau_{[\gamma_d]}$,$\tau_{[\gamma_{d+1}]}$,τ_{i_d} are arranged in clockwise order around $\triangle_d$.

For $k = 1, \ldots, d-1$, let γ_k denote the segment of γ between the points p_k and p_{k+1}, and let $\triangle_k$ denote the (unique) ideal triangle of T^o that γ_k crosses. If $\triangle_k$ is not self-folded, let $\tau_{[\gamma_k]}$ denote the third side of $\triangle_k$ (which is not crossed by γ_k). Otherwise, let $\tau_{[\gamma_k]}$ be the radius of the self-folded triangle.

A path $\omega = (\omega_1, \omega_2, \ldots, \omega_{length(\omega)})$ *on T^o is a concatenation of T^o-steps such that the starting point of a step ω_i is the finishing point of the previous step ω_{i-1}. Given a fixed orientation of γ, we say that $\omega = (\omega_1, \ldots, \omega_{2d+1})$ is a* complete (T^o, γ)-path *from s to t if the following axioms hold:*

(T1) Each even step ω_{2k} ($k = 1, \ldots, d$) is a quasi-arc associated to arc τ_{i_k}. Recall that $\tau_{i_1}, \ldots, \tau_{i_d}$ is the sequence of arcs crossed by γ in order.

(T2) For $k = 0, \ldots, d$, each ω_{2k+1} traverses a side of the ideal triangle $\triangle_k$.

- *i) Moreover, for $k = 1, 2, \ldots, d-1$, let $[p_k, p_{k+1}]_\omega$ denote the segment of ω starting at the point p_k following ω_{2k}, continuing along ω_{2k+1} and $\omega_{2(k+1)}$ until the point p_{k+1}. Then the segment γ_k is homotopic to $[p_k, p_{k+1}]_\omega$.*
- *ii) The segment γ_0 is homotopic to the segment $[s, p_1]_\omega$ of the path starting at the point $s = p_0$ following ω_1 and ω_2 until the point p_1.*
- *iii) The segment γ_d is homotopic to the segment $[p_d, t]_\omega$ of the path starting at the point p_d following ω_{2d} and ω_{2d+1} until the point $p_{d+1} = t$.*

If there are punctures, then we mean homotopy in S minus the punctures.

(T3) The step ω_{2k+1} starts and finishes in the interior of $\triangle_k$ or at a boundary marked point. This means that, if ω_{2k+1} goes along a quasi-arc τ' associated to an arc

adjacent to a puncture, then τ' must be chosen so that its endpoint p' near the puncture is located in the interior of $\triangle_k$.

5.1.2 Weights and heights

We assign a Laurent monomial weight and a height monomial (as in [Sch10]) to each T°-path. The Laurent monomial weight is as defined in Definition 4.2.6.

Definition 5.1.3 (Laurent monomial from a T°-path)**.** *We identify each step ω_i with the label of the quasi-arc/boundary edge τ which it traverses, and set $x(\omega) := x_\tau$. If τ is a boundary edge, set $x(\omega) := 1$. Define the Laurent monomial $x(\omega)$ corresponding to a complete (T^o, γ)-path ω by*

$$x(\omega) = \prod_{i \text{ odd}} x_{\omega_i} \prod_{i \text{ even}} x_{\omega_i}^{-1}.$$

Remark 5.1.4. *Two or more (T^o, γ)-paths may correspond to the same Laurent monomial, e.g., see Example 4.2.9. For each (T^o, γ)-path ω, the denominator of $x(\omega)$, before reducing, is equal to $x_{i_1}\, x_{i_2} \ldots x_{i_d}$ which corresponds to the arcs $\tau_{i_1}, \ldots, \tau_{i_d}$ of T^o which cross γ.*

The following definition is equivalent of [Sch10, Section 3.2] (and also discussed in [MS10, Section 5]). Note that, due to our choice of convention in Definition 2.2.9 (signed adjacency matrix of an ideal triangulation), our convention agrees with the convention of [Sch10, MS10] but is opposite of the more recent papers [MSW11, MSW13].

Definition 5.1.5 (γ-oriented even steps)**.** *Let ω be a (T^o, γ)-path. We say that ω_{2k} is* γ-oriented *if the orientation of ω_{2k} in the path ω crosses γ_k from the right of γ_k to the left of γ_k when viewed from outside the surface. See Fig. 5.1 and 5.2.*

Define

$$h(\omega) = \prod_{k:\omega_{2k} \text{ is } \gamma\text{-oriented}} h_{\omega_{i_k}}$$

Definition 5.1.6 (Specialized height monomial)**.** *Following [MSW11, Def. 4.9], we*

define the specialized height monomial $y(\omega)$ *of* ω *to be the specialization* $\Phi(h_\omega)$*, where*

$$\Phi(h_\tau) := \begin{cases} y_\tau & \text{if } \tau \text{ is not the side of a self-folded triangle,} \\ y_r/y_{r^{(P)}} & \text{if } \tau \text{ is the radius } r \text{ of a self-folded triangle enclosing } \text{P}, \text{ and} \\ y_{r^{(P)}} & \text{if } \tau \text{ is an } \ell\text{-loop enclosing a radius } r \text{ and a puncture } \text{P}. \end{cases}$$

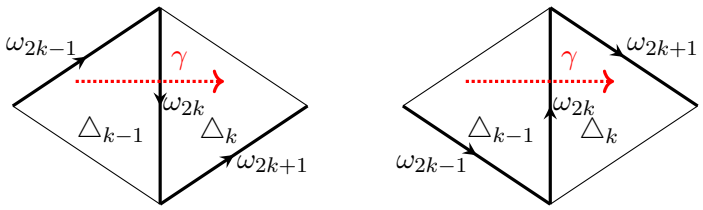

Figure 5.1: Two examples of a complete T°-path subsequence $(\omega_{2k-1}, \omega_{2k}, \omega_{2k+1})$. On the left, ω_{2k} is *not* γ-oriented. On the right, ω_{2k} is γ-oriented.

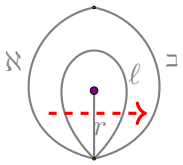

(a) γ crosses r in the counterclockwise direction.

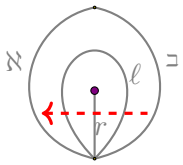

(b) γ crosses r in the clockwise direction.

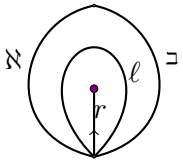

(c) Orientation of r which makes an even step be γ-oriented if γ crosses r in the counterclockwise direction.

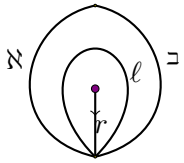

(d) Orientation of r which makes an even step be γ-oriented if γ crosses r in the clockwise direction.

Figure 5.2: Whether or not an even step along the radius r of a self-folded triangle is γ-orientated.

5.1.3 Formula for ordinary arcs

We generalize [Sch10, Theorem 3.1] and [ST09, Theorem 3.2] to surfaces with punctures. The special case when (S, M) is a once-punctured polygon is discussed in Section 4.2.

Theorem 5.1.1 (T^o-path formula for arcs)**.** *Let (S, M) be a marked surface with or without punctures with a tagged triangulation T. Let $\mathcal{A}$ be the corresponding cluster algebra with principal coefficients with respect to T. Let T^o be the corresponding ideal triangulation. Let $\gamma \notin T^o$ be an ordinary arc in S. Then the Laurent expansion of x_γ, in $\mathcal{A}$, with respect to T is given by*

$$x_\gamma = \sum_{\omega} x(\omega)\ y(\omega),$$

where the sum is taken over all (T^o, γ)-paths. The formula does not depend on the choice of orientation on γ. In the coefficient-free setting, set $y(\omega) := 1$ for all ω.

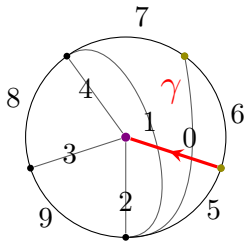

Figure 5.3: Ideal triangulation T° and an ordinary arc γ.

Example 5.1.7. *Consider the ideal triangulation T° and a radial arc γ illustrated in Fig. 5.3. We see that there are precisely 3 complete (T°, γ)-paths,*

$(6, \textcircled{\mathbf{0}}, 1, \textcircled{\mathbf{1}}, 2)$*, where both even steps are γ-oriented,*

$(5, \mathbf{0}, 7, \textcircled{\mathbf{1}}, 2)$*, where the 4th step (along edge 1) is γ-oriented, and*

$(5, \mathbf{0}, 0, \mathbf{1}, 4)$*, where neither of the even steps is γ-oriented.*

Applying Theorem 5.1.1, we find that x_γ is equal to

$$x_\gamma = \frac{x_1x_2x_6\ y_0y_1 + x_2x_5x_7\ y_1 + x_0x_4x_5}{x_0x_1}.$$

5.2 Formulas for tagged arcs with notches

We now present T-path versions of the snake graph formulas [MSW11, Theorems 4.17, 4.20] for cluster variables associated to tagged arcs which have notches. Let T° be an ideal triangulation of (S, M) which is not a closed surface with exactly two marked points. Let γ be a tagged arc with plain notchings between a puncture P and a marked point s (possibly $s = \text{P}$). For simplicity, we only consider the case for $\gamma \notin T^\circ$.

Choose an orientation of γ so that γ finishes at P. Let $\tau_{i_1}, \ldots, \tau_{i_d}$ be the arcs crossed by γ, and let $s = p_0, p_1, \ldots, p_d, \text{P}$ be the points of intersection of γ and T.

Let ℓ_γ^{P} be the loop (oriented clockwise) which cuts out a monogon (enclosing the puncture P) containing γ. If γ is adjacent to a second puncture Q, let ℓ_γ^{Q} be a noose based at P (oriented clockwise) which cuts out a monogon (enclosing the puncture Q) containing γ. If γ is a loop, note that ℓ_γ^{P} (respectively, ℓ_γ^{Q}) has two self-intersections. See [MSW11, Fig. 9].

As in [MSW11, Remark4.12], we may assume that no tagged arc in T is notched at either P or Q (note that this means that there are no loops in T° cutting out once-punctured monogons around P or Q).

Continuing with our previous terminology, we say that an arc is a *radius* if at least one of its endpoints is a puncture. Let $\rho_1, \ldots, \rho_f$ (where $f \geq 2$) be all the radii of T° which are adjacent to P, in clockwise order from the finishing endpoint of γ. If ρ_i is a loop, it appears twice on the list. Let $p_{d+1}, \ldots, p_{d+f}$ be the points of intersection of ℓ_γ^{P} with $\rho_1, \ldots, \rho_f$, in order.

In case γ is adjacent to another puncture Q (possibly $\text{Q} = \text{P}$), we denote the radii emanating from Q similarly; let $\eta_1, \ldots, \eta_g$ (where $g \geq 2$) be all the radii of T° which are adjacent to Q, in clockwise order from the starting point of γ.

5.2.1 Paths for tagged arcs with one notching $\gamma^{(P)}$

Consider a curve $\overline{\gamma}_+^{(P)}$ which follows ℓ_γ^{P} from its starting point but finishes in the interior of the ideal triangle $\triangle_{d+f}$ (with sides $\tau_{i_d}, \rho_1, \rho_f$), just after ℓ_γ^{P} crosses all the radii ρ_1, $\ldots$, ρ_f, in this order. Then $s = p_0, p_1, \ldots, p_{d+f}$ are the points of intersection of $\overline{\gamma}_+^{(P)}$ and T°, in this order.

Let $\overline{\gamma}_-^{(P)}$ be the curve which follows the opposite orientation $\ell_{\gamma_-}^{\text{P}}$ of ℓ_γ^{P} from the

beginning until right after $\ell^{\mathrm{P}}_{\gamma_-}$ crosses all of $\rho_f, \ldots, \rho_1$, in this order. See Fig. 5.4.

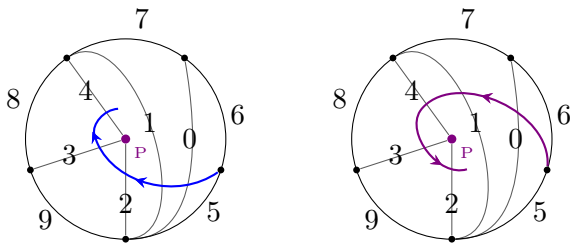

Figure 5.4: The $\overline{\gamma}^{(P)}_+$ (left) and $\overline{\gamma}^{(P)}_-$ (right) curves for the arc γ from Fig. 5.3.

Definition 5.2.1. *Assume we have the same setup as above. We say that* $\omega^+ = \{\omega_1, \ldots, \omega_{2(d+f)}\}$ *is a* $\left(T^\circ, \overline{\gamma}^{(P)}_+\right)$*-path if it satisfies the following axioms:*

(T0) ω^+ *starts from* s *and finishes at (the vicinity of) the puncture* P*.*

(T1) The even steps ω_{2k} $(k = 1, \ldots, d+f)$ *are quasi-arcs associated to* $\tau_{i_1}, \ldots, \tau_{i_d}, \rho_1, \ldots, \rho_f$*, in this order.*

(T2) For $k = 1, \ldots, d+f$*, the segment of* $\overline{\gamma}^{(P)}_+$ *from* p_k *to* p_{k+1} *is homotopic to* ω *starting at the point* p_k *following* w_{2k}*, continuing along* w_{2k+1} *and* $w_{2(k+1)}$ *until the point* p_{k+1}*.*

(T3) The step ω_{2k+1} *starts and finishes in the interior of* $\triangle_k$ *or at a boundary marked point. This means that, if* ω_{2k+1} *goes along a quasi-arc* τ' *associated to an arc adjacent to a puncture,* τ' *must be chosen so that its endpoint near said puncture is located in the interior of* $\triangle_k$*.*

We define a $\left(T^\circ, \overline{\gamma}^{(P)}_-\right)$*-path* ω^-*, starting from* s *and finishing at (the vicinity of) the puncture* P*, similarly so that the even steps of* ω^- *traverse* $\tau_{i_1}, \ldots, \tau_{i_d}, \rho_f, \ldots, \rho_1$*, in this order.*

Definition 5.2.2 (equivalence class)**.** *A* $(T^\circ, \gamma^{(P)})$*-path* $[\omega]$ *is an equivalence class of* $\left(T^\circ, \overline{\gamma}^{(P)}_+\right)$ *and* $\left(T^\circ, \overline{\gamma}^{(P)}_-\right)$*-paths. The equivalence relation is defined as follows. A* $\left(T^\circ, \overline{\gamma}^{(P)}_+\right)$*-path* ω^+ *and* $\left(T^\circ, \overline{\gamma}^{(P)}_-\right)$*-path* ω^- *are equivalent if the following holds:*

1. *The subpaths formed by their first* $(2d+1)$*-th steps coincide.*

2. *The subpath formed by steps* $\omega^-_{2(d+1)}, \ldots, \omega^-_{2(d+f)}$ *of* ω^- *is the reverse of the subpath formed by steps* $\omega^+_{2(d+1)}, \ldots, \omega^+_{2(d+f)}$ *of* ω^- *of* ω^+.

Otherwise, no two distinct $\left(T^\circ, \overline{\gamma}^{(P)}_+\right)$ *or* $\left(T^\circ, \overline{\gamma}^{(P)}_-\right)$*-paths are equivalent.*

Definition 5.2.3 (weights)**.** *Let* $[\omega]$ *be a* $(T^\circ, \gamma^{(P)})$*-path containing a representative* $\left(T^\circ, \overline{\gamma}^{(P)}_+\right)$ *or* $\left(T^\circ, \overline{\gamma}^{(P)}_-\right)$*-path* $W = (w_1, \ldots, w_{2(d+f)})$*. Let*

$$x(W) := \prod_{k \text{ odd}} x_{w_k} \prod_{k \text{ even}} x^{-1}_{w_k}, \text{ in other words,}$$
$$x(W) := \frac{\prod_{k \text{ odd}} x_{w_k}}{x(\tau_{i_1}) \ldots x(\tau_{i_d})\, x(\rho_1) \ldots x(\rho_f)}.$$

By construction, if W_a *and* W_b *belong to the same equivalent class* $[\omega]$*, then* $x(W_a) = x(W_b)$*, hence we write*

$$x([\omega]) := x(W_a) = x(W_b).$$

As in Section 5.1, we define height functions corresponding to $(T^\circ, \gamma^{(P)})$-paths.

Definition 5.2.4 ($\gamma^{(P)}$-oriented even steps)**.** *Let* ζ *be either the curve* $\overline{\gamma}^{(P)}_+$ *or* $\overline{\gamma}^{(P)}_-$*. Suppose* ω *is a* (T°, ζ)*-path. If* $\omega = (\omega_1, \ldots, \omega_{2(d+f)})$ *is a* (T°, ζ)*-path, we say that* ω_{2k} *is* $\gamma^{(P)}$*-oriented if, when* ω_{2k} *crosses* ζ *at* p_k*, it enters* ζ *from the right side of* ζ*. See Fig. 5.5.*

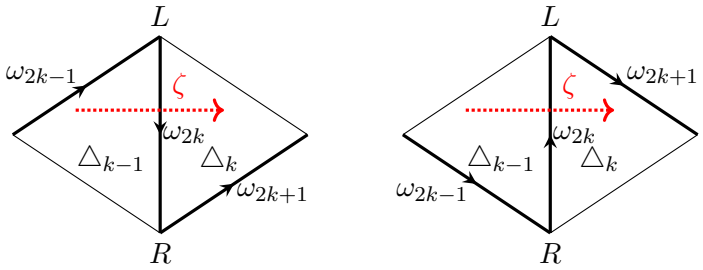

Figure 5.5: Two examples of a (T^o, ζ)-path subsequence $(\omega_{2k-1}, \omega_{2k}, \omega_{2k+1})$. On the left, ω_{2k} is *not* ζ-oriented. On the right, ω_{2k} is ζ-oriented.

Definition 5.2.5 (height monomial and specialized height monomial)**.** *Let* $W = (\omega_1, \ldots, \omega_{2(d+f)})$ *be a* $\left(T^\circ, \overline{\gamma}^{(P)}_+\right)$ *or* $\left(T^\circ, \overline{\gamma}^{(P)}_-\right)$*-path. We define the* height monomial

$h(W)$ by

$$h(W) := \prod_{k:\omega_{2k} \text{ is } \gamma^{(P)}\text{-oriented}} h_{w_{2k}}$$

One can check, if W_a and W_b belong to the same equivalent class $[\omega]$, then $h(W_a) = h(W_b)$, hence we write

$$h([\omega]) := h(W_a) = h(W_b).$$

We define the specialized height monomial *$y([\omega])$ of $[\omega]$ to be the specialization $\Phi(h([\omega]))$, where Φ is as defined earlier in Definition 5.1.6.*

Theorem 5.2.6 (Formula for $\gamma^{(P)}$)**.** *The T°-path expansion of $\gamma^{(P)}$ is given by*

$$x_{\gamma^{(P)}} = \sum_{[\omega]} x([\omega])\, y([\omega])$$

where the sum is over all $(T^\circ, \gamma^{(P)})$-paths $[\omega]$.

Example 5.2.7. *Consider the ideal triangulation T° and arc γ in Fig. 5.3. The curves $\overline{\gamma}_+^{(P)}$ and $\overline{\gamma}_-^{(P)}$ curves are illustrated in Fig. 5.4.*

We find that there are precisely 9 classes of $(T^\circ, \gamma^{(P)})$-paths. We list the path/s that each class contains. The $\pm$ sign at the end of the sequence indicates whether the sequence is a $\left(T^\circ, \overline{\gamma}_+^{(P)}\right)$-path or a $\left(T^\circ, \overline{\gamma}_-^{(P)}\right)$-path. The even steps are written in bold, and the $\gamma^{(P)}$-oriented even steps are circled:

i. $\big(6, \textcircled{\textbf{0}}, 1, \textcircled{\textbf{1}}, 1, \textcircled{\textbf{4}}, 3, \textcircled{\textbf{3}}, 2, \textcircled{\textbf{2}}\big)^-$

ii. $\big(6, \textcircled{\textbf{0}}, 1, \textcircled{\textbf{1}}, 2, \textcircled{\textbf{2}}, 2, \textcircled{\textbf{3}}, 8, \mathbf{4}\big)^+$, $\big(6, \textcircled{\textbf{0}}, 1, \textcircled{\textbf{1}}, 2, \mathbf{4}, 8, \textcircled{\textbf{3}}, 2, \textcircled{\textbf{2}}\big)^-$

iii. $\big(5, \mathbf{0}, 7, \textcircled{\textbf{1}}, 1, \textcircled{\textbf{4}}, 3, \textcircled{\textbf{3}}, 2, \textcircled{\textbf{2}}\big)^-$

iv. $\big(6, \textcircled{\textbf{0}}, 1, \textcircled{\textbf{1}}, 2, \textcircled{\textbf{2}}, 9, \mathbf{3}, 4, \mathbf{4}\big)^+$, $\big(6, \textcircled{\textbf{0}}, 1, \textcircled{\textbf{1}}, 2, \mathbf{4}, 4, \mathbf{3}, 9, \textcircled{\textbf{2}}\big)^-$

v. $\big(5, \mathbf{0}, 7, \textcircled{\textbf{1}}, 2, \textcircled{\textbf{2}}, 2, \textcircled{\textbf{3}}, 8, \mathbf{4}\big)^+$, $\big(5, \mathbf{0}, 7, \textcircled{\textbf{1}}, 2, \mathbf{4}, 8, \textcircled{\textbf{3}}, 2, \textcircled{\textbf{2}}\big)^-$

vi. $\big(5, \mathbf{0}, 7, \textcircled{\textbf{1}}, 2, \textcircled{\textbf{2}}, 9, \mathbf{3}, 4, \mathbf{4}\big)^+$, $\big(5, \mathbf{0}, 7, \textcircled{\textbf{1}}, 2, \mathbf{4}, 4, \mathbf{3}, 9, \textcircled{\textbf{2}}\big)^-$

vii. $\big(5, \mathbf{0}, 0, \mathbf{1}, 4, \textcircled{\textbf{2}}, 2, \textcircled{\textbf{3}}, 8, \mathbf{4}\big)^+$, $\big(5, \mathbf{0}, 0, \mathbf{1}, 4, \mathbf{4}, 8, \textcircled{\textbf{3}}, 2, \textcircled{\textbf{2}}\big)^-$

viii. $\left(5, \mathbf{0}, 0, \mathbf{1}, 4, \textcircled{\mathbf{2}}, 9, \mathbf{3}, 4, \mathbf{4}\right)^{+}, \quad \left(5, \mathbf{0}, 0, \mathbf{1}, 4, \mathbf{4}, 4, \mathbf{3}, 9, \textcircled{\mathbf{2}}\right)^{-}$

ix. $\left(5, \mathbf{0}, 0, \mathbf{1}, 1, \mathbf{2}, 3, \mathbf{3}, 4, \mathbf{4}\right)^{+}$

We describe each $(T^{\circ}, \gamma^{(P)})$*-path class:*

- *The top-most* $(T^{\circ}, \gamma^{(P)})$*-path class, item (i), contains exactly one path, a* $\left(T^{\circ}, \overline{\gamma}_{-}^{(P)}\right)$*-path. Every even step is* $\gamma^{(P)}$*-oriented.*

- *The next* $(T^{\circ}, \gamma^{(P)})$*-path class, item (ii), contains exactly two paths, a* $\left(T^{\circ}, \overline{\gamma}_{+}^{(P)}\right)$*-path (left) and a* $\left(T^{\circ}, \overline{\gamma}_{-}^{(P)}\right)$*-path (right). The even steps along* 0, 1, 2, *and* 3 *are* $\gamma^{(P)}$*-oriented.*
- *The third* $(T^{\circ}, \gamma^{(P)})$*-path class, item (iii), contains exactly one path, a* $\left(T^{\circ}, \overline{\gamma}_{-}^{(P)}\right)$*-path. The even steps along* 1, 2, 3, *and* 4 *are* $\gamma^{(P)}$*-oriented.*

- *The next* $(T^{\circ}, \gamma^{(P)})$*-path class, item (iv), contains exactly two paths, a* $\left(T^{\circ}, \overline{\gamma}_{+}^{(P)}\right)$*-path (left) and a* $\left(T^{\circ}, \overline{\gamma}_{-}^{(P)}\right)$*-path (right). The even steps along* 0, 1, *and* 2 *are* $\gamma^{(P)}$*-oriented.*
- *The next* $(T^{\circ}, \gamma^{(P)})$*-path class, item (v), contains exactly two paths, a* $\left(T^{\circ}, \overline{\gamma}_{+}^{(P)}\right)$*-path (left) and a* $\left(T^{\circ}, \overline{\gamma}_{-}^{(P)}\right)$*-path (right). The even steps along* 1, 2, *and* 3 *are* $\gamma^{(P)}$*-oriented.*

- *The* $(T^{\circ}, \gamma^{(P)})$*-path class, item (vi), contains two paths, a* $\left(T^{\circ}, \overline{\gamma}_{+}^{(P)}\right)$*-path (left) and a* $\left(T^{\circ}, \overline{\gamma}_{-}^{(P)}\right)$*-path (right). The even steps along* 1 *and* 2 *are* $\gamma^{(P)}$*-oriented.*
- *The* $(T^{\circ}, \gamma^{(P)})$*-path class, item (vii), contains two paths, a* $\left(T^{\circ}, \overline{\gamma}_{+}^{(P)}\right)$*-path (left) and a* $\left(T^{\circ}, \overline{\gamma}_{-}^{(P)}\right)$*-path (right). The even steps along* 2 *and* 3 *are* $\gamma^{(P)}$*-oriented.*

- *The second-from-bottom* $(T^{\circ}, \gamma^{(P)})$*-path class, item (viii), contains two paths, a* $\left(T^{\circ}, \overline{\gamma}_{+}^{(P)}\right)$*-path (left) and a* $\left(T^{\circ}, \overline{\gamma}_{-}^{(P)}\right)$*-path (right). The even step along* 2 *is* $\gamma^{(P)}$*-oriented.*

- *The bottom-most $(T^\circ, \gamma^{(P)})$-path class, item (ix), contains exactly one path, a $\left(T^\circ, \overline{\gamma}_+^{(P)}\right)$-path. None of the even steps is $\gamma^{(P)}$-oriented.*

Applying Theorem 5.2.6, we compute the Laurent expansion of $x_{\gamma^{(P)}}$ to be

$$\begin{gathered} x_{\gamma^{(P)}} = \Big(x_1^2 x_2 x_3 x_6 \ y_0 y_1 y_2 y_3 y_4 + \\ x_1 x_2^2 x_6 x_8 \ y_0 y_1 y_2 y_3 + x_1 x_2 x_3 x_5 x_7 \ y_1 y_2 y_3 y_4 + \\ x_1 x_2 x_4 x_6 x_9 \ y_0 y_1 y_2 + x_2^2 x_5 x_7 x_8 \ y_1 y_2 y_3 + \\ x_2 x_4 x_5 x_7 x_9 \ y_1 y_2 + x_0 x_2 x_4 x_5 x_8 \ y_2 y_3 + \\ x_0 x_4^2 x_5 x_9 \ y_2 + \\ x_0 x_1 x_3 x_4 x_5 \Big) / \\ (x_0 x_1 x_2 x_3 x_4)\,. \end{gathered}$$

5.2.2 Paths for tagged arcs with two notchings $\gamma^{(P,Q)}$

Let P and Q (possibly P = Q) be two punctures, and let γ be an ordinary arc between P and Q. Recall that $\eta_1, \ldots, \eta_g$ (where $g \geq 2$) denote the radii emanating from Q, in clockwise order so that η_1 is clockwise of the endpoint of γ at Q and η_g is counterclockwise of the endpoint of γ at Q.

Definition 5.2.8. *We define the following four curves: an "S"-shaped curve $\overline{\gamma}_{+,+}^{(P,Q)}$, a "C"-shaped curve $\overline{\gamma}_{+,-}^{(P,Q)}$, a "C"-shaped curve $\overline{\gamma}_{-,+}^{(P,Q)}$, and a "Z"-shaped curve $\overline{\gamma}_{-,-}^{(P,Q)}$.*

1. *We define an "S"-shaped curve $\overline{\gamma}_{+,+}^{(P,Q)}$, which starts in the interior of the ideal triangle with edges τ_{i_1}, η_1, and η_g, and ends in the interior of the ideal triangle with edges τ_{i_d}, ρ_1, and ρ_f, as follows. See Fig. 5.6 (top left).*
   - *The curve $\overline{\gamma}_{+,+}^{(P,Q)}$ crosses $\eta_g, \ldots, \eta_1, \tau_{i_1}, \ldots, \tau_{i_d}, \rho_1, \ldots, \rho_f$, in this order;*
   - *First, it follows the opposite orientation of ℓ_γ^Q as it crosses all of the radii $\eta_g, \ldots, \eta_1$, in this order;*
   - *Next, it follows the orientation of γ as it crosses $\tau_{i_1}, \ldots, \tau_{i_d}$;*
   - *Finally, it follows the orientation of ℓ_γ^P as it crosses all of the radii ρ_1, ..., ρ_f, in this order.*

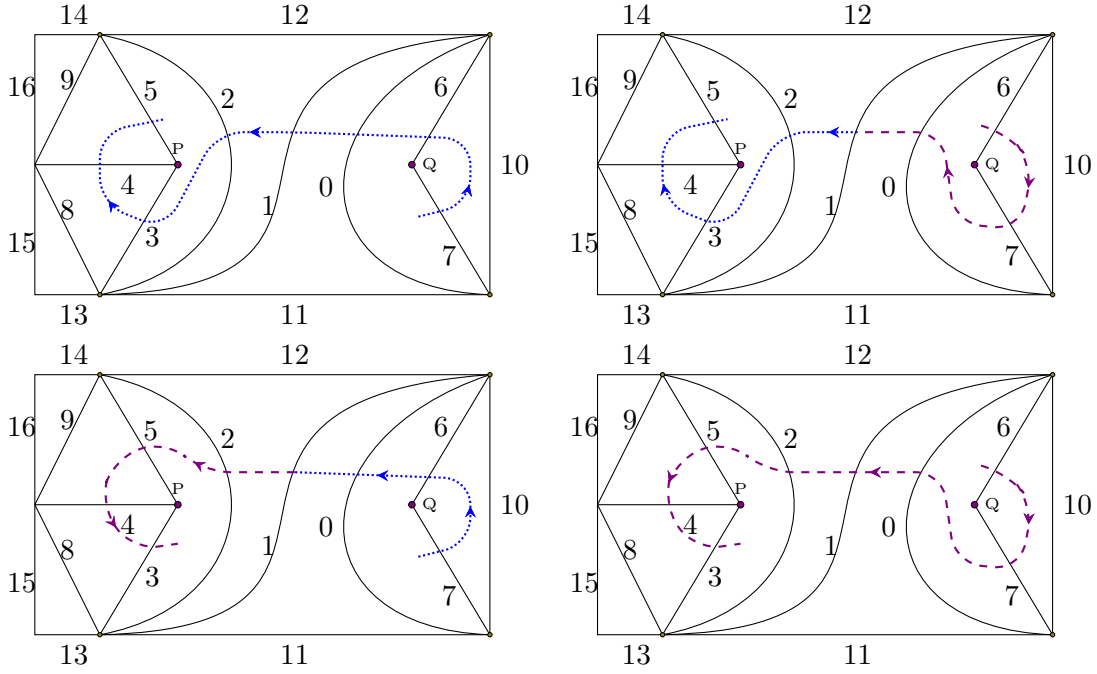

Figure 5.6: Top left: "S"-shaped curve $\overline{\gamma}^{(P,Q)}_{+,+}$. Top right: A ""C"-shaped curve $\overline{\gamma}^{(P,Q)}_{+,-}$. Bottom left: A "C"-shaped curve $\overline{\gamma}^{(P,Q)}_{-,+}$. Bottom Right: "Z"-shaped curve $\overline{\gamma}^{(P,Q)}_{-,-}$.

Let $p_{(1-g)}, \ldots, p_{d+f}$ denote that the $(g+d+f)$ points of intersection of $\overline{\gamma}^{(P,Q)}_{+,+}$ and T°, that is, the intersection of $\overline{\gamma}^{(P,Q)}_{+,+}$ and the arcs $\eta_g, \ldots, \eta_1, \tau_{i_1}, \ldots, \tau_{i_d}, \rho_1, \ldots, \rho_f$.

2. *We define an "C"-shaped curve $\overline{\gamma}^{(P,Q)}_{+,-}$, which starts in the interior of the ideal triangle with edges τ_{i_1}, η_1, and η_g, and ends in the interior of the ideal triangle with edges τ_{i_d}, ρ_1, and ρ_f, as follows. See Fig. 5.6 (top right).*

   - *The curve $\overline{\gamma}^{(P,Q)}_{+,-}$ crosses $\eta_1, \ldots, \eta_g, \tau_{i_1}, \ldots, \tau_{i_d}, \rho_1, \ldots, \rho_f$, in this order;*
   - *First, it follows the same orientation of ℓ^Q_γ as it crosses all of the radii $\eta_1, \ldots, \eta_g$, in this order;*
   - *Next, it follows the orientation of γ as it crosses $\tau_{i_1}, \ldots, \tau_{i_d}$;*
   - *Finally, it follows the orientation of ℓ^P_γ as it crosses all of the radii ρ_1, …, ρ_f, in this order.*

Let $p_{(1-g)}, \ldots, p_{d+f}$ denote that the $(g+d+f)$ points of intersection of $\overline{\gamma}^{(P,Q)}_{+,-}$ and T°, that is, the intersection of $\overline{\gamma}^{(P,Q)}_{+,-}$ and the arcs $\eta_1, \ldots, \eta_g$, $\tau_{i_1}, \ldots, \tau_{i_d}$, $\rho_1, \ldots, \rho_f$.

3. *We define an "C"-shaped curve $\overline{\gamma}^{(P,Q)}_{-,+}$, which starts in the interior of the ideal triangle with edges τ_{i_1}, η_1, and η_g, and ends in the interior of the ideal triangle with edges τ_{i_d}, ρ_1, and ρ_f, as follows. See Fig. 5.6 (bottom left).*

   - *The curve $\overline{\gamma}^{(P,Q)}_{-,+}$ crosses $\eta_g, \ldots, \eta_1, \tau_{i_1}, \ldots, \tau_{i_d}, \rho_1, \ldots, \rho_f$, in this order;*
   - *First, it follows the opposite orientation of ℓ^Q_γ as it crosses all of the radii $\eta_g, \ldots, \eta_1$, in this order;*
   - *Next, it follows the orientation of γ as it crosses $\tau_{i_1}, \ldots, \tau_{i_d}$;*
   - *Finally, it follows the opposite orientation of ℓ^P_γ as it crosses all of the radii ρ_f, $\ldots$, ρ_1, in this order.*

   Let $p_{(1-g)}, \ldots, p_{d+f}$ denote that the $(g+d+f)$ points of intersection of $\overline{\gamma}^{(P,Q)}_{-,+}$ and T°, that is, the intersection of $\overline{\gamma}^{(P,Q)}_{-,+}$ and the arcs $\eta_g, \ldots, \eta_1$, $\tau_{i_1}, \ldots, \tau_{i_d}$, $\rho_f, \ldots, \rho_1$.

4. *Let $\overline{\gamma}^{(P,Q)}_{-,-}$ be the "Z"-shaped curve with the same starting point and finishing point as $\overline{\gamma}^{(P,Q)}_{+,+}$, defined as follows. See Fig. 5.6 (bottom right).*

   - *The curve $\overline{\gamma}^{(P,Q)}_{-,-}$ crosses $\eta_1, \ldots, \eta_g, \tau_{i_1}, \ldots, \tau_{i_d}, \rho_f, \ldots, \rho_1$, in this order;*
   - *First, it follows the orientation of ℓ^Q_γ as it crosses all the radii $\eta_1, \ldots, \eta_g$, in this order;*
   - *Next, it follows the orientation of γ as it crosses $\tau_{i_1}, \ldots, \tau_{i_d}$;*
   - *Finally, it follows the opposite orientation of ℓ^P_γ as it crosses all of the radii ρ_f, $\ldots$, ρ_1, in this order.*

   Let $p_{(1-g)}, \ldots, p_{d+f}$ denote that the $(g+d+f)$ points of intersection of $\overline{\gamma}^{(P,Q)}_{-,-}$ and T°, that is, the intersection of $\overline{\gamma}^{(P,Q)}_{-,-}$ and the arcs $\eta_1, \ldots, \eta_g, \tau_{i_1}, \ldots, \tau_{i_d}, \rho_f, \ldots, \rho_1$.

Definition 5.2.9. *We say that $\omega^{+,+} = \{\omega_{2(1-g)}, \ldots, \omega_0, \quad \omega_1, \ldots, \omega_{2d+1}, \quad \omega_{2(d+1)}, \ldots, \omega_{2(d+f)}\}$ is a $\left(T^\circ, \overline{\gamma}^{(P,Q)}_{+,+}\right)$-*path *if it satisfies the following axioms:*

(T0) $\omega^{+,+}$ starts from (the vicinity of) the puncture $_Q$ and finishes at (the vicinity of) the puncture $_P$.

(T1) The even-numbered steps ω_{2k} $(k = 1-g, \ldots, d+f)$ *are quasi-arcs associated to* $\eta_g, \ldots, \eta_1, \tau_{i_1}, \ldots, \tau_{i_d}, \rho_1, \ldots, \rho_f$, *in this order.*

(T2) For each k, *the segment of* $\overline{\gamma}^{(P,Q)}_{+,+}$ *from* p_k *to* p_{k+1} *is homotopic to* $\omega^{+,+}$ *starting at the point* p_k *following* w_{2k}, *continuing along* w_{2k+1} *and* $w_{2(k+1)}$ *until the point* p_{k+1}. *(Therefore, the "S"-shaped curve* $\overline{\gamma}^{(P,Q)}_{+,+}$ *is homotopic to* $\omega^{+,+}$.*)*

(T3) The step ω_{2k+1} *starts and finishes in the interior of* $\triangle_k$ *or at a boundary marked point. This means that, if* ω_{2k+1} *goes along a quasi-arc* τ' *associated to an arc adjacent to a puncture,* τ' *must be chosen so that its endpoint near said puncture is located in the interior of* $\triangle_k$.

We define a $\left(T^\circ, \overline{\gamma}^{(P,Q)}_{+,-}\right)$*-path* $\omega^{+,-}$, *starting from (the vicinity of)* Q *and finishing at (the vicinity of)* P, *similarly so that the even steps of* $\omega^{+,-}$ *traverse* $\eta_1, \ldots, \eta_g, \tau_{i_1}, \ldots, \tau_{i_d}, \rho_1, \ldots, \rho_f$, *in this order. That is,* $\omega^{+,-}$ *is homotopic to the "C"-shaped curve* $\overline{\gamma}^{(P,Q)}_{+,-}$.

We define a $\left(T^\circ, \overline{\gamma}^{(P,Q)}_{-,+}\right)$*-path* $\omega^{-,+}$, *starting from (the vicinity of)* Q *and finishing at (the vicinity of)* P, *similarly so that the even steps of* $\omega^{-,+}$ *traverse* $\eta_g, \ldots, \eta_1, \tau_{i_1}, \ldots, \tau_{i_d}, \rho_f, \ldots, \rho_1$, *in this order. That is,* $\omega^{-,+}$ *is homotopic to the "C"-shaped curve* $\overline{\gamma}^{(P,Q)}_{-,+}$.

We define a $\left(T^\circ, \overline{\gamma}^{(P,Q)}_{-,-}\right)$*-path* $\omega^{-,-}$, *starting from (the vicinity of)* Q *and finishing at (the vicinity of)* P, *similarly so that the even steps of* $\omega^{-,-}$ *traverse* $\eta_1, \ldots, \eta_g, \tau_{i_1}, \ldots, \tau_{i_d}, \rho_f, \ldots, \rho_1$, *in this order. That is,* $\omega^{-,-}$ *is homotopic to the "Z"-shaped curve* $\overline{\gamma}^{(P,Q)}_{-,-}$.

Definition 5.2.10 (equivalence class)**.** *A* $(T^\circ, \gamma^{(P,Q)})$-path $[\omega]$ *is an equivalence class of* $\left(T^\circ, \overline{\gamma}^{(P,Q)}_{+,+}\right)$, $\left(T^\circ, \overline{\gamma}^{(P,Q)}_{+,-}\right)$, $\left(T^\circ, \overline{\gamma}^{(P,Q)}_{-,+}\right)$ *and* $\left(T^\circ, \overline{\gamma}^{(P,Q)}_{-,-}\right)$*-paths. The equivalence relation is defined as follows.*

A $\left(T^\circ, \overline{\gamma}^{(P,Q)}_{p_1,q_1}\right)$*-path* ω^{p_1,q_1} *and another distinct path* $\left(T^\circ, \overline{\gamma}^{(P,Q)}_{p_2,q_2}\right)$*-path* ω^{p_2,q_2} *are equivalent if and only if the following holds:*

1. *Either* p_1 *is the opposite sign of* p_2, *or* q_1 *is the opposite sign of* q_2.
2. *The subpaths of* ω^{p_1,q_1} *and* ω^{p_2,q_2} *formed by the middle steps, indexed by* $1, 2, \ldots, 2d+1$, *coincide.*

3. (a) *The subpath formed by steps of* ω^{p_2,q_2} *which are indexed by* $2(d+1)$ *through* $2(d+f)$ *either coincides with or is the opposite orientation of the subpath formed by steps of* ω^{p_1,q_1} *indexed by* $2(d+1)$ *through* $2(d+f)$.

   (b) *The subpath formed by steps of* ω^{p_2,q_2} *which are indexed by* $2(1-g)$, $2(1-g)+1, \ldots, -1, 0$ *either coincides with or is the opposite orientation of the subpath formed by steps of* ω^{p_1,q_1} *indexed by the same numbers* $2(1-g)$, $2(1-g)+1, \ldots, -1, 0$.

Remark 5.2.11. *In Section 5.5, it will become apparent that a* $(T^\circ, \gamma^{(P,Q)})$*-path class contains either one, two, or four paths.*

Next, we define the weight $x([\omega])$ and the specialized height monomial $y([\omega])$ of ω in the same manner as Definition 5.2.3 and Definition 5.2.5.

Definition 5.2.12 (weights)**.** *Let* $[\omega]$ *be a* $(T^\circ, \gamma^{(P,Q)})$*-path with a representative* $\left(T^\circ, \overline{\gamma}^{(P,Q)}_{+,+}\right)$ *or* $\left(T^\circ, \overline{\gamma}^{(P,Q)}_{-,-}\right)$*-path* $W = (\omega_{2(1-g)}, \ldots, \omega_{2(d+f)})$*. Let*

$$x(W) = \prod_{k \text{ odd}} x_{w_k} \prod_{k \text{ even}} x_{w_k}^{-1}, \text{ in other words,}$$

$$x(W) = \frac{\prod_{k \text{ odd}} x_{w_k}}{x(\eta_1)\ldots x(\eta_g)x(\tau_{i_1})\ldots x(\tau_{i_d})x(\rho_1)\ldots x(\rho_f)}.$$

By construction, if W_a *and* W_b *belong to the same equivalent class* $[\omega]$*, then* $x(W_a) = x(W_b)$*, hence we write*

$$x([\omega]) := x(W_a) = x(W_b).$$

Definition 5.2.13 ($\gamma^{(P,Q)}$-oriented steps)**.** *Let* ζ *be either the curve* $\overline{\gamma}^{(P,Q)}_{+,+}$, $\overline{\gamma}^{(P,Q)}_{+,-}$, $\overline{\gamma}^{(P,Q)}_{-,+}$, *or* $\overline{\gamma}^{(P,Q)}_{-,-}$*. Suppose* ω *is a* (T°, ζ)*-path. If* ω *is a* (T°, ζ)*-path, we say that* ω_{2k} *is* $\gamma^{(P,Q)}$*-oriented if, when* ω_{2k} *crosses* ζ *at* p_k*, it enters* ζ *from the right side of* ζ*. See Fig. 5.5.*

Definition 5.2.14 (height monomial and specialized height monomial for a $(T^\circ, \overline{\gamma}^{(P,Q)})$-path)**.** *Let* $W = (\omega_{2(1-g)}, \ldots, \omega_{2(d+f)})$ *be a* $\left(T^\circ, \overline{\gamma}^{(P,Q)}_{+,+}\right)$ *or* $\left(T^\circ, \overline{\gamma}^{(P,Q)}_{-,-}\right)$*-path. We define the* height monomial $h(\omega)$ *by*

$$h(W) := \prod_{k:\omega_{2k} \text{ is } \gamma^{(P,Q)}\text{-oriented}} h_{w_{2k}}$$

One can check, if W_a and W_b belong to the same equivalent class $[\omega]$, then $h(W_a) = h(W_b)$, hence we write

$$h([\omega]) := h(W_a) = h(W_b).$$

We define the specialized height monomial *$y([\omega])$ of $[\omega]$ to be the specialization $\Phi(h([\omega]))$, where Φ is as defined earlier in Definition 5.1.6.*

Theorem 5.2.15 (Formula for $\gamma^{(P,\,Q)}$)**.** *Then the T°-path expansion of $\gamma^{(P,\,Q)}$ is given by*

$$x_{\gamma^{(P,\,Q)}} = \sum_{[\omega]} x([\omega])\, y([\omega])$$

where the sum is over all $(T^\circ, \gamma^{(P,\,Q)})$-paths $[\omega]$.

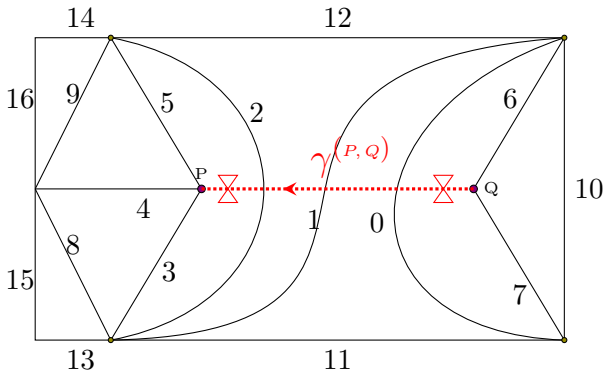

Figure 5.7: Ideal triangulation T° and doubly-notched arc $\gamma^{(P,\,Q)}$.

Example 5.2.16. *Consider the ideal triangulation T° and doubly-notched arc $\gamma^{(P,\,Q)}$ in Fig. 5.7. The "S"-shaped curve $\overline{\gamma}^{(P,\,Q)}_{+,+}$, the two "C"-shaped curves $\overline{\gamma}^{(P,\,Q)}_{+,-}$ and $\overline{\gamma}^{(P,\,Q)}_{-,+}$, and the "Z"-shaped curve $\overline{\gamma}^{(P,\,Q)}_{-,-}$ are illustrated in Fig. 5.6. We find that there are precisely* 30 *$(T^\circ, \gamma^{(P,\,Q)})$-paths. We list the path/s that each class contains. The $\pm$ symbols at the end of the sequence indicate whether the sequence is a $\left(T^\circ, \overline{\gamma}^{(P,\,Q)}_{+,+}\right)$, $\left(T^\circ, \overline{\gamma}^{(P,\,Q)}_{+,-}\right)$, $\left(T^\circ, \overline{\gamma}^{(P,\,Q)}_{-,+}\right)$, or $\left(T^\circ, \overline{\gamma}^{(P,\,Q)}_{-,-}\right)$-path. The even steps are written in bold, and the $\gamma^{(P,\,Q)}$-oriented even steps are circled:*

1. There is exactly one path,

$$\big(\textcircled{\textbf{6}}, 6, \textcircled{\textbf{7}}, 0, \textcircled{\textbf{0}}, 0, \textcircled{\textbf{1}}, 2, \textcircled{\textbf{2}}, 2, \textcircled{\textbf{5}}, 4, \textcircled{\textbf{4}}, 3, \textcircled{\textbf{3}}\big)^{-,-},$$

in this class.

2. $\big(\mathbf{7}, 10, \textcircled{\textbf{6}}, 6, \textcircled{\textbf{0}}, 0, \textcircled{\textbf{1}}, 2, \textcircled{\textbf{2}}, 2, \textcircled{\textbf{5}}, 4, \textcircled{\textbf{4}}, 3, \textcircled{\textbf{3}}\big)^{-,+}$,
   $\big(\textcircled{\textbf{6}}, 10, \mathbf{7}, 6, \textcircled{\textbf{0}}, 0, \textcircled{\textbf{1}}, 2, \textcircled{\textbf{2}}, 2, \textcircled{\textbf{5}}, 4, \textcircled{\textbf{4}}, 3, \textcircled{\textbf{3}}\big)^{-,-}$,
3. $\big(\textcircled{\textbf{6}}, 6, \textcircled{\textbf{7}}, 0, \textcircled{\textbf{0}}, 0, \textcircled{\textbf{1}}, 2, \textcircled{\textbf{2}}, 3, \textcircled{\textbf{3}}, 3, \textcircled{\textbf{4}}, 9, \mathbf{5}\big)^{+,-}$,
   $\big(\textcircled{\textbf{6}}, 6, \textcircled{\textbf{7}}, 0, \textcircled{\textbf{0}}, 0, \textcircled{\textbf{1}}, 2, \textcircled{\textbf{2}}, 3, \mathbf{5}, 9, \textcircled{\textbf{4}}, 3, \textcircled{\textbf{3}}\big)^{-,-}$.
4. *There is exactly one path in this class,*
   $\big(\textcircled{\textbf{6}}, 6, \textcircled{\textbf{7}}, 0, \textcircled{\textbf{0}}, 11, \mathbf{1}, 12, \textcircled{\textbf{2}}, 2, \textcircled{\textbf{5}}, 4, \textcircled{\textbf{4}}, 3, \textcircled{\textbf{3}}\big)^{-,-}$.

5. $\big(\mathbf{7}, 10, \textcircled{\textbf{6}}, 6, \textcircled{\textbf{0}}, 0, \textcircled{\textbf{1}}, 2, \textcircled{\textbf{2}}, 3, \textcircled{\textbf{3}}, 3, \textcircled{\textbf{4}}, 9, \mathbf{5}\big)^{+,+}$,
   $\big(\textcircled{\textbf{6}}, 10, \mathbf{7}, 6, \textcircled{\textbf{0}}, 0, \textcircled{\textbf{1}}, 2, \textcircled{\textbf{2}}, 3, \textcircled{\textbf{3}}, 3, \textcircled{\textbf{4}}, 9, \mathbf{5}\big)^{+,-}$,
   $\big(\mathbf{7}, 10, \textcircled{\textbf{6}}, 6, \textcircled{\textbf{0}}, 0, \textcircled{\textbf{1}}, 2, \textcircled{\textbf{2}}, 3, \mathbf{5}, 9, \textcircled{\textbf{4}}, 3, \textcircled{\textbf{3}}\big)^{-,+}$,
   $\big(\textcircled{\textbf{6}}, 10, \mathbf{7}, 6, \textcircled{\textbf{0}}, 0, \textcircled{\textbf{1}}, 2, \textcircled{\textbf{2}}, 3, \mathbf{5}, 9, \textcircled{\textbf{4}}, 3, \textcircled{\textbf{3}}\big)^{-,-}$.
6. $\big(\mathbf{7}, 10, \textcircled{\textbf{6}}, 6, \textcircled{\textbf{0}}, 11, \mathbf{1}, 12, \textcircled{\textbf{2}}, 2, \textcircled{\textbf{5}}, 4, \textcircled{\textbf{4}}, 3, \textcircled{\textbf{3}}\big)^{-,+}$,
   $\big(\textcircled{\textbf{6}}, 10, \mathbf{7}, 6, \textcircled{\textbf{0}}, 11, \mathbf{1}, 12, \textcircled{\textbf{2}}, 2, \textcircled{\textbf{5}}, 4, \textcircled{\textbf{4}}, 3, \textcircled{\textbf{3}}\big)^{-,-}$.
7. $\big(\textcircled{\textbf{6}}, 6, \textcircled{\textbf{7}}, 0, \textcircled{\textbf{0}}, 0, \textcircled{\textbf{1}}, 2, \textcircled{\textbf{2}}, 3, \textcircled{\textbf{3}}, 8, \mathbf{4}, 5, \mathbf{5}\big)^{+,-}$,
   $\big(\textcircled{\textbf{6}}, 6, \textcircled{\textbf{7}}, 0, \textcircled{\textbf{0}}, 0, \textcircled{\textbf{1}}, 2, \textcircled{\textbf{2}}, 3, \mathbf{5}, 5, \mathbf{4}, 8, \textcircled{\textbf{3}}\big)^{-,-}$.
8. $\big(\textcircled{\textbf{6}}, 6, \textcircled{\textbf{7}}, 0, \textcircled{\textbf{0}}, 11, \mathbf{1}, 12, \textcircled{\textbf{2}}, 3, \textcircled{\textbf{3}}, 3, \textcircled{\textbf{4}}, 9, \mathbf{5}\big)^{+,-}$,
   $\big(\textcircled{\textbf{6}}, 6, \textcircled{\textbf{7}}, 0, \textcircled{\textbf{0}}, 11, \mathbf{1}, 12, \textcircled{\textbf{2}}, 3, \mathbf{5}, 9, \textcircled{\textbf{4}}, 3, \textcircled{\textbf{3}}\big)^{-,-}$.

9. $\big(\mathbf{7}, 10, \textcircled{\textbf{6}}, 6, \textcircled{\textbf{0}}, 0, \textcircled{\textbf{1}}, 2, \textcircled{\textbf{2}}, 3, \textcircled{\textbf{3}}, 8, \mathbf{4}, 5, \mathbf{5}\big)^{+,+}$,
   $\big(\textcircled{\textbf{6}}, 10, \mathbf{7}, 6, \textcircled{\textbf{0}}, 0, \textcircled{\textbf{1}}, 2, \textcircled{\textbf{2}}, 3, \textcircled{\textbf{3}}, 8, \mathbf{4}, 5, \mathbf{5}\big)^{+,-}$,
   $\big(\mathbf{7}, 10, \textcircled{\textbf{6}}, 6, \textcircled{\textbf{0}}, 0, \textcircled{\textbf{1}}, 2, \textcircled{\textbf{2}}, 3, \mathbf{5}, 5, \mathbf{4}, 8, \textcircled{\textbf{3}}\big)^{-,+}$,
   $\big(\textcircled{\textbf{6}}, 10, \mathbf{7}, 6, \textcircled{\textbf{0}}, 0, \textcircled{\textbf{1}}, 2, \textcircled{\textbf{2}}, 3, \mathbf{5}, 5, \mathbf{4}, 8, \textcircled{\textbf{3}}\big)^{-,-}$.

10. $\big(\mathbf{7},10,\textcircled{\mathbf{6}},6,\textcircled{\mathbf{0}},11,\mathbf{1},12,\textcircled{\mathbf{2}},3,\textcircled{\mathbf{3}},3,\textcircled{\mathbf{4}},9,\mathbf{5}\big)^{+,+}$,
$\big(\textcircled{\mathbf{6}},10,\mathbf{7},6,\textcircled{\mathbf{0}},11,\mathbf{1},12,\textcircled{\mathbf{2}},3,\textcircled{\mathbf{3}},3,\textcircled{\mathbf{4}},9,\mathbf{5}\big)^{+,-}$,
$\big(\mathbf{7},10,\textcircled{\mathbf{6}},6,\textcircled{\mathbf{0}},11,\mathbf{1},12,\textcircled{\mathbf{2}},3,\mathbf{5},9,\textcircled{\mathbf{4}},3,\textcircled{\mathbf{3}}\big)^{-,+}$,
$\big(\textcircled{\mathbf{6}},10,\mathbf{7},6,\textcircled{\mathbf{0}},11,\mathbf{1},12,\textcircled{\mathbf{2}},3,\mathbf{5},9,\textcircled{\mathbf{4}},3,\textcircled{\mathbf{3}}\big)^{-,-}$.

11. $\big(\mathbf{7},10,\textcircled{\mathbf{6}},7,\mathbf{0},1,\mathbf{1},12,\textcircled{\mathbf{2}},2,\textcircled{\mathbf{5}},4,\textcircled{\mathbf{4}},3,\textcircled{\mathbf{3}}\big)^{-,+}$,
$\big(\textcircled{\mathbf{6}},10,\mathbf{7},7,\mathbf{0},1,\mathbf{1},12,\textcircled{\mathbf{2}},2,\textcircled{\mathbf{5}},4,\textcircled{\mathbf{4}},3,\textcircled{\mathbf{3}}\big)^{-,-}$.

12. $\big(\textcircled{\mathbf{6}},6,\textcircled{\mathbf{7}},0,\textcircled{\mathbf{0}},11,\mathbf{1},12,\textcircled{\mathbf{2}},3,\textcircled{\mathbf{3}},8,\mathbf{4},5,\mathbf{5}\big)^{+,-}$,
$\big(\textcircled{\mathbf{6}},6,\textcircled{\mathbf{7}},0,\textcircled{\mathbf{0}},11,\mathbf{1},12,\textcircled{\mathbf{2}},3,\mathbf{5},5,\mathbf{4},8,\textcircled{\mathbf{3}}\big)^{-,-}$.

13. $\big(\textcircled{\mathbf{6}},6,\textcircled{\mathbf{7}},0,\textcircled{\mathbf{0}},11,\mathbf{1},1,\mathbf{2},5,\textcircled{\mathbf{3}},3,\textcircled{\mathbf{4}},9,\mathbf{5}\big)^{+,-}$,
$\big(\textcircled{\mathbf{6}},6,\textcircled{\mathbf{7}},0,\textcircled{\mathbf{0}},11,\mathbf{1},1,\mathbf{2},5,\mathbf{5},9,\textcircled{\mathbf{4}},3,\textcircled{\mathbf{3}}\big)^{-,-}$.

14. This class contains exactly one path, $\big(\mathbf{7},7,\mathbf{6},0,\mathbf{0},1,\mathbf{1},12,\textcircled{\mathbf{2}},2,\textcircled{\mathbf{5}},4,\textcircled{\mathbf{4}},3,\textcircled{\mathbf{3}}\big)^{-,+}$.

15. $\big(\mathbf{7},10,\textcircled{\mathbf{6}},6,\textcircled{\mathbf{0}},11,\mathbf{1},12,\textcircled{\mathbf{2}},3,\textcircled{\mathbf{3}},8,\mathbf{4},5,\mathbf{5}\big)^{+,+}$,
$\big(\textcircled{\mathbf{6}},10,\mathbf{7},6,\textcircled{\mathbf{0}},11,\mathbf{1},12,\textcircled{\mathbf{2}},3,\textcircled{\mathbf{3}},8,\mathbf{4},5,\mathbf{5}\big)^{+,-}$,
$\big(\mathbf{7},10,\textcircled{\mathbf{6}},6,\textcircled{\mathbf{0}},11,\mathbf{1},12,\textcircled{\mathbf{2}},3,\mathbf{5},5,\mathbf{4},8,\textcircled{\mathbf{3}}\big)^{-,+}$,
$\big(\textcircled{\mathbf{6}},10,\mathbf{7},6,\textcircled{\mathbf{0}},11,\mathbf{1},12,\textcircled{\mathbf{2}},3,\mathbf{5},5,\mathbf{4},8,\textcircled{\mathbf{3}}\big)^{-,-}$.

16. $\big(\mathbf{7},10,\textcircled{\mathbf{6}},6,\textcircled{\mathbf{0}},11,\mathbf{1},1,\mathbf{2},5,\textcircled{\mathbf{3}},3,\textcircled{\mathbf{4}},9,\mathbf{5}\big)^{+,+}$,
$\big(\textcircled{\mathbf{6}},10,\mathbf{7},6,\textcircled{\mathbf{0}},11,\mathbf{1},1,\mathbf{2},5,\textcircled{\mathbf{3}},3,\textcircled{\mathbf{4}},9,\mathbf{5}\big)^{+,-}$,
$\big(\mathbf{7},10,\textcircled{\mathbf{6}},6,\textcircled{\mathbf{0}},11,\mathbf{1},1,\mathbf{2},5,\mathbf{5},9,\textcircled{\mathbf{4}},3,\textcircled{\mathbf{3}}\big)^{-,+}$,
$\big(\textcircled{\mathbf{6}},10,\mathbf{7},6,\textcircled{\mathbf{0}},11,\mathbf{1},1,\mathbf{2},5,\mathbf{5},9,\textcircled{\mathbf{4}},3,\textcircled{\mathbf{3}}\big)^{-,-}$.

17. $\big(\mathbf{7},10,\textcircled{\mathbf{6}},7,\mathbf{0},1,\mathbf{1},12,\textcircled{\mathbf{2}},3,\textcircled{\mathbf{3}},3,\textcircled{\mathbf{4}},9,\mathbf{5}\big)^{+,+}$,
$\big(\textcircled{\mathbf{6}},10,\mathbf{7},7,\mathbf{0},1,\mathbf{1},12,\textcircled{\mathbf{2}},3,\textcircled{\mathbf{3}},3,\textcircled{\mathbf{4}},9,\mathbf{5}\big)^{+,-}$,
$\big(\mathbf{7},10,\textcircled{\mathbf{6}},7,\mathbf{0},1,\mathbf{1},12,\textcircled{\mathbf{2}},3,\mathbf{5},9,\textcircled{\mathbf{4}},3,\textcircled{\mathbf{3}}\big)^{-,+}$,
$\big(\textcircled{\mathbf{6}},10,\mathbf{7},7,\mathbf{0},1,\mathbf{1},12,\textcircled{\mathbf{2}},3,\mathbf{5},9,\textcircled{\mathbf{4}},3,\textcircled{\mathbf{3}}\big)^{-,-}$.

18. $\big(\textcircled{\mathbf{6}},6,\textcircled{\mathbf{7}},0,\textcircled{\mathbf{0}},11,\mathbf{1},1,\mathbf{2},5,\textcircled{\mathbf{3}},8,\mathbf{4},5,\mathbf{5}\big)^{+,-}$,
$\big(\textcircled{\mathbf{6}},6,\textcircled{\mathbf{7}},0,\textcircled{\mathbf{0}},11,\mathbf{1},1,\mathbf{2},5,\mathbf{5},5,\mathbf{4},8,\textcircled{\mathbf{3}}\big)^{-,-}$.

19. $\big(\mathbf{7},7,\mathbf{6},0,\mathbf{0},1,\mathbf{1},12,\textcircled{\mathbf{2}},3,\textcircled{\mathbf{3}},3,\textcircled{\mathbf{4}},9,\mathbf{5}\big)^{+,+}$,
$\big(\mathbf{7},7,\mathbf{6},0,\mathbf{0},1,\mathbf{1},12,\textcircled{\mathbf{2}},3,\mathbf{5},9,\textcircled{\mathbf{4}},3,\textcircled{\mathbf{3}}\big)^{-,+}$,

20. $\big(\mathbf{7}, 10, \textcircled{\mathbf{6}}, 6, \textcircled{\mathbf{0}}, 11, \mathbf{1}, 1, \mathbf{2}, 5, \textcircled{\mathbf{3}}, 8, \mathbf{4}, 5, \mathbf{5}\big)^{+,+}$,
$\big(\textcircled{\mathbf{6}}, 10, \mathbf{7}, 6, \textcircled{\mathbf{0}}, 11, \mathbf{1}, 1, \mathbf{2}, 5, \textcircled{\mathbf{3}}, 8, \mathbf{4}, 5, \mathbf{5}\big)^{+,-}$,
$\big(\mathbf{7}, 10, \textcircled{\mathbf{6}}, 6, \textcircled{\mathbf{0}}, 11, \mathbf{1}, 1, \mathbf{2}, 5, \mathbf{5}, 5, \mathbf{4}, 8, \textcircled{\mathbf{3}}\big)^{-,+}$,
$\big(\textcircled{\mathbf{6}}, 10, \mathbf{7}, 6, \textcircled{\mathbf{0}}, 11, \mathbf{1}, 1, \mathbf{2}, 5, \mathbf{5}, 5, \mathbf{4}, 8, \textcircled{\mathbf{3}}\big)^{-,-}$.

21. $\big(\mathbf{7}, 10, \textcircled{\mathbf{6}}, 7, \mathbf{0}, 1, \mathbf{1}, 12, \textcircled{\mathbf{2}}, 3, \textcircled{\mathbf{3}}, 8, \mathbf{4}, 5, \mathbf{5}\big)^{+,+}$,
$\big(\textcircled{\mathbf{6}}, 10, \mathbf{7}, 7, \mathbf{0}, 1, \mathbf{1}, 12, \textcircled{\mathbf{2}}, 3, \textcircled{\mathbf{3}}, 8, \mathbf{4}, 5, \mathbf{5}\big)^{+,-}$,
$\big(\mathbf{7}, 10, \textcircled{\mathbf{6}}, 7, \mathbf{0}, 1, \mathbf{1}, 12, \textcircled{\mathbf{2}}, 3, \mathbf{5}, 5, \mathbf{4}, 8, \textcircled{\mathbf{3}}\big)^{-,+}$,
$\big(\textcircled{\mathbf{6}}, 10, \mathbf{7}, 7, \mathbf{0}, 1, \mathbf{1}, 12, \textcircled{\mathbf{2}}, 3, \mathbf{5}, 5, \mathbf{4}, 8, \textcircled{\mathbf{3}}\big)^{-,-}$.

22. $\big(\mathbf{7}, 10, \textcircled{\mathbf{6}}, 7, \mathbf{0}, 1, \mathbf{1}, 1, \mathbf{2}, 5, \textcircled{\mathbf{3}}, 3, \textcircled{\mathbf{4}}, 9, \mathbf{5}\big)^{+,+}$,
$\big(\textcircled{\mathbf{6}}, 10, \mathbf{7}, 7, \mathbf{0}, 1, \mathbf{1}, 1, \mathbf{2}, 5, \textcircled{\mathbf{3}}, 3, \textcircled{\mathbf{4}}, 9, \mathbf{5}\big)^{+,-}$,
$\big(\mathbf{7}, 10, \textcircled{\mathbf{6}}, 7, \mathbf{0}, 1, \mathbf{1}, 1, \mathbf{2}, 5, \mathbf{5}, 9, \textcircled{\mathbf{4}}, 3, \textcircled{\mathbf{3}}\big)^{-,+}$,
$\big(\textcircled{\mathbf{6}}, 10, \mathbf{7}, 7, \mathbf{0}, 1, \mathbf{1}, 1, \mathbf{2}, 5, \mathbf{5}, 9, \textcircled{\mathbf{4}}, 3, \textcircled{\mathbf{3}}\big)^{-,-}$.

23. $\big(\textcircled{\mathbf{6}}, 6, \textcircled{\mathbf{7}}, 0, \textcircled{\mathbf{0}}, 11, \mathbf{1}, 1, \mathbf{2}, 2, \mathbf{3}, 4, \mathbf{4}, 5, \mathbf{5}\big)^{+,-}$.

24. $\big(\mathbf{7}, 7, \mathbf{6}, 0, \mathbf{0}, 1, \mathbf{1}, 12, \textcircled{\mathbf{2}}, 3, \textcircled{\mathbf{3}}, 8, \mathbf{4}, 5, \mathbf{5}\big)^{+,+}$.

25. $\big(\mathbf{7}, 7, \mathbf{6}, 0, \mathbf{0}, 1, \mathbf{1}, 1, \mathbf{2}, 5, \textcircled{\mathbf{3}}, 3, \textcircled{\mathbf{4}}, 9, \mathbf{5}\big)^{+,+}$,
$\big(\mathbf{7}, 7, \mathbf{6}, 0, \mathbf{0}, 1, \mathbf{1}, 1, \mathbf{2}, 5, \mathbf{5}, 9, \textcircled{\mathbf{4}}, 3, \textcircled{\mathbf{3}}\big)^{-,+}$.

26. $\big(\mathbf{7}, 10, \textcircled{\mathbf{6}}, 6, \textcircled{\mathbf{0}}, 11, \mathbf{1}, 1, \mathbf{2}, 2, \mathbf{3}, 4, \mathbf{4}, 5, \mathbf{5}\big)^{+,+}$,
$\big(\textcircled{\mathbf{6}}, 10, \mathbf{7}, 6, \textcircled{\mathbf{0}}, 11, \mathbf{1}, 1, \mathbf{2}, 2, \mathbf{3}, 4, \mathbf{4}, 5, \mathbf{5}\big)^{+,-}$.

27. $\big(\mathbf{7}, 10, \textcircled{\mathbf{6}}, 7, \mathbf{0}, 1, \mathbf{1}, 1, \mathbf{2}, 5, \textcircled{\mathbf{3}}, 8, \mathbf{4}, 5, \mathbf{5}\big)^{+,+}$,
$\big(\textcircled{\mathbf{6}}, 10, \mathbf{7}, 7, \mathbf{0}, 1, \mathbf{1}, 1, \mathbf{2}, 5, \textcircled{\mathbf{3}}, 8, \mathbf{4}, 5, \mathbf{5}\big)^{+,-}$,
$\big(\mathbf{7}, 10, \textcircled{\mathbf{6}}, 7, \mathbf{0}, 1, \mathbf{1}, 1, \mathbf{2}, 5, \mathbf{5}, 5, \mathbf{4}, 8, \textcircled{\mathbf{3}}\big)^{-,+}$,
$\big(\textcircled{\mathbf{6}}, 10, \mathbf{7}, 7, \mathbf{0}, 1, \mathbf{1}, 1, \mathbf{2}, 5, \mathbf{5}, 5, \mathbf{4}, 8, \textcircled{\mathbf{3}}\big)^{-,-}$.

28. $\big(\mathbf{7}, 7, \mathbf{6}, 0, \mathbf{0}, 1, \mathbf{1}, 1, \mathbf{2}, 5, \textcircled{\mathbf{3}}, 8, \mathbf{4}, 5, \mathbf{5}\big)^{+,+}$,
$\big(\mathbf{7}, 7, \mathbf{6}, 0, \mathbf{0}, 1, \mathbf{1}, 1, \mathbf{2}, 5, \mathbf{5}, 5, \mathbf{4}, 8, \textcircled{\mathbf{3}}\big)^{-,+}$.

29. $\big(\mathbf{7}, 10, \textcircled{\mathbf{6}}, 7, \mathbf{0}, 1, \mathbf{1}, 1, \mathbf{2}, 2, \mathbf{3}, 4, \mathbf{4}, 5, \mathbf{5}\big)^{+,+}$,
$\big(\textcircled{\mathbf{6}}, 10, \mathbf{7}, 7, \mathbf{0}, 1, \mathbf{1}, 1, \mathbf{2}, 2, \mathbf{3}, 4, \mathbf{4}, 5, \mathbf{5}\big)^{+,-}$.

30. This class contains exactly one path,

$$(\mathbf{7},7,\mathbf{6},0,\mathbf{0},1,\mathbf{1},1,\mathbf{2},2,\mathbf{3},4,\mathbf{4},5,\mathbf{5})^{+,+}.$$

Applying Theorem 5.2.15, we compute $x_{\gamma^{(P,\,Q)}}$ *to be*

$$\begin{aligned}
x_{\gamma^{(P,\,Q)}} = \Big(& x_0^2x_2^2x_3x_4x_6\ y_0y_1y_2y_3y_4y_5y_6y_7 + \\
& \big(x_0x_2^2x_3x_4x_6x_{10}\ y_0y_1y_2y_3y_4y_5y_6 + x_0^2x_2x_3^2x_6x_9\ y_0y_1y_2y_3y_4y_6y_7 + \\
& x_0x_2x_3x_4x_6x_{11}x_{12}\ y_0y_2y_3y_4y_5y_6y_7\big) + \\
& \big(x_0x_2x_3^2x_6x_9x_{10}\ y_0y_1y_2y_3y_4y_6 + x_2x_3x_4x_6x_{10}x_{11}x_{12}\ y_0y_2y_3y_4y_5y_6 + \\
& x_0^2x_2x_3x_5x_6x_8\ y_0y_1y_2y_3y_6y_7 + x_0x_3^2x_6x_9x_{11}x_{12}\ y_0y_2y_3y_4y_6y_7\big) + \\
& \big(x_0x_2x_3x_5x_6x_8x_{10}\ y_0y_1y_2y_3y_6 + x_3^2x_6x_9x_{10}x_{11}x_{12}\ y_0y_2y_3y_4y_6 + \\
& x_1x_2x_3x_4x_7x_{10}x_{12}\ y_2y_3y_4y_5y_6 + \\
& x_0x_3x_5x_6x_8x_{11}x_{12}\ y_0y_2y_3y_6y_7 + x_0x_1x_3x_5x_6x_9x_{11}\ y_0y_3y_4y_6y_7\big) + \\
& \big(x_0x_1x_2x_3x_4x_7x_{12}\ y_2y_3y_4y_5 + x_3x_5x_6x_8x_{10}x_{11}x_{12}\ y_0y_2y_3y_6 + \\
& x_1x_3x_5x_6x_9x_{10}x_{11}\ y_0y_3y_4y_6 + x_1x_3^2x_7x_9x_{10}x_{12}\ y_2y_3y_4y_6 + x_0x_1x_5^2x_6x_8x_{11}\ y_0y_3y_6y_7\big) + \\
& \big(x_0x_1x_3^2x_7x_9x_{12}\ y_2y_3y_4 + x_1x_5^2x_6x_8x_{10}x_{11}\ y_0y_3y_6 + \\
& x_1x_3x_5x_7x_8x_{10}x_{12}\ y_2y_3y_6 + x_1^2x_3x_5x_7x_9x_{10}\ y_3y_4y_6 + x_0x_1x_2x_4x_5x_6x_{11}\ y_0y_6y_7\big) + \\
& \big(x_0x_1x_3x_5x_7x_8x_{12}\ y_2y_3 + x_0x_1^2x_3x_5x_7x_9\ y_3y_4 + \\
& x_1x_2x_4x_5x_6x_{10}x_{11}\ y_0y_6 + x_1^2x_5^2x_7x_8x_{10}\ y_3y_6\big) + \\
& x_0x_1^2x_5^2x_7x_8\ y_3 + x_1^2x_2x_4x_5x_7x_{10}\ y_6\big) + \\
& x_0x_1^2x_2x_4x_5x_7\Big) \Big/ \\
& (x_0x_1x_2x_3x_4x_5x_6x_7)\,.
\end{aligned}$$

5.3 Proof of Theorem 5.1.1: formula for an ordinary arc γ

5.3.1 Backtracks and non-backtracks

We extend the notion of backtrack and non-backtrack cycles (see Definition 4.2.4) to a general punctured surface.

Definition 5.3.1 (backtrack cycle, non-backtrack cycle, quasi-backtrack, and quasi-non-backtrack)**.** *Let $\gamma \notin T^\circ$ and let $\omega = (\omega_1, \ldots, \omega_{2d+1})$ be a (T°, γ)-path. Let τ be an arc of T° (possibly a loop), and let (ω_j, ω_{j+1}) be a pair of consecutive quasi-arcs, both associated to τ.*

1. *We say that (ω_j, ω_{j+1}) is a* cycle *if the starting point of ω_j coincides with the ending point of ω_{j+1}. Note that a cycle is only possible when this point is a marked point on the boundary.*

   i) A cycle (ω_j, ω_{j+1}) is called a backtrack*, denoted by $(\underline{\tau, \tau})$, if it is contractible.*

   ii) A cycle (ω_j, ω_{j+1}) is called a non-backtrack*, denoted by $(\boldsymbol{\tau, \tau})$, otherwise.*

2. *Suppose that (ω_j, ω_{j+1}) is not quite a cycle, but the starting point of ω_j and the ending point of ω_{j+1} are two (non-marked) points ${}_Q{}'$ and ${}_Q{}''$ in the vicinity of a puncture ${}_Q$ (where ${}_Q$ is an endpoint of τ).*

   i) Then we define quasi-backtracks *as follows. (Note that we only define a quasi-backtrack when τ is adjacent to at least one puncture.)*

   a. Suppose that τ has a second endpoint v that is a boundary marked point. We say that (ω_j, ω_{j+1}), denoted by $(\overline{\tau, \tau})$, is a quasi-backtrack if it is a concatenation of two quasi-arcs

   $$ {}_Q{}' \rightsquigarrow v \rightsquigarrow {}_Q{}''. $$

   b. Suppose that τ is adjacent to another puncture ${}_P$ distinct from ${}_Q$, or τ is a loop (where we write ${}_P := {}_Q$). We say that (ω_j, ω_{j+1}), denoted by $(\overline{\tau, \tau})$, is a quasi-backtrack if (ω_j, ω_{j+1}) is a concatenation of two quasi-arcs

   $$ {}_Q{}' \rightsquigarrow {}_P{}' \rightsquigarrow {}_Q{}'', $$

where $_P'$ *is a (non-marked) point in the vicinity of* $_P$*, such that the cycle formed by concatenating* $_Q' \rightsquigarrow {}_P' \rightsquigarrow {}_Q''$ *and the short curve between* $_Q'$ *and* $_Q''$ *(within the disk* D_Q*) is either contractible to* $_Q$ *or contractible.*

ii) Finally, we define quasi-non-backtracks *as follows. Suppose that* τ *is adjacent to another puncture* $_P$ *distinct from* $_Q$*, or* τ *is a loop (where we write* $_P := {}_Q$*). We say that* (ω_j, ω_{j+1}) *is a quasi-non-backtrack, denoted by* $(\boldsymbol{\tau}, \boldsymbol{\tau})$*, if* (ω_j, ω_{j+1}) *is a concatenation of two quasi-arcs*

$$_Q' \rightsquigarrow {}_P' \rightsquigarrow {}_Q'',$$

where $_P'$ *is a (non-marked) point in the vicinity of* $_P$*, such that the cycle formed by concatenating* $_Q' \rightsquigarrow {}_P' \rightsquigarrow {}_Q''$ *and the short curve between* $_Q'$ *and* $_Q''$ *(within the disk* D_Q *around* $_Q$*) is* not *contractible and* not *contractible to* $_Q$*.*

We will explain in Proposition 5.3.2 that a non-backtrack cycle or a quasi-non-backtrack (as defined in Definition 5.3.1) can only appear in a (T°, γ)-path if τ is the radius of a self-folded triangle of T°. As in Remark 4.2.5(2a), we say that (ω_j, ω_{j+1}) is a *counterclockwise non-backtrack* or *counterclockwise quasi-non-backtrack* if it goes counterclockwise (see Figs. 5.8(b) and 5.9(b)). We say that (ω_j, ω_{j+1}) is a *clockwise non-backtrack* or *clockwise quasi-non-backtrack* if it goes clockwise (Figs. 5.8(c) and 5.9(c)).

5.3.2 A non-backtrack cycle or quasi-non-backtrack can only go along a self-folded triangle's radius

The following proposition is the analog of Proposition 4.2.13 (from the previous chapter) for a general marked surface.

Proposition 5.3.2. *Let* T° *be an ideal triangulation. Suppose* γ *is an ordinary arc which crosses* $\tau \in T^\circ$*, and let* $\omega = (\omega_1, \ldots, \omega_{2d+1})$ *be a* (T°, γ)*-path. Suppose* (ω_j, ω_{j+1}) *is a pair of steps both going along quasi-arcs associated to* τ*.*

1) *Suppose* $\tau \in T^\circ$ *(possibly a loop) is* not *the radius of a self-folded triangle of* T°*. Then* (ω_j, ω_{j+1}) *follow two opposite orientations of* τ *in such a way that* (ω_j, ω_{j+1})

is a backtrack cycle (see Fig. 5.10(a)) or a quasi-backtrack (see Figs. 5.10(b) and 5.11).

2) *Suppose that τ is the radius of a self-folded triangle. Then (ω_j, ω_{j+1}) is one of the following:*

   - *a backtrack cycle or a quasi-backtrack (Figs. 5.8(a) and 5.9(a)),*
   - *a counterclockwise non-backtrack cycle or a counterclockwise quasi-non-backtrack (Figs. 5.8(b) and 5.9(b)),*
   - *a clockwise non-backtrack cycle or a clockwise quasi-non-backtrack (Figs. 5.8(c) and 5.9(c)).*

5.3.3 A (T°, γ)-path ω on S, M is uniquely determined by its sequence of labels

The proof of Proposition 4.2.16 (discussed in Section 4.2.2) carries over to the following proposition for the case of a general marked surface (S, M):

Proposition 5.3.3. *A (T°, γ)-path ω on (S, M) is uniquely determined by its sequence of labels $(\omega_1, \ldots, \omega_{2d+1})$, forgetting the orientations of the steps and whether a consecutive pair is a non-backtrack or a backtrack (respectively, a quasi-non-backtrack or a quasi-backtrack).*

5.3.4 Proof of Theorem 5.1.1

Proof of Theorem 5.1.1. We repeat the same argument given in Chapter 4. For an ordinary arc γ, [MS10] gives a natural, explicit bijection F between the complete (T^o, γ)-paths ω and the perfect matchings P of a certain graph (called snake graph) G_γ corresponding to γ and T^o for unpunctured (S, M). This bijection F preserves both the weight $x(P)$ and height $y(P)$ of a matching, which are described in [MSW11, Sec. 4.3]. What we mean by that is, if $F(P) = \omega$, then

$$\left(\prod_{k=1}^{d} \frac{1}{x(\tau_{i_k})}\right) x(P) = x(\omega), \text{ and}$$

$$y(P) = y(\omega).$$

Since, by [MSW11, Thm. 4.10],

$$x_\gamma = \left(\prod_{k=1}^{d} \frac{1}{x(\tau_{i_k})} \right) \sum_P x(P)\ y(P)$$

where the sum is taken over all perfect matchings P of G_γ, the result follows. $\square$

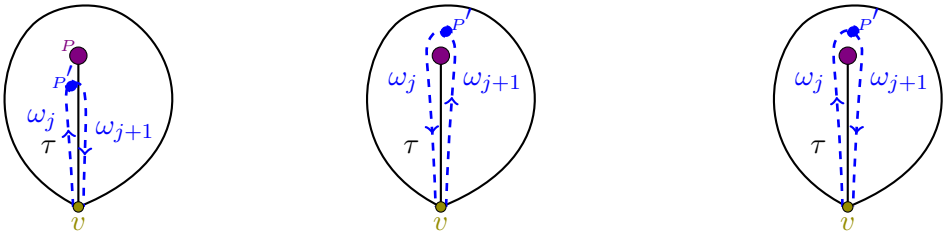

(a) Backtrack cycle $(\underline{\tau,\tau})$. (b) Counterclockwise non-backtrack cycle $(\boldsymbol{\tau,\tau})$. (c) Clockwise non-backtrack cycle $(\boldsymbol{\tau,\tau})$.

Figure 5.8: The three possibilities of a pair (ω_j, ω_{j+1}) of consecutive steps along τ (between a boundary marked point v and a puncture P) if T° has a self-folded triangle with τ as the radius.

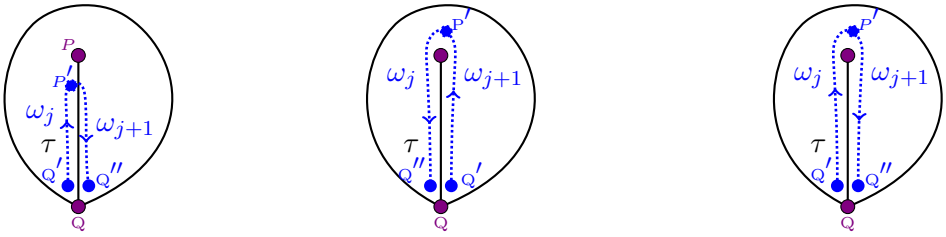

(a) Quasi-backtrack $(\overline{\tau,\tau})$. (b) Counterclockwise quasi-non-backtrack $(\overline{\boldsymbol{\tau,\tau}})$. (c) Clockwise quasi-non-backtrack $(\overline{\boldsymbol{\tau,\tau}})$.

Figure 5.9: The three possibilities of a pair (ω_j, ω_{j+1}) of consecutive steps along τ (between two punctures P and Q) if T° has a self-folded triangle with τ as the radius.

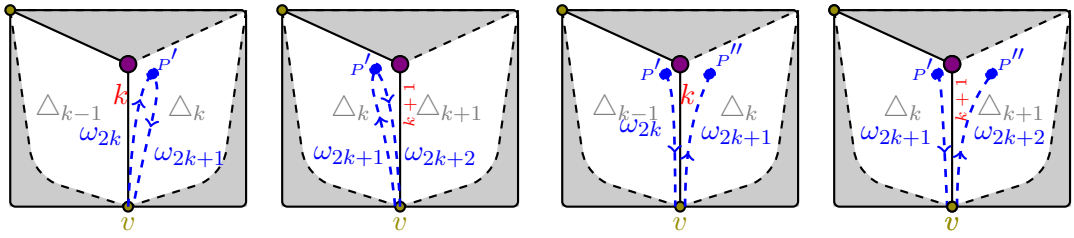

(a) Backtrack cycle $(\underline{\omega_{2k}, \omega_{2k+1}})$ or $(\underline{\omega_{2k+1}, \omega_{2k+2}})$. (b) Quasi-backtrack $(\overline{\omega_{2k}, \omega_{2k+1}})$ or $(\overline{\omega_{2k+1}, \omega_{2k+2}})$.

Figure 5.10: Possibilities for pair (ω_j, ω_{j+1}) of consecutive steps along τ if τ is not the radius of a self-folded triangle of T° and if τ is between a boundary marked point and a puncture P.

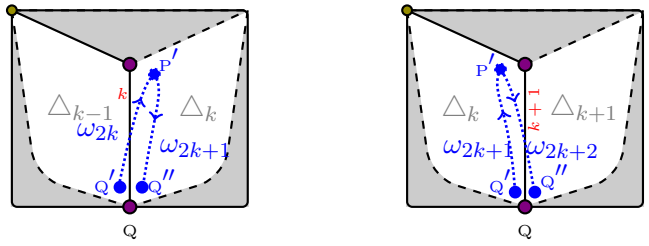

(a) Quasi-backtrack $(\overline{\omega_{2k}, \omega_{2k+1}})$. (b) Quasi-backtrack $(\overline{\omega_{2k+1}, \omega_{2k+2}})$.

Figure 5.11: A pair (ω_j, ω_{j+1}) of consecutive steps along τ must be a quasi-backtrack if τ is not the radius of a self-folded triangle of T° and if τ is between two punctures P and Q.

5.4 Proof of Theorem 5.2.6: formula for $\gamma^{(P)}$

The argument presented in this section is a T-path analog of the proof of [MSW11, Theorem 4.17] given in [MSW11, Section 12.1].

Lemma 5.4.1. *If ω is a complete (T°, ℓ_γ^P)-path, then one of these must hold: either the odd step ω_{2d+1} finishes at* P*, or the even step $\omega_{2(d+f)}$ finishes at* P*.*

Proof. Suppose the odd step ω_{2d+1} does not end at P. Recall that, by (T1), the previous even step ω_{2d} must traverse τ_{i_d} and the next even step ω_{2d+2} must traverse ρ_1. Therefore, the starting point of step ω_{2d+1} must be adjacent to τ_{i_d}, and the ending point of ω_{2d+1} must be adjacent to ρ_1. But the ending point of ω_{2d+1} cannot be P by assumption. Hence ω_{2d+1} must go along τ_{i_d} and ending at the vertex v_{ρ_1} adjacent to ρ_1. If τ_{i_d} is a loop, then ω_{2d+1} goes clockwise.

Now we have no choice but requiring $\omega_{2(d+1)}$ to go along ρ_1 and ending at P. This in turn requires the next two steps to be a backtrack along ρ_2 from P back to itself, forcing the next two steps (if any) to be a backtrack along ρ_3 back to P, and so on. Therefore, we conclude that $\omega_{2(d+f)}$ ends at P. □

Definition 5.4.2 (Sets $\Omega(\gamma)$ and $S\Omega(\gamma^{(P)})$)**.** *Let γ be an ordinary arc. We let $\Omega(\gamma)$ denote the set of complete (T°, γ)-paths. If γ is not a loop, we let $S\Omega(\gamma^{(P)})$ be the set of $(T^\circ, \gamma^{(P)})$-paths.*

We prove Theorem 5.2.6 by constructing a bijection ψ between pairs $(W_1, [W_2])$ in $\Omega(\gamma) \times S\Omega(\gamma^{(P)})$ and complete $(T^\circ, \ell_\gamma^{\mathrm{P}})$-paths in $\Omega(\ell_\gamma^{\mathrm{P}})$. This bijection will be weight-preserving and height-preserving, in the sense that, if $\psi(W_1, [W_2]) = W_3$, then $x(W_1)\, x([W_2]) = x(W_3)$ and $h(W_1)\, h([W_2]) = h(W_3)$.

This gives

$$\sum_{W_3 \in \Omega(\ell_\gamma^{\mathrm{P}})} = \left(\sum_{W_1 \in \Omega(\gamma)} x(W_1)\, h(W_1) \right) \left(\sum_{[W_2] \in S\Omega(\gamma^{(P)})} x([W_2])\, h([W_2]) \right). \tag{5.4.1}$$

After applying Φ, the left-hand-side and first term on the right are equal to $x_{\ell_\gamma^{\mathrm{P}}}$ and x_γ, given by Theorem 5.1.1, which allows us to express $x_{\gamma^{(P)}} = \left(x_{\ell_\gamma^{\mathrm{P}}}\right)/(x_\gamma)$ in terms of $\left(\sum_{[W_2] \in S\Omega(\gamma^{(P)})} x([W_2])\, y([W_2])\right)$.

Proof of Theorem 5.2.6. Write $\ell_\gamma = \ell_\gamma^{\text{P}}$, and orient it clockwise. As indicated above, we define a map

$$\psi : \Omega(\gamma) \times S\Omega(\gamma^{(P)}) \to \Omega(\ell_\gamma) \text{ by}$$

$$\psi(W_1, [W_2]) = \begin{cases} [W_2]^+ \cup W_{1-} & \text{if } [W_2] \text{ contains a } \left(T^\circ, \overline{\gamma}_+^{(P)}\right)\text{-path} \\ W_1 \cup [W_2]_-^- & \text{if } [W_2] \text{ contains exactly} \\ & \text{one path, a } \left(T^\circ, \overline{\gamma}_-^{(P)}\right)\text{-path} \end{cases}$$

where:

- $[W_2]^+ \cup W_{1-}$ is the following concatenation. Start with the $\left(T^\circ, \overline{\gamma}_+^{(P)}\right)$-path of $[W_2]$ which goes clockwise, ending at P, followed by the reverse of the (T°, γ)-path W_1.
- $W_1 \cup [W_2]_-^-$ is the following concatenation. Start with the (T°, γ)-path W_1, ending at P, followed by the reverse of the $\left(T^\circ, \overline{\gamma}_-^{(P)}\right)$-path of $[W_2]$.

It is clear that $\psi(W_1, [W_2])$ is a (T°, ℓ_γ)-path.

We show that ψ is a bijection by exhibiting its inverse. For $W_3 \in \Omega(\ell_\gamma)$, define $\varphi : \Omega(\ell_\gamma) \to \Omega(\gamma) \times S\Omega(\gamma^{(P)})$ as follows. Let $W_3 \in \Omega(\ell_\gamma^{\text{P}})$. By Lemma 5.4.1, one of these must hold: the even step $\omega_{2(d+f)}$ of W_3 ends at P, or the odd step ω_{2d+1} ends at P.

If we are in the first case (the even step $\omega_{2(d+f)}$ of W_3 ends at P), let $\varphi(W_3) := (W_1, [W_2])$ where W_1 is the $2d+1$-length path consisting of the last $2d+1$ steps of W_3, but reversed in order and traversing the opposite orientation; and W_2 is the even-length path consisting of the first $2(d+f)$ steps of W_3. Then W_2 is a $\left(T^\circ, \overline{\gamma}_+^{(P)}\right)$-path by construction.

Otherwise, if the even step $\omega_{2(d+f)}$ of W_3 starts at P and ends at s_f, then the odd step ω_{2d+1} must end at at P. Let $\varphi(W_3) := (W_1, [W_2])$ where W_1 is the $2d+1$-length path consisting of the first $2d+1$ steps of W_3; and W_2 is the even-length path consisting of the last $2(d+f)$ steps of W_3, but reversed in order and traversing the opposite orientation. Then W_2 is a $\left(T^\circ, \overline{\gamma}_-^{(P)}\right)$-path by construction.

For both cases, W_1 is a complete (T°, γ)-path by construction. It is also straightforward to show that these two maps are inverses.

We now show that the bijection ψ is weight-preserving. Since the bijection maps a step to another step, and it preserves the parity of each step (that is, whether a step is an odd or an even-numbered step), we obtain $x(W_3) = x(W_1)\, x([W_2])$, and we conclude that ψ is weight-preserving.

To see that ψ is height-preserving, let $W_3 = \psi(W_1, [W_2])$ for some $(W_1, [W_2]) \in \Omega(\gamma) \times S\Omega(\gamma^{(P)})$. We first consider the case where $[W_2]$ contains a representative $\left(T^\circ, \overline{\gamma}_+^{(P)}\right)$-path $[W_2]^+$ which goes clockwise around P. Recall that both ℓ_γ and $\overline{\gamma}_+^{(P)}$ is set to go clockwise around P. By definition of ψ, the orientation of the steps of $[W_2]^+$ agrees with the orientation of the first $2(d+f)$ steps of W_3. Hence, the height corresponding to each of the first $(d+f)$ even steps of W_3 is equal to the height of each of the even steps of $[W_2]_+$. Since the height of a complete (T°, γ)-path is independent of our choice of orientation for γ, the height corresponding to each of the last d even steps of W_3 is equal to the height of each of the even steps of W_1. Hence $h(W_3) = h(W_1)\, h([W_2])$ in this case.

Next, consider the case where $[W_2]$ contains exactly one element, a $\left(T^\circ, \overline{\gamma}_+^{(P)}\right)$-path $[W_2]^-$ homotopic to the curve $\overline{\gamma}_-^{(P)}$ which goes counterclockwise around P. Even though $\overline{\gamma}_-^{(P)}$ goes the opposite direction as ℓ_γ, the path $[W_2]^-$ also goes the opposite direction when crossing the radii $\rho_1, \ldots, \rho_f$. Hence the heights of the last $(d+f)$ even steps of W_3 are equal to the heights corresponding to the even steps of $[W_2]^-$. The heights corresponding to the first d even steps of W_3 are equal to the heights of the even steps of W_1. We conclude that ψ is also height-preserving in this case.

Because ψ is weight-preserving and height-preserving, we have (5.4.1). Applying Φ gives

$$\sum_{W_3 \in \Omega(\ell_\gamma^{\mathrm{P}})} = \left(\sum_{W_1 \in \Omega(\gamma)} x(W_1)\, y(W_1) \right) \left(\sum_{[W_2] \in S\Omega(\gamma^{(P)})} x([W_2])\, y([W_2]) \right). \tag{5.4.2}$$

We now use the identity $x_{\ell_\gamma} = x_\gamma\, x_{\gamma^{(P)}}$ and obtain

$$x_{\gamma^{(P)}} = \left(\sum_{W \in \Omega(\ell_\gamma^{\mathrm{P}})} x(W)\, y(W) \right) \Bigg/ \left(\sum_{W \in \Omega(\gamma)} x(W)\, y(W) \right). \tag{5.4.3}$$

Comparing (5.4.2) and (5.4.3) yields the desired formula. □

5.5 Proof of Theorem 5.2.15: formula for $\gamma^{(P,Q)}$

5.5.1 γ-compatible pair of snake graph matchings

First, we recall the notion of γ-*symmetric matchings* and γ-*compatible pair of matchings*, as defined in [MSW11, Sec 4.4].

Definition 5.5.1 (*Subgraphs $G_{\gamma^{(P)},1}$, $G_{\gamma^{(P)},2}$, $H_{\gamma^{(P)},1}$, and $H_{\gamma^{(P)},2}$ of $G_{\ell_\gamma^P}$*)**.** *Since ℓ_γ^P is a loop cutting out a once-punctured monogon with radius γ and puncture P, the graph $G_{\ell_\gamma^P}$ contains two disjoint connected subgraphs, one on each end, both of which are isomorphic to G_γ. Therefore each subgraph consists of a union of tiles $\square_{\tau_{i_1}}$ through $\square_{\tau_{i_d}}$; we let $G_{\gamma^{(P)},1}$ and $G_{\gamma^{(P)},2}$ denote these two subgraphs.*

Let v_1 and v_2 be the two vertices of tiles $\square_{\tau_{i_d}}$ in $G_{\ell_\gamma^P}$ incident to the edges labeled ρ_1 and ρ_f. For $i \in \{1,2\}$, we let $H_{\gamma^{(P)},i}$ be the connected subgraph of $G_{\gamma^{(P)},i}$ which is obtained by deleting v_i and the two edges incident to v_i. See Fig. [MSW11, Def. 4.14] Fig. [MSW11, Fig. 8] for more details.

Definition 5.5.2 (γ-symmetric matching)**.** *A perfect matching P of $G_{\ell_\gamma^P}$ is called* γ-symmetric *if the restrictions of P to the two ends satisfy $P|_{H_{\gamma^{(P)},1}} \cong P|_{H_{\gamma^{(P)},2}}$.*

Lemma 5.5.3 ([MSW11, Lemma 12.4])**.** *If P is a γ-symmetric perfect matching of the snake graph $G_{\ell_\gamma^P}$ corresponding to the ℓ-loop ℓ_γ^P, then P restricts to a perfect matching on its first d tiles or on its last d tiles.*

Lemma 5.5.4. *Let P be a γ-symmetric matching of the snake graph corresponding to ℓ_γ^P. If each of the restriction of P to the first d tiles and the restriction of P to the last d tiles is a perfect matching, then they coincide.*

Proof. Since P is γ-symmetric, the matchings on the first d tiles and the last d tiles coincide except for the two edges (labeled ρ_1 and ρ_f) which are adjacent to the northeast-most vertex v_1 (respectively, southwest-most vertex v_2). To have a perfect matching on each d-tile subgraph, one of the edges labeled ρ_1 and ρ_f must be marked. Marking ρ_1 on one d-tile subgraph and marking ρ_f on the other d-tile subgraph would violate the perfect matching condition of P. □

Definition 5.5.5 (γ-compatible pair of snake graph perfect matchings)**.** *As in [MSW11, Def. 4.18], assume that the tagged triangulation T does not contain either γ, $\gamma^{(P)}$, or $\gamma^{(Q)}$. Let P_P and P_Q be γ-symmetric matchings of the snake graphs corresponding to ℓ_γ^P and ℓ_γ^Q, respectively. By Lemma 5.5.3, either the edges of the last d tiles or the first d tiles of P_P (respectively, P_Q) is a perfect matching. We say that (P_P, P_Q) is a* γ-compatible *pair if at least one of these holds:*

the perfect matching of the last d tiles of P_P is isomorphic to the perfect matching of the last d tiles of P_Q; or
the perfect matching of the last d tiles of P_P is isomorphic to the perfect matching of the first d tiles of P_Q; or
the perfect matching of the first d tiles of P_P is isomorphic to the perfect matching of the last d tiles of P_Q; or
the perfect matching of the first d tiles of P_P is isomorphic to the perfect matching of the first d tiles of P_Q.

Fig. 5.12 illustrates the graphs ℓ_γ^P (left) and ℓ_γ^Q (right) for the setup from Fig. 5.7.

5.5.2 Maps *path* and *pm* between γ-compatible pairs and $(T^\circ, \gamma^{(P,Q)})$-paths

Definition 5.5.6 (*path* map)**.** *We construct a map*

$$path : \left\{\gamma\text{-compatible pair of matchings of } \left(G_{\ell_\gamma^P}, G_{\ell_\gamma^Q}\right)\right\} \to \left\{\left(T^\circ, \gamma^{(P,Q)}\right)\text{-paths}\right\},$$

as follows. Let (P_P, P_Q) be a γ-compatible pair.

Suppose that the edges of P_P and P_Q on the last d tiles of the corresponding snake graphs form perfect matchings. We then construct a $\left(T^\circ, \overline{\gamma}_{+,+}^{(P,Q)}\right)$-path $\omega^{+,+}$ which depends on (P_P, P_Q), as follows.

First, let $G_{\tau_{i_d},\ldots,\tau_{i_1},\eta_1,\ldots,\eta_g}$ be the connected subgraph of $G_{\ell_\gamma^Q}$ constructed by removing the last d tiles of $G_{\ell_\gamma^Q}$. The tiles of $G_{\tau_{i_d},\ldots,\tau_{i_1},\eta_1,\ldots,\eta_g}$ have diagonals labeled $\tau_{i_d}, \ldots, \tau_{i_1}, \eta_1, \ldots, \eta_g$, ordered as it goes east or north.

We associate a path $\omega^{+,+}(P_Q)$ on this subgraph (including the diagonals) to P_Q as follows. We use the same technique of [MS10], but we will start at the northeast-most

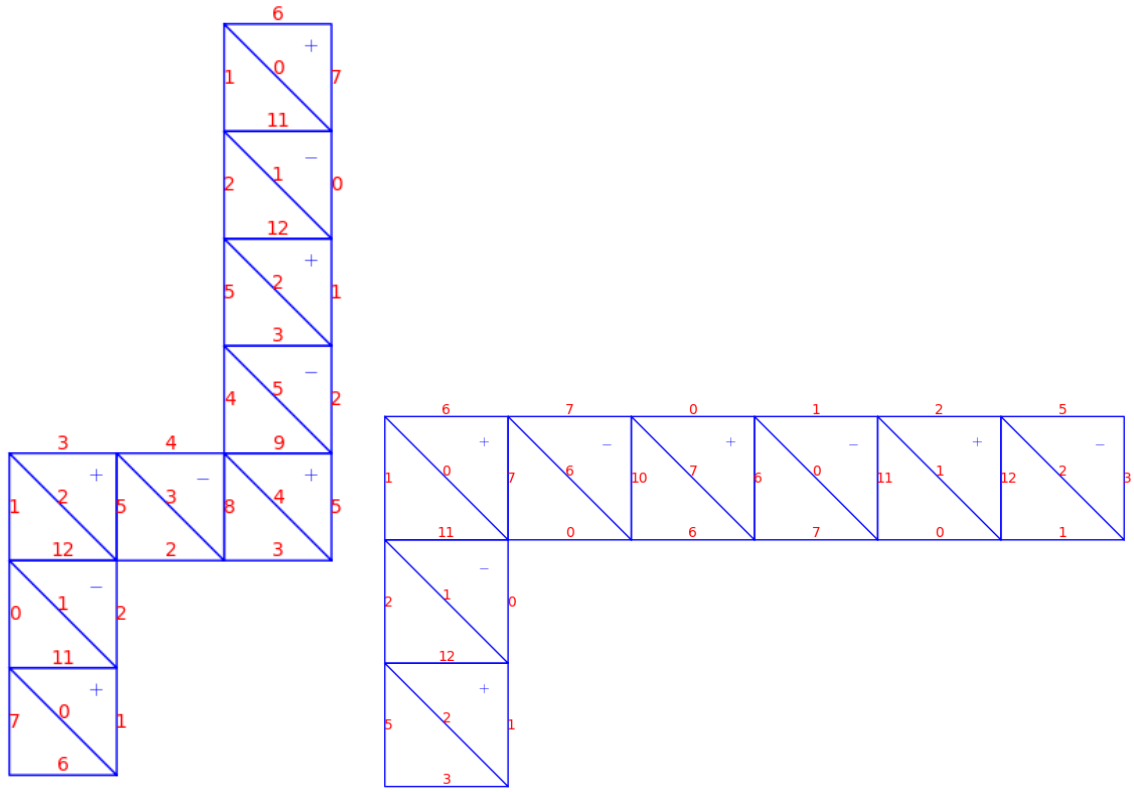

Figure 5.12: Snake graphs corresponding to ordinary arcs ℓ_γ^{P} (left) and ℓ_γ^{Q} (right), where γ is illustrated in Fig. 5.7.

tile and finish at the southwest-most tile (the opposite direction of how the snake graph is built). Start from the point v shared by $\square_{\eta_g}$ and $\square'_{\tau_{i_d}}$ (the $(d+g+1)$-th tile of the snake graph $G_{\ell_\gamma^Q}$) such that v is adjacent to the diagonal of $\square_{\eta_g}$. (If $\square'_{\tau_{i_d}}$ is north of $\square_{\eta_g}$, then v is the northwest corner of $\square_{\eta_g}$; if $\square'_{\tau_{i_d}}$ is east of $\square_{\eta_g}$, then v is the southeast corner of $\square_{\eta_g}$). Then go along the diagonal of the tile $\square_{\eta_g}$ to its other endpoint v', then along the (unique) edge $e(v')$ of P_Q which covers v'. Note that, since the restriction of P_Q on the last d tiles is a perfect matching, the other endpoint (which is not v') of this unique edge $e(v')$ must be a vertex of the tile $\square_{\eta_{g-1}}$. Continue along the diagonal of the tile $\square_{\eta_{g-1}}$, and so forth. Continue in this way until we get to go along the diagonal at the southwest-most tile, $\square_{\tau_{i_d}}$, i.e, the first tile of both $G_{\ell_\gamma^Q}$ and $G_{\tau_{i_d},\ldots,\tau_{i_1},\eta_1,\ldots,\eta_g}$. This path $\omega^{+,+}(P_Q)$ finishes at this endpoint v'' of this diagonal. Note that v'' is either the

northwest-most corner or the southeast-most corner of $\square_{\tau_{i_d}}$.

Next, let $G_{\tau_{i_1},\ldots,\tau_{i_d},\rho_1,\ldots,\rho_f}$ *be the connected subgraph of* $G_{\ell_\gamma^P}$*, which is the result of removing the last* d *tiles of* $G_{\ell_\gamma^P}$*. The tiles of* $G_{\tau_{i_1},\ldots,\tau_{i_d},\rho_1,\ldots,\rho_f}$ *have diagonals labeled* $\tau_{i_1},\ldots,\tau_{i_d},\rho_1,\ldots,\rho_f$*. We associate a path* $\omega^{+,+}(P_P)$ *on this subgraph to* P_P *in a similar manner as before, but, this time we go in the same direction as how a snake graph is built (by progressing either north or east). Let* s *be the southwest-most corner of the first tile* $\square_{\tau_{i_1}}$*, and let* $e(s)$ *denote the edge of* P_P *which covers* s*. Let* v *be the other point of* $\square_{\tau_{i_1}}$ *which is covered by* $e(s)$*. (That is, if* $e(s)$ *is the southern edge, then* v *is the southeast corner of* $\square_{\tau_{i_1}}$*; if* $e(s)$ *is the western edge, then* v *is the northwest corner of* $\square_{\tau_{i_1}}$*). Then the path* $\omega^{+,+}(P_P)$ *starts from the point* v*, going along the diagonal of the tile* $\square_{\tau_{i_1}}$*, then along the unique edge* e *of* P_P *that is incident to the other endpoint of that diagonal. Continue along the diagonal of the tile* $\square_{\tau_{i_2}}$*, and so forth. Continue in this way until we get to go along the diagonal at the northeast-most tile,* $\square_{\rho_f}$*, of* $G_{\tau_{i_1},\ldots,\tau_{i_d},\rho_1,\ldots,\rho_f}$*. This step along this diagonal ends at a corner* v'' *of* $\square_{\rho_f}$ *which is also a corner of the next tile,* $\square'_{\tau_{i_d}}$ *(the* $(d+f+1)$*-th tile of* $G_{\ell_\gamma^P}$*). This must happen because the restriction of* P_P *on the last* d *tiles of* $G_{\ell_\gamma^P}$ *is a perfect matching. Our path* $\omega^{+,+}(P_P)$ *ends at* v''*.*

We then fold each of $\omega^{+,+}(P_Q)$ *and* $\omega^{+,+}(P_P)$ *onto a lifted, triangulated polygon containing lifts of* ℓ_γ^P *and* ℓ_γ^Q *and then again onto* T°*. The last* $(2d-1)$ *steps of* $\omega^{+,+}(P_Q)$ *and the first* $(2d-1)$ *steps of* $\omega^{+,+}(P_P)$*, after this folding onto* T°*, coincide. We identify these* $2d-1$ *steps. The resulting path is a path of length* $2g+(2d-1)+2f$ *which is homotopic to an "S" shape as it crosses* $\eta_g,\ldots,\eta_1,\tau_{i_1},\ldots,\tau_{i_d},\rho_1,\ldots,\rho_f$*. This path is a* $\left(T^\circ,\overline{\gamma}_{+,+}^{(P,\,Q)}\right)$*-path, and we denote it by* $\omega^{+,+}$*. We set*

$$path(P_P,P_Q)$$

to be the equivalence class containing $\omega^{+,+}$*.*

Suppose that one of the restrictions of P_P *and* P_Q *to the last* d *tiles of the corresponding snake graphs* $G_{\ell_\gamma^P}$ *and* $G_{\ell_\gamma^Q}$ *(respectively) does not form a perfect matching. But suppose that the restrictions of* P_P *and* P_Q *on the first* d *tiles of* $G_{\ell_\gamma^P}$ *and* $G_{\ell_\gamma^Q}$ *(respectively) are perfect matchings. We construct a* $\left(T^\circ,\overline{\gamma}_{-,-}^{(P,\,Q)}\right)$*-path* $\omega^{-,-}$ *which depends*

on (P_P, P_Q) in a similar manner.

In this situation, first consider the subgraph $G_{\eta_1,\ldots,\eta_g,\tau_{i_1},\ldots,\tau_{i_d}}$ of $G_{\ell_\gamma^Q}$, created by removing the first d tiles of $G_{\ell_\gamma^Q}$. The tiles of this subgraph have diagonals labeled $\eta_1, \ldots, \eta_g, \tau_{i_1}, \ldots, \tau_{i_d}$. We define a path $\omega^{-,-}(P_Q)$ on this subgraph which starts by traversing the diagonal of the first tile $\square_{\eta_1}$ and finishes after it traverses the diagonal of the last tile $\square_{\tau_{i_d}}$ of the subgraph.

Second, consider the subgraph $G_{\rho_1,\ldots,\rho_f,\tau_{i_d},\ldots,\tau_{i_1}}$ of $G_{\ell_\gamma^P}$, created by removing the first d tiles of $G_{\ell_\gamma^P}$. The tiles of this subgraph have diagonals labeled $\rho_1, \ldots, \rho_f, \tau_{i_d}, \ldots, \tau_{i_1}$. We define a path $\omega^{-,-}(P_P)$ on this subgraph which starts by traversing the diagonal of the last tile $\square_{\tau_{i_1}}$ and finishes after it traverses the diagonal of the first tile $\square_{\rho_1}$ of the subgraph.

As before, we fold each of $\omega^{-,-}(P_Q)$ and $\omega^{-,-}(P_P)$ and onto T°. The last $(2d-1)$ steps of $\omega^{-,-}(P_Q)$ and the first $(2d-1)$ steps of $\omega^{-,-}(P_P)$, after this folding onto T°, coincide. We identify these $(2d-1)$ steps. The resulting path is of length $2g+(2d-1)+2f$ and is homotopic to a "Z" shape as it crosses $\eta_1, \ldots, \eta_g, \tau_{i_1}, \ldots, \tau_{i_d}, \rho_f, \ldots, \rho_1$. This path is a $\left(T^\circ, \overline{\gamma}_{-,-}^{(P,Q)}\right)$-path, and we denote it by $\omega^{-,-}$. We set

$$path(P_P, P_Q)$$

to be the equivalence class containing $\omega^{-,-}$.

Suppose neither of the two scenarios above holds, but suppose that the restriction of P_P on the last d tiles and the restriction of P_Q on the first d tiles are perfect matchings. Then, similarly, we construct a $\left(T^\circ, \overline{\gamma}_{+,-}^{(P,Q)}\right)$-path $\omega^{+,-}$ which depends on (P_P, P_Q) in a similar manner.

Otherwise, if the restriction of P_P on the first d tiles and the restriction of P_Q on the last d tiles are perfect matchings, we construct a $\left(T^\circ, \overline{\gamma}_{-,+}^{(P,Q)}\right)$-path $\omega^{-,+}$ which depends on (P_P, P_Q) in a similar manner.

We will show that *path* is a bijection by exhibiting its inverse.

Definition 5.5.7 (pm map)**.** *We construct a map*

$$pm : \left\{\left(T^\circ, \gamma^{(P,\,Q)}\right)\text{-paths}\right\} \to \left\{\gamma\text{-compatible pair of matchings of } \left(G_{\ell_\gamma^P}, G_{\ell_\gamma^Q}\right)\right\},$$

as follows. First, suppose $[w]$ *contains a* $\left(T^\circ, \overline{\gamma}_{+,+}^{(P,\,Q)}\right)$*-path* $\omega^{+,+}$*. Let* $G_{\tau_{i_d},\ldots,\tau_{i_1},\eta_1,\ldots,\eta_g}$ *be the subgraph of* $G_{\ell_\gamma^Q}$ *with all the tiles of* $G_{\ell_\gamma^Q}$ *except for the last* d *tiles, as defined previously. We take the first* $2g + (2d-1)$ *steps of* $\omega^{+,+}$*, which crosses* $\eta_g, \ldots, \eta_1, \tau_{i_1}, \ldots, \tau_{i_d}$ *(in that order) in* T° *and unfold this onto a path* $G(\omega^{+,+})$ *along edges and diagonals of* $G_{\tau_{i_d},\ldots,\tau_{i_1},\eta_1,\ldots,\eta_g}$ *(as in [MS10]), so that:*

- $G(\omega^{+,+})$ *starts by traversing the diagonal of the last tile* $\square_{\eta_g}$ *of* $G_{\tau_{i_d},\ldots,\tau_{i_1},\eta_1,\ldots,\eta_g}$*, starting from the point shared by* $\square_{\eta_g}$ *and the tile either north or east of it,* $\square'_{\tau_{i_1}}$ *(the* $(d+g+1)$*-th tile of the snake graph* $G_{\ell_\gamma^Q}$*);*
- $G(\omega^{+,+})$ *finishes by traversing the diagonal of the first tile* $\square_{\tau_{i_d}}$ *of* $G_{\tau_{i_d},\ldots,\tau_{i_1},\eta_1,\ldots,\eta_g}$*, finishing at either the northwest-most or southeast-most corner of* $\square_{\tau_{i_d}}$*;*
- *the even-numbered steps of* $\omega^{+,+}$ *correspond to steps of* $G(\omega^{+,+})$ *along the tiles' diagonals, and the odd-numbered steps of* $\omega^{+,+}$ *correspond to steps of* $G(\omega^{+,+})$ *along one of the four edges of the tiles.*

Next, remove all diagonals, resulting in a matching $pm^Q(\omega^{+,+})$ *of* $G_{\tau_{i_d},\ldots,\tau_{i_1},\eta_1,\ldots,\eta_g}$*. Note that this matching* $pm^Q(\omega^{+,+})$ *is not a perfect matching of* $G_{\tau_{i_d},\ldots,\tau_{i_1},\eta_1,\ldots,\eta_g}$*. In particular, the southwest-most point* s *of this graph is not covered by any edge of* $pm^Q(\omega^{+,+})$*. We add a unique edge such that* s *is now covered and the result is still a matching. Next, put this matching onto the snake graph* $G_{\ell_\gamma^Q}$*. We add edges along the last* d *tiles (to match the edges of the first* d *tiles), possibly adding an extra edge along* $\square'_{\tau_{i_1}}$ *to turn this into a perfect matching, so that we get a* γ*-symmetric matching* P_Q*.*

We take the last $(2d-1)+2f$ *steps of* $\omega^{+,+}$*, which crosses* $\tau_{i_1}, \ldots, \tau_{i_d}, \rho_1, \ldots, \rho_f$ *(in that order) in* T° *and unfold this onto the edges* $G_{\tau_{i_1},\ldots,\tau_{i_d},\rho_1,\ldots,\rho_f}$ *as before. Next, remove all diagonals, resulting in a matching* $pm^P(\omega^{+,+})$ *of* $G_{\tau_{i_1},\ldots,\tau_{i_d},\rho_1,\ldots,\rho_f}$*. This matching* $pm^P(\omega^{+,+})$ *is not a perfect matching of* $G_{\tau_{i_1},\ldots,\tau_{i_d},\rho_1,\ldots,\rho_f}$*; in particular, the southwest-most point* s *of this graph is not covered by any edge. We add a unique edge such that* s *is now covered and the result is still a matching. Next, put this matching onto the*

snake graph $G_{\ell_\gamma^P}$. We match the edges along the last d tiles so that we get a γ-symmetric matching P_P.

Since the middle $(2d-1)$ steps are the same steps by definition, the restriction of P_Q and the restriction of P_P to the last d tiles of the snake graphs $G_{\ell_\gamma^Q}$ and $G_{\ell_\gamma^P}$ (respectively) are clearly isomorphic. Hence (P_P, P_Q) is a γ-compatible pair.

Next, suppose $[w]$ does not contain any $\left(T^\circ, \overline{\gamma}_{+,+}^{(P,Q)}\right)$-path but it contains a $\left(T^\circ, \overline{\gamma}_{-,-}^{(P,Q)}\right)$-path $w^{-,-}$. We construct γ-compatible matchings P_Q and P_P in a similar manner as before, where the restriction of P_Q and the restriction of P_P to the first d tiles of the snake graphs $G_{\ell_\gamma^Q}$ and $G_{\ell_\gamma^P}$ (respectively) are isomorphic.

Otherwise, suppose $[w]$ contains a $\left(T^\circ, \overline{\gamma}_{+,-}^{(P,Q)}\right)$-path $w^{+,-}$. We construct γ-compatible matchings P_Q and P_P in a similar manner as before, where the restriction of P_Q to the first d tiles of the snake graph $G_{\ell_\gamma^Q}$ and the restriction of P_P to the last d tiles of the snake graph $G_{\ell_\gamma^P}$ (respectively) are isomorphic.

If neither of the above scenarios hold, then $[w]$ must contain a $\left(T^\circ, \overline{\gamma}_{-,+}^{(P,Q)}\right)$-path $w^{-,+}$. We construct γ-compatible matchings P_Q and P_P in a similar manner as before, where the restriction of P_Q to the last d tiles of the snake graph $G_{\ell_\gamma^Q}$ and the restriction of P_P to the first d tiles of the snake graph $G_{\ell_\gamma^P}$ (respectively) are isomorphic.

5.5.3 Proof that *path* is a weight and heigh-preserving bijection

Proof of Theorem 5.2.15. By construction, the maps *path* and *pm* defined in Definitions 5.5.6 and 5.5.7 are inverses, hence *path* is a bijection.

To prove Theorem 5.2.15, we look to [MSW11, Theorem 4.20], which states that

$$x_{\gamma^{(P,Q)}} = \frac{1}{x_{\eta_g} \dots x_{\eta_1} x_{\tau_{i_1}} \dots x_{\tau_{i_d}} x_{\rho_1} \dots x_{\rho_f}} \sum_{(P_{\mathrm{P}}, P_{\mathrm{Q}})} \frac{x(P_{\mathrm{P}})\, x(P_{\mathrm{Q}})}{x(P_{\mathrm{restr}})^3} \frac{y(P_{\mathrm{P}})\, y(P_{\mathrm{Q}})}{y(P_{\mathrm{restr}})^3} \tag{5.5.1}$$

where the sum is over all γ-compatible pairs of matchings $(P_{\mathrm{P}}, P_{\mathrm{Q}})$ of $(G_{\ell_\gamma^{\mathrm{P}}}, G_{\ell_\gamma^{\mathrm{Q}}})$, and P_{restr} is the restriction of P_{P} to a perfect matching on either the last or the first d tiles of $G_{\ell_\gamma^{\mathrm{P}}}$. There are $d+1$ edges in P_{restr}.

We now show that the bijection *path* is weight-preserving, in the sense that, given a γ-compatible pair $(P_{\mathrm{P}}, P_{\mathrm{Q}})$, if $[\omega] = path(P_{\mathrm{P}}, P_{\mathrm{Q}})$, then

$$\frac{1}{x_{\eta_g} \dots x_{\eta_1} x_{\tau_{i_1}} \dots x_{\tau_{i_d}} x_{\rho_1} \dots x_{\rho_f}} \frac{x(P_{\mathrm{P}})\, x(P_{\mathrm{Q}})}{x(P_{\mathrm{restr}})^3} = x\left([\omega]\right). \tag{5.5.2}$$

Without loss of generality, assume that the restrictions of P_{P} and P_{Q} to the last d tiles of the snake graphs $G_{\ell_\gamma^{\mathrm{P}}}$ and $G_{\ell_\gamma^{\mathrm{Q}}}$ (respectively) are perfect matchings. Let P_{restr} denote the restriction of P_{P} to the last d tiles. Let ω denote the $\left(T^\circ, \overline{\gamma}_{+,+}^{(P,\,Q)}\right)$-path in the equivalence class $path(P_{\mathrm{P}}, P_{\mathrm{Q}})$.

First, we prove that

$$\frac{x(P_{\mathrm{P}})\, x(P_{\mathrm{Q}})}{x(P_{\mathrm{restr}})^3} = \prod_{\text{odd steps } \omega_{(1-g)-1}, \cdots, \omega_{2(d+f)-1} \text{ of } \omega} x\left(\omega_{2k+1}\right). \tag{5.5.3}$$

Let s_{P} and s_{Q} be the southwest-most vertices of the the snake graphs $G_{\ell_\gamma^{\mathrm{P}}}$ and $G_{\ell_\gamma^{\mathrm{Q}}}$, respectively. Let $edge(s_{\mathrm{P}})$ denote the edge of P_{P} (of the first tile, $\square_{\tau_{i_1}}$, of $G_{\ell_\gamma^{\mathrm{P}}}$) which covers s_{P}. Let $edge(s_{\mathrm{Q}})$ denote the edge of P_{Q} (of the first tile, $\square_{\tau_{i_d}}$, of $G_{\ell_\gamma^{\mathrm{Q}}}$) which covers s_{Q}. Note that $edge(s_{\mathrm{P}})$ is labeled either by η_1 or η_g, and $edge(s_{\mathrm{P}})$ is labeled either by ρ_1 or ρ_f.

By construction of ω, we have

$$\frac{x\left(P_{\mathrm{Q}}\right)}{x\left(P_{\mathrm{restr}}\right)} = x\begin{pmatrix}\text{the first}\\ g \text{ odd}\\ \text{steps of } \omega\end{pmatrix} x\begin{pmatrix}\text{the next}\\ d-1 \text{ odd}\\ \text{steps of } \omega\end{pmatrix} x\begin{pmatrix}\text{the last}\\ f \text{ odd}\\ \text{steps of}\\ \omega\end{pmatrix} x\Big(edge(s_{\mathrm{Q}})\Big), \tag{5.5.4}$$

$$\frac{x\left(P_{\mathrm{P}}\right)}{x\left(P_{\mathrm{restr}}\right)} = x\begin{pmatrix}\text{the first}\\ g \text{ odd}\\ \text{steps of } \omega\end{pmatrix} x\begin{pmatrix}\text{the next}\\ d-1 \text{ odd}\\ \text{steps of } \omega\end{pmatrix} x\begin{pmatrix}\text{the last}\\ f \text{ odd}\\ \text{steps of}\\ \omega\end{pmatrix} x\Big(edge(s_{\mathrm{P}})\Big). \tag{5.5.5}$$

Next, we have

$$x\left(P_{\text{restr}}\right) = x\begin{pmatrix}\text{the}\\ \text{middle}\\ d-1 \text{ odd}\\ \text{steps of } \omega\end{pmatrix} x\Big(edge(s_{\text{P}})\Big)x\Big(edge(s_{\text{Q}})\Big). \tag{5.5.6}$$

Multiplying (5.5.4) and (5.5.5) gives us

$$\begin{aligned}\frac{x(P_{\text{Q}})\,x(P_{\text{P}})}{x(P_{\text{restr}})^2} = x\begin{pmatrix}\text{the first}\\ g \text{ odd}\\ \text{steps of } \omega\end{pmatrix} x\begin{pmatrix}\text{the}\\ \text{middle}\\ d-1 \text{ odd}\\ \text{steps of } \omega\end{pmatrix}^2 x\Big(edge(s_{\text{Q}})\Big)\\ x\Big(edge(s_{\text{P}})\Big)x\begin{pmatrix}\text{the last}\\ f \text{ odd}\\ \text{steps of}\\ \omega\end{pmatrix}.\end{aligned} \tag{5.5.7}$$

Combining (5.5.7) and (5.5.6), we get

$$\begin{aligned}\frac{x(P_{\text{Q}})\,x(P_{\text{P}})}{x(P_{\text{restr}})^3} &= x\begin{pmatrix}\text{the first}\\ g \text{ odd}\\ \text{steps of } \omega\end{pmatrix} x\begin{pmatrix}\text{the}\\ \text{middle}\\ d-1 \text{ odd}\\ \text{steps of } \omega\end{pmatrix} x\begin{pmatrix}\text{the last}\\ f \text{ odd}\\ \text{steps of}\\ \omega\end{pmatrix}\\ &= x\begin{pmatrix}\text{all odd}\\ \text{steps of}\\ \omega\end{pmatrix},\end{aligned}$$

which proved (5.5.3).

Since the even-numbered steps of ω go along precisely the arcs $\eta_g, \ldots, \eta_1, \ldots, \tau_{i_1}, \ldots, \tau_{i_1}, \ldots, \rho_1, \ldots, \rho_f$, we conclude (5.5.2), as needed.

The bijection *path* is also height-preserving, in the sense that

$$\frac{h(P_{\text{P}})\,h(P_{\text{Q}})}{h(P_{\text{restr}})^3} = h(\omega). \tag{5.5.8}$$

To see this, we argue that

$$\frac{h(P_{\mathrm{Q}})}{h(P_{\mathrm{restr}})^2} = h\big(\text{the first } g \text{ even steps of } \omega, \text{ along } \eta_g, \ldots, \eta_1\big), \tag{5.5.9}$$

$$h(P_{\mathrm{restr}}) = h\big(\text{the middle } d \text{ even steps of } \omega, \text{ along } \tau_{i_1}, \ldots, \tau_{i_d}\big), \tag{5.5.10}$$

$$\frac{h(P_{\mathrm{P}})}{h(P_{\mathrm{restr}})^2} = h\big(\text{the last } f \text{ even steps of } \omega, \text{ along } \rho_1, \ldots, \rho_f\big). \tag{5.5.11}$$

This is evident from the folding map of [MS10] between the matchings on snake graphs and the T°-paths. See [MS10, Section 5] for more details.

Combining (5.5.3) and (5.5.8), after applying Φ, we deduce that

$$\frac{1}{x_{\eta_g} \ldots x_{\eta_1} x_{\tau_{i_1}} \ldots x_{\tau_{i_d}} x_{\rho_1} \ldots x_{\rho_f}} \frac{x(P_{\mathrm{P}})\, x(P_{\mathrm{Q}})}{x(P_{\mathrm{restr}})^3} \frac{y(P_{\mathrm{P}})\, y(P_{\mathrm{Q}})}{y(P_{\mathrm{restr}})^3} = x(\omega) y(\omega). \tag{5.5.12}$$

This concludes the proof of Theorem 5.2.15. □

References

[BCI74] D. Broline, D. W. Crowe, and I. M. Isaacs. The geometry of frieze patterns. *Geometriae Dedicata*, 3:171–176, 1974.

[BFPT16] Karin Baur, Klemens Fellner, Mark James Parsons, and Manuela Tschabold. Growth behaviour of periodic tame friezes. *arXiv preprint arXiv:1603.02127*, 2016.

[BM09] Karin Baur and Robert J. Marsh. Frieze patterns for punctured discs. *J. Algebraic Combin.*, 30(3):349–379, 2009, 0711.1443.

[BPT16] Karin Baur, Mark J. Parsons, and Manuela Tschabold. Infinite friezes. *European J. Combin.*, 54:220–237, 2016.

[CC73] John H Conway and HSM Coxeter. Triangulated polygons and frieze patterns. *The Mathematical Gazette*, 57(400):87–94, 1973.

[CC06] Philippe Caldero and Frédéric Chapoton. Cluster algebras as Hall algebras of quiver representations. *Comment. Math. Helv.*, 81(3):595–616, 2006.

[Cer11] Giovanni Cerulli Irelli. Positivity in skew-symmetric cluster algebras of finite type. *preprint arXiv:1102.3050*, 2011, 1102.3050.

[CKLFP13] Giovanni Cerulli Irelli, Bernhard Keller, Daniel Labardini-Fragoso, and Pierre-Guy Plamondon. Linear independence of cluster monomials for skew-symmetric cluster algebras. *Compos. Math.*, 149(10):1753–1764, 2013, 1203.1307.

[CLF12] Giovanni Cerulli Irelli and Daniel Labardini-Fragoso. Quivers with potentials associated to triangulated surfaces, Part III: tagged triangulations and cluster monomials. *Compos. Math.*, 148(6):1833–1866, 2012, 1108.1774.

[CK08] Philippe Caldero and Bernhard Keller. From triangulated categories to cluster algebras. *Invent. Math.*, 172(1):169–211, 2008, math.RT/0506018.

[CLS15] Ilke Canakci, Kyungyong Lee, and Ralf Schiffler. On cluster algebras from unpunctured surfaces with one marked point. *Proc. Amer. Math. Soc. Ser. B*, 2:35–49, 2015.

[Cox71] H. S. M. Coxeter. Frieze patterns. *Acta Arith.*, 18:297–310, 1971.

[CP03] Gabriel D. Carroll and Gregory Price. Two new combinatorial models for the ptolemy recurrence. *unpublished memo*, 2003.

[CP15] Cesar Ceballos and Vincent Pilaud. Cluster algebras of type D: pseudotriangulations approach. *Electron. J. Combin.*, 22(4):Paper 4.44, 27, 2015.

[Dev16] The Sage Developers. *SageMath, the Sage Mathematics Software System (Version 7.2)*, The Sage Development Team, 2016. `http://www.sagemath.org`.

[DT13] Grégoire Dupont and Hugh Thomas. Atomic bases of cluster algebras of types A and $\tilde{A}$. *Proc. Lond. Math. Soc.*, 107(4):825–850, 2013, 1106.3758.

[FG06] Vladimir Fock and Alexander Goncharov. Moduli spaces of local systems and higher Teichmüller theory. *Publ. Math. Inst. Hautes Études Sci.*, (103):1–211, 2006, math.AG/0311149.

[FG09] Vladimir V. Fock and Alexander B. Goncharov. Cluster ensembles, quantization and the dilogarithm. *Ann. Sci. Éc. Norm. Supér. (4)*, 42(6):865–930, 2009, math.AG/0311245.

[FST08] Sergey Fomin, Michael Shapiro, and Dylan Thurston. Cluster algebras and triangulated surfaces. I. Cluster complexes. *Acta Math.*, 201(1):83–146, 2008, math.RA/0608367.

[FST12] Anna Felikson, Michael Shapiro, and Pavel Tumarkin. Skew-symmetric cluster algebras of finite mutation type. *J. Eur. Math. Soc. (JEMS)*, 14(4):1135–1180, 2012.

[FT12] Sergey Fomin and Dylan Thurston. Cluster algebras and triangulated surfaces. part II: Lambda lengths. *arXiv preprint arXiv:1210.5569*, 2012.

[FZ02] Sergey Fomin and Andrei Zelevinsky. Cluster algebras. I. Foundations. *J. Amer. Math. Soc.*, 15(2):497–529, 2002, math.RT/0104151.

[FZ03] Sergey Fomin and Andrei Zelevinsky. Cluster algebras. II. Finite type classification. *Invent. Math.*, 154(1):63–121, 2003, math.RA/0208229.

[FZ07] Sergey Fomin and Andrei Zelevinsky. Cluster algebras. IV. Coefficients. *Compos. Math.*, 143(1):112–164, 2007.

[GHKK14] Mark Gross, Paul Hacking, Sean Keel, and Maxim Kontsevich. Canonical bases for cluster algebras. *preprint arXiv:1411.1394*, 2014.

[GM15] Emily Gunawan and Gregg Musiker. T-path formula and atomic bases for cluster algebras of type D. *SIGMA Symmetry Integrability Geom. Methods Appl.*, 11:060, 2015.

[GSV05] Michael Gekhtman, Michael Shapiro, and Alek Vainshtein. Cluster algebras and Weil–Petersson forms. *Duke Math. J.*, 127(2):291–311, 2005, math.QA/0309138.

[HL10] David Hernandez and Bernard Leclerc. Cluster algebras and quantum affine algebras. *Duke Math. J.*, 154(2):265–341, 2010, 0903.1452.

[LLZ14] Kyungyong Lee, Li Li, and Andrei Zelevinsky. Positivity and tameness in rank 2 cluster algebras. *J. Algebraic Combin.*, 40(3):823–840, 2014, 1303.5806.

[LS15] Kyungyong Lee and Ralf Schiffler. Positivity for cluster algebras. *Ann. of Math. (2)*, 182(1):73–125, 2015.

[MS10] Gregg Musiker and Ralf Schiffler. Cluster expansion formulas and perfect matchings. *J. Algebraic Combin.*, 32(2):187–209, 2010, 0810.3638.

[MSW11] Gregg Musiker, Ralf Schiffler, and Lauren Williams. Positivity for cluster algebras from surfaces. *Adv. Math.*, 227(6):2241–2308, 2011, 0906.0748.

[MSW13] Gregg Musiker, Ralf Schiffler, and Lauren Williams. Bases for cluster algebras from surfaces. *Compos. Math.*, 149(2):217–263, 2013, 1110.4364.

[Mul13] Greg Muller. Locally acyclic cluster algebras. *Adv. Math.*, 233:207–247, 2013.

[MW13] Gregg Musiker and Lauren Williams. Matrix formulae and skein relations for cluster algebras from surfaces. *Int. Math. Res. Not. IMRN*, (13):2891–2944, 2013.

[Nak11] Hiraku Nakajima. Quiver varieties and cluster algebras. *Kyoto J. Math.*, 51(1):71–126, 2011, 0905.0002.

[Pro02] James Propp. Lattice structure for orientations of graphs. *arXiv preprint math/0209005*, 2002.

[Pro05] James Propp. The combinatorics of frieze patterns and markoff numbers. *arXiv preprint math/0511633*, 2005.

[SCc08] The Sage-Combinat community. *Sage-Combinat: enhancing Sage as a toolbox for computer exploration in algebraic combinatorics*, 2008. `http://combinat.sagemath.org`.

[Sch08a] Ralf Schiffler. A cluster expansion formula (A_n case). *Electron. J. Combin.*, 15(1):Research paper 64, 9, 2008.

[Sch08b] Ralf Schiffler. A geometric model for cluster categories of type D_n. *J. Algebraic Combin.*, 27(1):1–21, 2008, math.RT/0608264.

[Sch10] Ralf Schiffler. On cluster algebras arising from unpunctured surfaces. II. *Adv. Math.*, 223(6):1885–1923, 2010, 0809.2593.

[Smi15] David Smith. Infinite friezes and triangulations of the strip. *arXiv preprint arXiv:1512.05842*, 2015.

[ST09] Ralf Schiffler and Hugh Thomas. On cluster algebras arising from unpunctured surfaces. *Int. Math. Res. Not.*, 2009(17):3160–3189, 2009, 0712.4131.

[SZ04] Paul Sherman and Andrei Zelevinsky. Positivity and canonical bases in rank 2 cluster algebras of finite and affine types. *Mosc. Math. J.*, 4(4):947–974, 2004, math.RT/0307082.

[Tsc15] Manuela Tschabold. Arithmetic infinite friezes from punctured discs. *arXiv preprint arXiv:1503.04352*, 2015.

[Yur16] Toshiya Yurikusa. A new cluster expansion formula for cluster algebras in type a. *arXiv preprint arXiv:1605.07557*, 2016.